Hydrogeological processes and Geological Settings over Europe controlling dissolved geogenic and anthropogenic elements in groundwater of relevance to human health and the status of dependent ecosystems - HOVER

Deliverable 5.3

Modelling nitrate and pesticide transport: Assessments of N travel times

Authors and affiliations:

Matthew Ascott (NERC)
Lei Wang (NERC)
Hans Peter Broers (TNO)
Mariëlle van Vliet (TNO)
Gijs Janssen (Deltares)
Laurence Gourcy (BRGM)
Stéphanie Pinson (BRGM)
Eline Malcuit (BRGM)
Nicolas Surdyk (BRGM)
Ozren Larva (HGI)
Željka Brkić (HGI)
Henry Debattista (MTI)
Annette Rosenbom (GEUS)
Klaus Hinsby (GEUS)
Janko Urbanc (GeoZS)
Katie Tedd (GSI)

E-mail of lead author:
matta@bgs.ac.uk

Version: no. 1

This report is part of a project that has received funding by the European Union's Horizon 2020 research and innovation programme under grant agreement number 731166.

Deliverable Data		
Deliverable number	D5.3	
Dissemination level	Public	
Deliverable name	Modelling nitrate and pesticide transport	
Work package	WP5 Nitrate and pesticides transport from soil to groundwater receptors	
Lead WP/Deliverable beneficiary	NERC (BGS)	
Deliverable status		
Submitted (Author(s))	22/12/2020	Matthew Ascott, Lei Wang
Verified (WP leader)	22/12/2020	Matthew Ascott
Approved (Coordinator)	22/12/2020	Laurence Gourcy

The GeoERA-Groundwater HOVER (Hydrogeological processes and Geological settings over Europe controlling dissolved geogenic and anthropogenic elements in groundwater of relevance to human health and the status of dependent ecosystems) project aims to gain an understanding of the controls on groundwater quality across Europe.

Within HOVER, Work Package 5 (WP5) aims to develop an improved understanding of the transport of nitrate (NO3) and pesticides (PST) from soil to groundwater receptors. The aim of the task 3 of WP5 (Task 5.3) is to use modelling approaches to assess N and PST travel times across different European settings. This report describes approaches to modelling nitrate and pesticide transport and associated travel times in unsaturated and saturated zones across the pilot areas of the methodological demonstration project HOVER WP5. For each pilot site, we detail the key drivers to the models developed, the modelling approach used and key results and outcomes. We then synthesize these models and compare approaches, results and outcomes across the different pilots.

TABLE OF CONTENTS

1 INTRODUCTION

1.1 Background to HOVER and WP5

The GeoERA-Groundwater HOVER (**H**ydrogeological processes and Geological settings **over** Europe controlling dissolved geogenic and anthropogenic elements in groundwater of relevance to human health and the status of dependent ecosystems) project aims to gain an understanding of the controls on groundwater quality across Europe.

Nitrate (N) and pesticides (PST) remain ubiquitous groundwater contaminants in Europe, and are major concerns for public and private water supply and aquatic ecosystems. Within HOVER, Work Package 5 (WP5) aims to develop an improved understanding of the transport of nitrate (NO_3) and pesticides (PST) from soil to groundwater receptors.

1.2 Background to Task 5.3 and this report

The aim of Task 5.3 (Modelling nitrate and pesticide transport through unsaturated and saturated zones to groundwater receptors) is to use modelling approaches to assess N and PST transport across a number of relevant European settings. For each pilot area, we detail the modelling approach, key results and outcomes. The countries participating in this report are shown in Figure 1.1 and the pilot areas are listed in Table 1.1. Chapters 2 to 10 of this report detail the individual pilot studies undertaken. In chapter 11, we then evaluate, compare and synthesize the different approaches taken and develop cross-pilot outputs. These cross-pilot outputs are also reported in the EGDI.

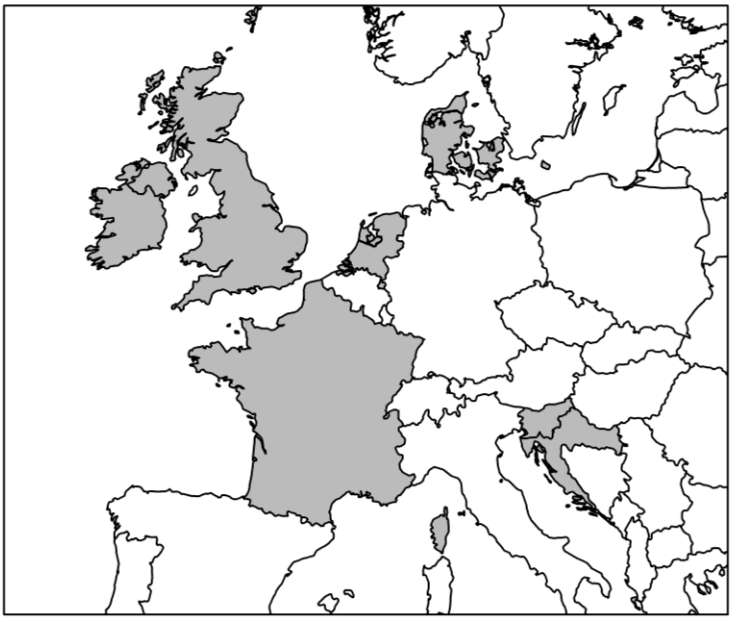

Figure 1.1 Countries contributing pilot studies to this report. Malta is not included in this figure due to scale.

Table 1.1 Pilot areas detailed in this report

Country	**Lead Author**	**Pilot study**	**Nitrate**	**Pesticides**
Continental	NERC (BGS)	Continental scale modelling of nitrate stored in the unsaturated zone	X	
UK		National scale modelling of nitrate storage and travel times	X	
France	BRGM	National scale nitrate travel time modelling	X	
Netherlands	TNO	Groundwater model evaluation in the Meuse catchment	X	X
Denmark	GEUS	National scale nitrate modelling, Pesticide Leaching Assessment Programme modelling	X	X
Croatia and Slovenia	GEO-ZS, HGI-CGS	Modelling nitrate concentration trends in the Drava aquifer	X	
Malta	MTI	Summary of BGS nitrate conceptual modelling studies	X	
Republic of Ireland	GSI	Summary of Source Apportionment Loading Methodology	X	

2 GLOBAL AND CONTINENTAL SCALE MODELLING OF NITRATE IN THE UNSATURATED ZONE

Matthew Ascott, Lei Wang
NERC (BGS), UK

2.1 Introduction

This case study reports the work of Ascott et al. (2017) where nitrate stored in the unsaturated zone was calculated at the global scale for the first time. Global scale N budgets used to quantify man's impact on the N cycle often assume a steady state over a 1 year timescale, with no net N accumulation. Research across a range of scales has shown this to be inappropriate, as there can be substantial storage of nitrate in soils, the vadose zone and groundwater (Ascott et al., 2016; Van Meter et al., 2016; Worrall et al., 2009; Worrall et al., 2015). Problems associated with time lag and storage of nitrate in the unsaturated zone have been identified at local (Costa et al., 2002; Gvirtzman and Magaritz, 1986; Kurtzman et al., 2013; McMahon et al., 2006; Pratt et al., 1972; Rudolph et al., 2015; Spalding and Kitchen, 1988; Wellings and Bell, 1980), regional (Foster et al., 1982; Johnston et al., 1998; Mercado, 1976) and national scales (Ascott et al., 2016; Fenton et al., 2011; Wang et al., 2013; Wang et al., 2016; Wang et al., 2012). The research reported here presents the first estimate of this problem at the global scale (Ascott et al., 2017). Here we also present the results at the continental scale for Europe, covering the GeoERA HOVER WP5 partners.

2.2 Modelling approach

2.2.1 Overarching framework

The modelling approach consists of a static coupling of existing models of global water table depth, groundwater recharge, near-surface porosity and nitrate leaching from the base of the soil zone. The model operates on a 0.5 degree grid cell size and annual for 1900 – 2000, and was developed in R. All driving datasets are available from the references cited by Ascott et al. (2017), and the model outputs are publically available via the UK National Geoscience Data Centre (Ascott, 2018).

2.2.2 Source term

Nitrate leaching from the base of the soil zone was derived from the global nutrient model IMAGE (Beusen et al., 2015) for 1900 to 2000. IMAGE has been detailed elsewhere (Beusen et al., 2015; Bouwman et al., 2013; Van Drecht et al., 2003) and the soil zone processes are briefly described here and in Figure 2.1. IMAGE uses the concept of an annual steady state soil N budget surplus, defined as the balance between soil N inputs and outputs. The soil N budget (N_{budget}) is calculated as:

$$N_{\text{budget}} = N_{\text{fix}} + N_{\text{dep}} + N_{\text{fert}} + N_{\text{man}} - N_{\text{withdr}} - N_{\text{vol}} \qquad (2.1)$$

Where N_{fix} is biological nitrogen fixation, N_{dep} is atmospheric N deposition, N_{fert} is application of N fertilizer, N_{man} is addition of manure and N_{withdr} and N_{vol} are loss terms for N withdrawal from harvesting and ammonia volatilisation respectively. When N_{budget} is positive, leaching, surface runoff and denitrification can occur. N leaching (N_{leach}) at the base of the soil zone is a fraction of the soil N budget excluding N loss via surface runoff (N_{sro}):

$$N_{\text{leach}} = f_{\text{leach}}(N_{\text{budget}} - N_{\text{sro}}) \qquad (2.2)$$

For further detail on soil N budget inputs, outputs and processes the reader is referred to previous modelling studies (Bouwman et al., 2013; Van Drecht et al., 2003).

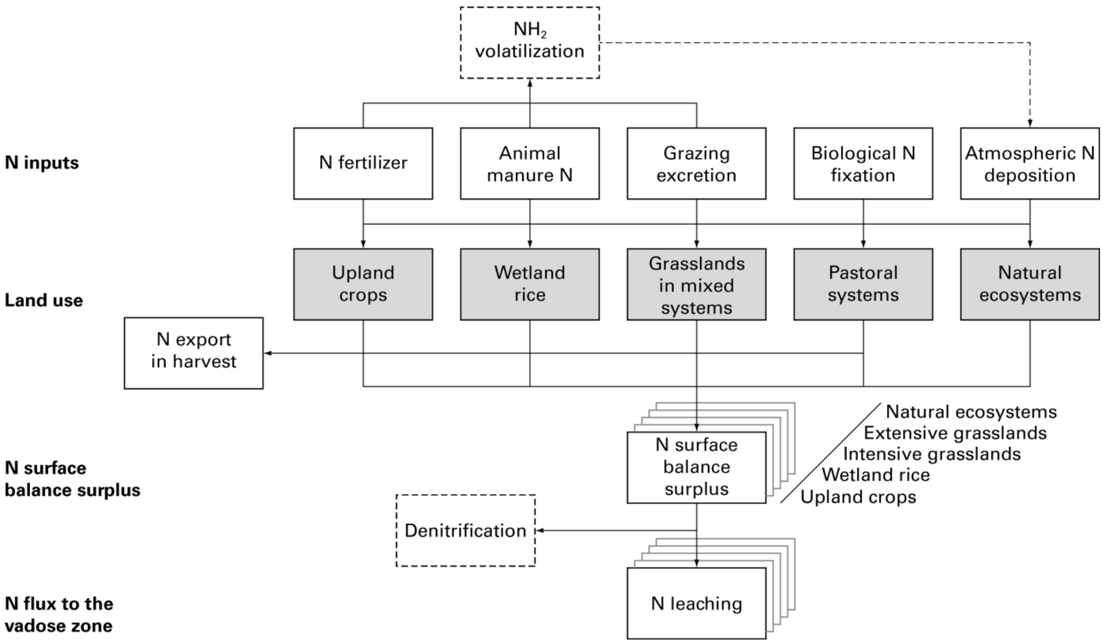

Figure 2.1 Scheme used to calculate N leaching at the base of the soil zone

2.2.3 Unsaturated zone

Travel time in the unsaturated zone was derived by estimating the depth to groundwater and nitrate velocity. Depth to groundwater mapping at 0.5 degree scale was derived from previously published maps by Fan et al. (2013). Velocity of nitrate (V_{NO3}, m year^{-1}) in the unsaturated zone was calculated using a piston flow model:

$$V_{\mathrm{NO3}} = \frac{R}{\emptyset} \tag{2.3}$$

Where R is the recharge rate (m year^{-1}) and Ø is effective porosity (dimensionless). Porosity estimates were derived from Gleeson et al. (2014) and global groundwater recharge mapping was derived from the PCR-GLOBWB model (Wada et al., 2010). Whilst recharge estimates derived using PCR-GLOBWB account for increased hydraulic conductivity with increased saturation, unsaturated zone velocities can also decrease with increased saturation associated with an increased cross-sectional area of flow (Sousa et al., 2013). Based on previous catchment and regional scale approaches (Fenton et al., 2011; Sousa et al., 2013; Vero et al., 2014; Wilson and Shokri, 2015), we accounted for this process separately from recharge in the calculation of deep unsaturated zone travel times. Estimates of travel time through the deep vadose zone calculated using equation 2.1 assumes a fully saturated matrix. This is supported by work which shows that unsaturated zone velocities calculated using this method agree well with observed velocities derived from unsaturated zone porewater profiles in limestone and sandstone aquifers (Wang et al., 2012). In partially saturated media, assuming 100% effective saturation will result in unsaturated zone velocities being underestimated and hence unsaturated zone storage being overestimated. N storage in unsaturated zones of strongly karstified aquifers with limited matrix porosity will also be overestimated. Global geological maps do not differentiate between karst and non-karst sedimentary carbonate rocks (Gleeson et al., 2011), so we explored the impact of these assumptions on model results through sensitivity analysis.

2.2.4 Representation of attenuation processes

It was assumed that nitrate is conservative in the unsaturated zone. This is supported by numerous studies (Rivett et al., 2008) which showed that the evidence for denitrification in the unsaturated zone is very limited, with just 1-2% of the nitrate leached removed (Rivett et al., 2007). In some specific local hydrogeological settings (e.g. where anaerobic conditions and organic carbon are present (Rivett et al., 2008)) denitrification in the unsaturated zone may occur, and in these areas the model may overestimate nitrate storage. At the global scale this was considered negligible.

2.2.5 Model calculation, sensitivity analysis and validation

For each grid cell, the unsaturated zone travel time and nitrate leaching history was used to derive estimates of nitrate stored across the whole thickness of the unsaturated zone on an annual basis. We undertook a heuristic sensitivity analysis by running the model using different inputs. We separately varied the vadose zone travel time and nitrate leaching input by +/-50%. We also varied vadose zone effective saturations (0.25, 0.5, 0.75 and 1) to account for variable cross-sectional area of flow in partially saturated media. We also separated areas underlain by sedimentary carbonate rocks (Gleeson et al., 2014) to account for rapid vadose zone transport in karstic aquifers with limited matrix porosity, and hence limited N storage.

A 2 step model validation was undertaken. First, the model results were compared against previously published national and catchment scale estimates of nitrate storage (England and Wales (Ascott et al., 2016) and the Thames catchment (Worrall et al., 2015). Second, distributions of modelled nitrate concentrations in recharge at the water table were compared against observed distributions of groundwater nitrate concentrations for Europe (European Environment Agency, 2015) and America (USGS, 2015). The comparison between modelled concentrations in recharge and observed concentrations does not directly validate estimates of nitrate storage, but it provides a sense-check that the nitrate inputs and unsaturated zone travel time estimates are reasonable.

2.3 Key results

2.3.1 Global scale results

Figure 2.2 shows the modelled global increase in nitrate stored in the unsaturated zone for 1900 to 2000. Total global storage in the year 2000 is estimated to be between 600 and 1800 Tg N. 10% of this is estimated to be located on carbonate unsaturated zones, where matrix porosity may be limited and thus the model may be overestimating nitrate storage. Total global unsaturated zone nitrate storage is between 7 and 200% of estimates of soil inorganic nitrogen storage (NO_3^- + NH_4^+, 940 (Prentice, 2008) – 25,000 (Lin et al., 2000) Tg).

Figure 2.3 shows the spatial distribution of increases in nitrate stored in the unsaturated zone. Areas of North America, China, Central and Eastern Europe have developed large amounts of nitrate stored in the vadose zone due to thick unsaturated zones, slow travel times and high nitrate loading. Estimates of nitrate stored in the unsaturated zone derived from the global model agree reasonably well with estimates from previous studies, see Table 2.1. Figure 2.4 shows modelled and observed concentrations in recharge and groundwater for the EU and the USA. The distributions show a reasonably good agreement, with a better agreement in the USA reflecting the much larger observational dataset available in the USA than in Europe.

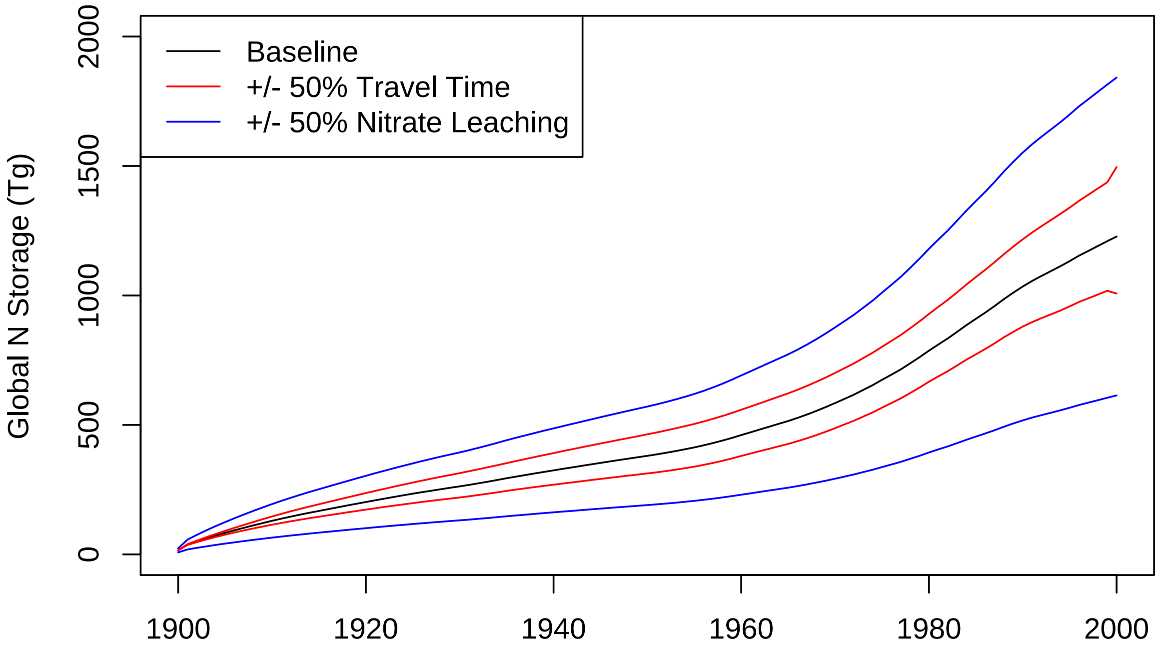

Figure 2.2 Modelled increases in nitrate stored in the unsaturated zone at the global scale

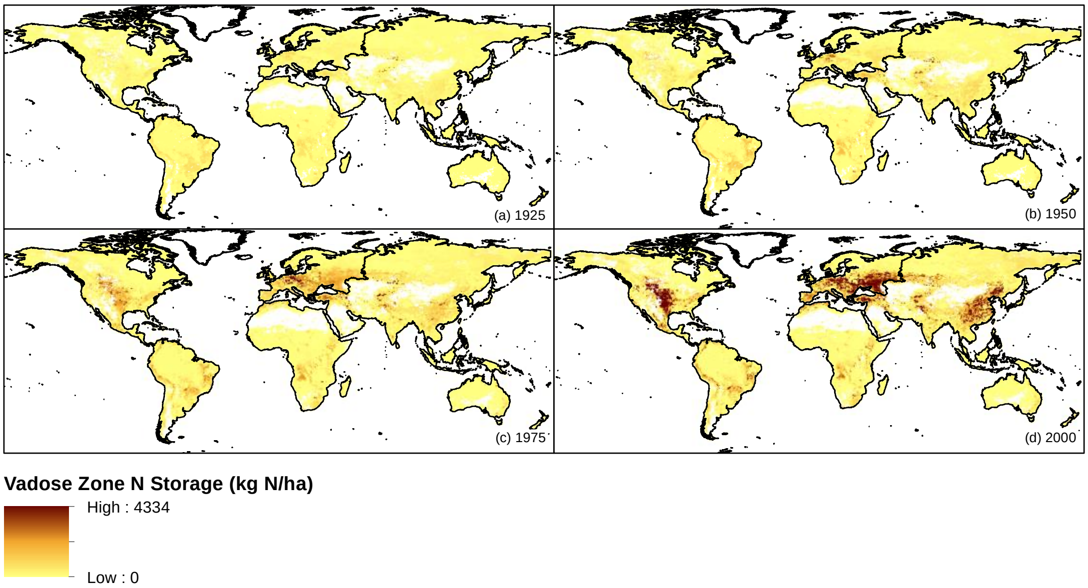

Figure 2.3 Spatial distribution of nitrate stored in the unsaturated zone for 1925 - 2000

Table 2.1 Estimates of nitrate storage (Tg N) in the unsaturated zone calculated using the global model and in previous studies

Area	Range of previous estimates	Peak global model storage estimate
England and Wales	0.016-0.24	0.059
Thames Basin, England	0.8-1.75	1.7

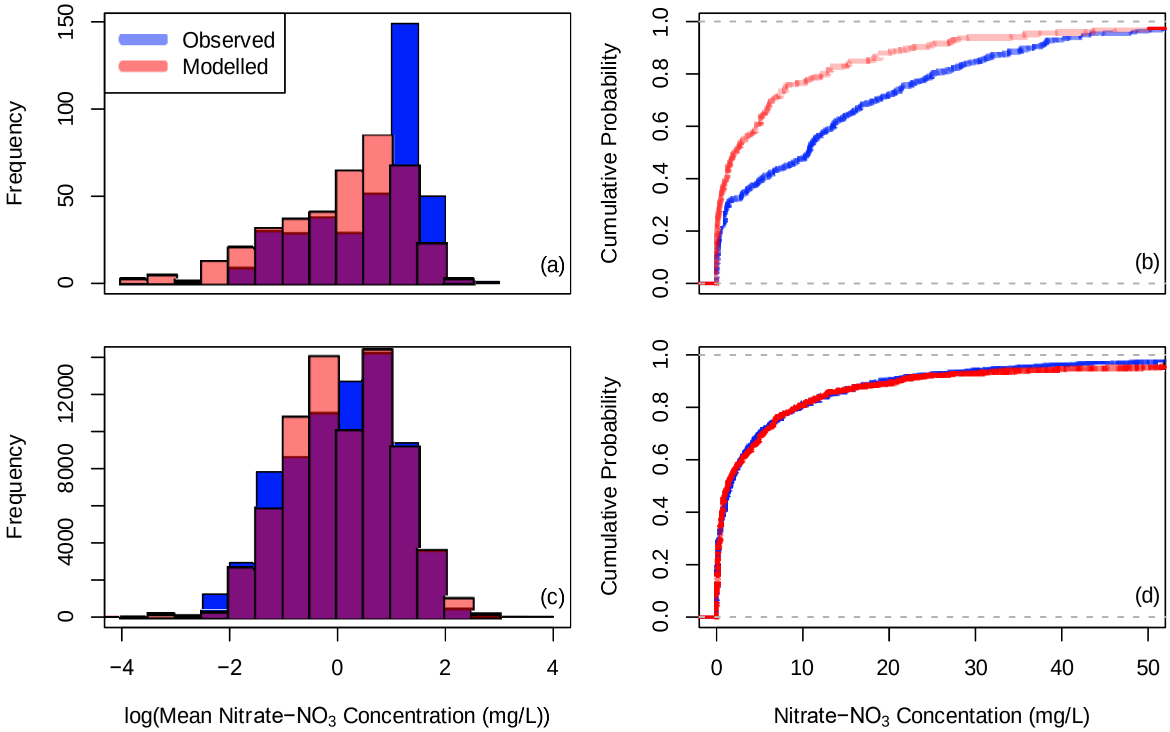

Figure 2.4 Observed (blue) and modelled (red) distributions of nitrate concentrations in groundwater and recharge respectively, for countries in the European Union (top) and the USA (bottom)

2.3.2 *Results for Europe*

Figure 2.5 shows patterns of nitrate stored in the unsaturated zone for the year 2000 in Europe. The model predicts nitrate storage to be relatively more significant in Central and Eastern Europe than Western Europe. The patterns of nitrate stored in the unsaturated zone broadly reflect the driving controls of water table depth and nitrate leaching from the base of the soil zone. On this basis four principal typologies of loading-travel time-storage can be derived:

- Areas which have high modelled historic nitrate leaching and deep water tables, resulting in significant unsaturated zone nitrate storage (for example Eastern Germany and the Czech Republic)
- Areas which have high modelled historic nitrate leaching and shallow water tables, resulting in limited unsaturated zone nitrate storage (for example the Netherlands and Denmark)
- Areas which have low modelled historic nitrate leaching and deep water tables, resulting in limited unsaturated zone nitrate storage (for example Alpine regions)
- Areas which have low modelled historic nitrate leaching and shallow water tables, resulting in limited unsaturated zone nitrate storage (for example Northern Russia, parts of Latvia and Estonia)

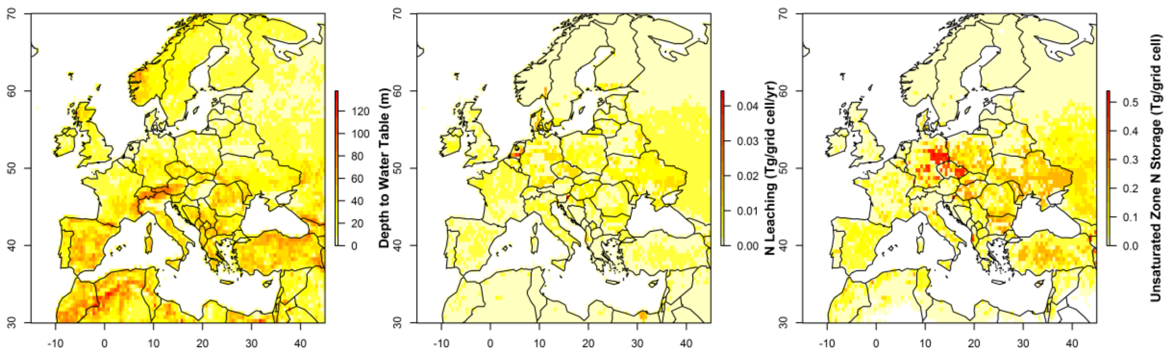

Figure 2.5 Depth to water table (left), nitrate leaching in 1987 (middle) and nitrate stored in the unsaturated zone in 2000 (right) in Europe

2.4 Outcomes of modelling

All model inputs and outputs are publicly available as discussed in section 2.2.1. The principal outcome of this research at the global scale has been an increased awareness of the issue of nitrate transport in the unsaturated zone. The research was reported by a number of national news agencies (BBC, The Times UK). As a result of this the increased awareness of this issue resulting from this research and the UK case study reported in section 3, the Environmental Audit Committee of the UK Government ran an enquiry into Nitrate, to which BGS submitted written and oral evidence (Ascott and Ward, 2018). Moreover, some of the principles of the global scale modelling have been based on case studies in the UK. These national scale approaches are being used to inform policymaking, as discussed further in section 3.

The global scale modelling here has the potential to be used as a screening to evaluate whether further regional to basin scale investigations into nitrate transport in the unsaturated zone are likely to be required. Ongoing work is currently evaluating the performance of the global scale model against regional scale modelling studies in the Loess Plateau of China (Turkeltaub et al., 2019; Turkeltaub et al., 2015). Future work seeks to refine the global scale model using more detailed local scale datasets and future scenarios of nitrate leaching. At present the model is currently constrained by the driving nitrate leaching data, which is only available on a 0.5 degree basis for 1900 – 2000.

3 UK

Lei Wang, Matthew Ascott
NERC (BGS), UK

3.1 Regional scale prediction of the arrival of peak nitrate concentrations at the water table and nitrate storage in the vadose zone: case studies from Great Britain

3.1.1 Introduction

This case study reports the “nitrate time bomb” model developed by Wang et al. (2012), which has been used to predict national-scale loading of nitrate at the water table, and calculate the total mass of nitrate contained in the vadose zone of aquifers in England and Wales (Ascott et al., 2016).

Using Great Britain as a case study, the work of Wang et al. (2012) shows significant regional variation in nitrate arrival times at the water table. Nitrate reaches the water table of most aquifers within 80 years from application, but there are contrasting outcomes for the two main aquifers, the Permo-Triassic sandstones and the Cretaceous Chalk, a fractured microporous limestone aquifer. Peak nitrate loading is predicted to have already arrived at the water table for over 90% of the Permo-Triassic sandstone aquifer. However, the projected peak nitrate input in about 60 % of the Chalk aquifer has not yet reached the water table; and this will continue to arrive over the next 60 years.

According to Ascott et al. (2016), the total mass of nitrate in the vadose zone of aquifers in England and Wales peaked in 2008 at 1400 kt N (800 to >1700 kt N from sensitivity analyses), which is approximately 2.5 to 6 times greater than saturated zone estimates for this period. Therefore, the subsurface is an important store of reactive nitrogen. Majority of the nitrate mass (~70%) is estimated to be in the Chalk.

3.1.2 Modelling approach

3.1.2.1 Overarching framework

The nitrate time bomb (NTB) was developed to address the question: when and how the nitrate time-lag in the groundwater system affects groundwater quality at catchment, regional, national and international scales. Great Britain, the contiguous land mass of the United Kingdom, has been used as a case study. In order to predict changes in average behaviour over a regional area (taken to be >100,000 km^2), it is necessary to develop a generic methodology with an appropriate level of conceptual complexity.

A relatively simple conceptual model has been developed based on identification of first order controls on trends in nitrate concentration in groundwater. Factors, such as average saturated groundwater flow and groundwater discharge rates, affect trends in nitrate concentration in groundwater. However, the first order control on trends in nitrate concentration in groundwater is the loading of nitrate at the water table. This in turn is primarily a function of the nitrate input function at the bottom of the soils, the rate of travel of nitrate through the unsaturated zone, and the thickness of the unsaturated zones. Other factors that have spatio-temporal variations, such as recharge rate, nitrate degradation, and diffusive and dispersive processes in the soil and unsaturated zones, also affect the loading of nitrate at the water table.

Based on this simple conceptual model (Figure 3.1), the nitrate time bomb (NTB) model code has been developed using C++ and is available for research purposes. The key model stakeholders include researchers, local governments, water companies and geological surveys.

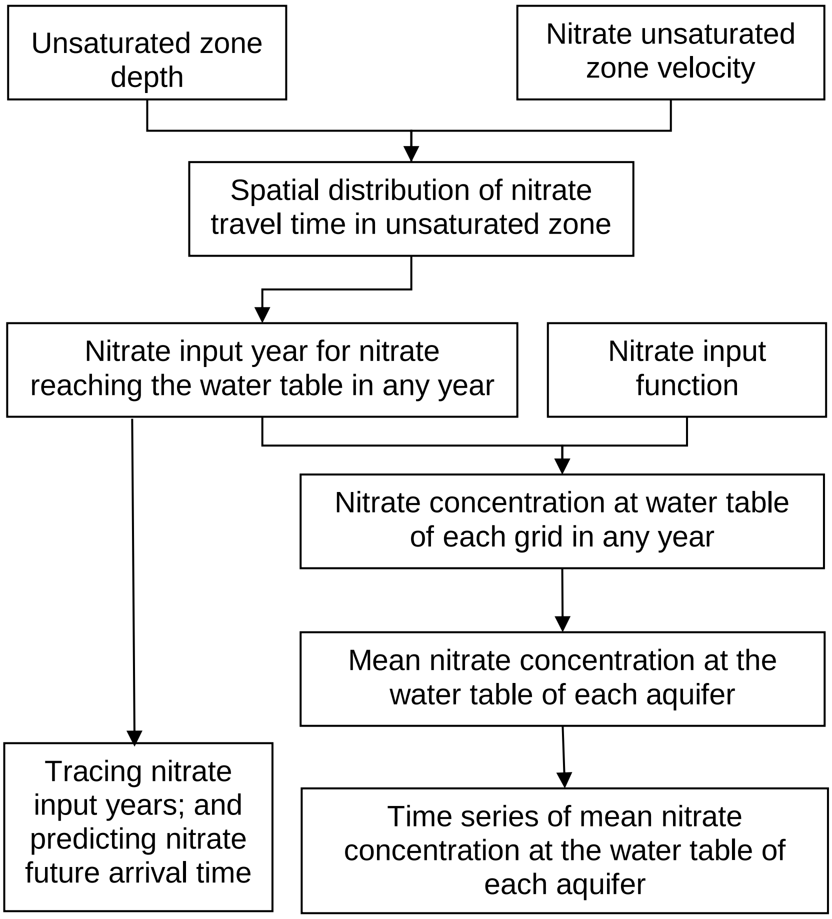

Figure 3.1. Flow chart of the conceptual model in the nitrate time bomb model

3.1.2.2 Source Term

The nitrate input function used in the present study is based on estimates of the time-varying nitrate content found in the unsaturated zone immediately beneath the soil layer. The nitrate input function curve (Figure 3.2) is divided into six time slices or spans which are defined as follows:

Span 1 (1925–1940) has a constant input of 25kg N ha^{-1} (Foster et al., 1982), which was derived based on a low level of industrialisation and very limited use of non-manure based fertilisers (Addiscott, 2005). This span reflects the pre-war level of nitrate input to groundwater and is based on. Span 2, from 1940 to 1955, consists of a 1 kg N ha^{-1} $year^{-1}$ rise in input from 25 kg N ha^{-1} in 1940 to 40 kg N ha^{-1} in 1955. This rise is the result of the gradual intensification of agriculture during and just after WWII (Foster et al., 1982). Span 3, from 1955 to 1975, has a steeper rise, i.e. 1.5 kg N ha^{-1} $year^{-1}$ from 40 kg N ha^{-1} in 1955 to 70 kg N ha^{-1} in 1975, which reflects the increases in the use of synthesized fertilisers to meet the food needs of an expanding population (Addiscott et al., 1991). In span 4 (from 1975 to 1990), there is a constant peak nitrate input value derived using the average value from the study of Lord et al. (1999). Span 5, from 1991 to 2020, has a gradual decline of 1 kg N ha^{-1} year $^{-1}$ from 70 kg N ha^{-1} in 1991 to 40 kg N ha^{-1} in 2020, thereby reflecting restrictions on fertiliser application as a result of the implementation on nitrate sensitive areas (Lord et al., 1999) and nitrate vulnerable zones. This is evidenced by a reduction about 30% in fertiliser use between 1990 and 2000 (ADAS, 2003).Finally, span 6 (from 2020 to 2050) at the end of the modelled input has a constant leaching rate of 40 kg N ha^{-1} assuming a return to nitrate input levels similar to those associated with early intensified farming in the mid-1950s.

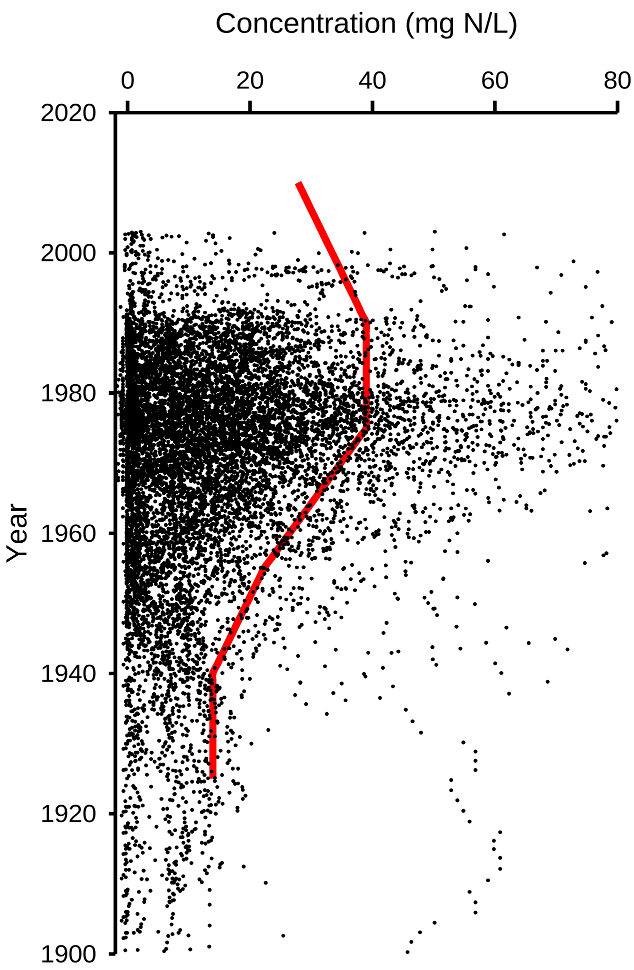

Figure 3.2. Nitrate input function (solid line) derived from literature data. Black dots show temporally corrected porewater nitrate concentrations from ~300 cored boreholes

In the case study of Ascott et al. (2015), the method described in section 3.2.2.2 has been used to prepare the nitrate loadings from agricultural land.

3.1.2.3 Unsaturated Zone

Movement of water, and hence nitrate, through the unsaturated zone is predominantly vertical. Even if at the site- or local-scale there is some lateral movement, because the modelling cell has a resolution of 1 km by 1 km, the assumption of vertical movement is reasonable. The unsaturated zone velocity and the depth to water are assumed to be broadly constant over the modelled period and can be relatively well characterised from current hydrogeological data. The assumption of a constant velocity implicitly requires an assumption that for each unit (1 km^2) cell the unsaturated zone has homogeneous hydrodynamic characteristics, i.e. the velocities used in the model are effective velocities at the modelling resolution.

For each 1 km by 1 km cell, the model requires an effective vertical velocity of nitrate in the unsaturated zone. The new digital 1:625,000 hydrogeological mapping of Great Britain (BGS, 2010) has been used to assign the spatially dependent nitrate velocities. Each of the bedrock formations was attributed with a water movement rate.

For some of the major aquifers, particularly on the Chalk, there are many studies looking at rates of water movement through the unsaturated zone (e.g. Foster and Smith-Carington, 1980; Geake and Foster 1989; Chilton and Foster, 1991; Barraclough et al., 1994). These rates generally agree with values calculated by dividing the effective rainfall by the matrix porosity to obtain the rate of water movement. Table 3.1 shows such rates for the Chalk, Sherwood Sandstone and Lincolnshire Limestone. The rate for the Lincolnshire Limestone is based on a relatively few profiles compared to the Chalk and Sherwood Sandstone. The effective rainfall figures were taken as the mean value from Chilton and Foster (1991) and the porosities from Bloomfield et al. (1995) and Allen et al. (1997). These values were also used for similar rocks, so the Sherwood Sandstone value was used for all the Permo-Triassic sandstones and conglomerates in Great Britain and the Lincolnshire Limestone value was used for all the Great Oolite and other Inferior Oolite rocks.

Table 3.1. Calculated rates of unsaturated water movement for selected major aquifers.

	Porosity (%)	**Effective rainfall (mm/a)**	**Unsaturated zone flow rate (m/a)**
White Chalk Subgroup	33.1	250	0.76
Grey Chalk Subgroup	27.9	250	0.90
Lincolnshire Limestone	18	200	1.11
Sherwood Sandstone	26	275	1.06

This estimate of velocity of travel through the unsaturated zone has been used to validate the nitrate input function derived in the previous section. Nitrate concentration data from the porewaters of almost 300 cored boreholes (Stuart, 2005) have been used to estimate the nitrate in infiltration entering the unsaturated zone during the past 100 years. This has been done by considering the date at which the samples were taken, their depth below ground surface and the estimate of velocity in the unsaturated zone. These are shown on Figure 3.2 as black dots. Their distribution is consistent with the overall modelled input function, with peak applications in the early 1980s.

The groundwater-level dataset has been estimated for each modelling cell (1km by 1km) across Great Britain using the datasets listed below:

- groundwater levels inferred from river base levels
- groundwater levels taken from contours on published hydrogeological maps (generally at 1:100,000 scale) and from other digitised contours
- point measurements from national networks of observation wells and from well inventories

Measurements that characterise confined aquifers are of no value when calculating the thickness of the unsaturated zones. The river-base-level surface is an interpolated surface that assumes that rivers are hydraulically connected to aquifers, and approximate to the water table in the aquifer. The river network used is derived from a gridded Digital Surface Model (NextMap DSM), with drainage densities appropriate to different hydrolithological units. When compared to available point measurements, it shows that the resulting dataset has a realistic water table in permeable unconfined aquifers. It worth noting that, as the Chalk aquifer has some of the largest depths to water table in Great Britain, and contoured observational data are available for this aquifer, the contours were incorporated in the study.

The depth to groundwater, or the depth of the unsaturated zones, was obtained by subtracting the mean groundwater levels from the NextMap DSM mean topographic elevations for each 1km by 1km modelling cell.

In order to avoid unrealistic estimations of groundwater levels in low permeability areas with pronounced topography, the dataset was filtered so that the maximum thickness of the unsaturated zone was constrained to no more than 10 metres in areas underlain by low permeability rocks.

3.1.2.4 Superficial deposits

Since the 1:625 000 hydrogeological map for the UK currently only shows the bedrock, areas where the bedrock is overlain by low permeability superficial deposits are portrayed incorrectly as having a highly productive aquifer at outcrop. In reality, these areas have a low recharge potential and there will not be significant amounts of recharge reaching the bedrock aquifer. In addition, denitrification is likely to occur within such superficial deposits and hence low potential nitrate inputs to the underlying aquifer. These areas have been masked out of the GIS analysis in this study using data from a national map of the recharge potential of the superficial deposits (SNIFFER, 2006; Griffiths, 2010). Areas where both the primary and secondary recharge potentials are low were used to define areas where no nitrate is assumed to reach the underlying aquifers.

3.1.2.5 Representation of attenuation processes

In both case studies, it is assumed that nitrate is conservative in the vadose zone above aquifers. This assumption is supported by studies which suggest that denitrification in the unsaturated zone is likely to be very limited Kinniburgh et al. (1994); Rivett et al. (2007). Field data indicate that vadose zone denitrification results in decreases in concentrations which represent just 1 – 2 % of nitrate input (Rivett et al., 2007). We also assume that nitrate moves through the vadose zone with a constant vertical velocity, no hydrodynamic dispersion and undergoes vertical transport through the matrix when in dual porosity media.

3.1.2.6 Calculating the total mass of nitrate in the unsaturated zones

The total mass of nitrate in the unsaturated zones was derived for each year between 1925 and 2050 using the equation below and aggregated to the national scale by aquifers.

$$N_{VZ} = \frac{\sum_{i=t-TT_{VZ}}^{t} NIF_i}{10^6} \tag{3.1}$$

where N_{VZ} (kt N) is the total nitrate in unsaturated zones for any year, t (years); TT_{VZ} (year) is the nitrate travel time in the unsaturated zones at a given grid cell; and NIF (kg N) is a time-variant nitrate input function. The nitrate storage in the unsaturated zones through time was calculated using the equation below:

$$NIF_t - Nout_t = \Delta N_{VZ} \tag{3.2}$$

where $Nout_t$ is the nitrate flux from the unsaturated zones to the saturated zone and ΔN_{VZ} is the change in unsaturated zones nitrate storage for any year t.

3.1.3 Key results

3.1.3.1 Prediction of the arrival of peak nitrate concentrations at the water table

The distribution of nitrate travel times in the unsaturated zones calculated (ranges between 1 and over 400 years) is shown in Figure 3.3. The results show that nitrate is projected to reach the water table of 88.1% of the areas of Great Britain within 20 years of input. It is predicted to take 1 year for nitrate to reach the water table in roughly 27% of areas and 20 years for 19%.

The areas of selected hydrogeological units which have not yet been affected by predicted peak nitrate concentrations are shown in Table 3.2. This includes significant areas of both major and locally important aquifers. The Cretaceous, Carboniferous, and the Devonian sandstones of Scotland are all strata that have pronounced relief and the model predicts a thick unsaturated zone. The distribution of peak arrival times predicted for the Chalk has a very long tail (Figure 3.4). The peak nitrate concentration in other aquifers with significant intergranular flow, such as the Cretaceous Greensands and karstic aquifers, the Zechstein Group dolomites and the Dinantian limestones, are predicted to have predominantly arrived. The remaining aquifers in Table 3.2 include the important Permo-Triassic sandstones and conglomerates and the Jurassic oolites where the predicted nitrate peak has arrived over the majority of the aquifer. However, the large outcrop area means that over 200 km^2 are projected to be still unaffected. Table 3.2 also gives the estimated mean arrival time for nitrate to the remaining unaffected areas. The average arrival time is predicted to be about 36 years, but some area most notably parts of the Chalk aquifer have > 50 years (Figure 3.5).

Nitrate concentrations calculated at the water table vary spatially due to the spatial variation of the thickness of the unsaturated zones. The average nitrate concentrations at the water table for each hydrogeological unit in different years were also calculated to simplify the concentration results. The results show that water arriving at the water table of poor and minor aquifers could have a higher nitrate concentration than that arriving in major aquifers in 2009, mostly because of the short travel time for nitrate in the unsaturated zones of these poor aquifers. Based on the input function, and unsaturated zone thickness and water velocity, a time series for nitrate concentration arriving at the water table of each aquifer in 1925-2070 was created. Figure 3.6 shows the modelled time series of the average nitrate concentration at the water table of the White Chalk and of the Triassic sandstones and conglomerates up to 2050. The modelled results show that peak nitrate has not yet reached the water table in about 60% of the Chalk, and the average nitrate concentrations reaching the Chalk water table will peak in 2020.

Table 3.2. Areas predicted to be unaffected by peak nitrate input in geological units with unaffected outcrop area of 200 km^2 or more in Great Britain and future arrival time for the remaining N peak

Unit	**Unaffected area (km^2)**	**Total area (km^2)**	**Unaffected (%)**	**Mean arrival time (years)**
White Chalk Subgroup	9695	15817	61.3	42.2
Yoredale Group	2053	5813	35.3	36.3
Millstone Grit Group	1664	4793	34.7	34.7
Pennine and South Wales Lower Coal Measures Formations	1267	3690	34.3	25.8
South Wales Upper Coal Measures Formation	836	1537	54.4	57.7
Permo-Triassic sandstone and conglomerate	708	8956	7.9	16.2
Middle Old Red Sandstone (Scotland)	683	3263	20.9	26.7
Grey Chalk Subgroup	517	1661	31.1	23.8
Ravenscar Group	490	833	58.8	30.1
Lambeth Group	419	1083	38.7	57.9
Arbuthnott-Garvock Group	394	2116	18.6	24.2
Inverclyde Group	369	1816	20.3	23.7
Pennine and South Wales Middle Coal Measures Formations	367	3051	12.0	18.9
Corallian Group	280	830	33.7	29.4
Stratheden Group	268	1329	20.2	23.3
Clackmannan Group	231	1941	11.9	14.6
Great Oolite Group	223	3546	6.3	16.5
Inferior Oolite Group	214	1803	11.9	23.8
Fell Sandstone Group	201	330	60.9	45.7
Strathmore Group	200	1190	16.8	28.7

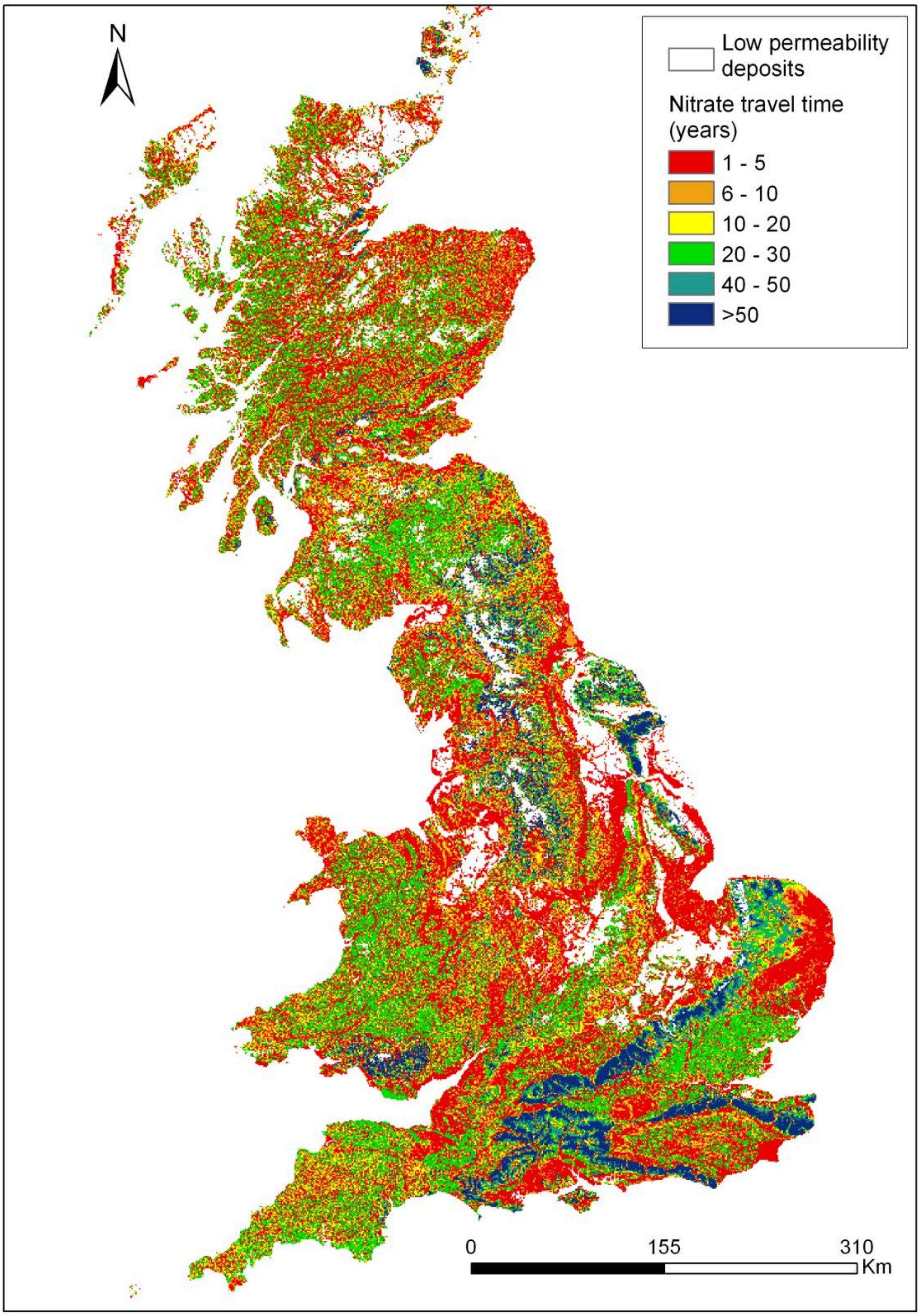

Figure 3.3. The distribution of predicted nitrate travel time in the bedrock unsaturated zone of Great Britain. Low permeability superficial deposits not coloured.

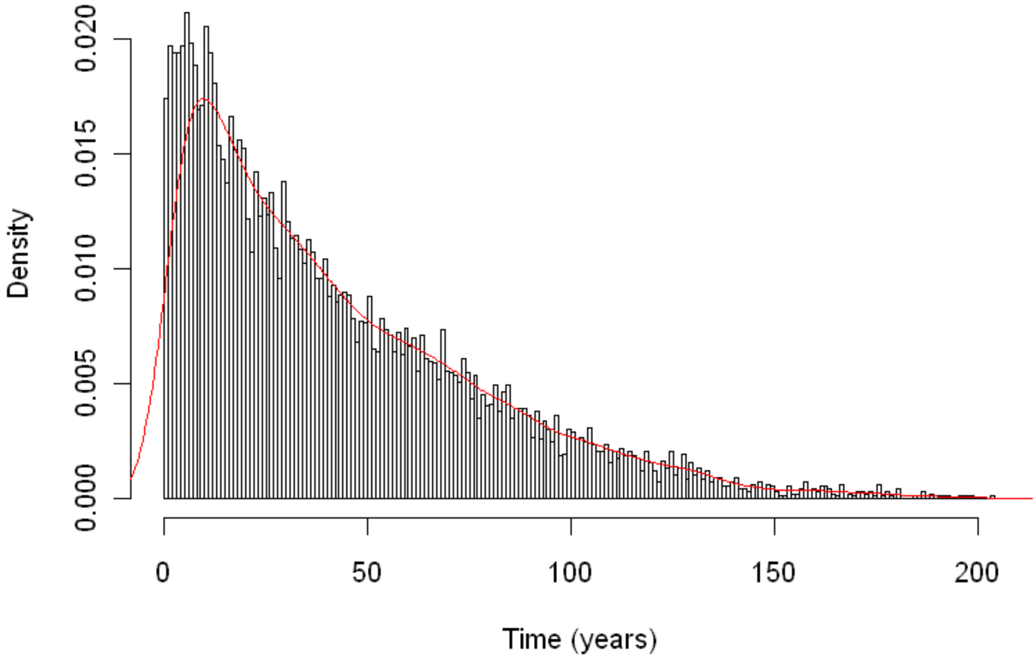

Figure 3.4. Density histogram for the times it takes the input peak to reach the water table in the Chalk

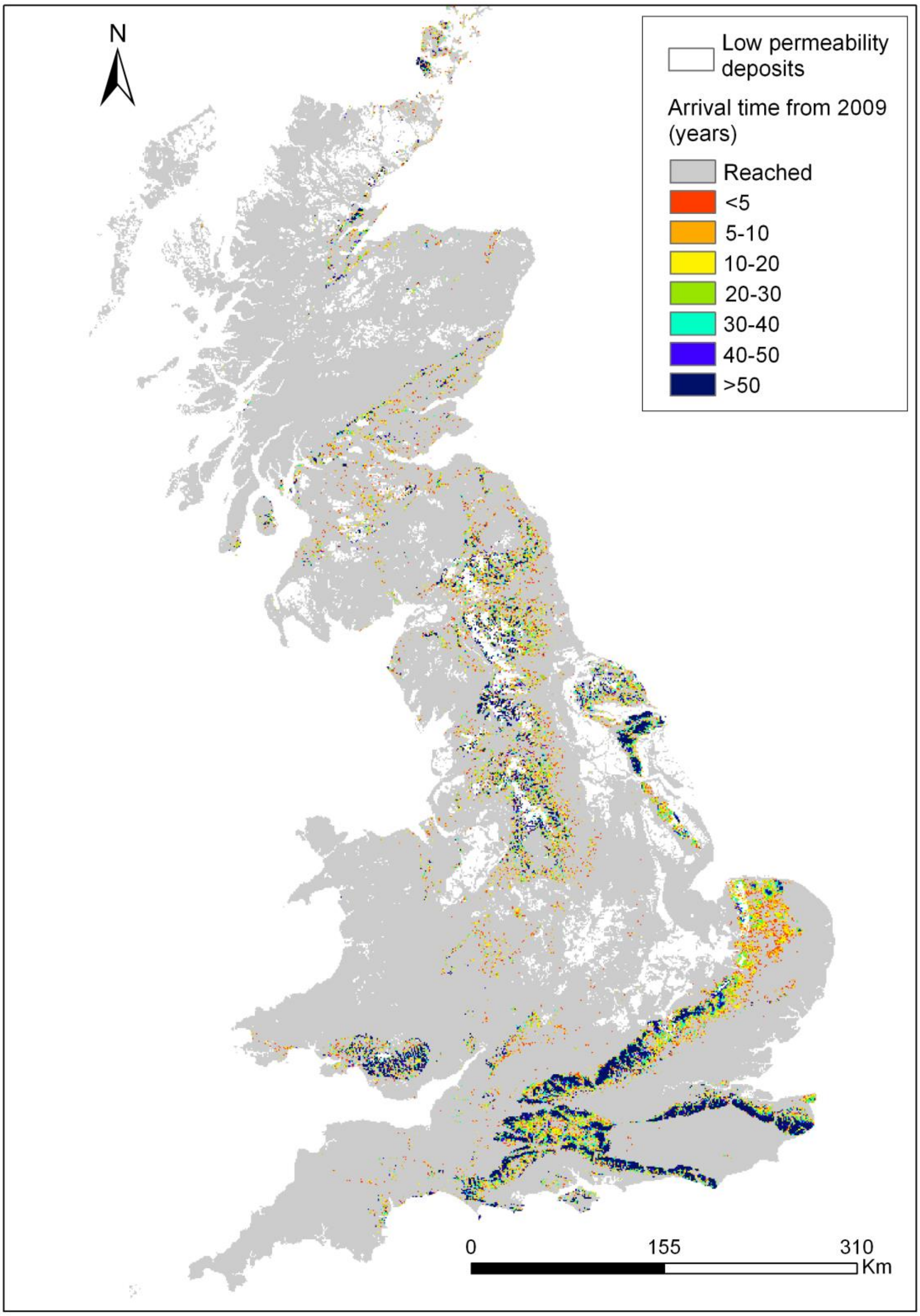

Figure 3.5. Model estimate of how long after 2009 the peak nitrate input will arrive at the water table. Low permeability superficial deposits not coloured.

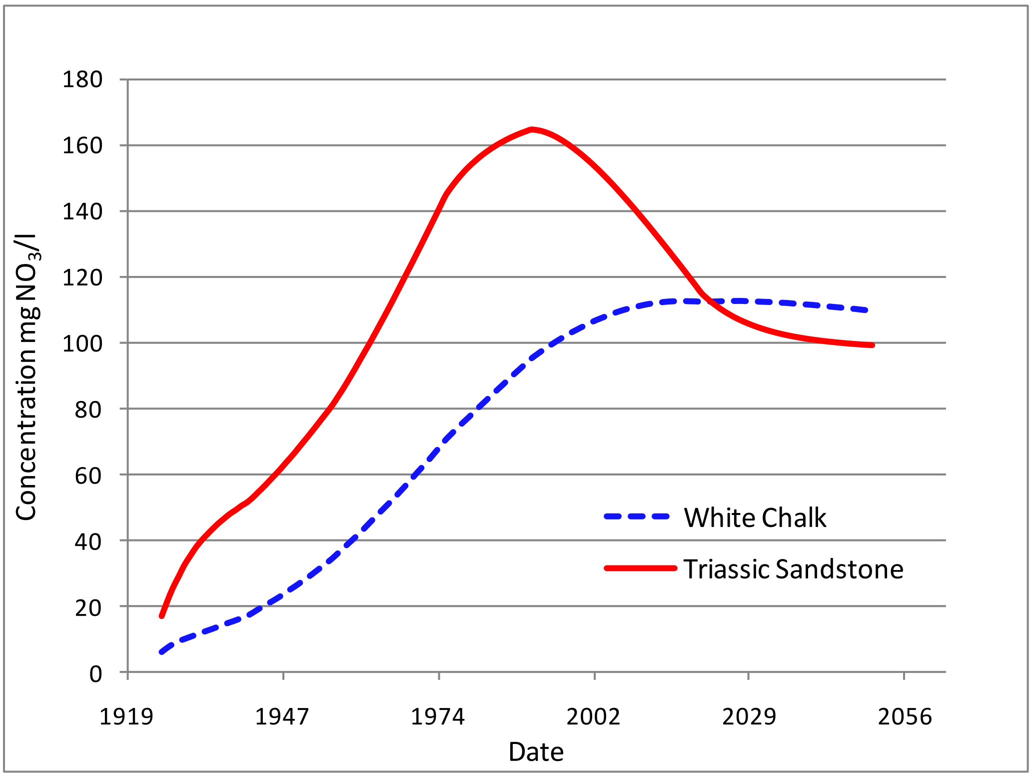

Figure 3.6. Predicted time series of nitrate concentration arriving at the water table of the two major aquifers of Great Britain

3.1.3.2 Unsaturated zones nitrate storage in England and Wales

The total mass of nitrate in the unsaturated zones has increased substantially through time, peaking at approximately 1400 kt N in 2008 (Figure 3.7 (c) and (d)). From 2008 onwards, the mass of nitrate in the unsaturated zones has been decreasing and the unsaturated zone is now a net source of nitrate to groundwater. The temporal change in nitrate storage in the unsaturated zones in 2015 is estimated to be approximately -5 kt N/a, whilst the flux from the unsaturated zones to groundwater was approximately 72 kt N/a in 2015.

The variability in total nitrate mass (Figure 3.7 (c)) is associated with using greater or smaller nitrate inputs as shown in Figure 3.7 (b). Based on sensitivity analysis, nitrate mass peaks of 1700 and 1200 kt N are estimated for the greater and smaller nitrate inputs respectively. Nitrate mass peaks of 1500 and 1300 kt N were estimated using conservative estimates of longer and short unsaturated zones travel times respectively (Figure 3.7 (d), +/- 15%). This also results in the peak nitrate mass occurring earlier (2007) for the shorter travel time distribution and later (2011) for longer travel times. A wider range of unsaturated zone nitrate masses was calculated using a wider range of unsaturated zones travel times based on reported maximum and minimum unsaturated zone velocities (Figure 3.7 (d), + 80%/-60%). The peak mass is reduced to 800 kt N in 1991 by using the -60% travel time. When using the +80% travel time, nitrate mass will be 1750 kt N in 2050 however this is still increasing.

Figure 3.8. shows that the increase in unsaturated zones nitrate storage is dominated by the Chalk, containing an estimated 70% of the total mass in 2015. According to the results, other aquifers also have increases. For example, the Permo-Triassic Sandstones, Oolitic Limestones and numerous other

locally important formations, have 4%, 3% and 23% total mass respectively in 2015. The Chalk, Permo-Trias and Oolites have peak mass years of 2015, 1991 and 1992 respectively.

The Chalk dominates the nitrate-storage increase in unsaturated zones due to its large outcrop area, extensive agricultural land use (87%) and extensive thick unsaturated zone (Wang et al., 2012). Figure 3.9 shows the spatial distribution of nitrate storage estimated in the unsaturated zones in 1960 and 2015. Increases in nitrate storage in the chalk of southern and north east England can be observed. Interfluve areas where unsaturated zones are thick have particularly large nitrate storage increases.

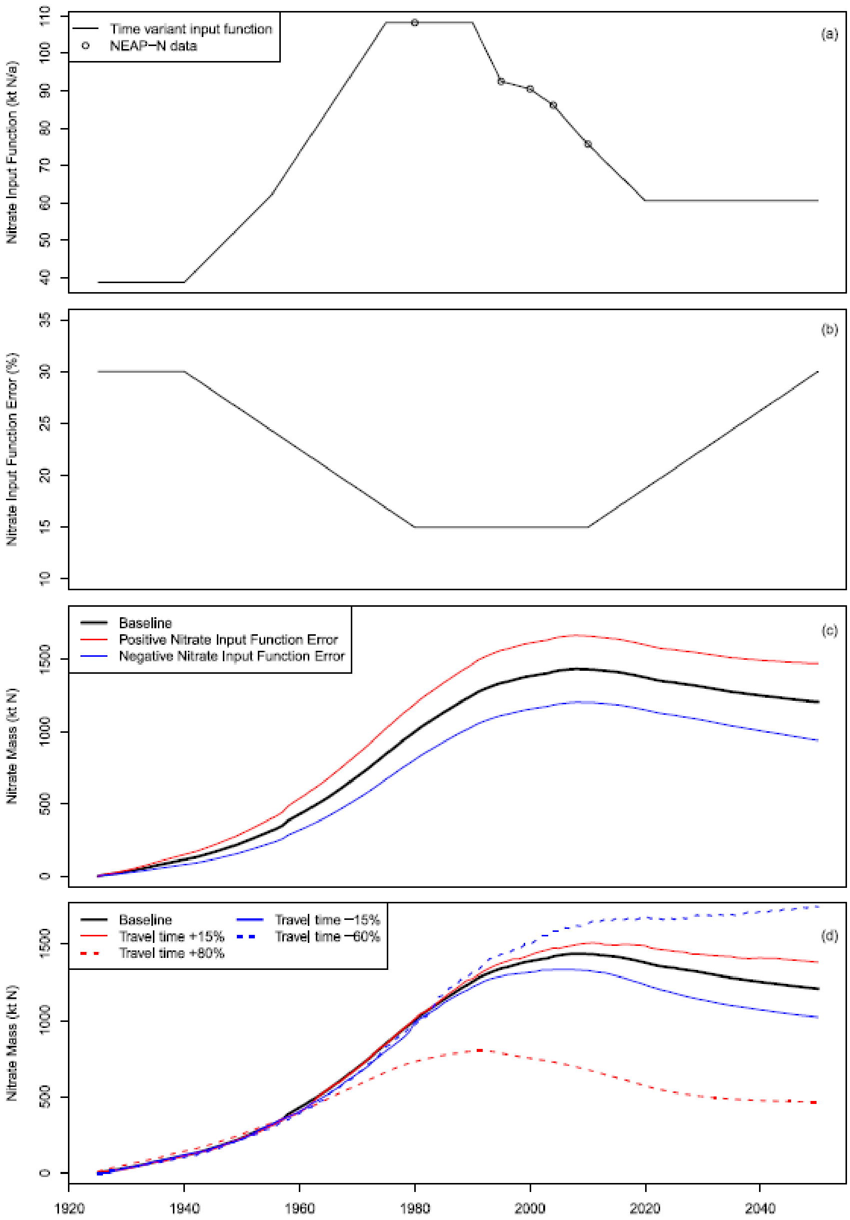

Figure 3.7. (a) Time variant nitrate input function, (b) nitrate input function error, (c) unsaturated zones nitrate mass considering input function uncertainty and (d) unsaturated zone nitrate mass considering travel time uncertainty.

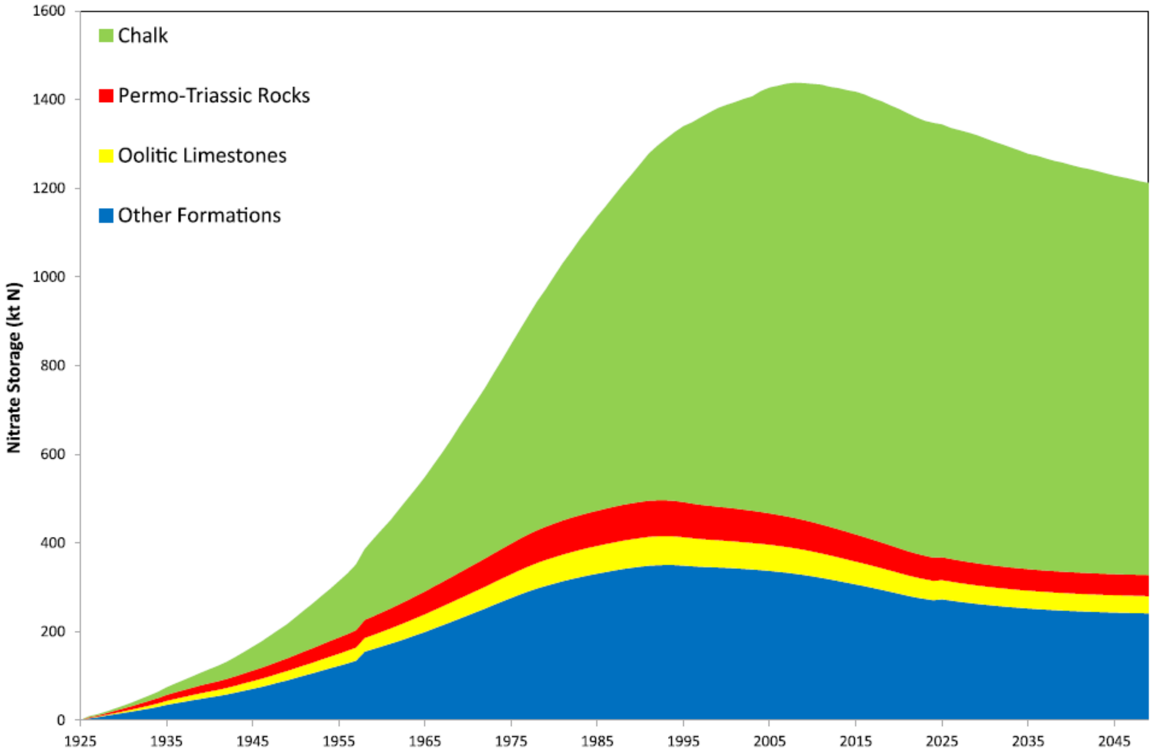

Figure 3.8. Change in unsaturated zone nitrate storage for 1925 – 2050 for moderate and highly productive aquifers.

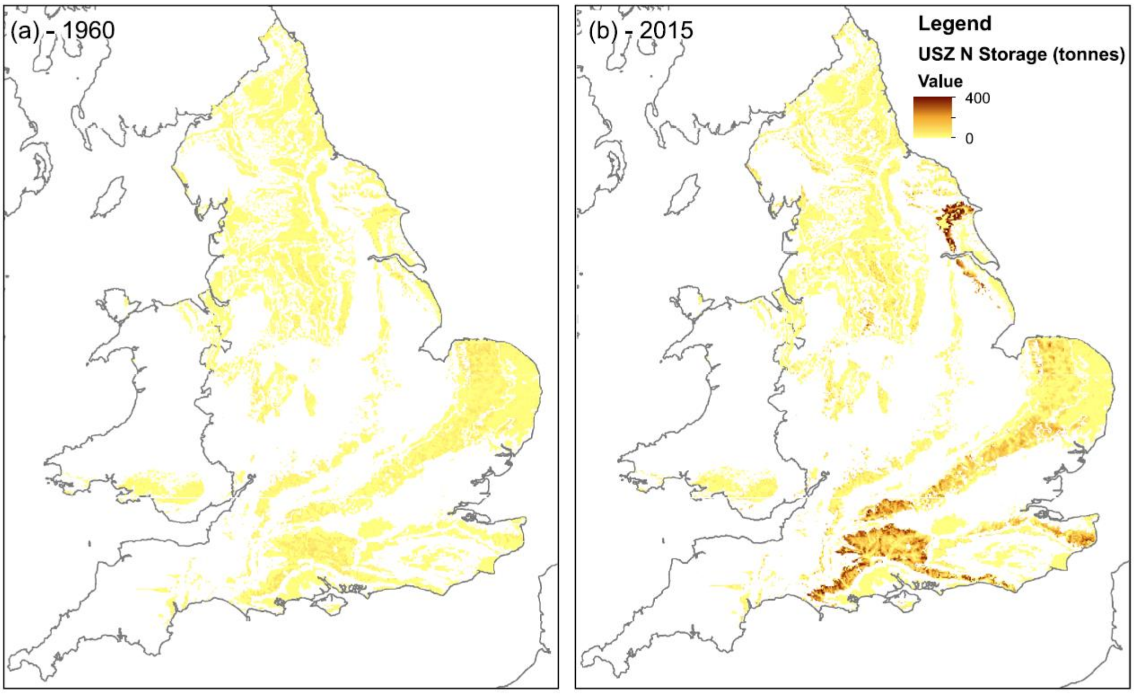

Figure 3.9. Spatial distribution of total vadose zone nitrate mass (as tonnes N per 1 km grid cell) in England and Wales in (a) 1960 and (b) 2015.

3.1.4 Outcomes of modelling

This the first time to estimate the arriving time of the peak nitrate loading at the water table for Great Britain. The results are useful to help policy-makers to better understand the impacts of nitrate time-lag in the groundwater system on water quality when implementing the EU Water Framework Directive. For example, the travel time in the unsaturated zones estimated, in this study have been used by Environment Agency. This first version of NTB model, which has focused on the nitrate transport in the unsaturated zones, has been further developed to simulate the nitrate transport in both unsaturated zones and saturated zones, which is discussed in the following section.

Estimating nitrate storage in the unsaturated zones is a first step in reducing the uncertainty in national scale N budgets. The methodology can assist environmental managers and policymakers in decision making with regards to national and regional scale catchment mitigation measures to improve water quality, in conjunction with groundwater flow modelling. The nitrate storage outputs reported in this chapter have been used by regional managers of the Environment Agency of England to illustrate why meeting timescales for nitrate trend reversal may be challenging in certain areas of the Chalk (Central Southern England, see Figure 3.9(b)). The outputs of this research have also been used as evidence in the UK Government Environmental Audit Committee on nitrate, to show that legacy nitrate remains an issue at the national scale.

3.2 The changing trend in nitrate concentrations in major aquifers across England and Wales from 1925 to 2150

3.2.1 Introduction

Wang et al. (2016) developed an approach to modelling groundwater nitrate at the national scale, to simulate the impacts of historical nitrate loading from agricultural land on the evolution of groundwater nitrate concentrations. An additional process-based component was constructed for the saturated zone of significant aquifers in England and Wales. This work introduced a spatio- temporal nitrate input function. The sensitivity analysis was undertaken using Monte Carlo simulations. Using national nitrate monitoring data, the model was calibrated. The model has been applied at 28 selected aquifer zones in England and Wales and time series of annual average nitrate concentrations along with annual spatially distributed nitrate concentration maps from 1925 to 2150 were generated. The results show that 16 aquifer zones have an increasing trend in nitrate concentration, while average nitrate concentrations in the remaining 12 are declining. The model thus enables the magnitude and timescale of groundwater nitrate response to be taken into account alongside current planning of land-management options for reducing nitrate losses.

3.2.2 Modelling approach

3.2.2.1 Overarching framework

The nitrate time bomb (NTB) model (Wang *et al.*, 2012) has been extended as described in the following sections, to investigate the impacts of historical nitrate loading from arable land on the changing trend in groundwater nitrate concentrations. The improved NTB model code has been developed using C++ and is available for research purpose. The key model stakeholders include researchers, local governments, water companies and geological surveys.

3.2.2.2 Introducing distributed historical and projected nitrate loadings from agricultural land

The single nitrate-input-function (section 3.1.2.2) only represents a national average, rather than a spatially distributed input based on the evolution of agricultural activity across England and Wales. NEAP-N (Anthony *et al.,* 1996; Environment Agency, 2007, Lord and Anthony, 2000; Silgram *et al.,* 2001) is a meta-model of the NITCAT (Lord, 1992) and NCYCLE (Scholefield *et al.,* 1991) models, with adjustments for climate and soil type (Anthony *et al.,* 1996). NEAP-N includes a water-balance model and a leaching algorithm. Using nitrate loss potential coefficients for each crop type, grassland type and livestock categories within the June Agricultural Census data, the model predicts the total annual nitrate loss from agricultural land across England and Wales. For this study, the NEAP-N loss potential coefficients used were revised in 1980, 1995, 2000, 2004 and 2010, corresponding to years with full agricultural census data for farms across England and Wales. This is to account for changes in nutrient applications (fertiliser and manure), crop yields and livestock yields (meat or milk) over time. The predicted NEAP-N nitrogen loadings (1 km by 1 km) for these years were used in this study to derive the spatio-temporal nitrate-input-functions. The trend of historical nitrogen loading in the original single nitrate-input-function of NTB was used to interpolate and extrapolate the data for the years other than the NEAP-N years. This enabled a nitrogen loading map to be calculated for each year from 1920 to 2050. Figure 3.10 shows two examples of the new derived nitrate-input functions for locations in ‘Chalk, Southern England’ and ‘Carboniferous Limestone, South Wales and South West England’.

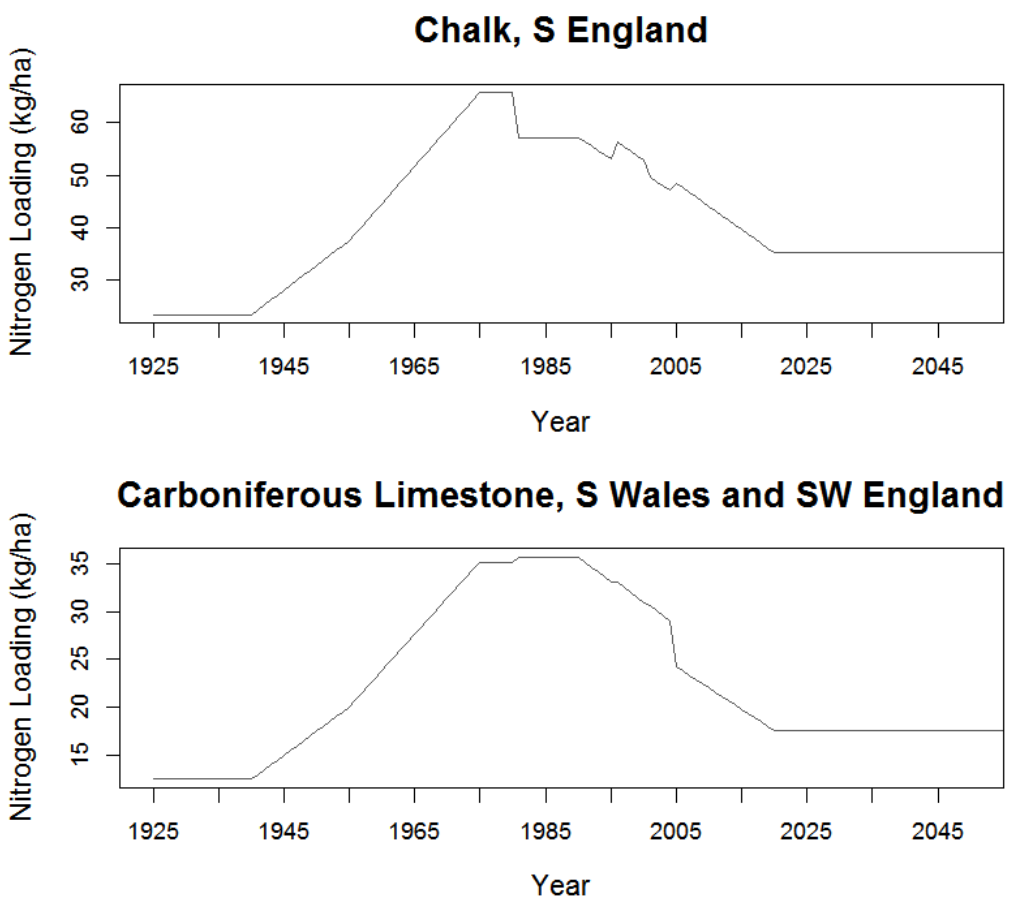

Figure 3.10. Derived nitrate-input-functions at two locations in England and Wales, using a combination of NEAP-N predictions and the single nitrate-input-function.

3.2.2.3 A national-scale conceptual model for nitrate transport and dilution in aquifers

A simplified hydrogeological conceptual model (

- Figure 3.11) was developed to simulate nitrate transport and dilution processes in major aquifers of England and Wales, on the basis of the following assumptions:
- groundwater recharge supplies water to aquifers as an input, and no lateral water flow in USZs were considered in this national-scale study
- groundwater flows out of the system through rivers in the form of baseflow as an output on an annual basis
- groundwater is disconnected from rivers where low permeability superficial deposits are present
- the total volume of groundwater (Vol_{total}) for an aquifer varies from year to year due to the change of groundwater recharge. Vol_{total} in a simulation year is the sum of the groundwater

background volume ($Vol_{background}$) and the annual groundwater recharge reaching the water table ($Vol_{recharge}$). Groundwater recharge and baseflow reach dynamic equilibrium whereby the amount of recharge equals that of baseflow in each of aquifer zone in a simulation year. It is assumed that $Vol_{background}$ remains same in each simulation year

- nitrate entering an aquifer is diluted throughout the total volume of groundwater in a simulation year
- the velocity of nitrate transport in aquifers is a function of aquifer permeability, hydraulic gradient and porosity
- the transport distance for groundwater and nitrate is simplified as the total distance between the location of recharge and nitrate entering the aquifer at the water table and their discharge point on the river network.

3.2.2.4 Nitrate transport velocity in the USZ

The key factors affecting pollutant velocity of transport in USZs include the groundwater recharge rate, aquifer porosity and the storage coefficient are important (Leonard and Knisel, 1988). The nitrate velocity in the USZ and hence the residence time can be expressed as (Rao and Davidson, 1985; Rao and Jessup, 1983):

$$V_{USZ,i} = \frac{q_i}{Sr_{aquifer} \cdot Rf_{aquifer}} \tag{3.3}$$

$$RTime_{USZ,i} = \frac{Thickness_{USZ,i}}{V_{USZ,i}} \tag{3.4}$$

where $Thickness_{USZ,i}$ is the thickness of USZ at cell i (Figure 3.11); $V_{USZ,i}$ (m year^{-1}) is the nitrate-transport velocity in the unsaturated zone; q_i (m year^{-1}) is groundwater recharge at cell i; $Rf_{aquifer}$ (-) is the retardation factor determined in the calibration procedure, and; $Sr_{aquifer}$ (-) is the specific retention for the rock. The specific retention represents how much water remains in the rock after it is drained by gravity, and is the difference between porosity and specific yield.

3.2.2.5 Methods for calculating nitrate concentrations in groundwater

The methods for calculating groundwater available for nitrate dilution, the velocity of nitrate transport in aquifers, and annual nitrate concentration in groundwater can be found in Wang et al. (2016).

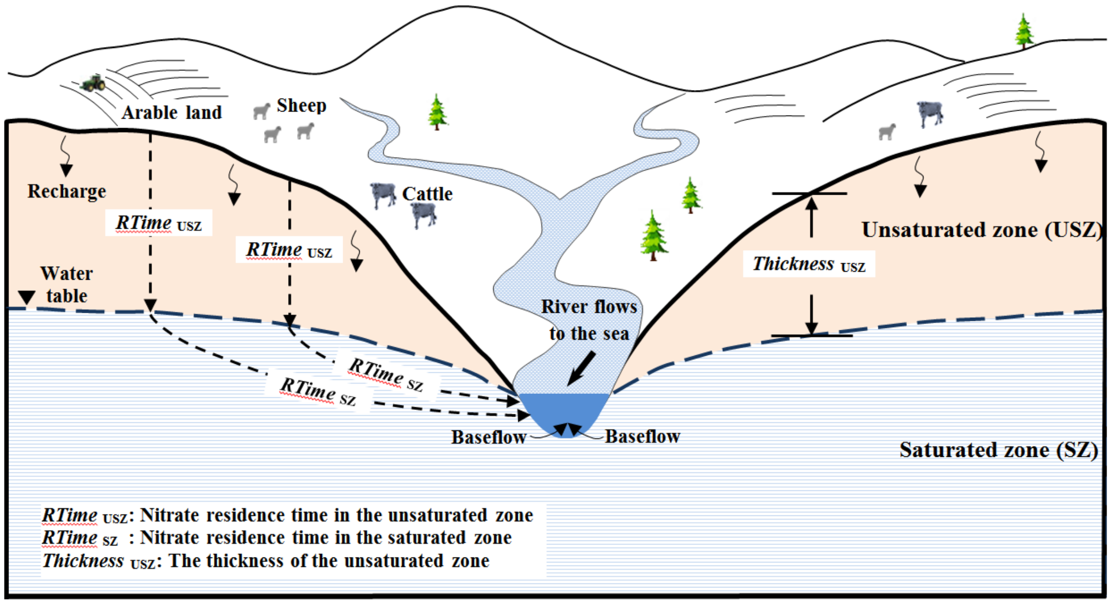

Figure 3.11. The conceptualisation of nitrate transport in the unsaturated and saturated zones.

3.2.2.6 Model construction and data

Twenty-eight important unconfined aquifer zones in England and Wales selected by focusing on those with > 10-year nitrate time-lag in the USZ and a baseflow index (BFI) > 0.4. BFI is the average ratio of annual baseflow to annual river flow in a catchment and represents how well aquifers and rivers are connected. The waters in these aquifer zones (Figure 3.12) are, therefore, those more likely to be affected by historical nitrate loading in the longer term than other areas. The digital 1: 250 000 hydrogeological mapping of Great Britain from the BGS (2015) and the hydrology of soil types (HOST) classification scheme (Boorman *et al.,* 1995) were used as the basis for identifying these key aquifer zones. The subdivision of large aquifers, such as the Chalk, into a series of areas reflects the scale at which published data on aquifer properties are available in Allen *et al.* (1997). The different aquifers are normally separated by aquitards and generally different zones of a specific aquifer are geographically separated. The study areas were discretised into 1 km by 1 km cells.

Cross-correlation has been used to reveal the significance of the water-table response to rainfall after a given time (Lee *et al.,* 2006), using the time series of monthly rainfall (1961 – 2011), from the Meteorological Office Rainfall and Evaporation Calculation System (MORECS) and groundwater level for 57 boreholes across the study area. The water-table response time Rp_q to rainfall events was calculated by setting to the period of time over which there is a correlation between groundwater level and rainfall at more than 95% confidence level.

A national-scale groundwater recharge model was built using the soil water balance model SLiM , which objectively estimates recharge and runoff using information on rainfall intensity, potential evapotranspiration, topography, soil type, crop type, and *BFI*. The model was calibrated using the observed river-flow data for 102 gauging stations (http://www.ceh.ac.uk/data/nrfa/). The long-term-average and time-variant recharge estimates were then used to simulate nitrate-transport velocity in the USZ and the groundwater volume $Vol_{total}(t)$, respectively.

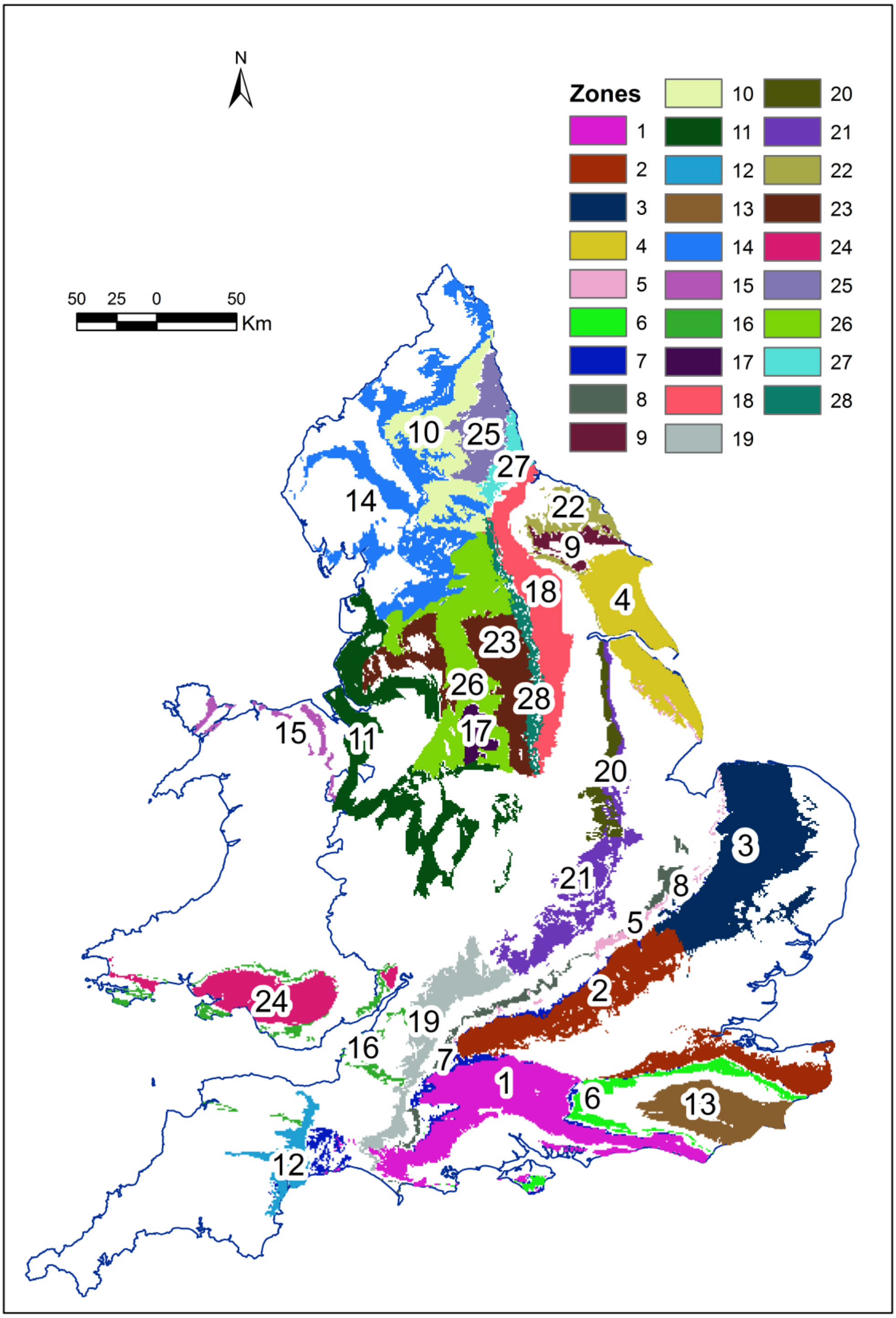

Figure 3.12. Aquifer zones identified in England and Wales

3.2.2.7 Model calibration and validation

Monte Carlo (MC) simulations were undertaken to calibrate the revised model. Please see more details in Wang et al. (2016). All parameters used in this study are summarised in Table 3.3. The fixed parameters were identified based on existing datasets and hydrogeological knowledge from hydrogeologists.

Table 3.3. Summary of parameters used in this case study

Fixed / Monte Carlo calibration	Parameter (units)	Description
Fixed	A_i (m^2)	The area for cell i
	q_i (m year^{-1})	The recharge value for cell i
	The nitrate-input-functions (kg/ha)	-
	Rp_q (year)	The water-table response time to recharge events
	GWL_i (m)	The groundwater level for cell i
	RL_i (m)	The river level for cell i
	ATT (-)	the nitrate attenuation factor in the USZ
	$Thickness_{USZ,i}$	The thickness of USZ at cell i
Monte Carlo Calibration	$\Phi_{aquifer}$ (-)	The porosity for an aquifer zone
	$Sy_{aquifer}$ (-)	The specific yield for an aquifer zone
	$Rf_{aquifer}$ (-)	The retardation factor for calculating the nitrate velocity in USZs
	$T_{aquifer}$ (m^2 day^{-1})	The transmissivity for an aquifer zone
	$D_{aquifer}$ (m)	Depth of active groundwater for an aquifer zone

Two sets of MC simulations were conducted to calibrate the model against:

1) the nitrate velocity values in USZ derived from measurements of porewaters from cores from bored boreholes (Wang et al., 2012), and;
2) the observed average nitrate concentrations for each aquifer zone calculated from monitoring data provided by the Environment Agency.

In the former, the bias (absolute difference) between simulated and observed nitrate velocity in USZs was used to evaluate the model fit. In the latter, the Nash-Sutcliffe efficiency (NSE) was adopted to calculate the goodness-of-fit between observed and modelled nitrate concentrations.

3.2.3 Key results

3.2.3.1 Estimates of nitrate concentration

Based on the calibrated model for the period 1925 to 2150, the annual nitrate concentrations for the 28 selected aquifer zones in England and Wales were simulated using spatially distributed recharge values for 1961 to 2011. Outside this period, the long-term average recharge value (1961 – 2011) was used. Figure 3.13 shows some examples of the modelled time series, which had well defined trends in the observed data. The nitrate concentration in the 'Chalk of southern England' is estimated to have reached its peak value of 35 mg NO_3 L^{-1} in the year 2014. The average nitrate concentration in the 'Thames Chalk' keeps rising until the peak value of 53 mg NO_3 L^{-1} is reached in the year 2036. A declining nitrate-concentration trend was found in 'Chalk, Southern England', 'Lower Greensand, Weald', 'Permo-Triassic Sandstone, Lancashire to West Midlands', 'Permo-Triassic Sandstone, South West England', 'Carboniferous Limestone, South Wales and South West England', 'Permo-Triassic Sandstone, Nottingham to North Yorkshire', 'Middle Jurassic limestone, Cotswolds to Dorset', 'Inferior Oolite, Lincolnshire', 'Middle Jurassic limestones (excluding Inferior Oolite, Lincolnshire), Lincolnshire to Oxfordshire', 'Middle Jurassic, Yorkshire', 'Coal Measures, Durham and Northumberland' and 'Millstone Grit, South Pennines'. The remaining 16 aquifer zones have an increasing trend in nitrate concentration. Annual distributed nitrate concentration maps from 1925 to 2150 were also generated and Figure 3.14, Figure 3.15 and Figure 3.16 show example results for 2000, 2015 and 2020 respectively.

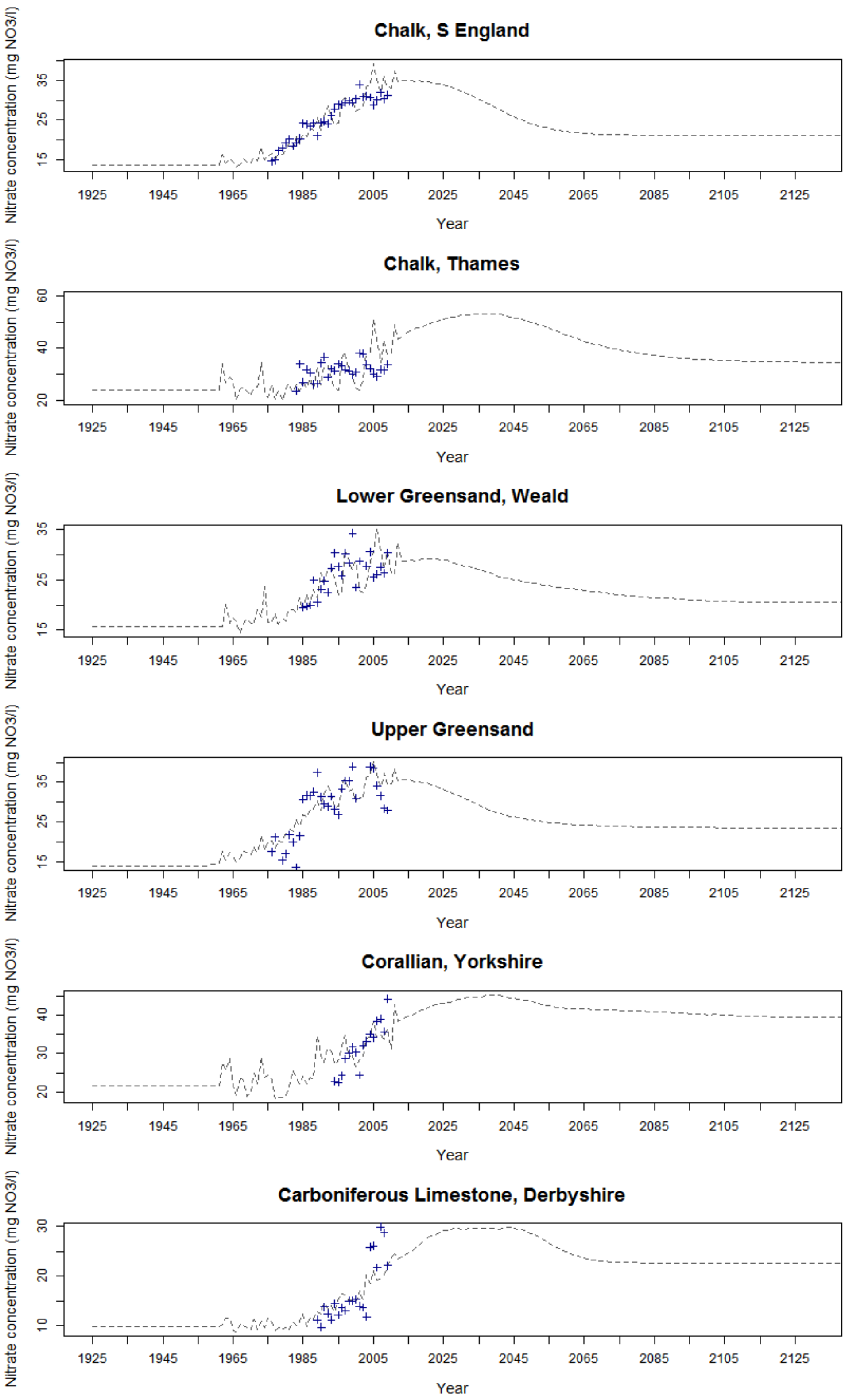

Figure 3.13. Time series of modelled and observed nitrate concentrations for example aquifer zones. The dashed lines are the modelled annual nitrate concentrations and the crosses are the observed values.

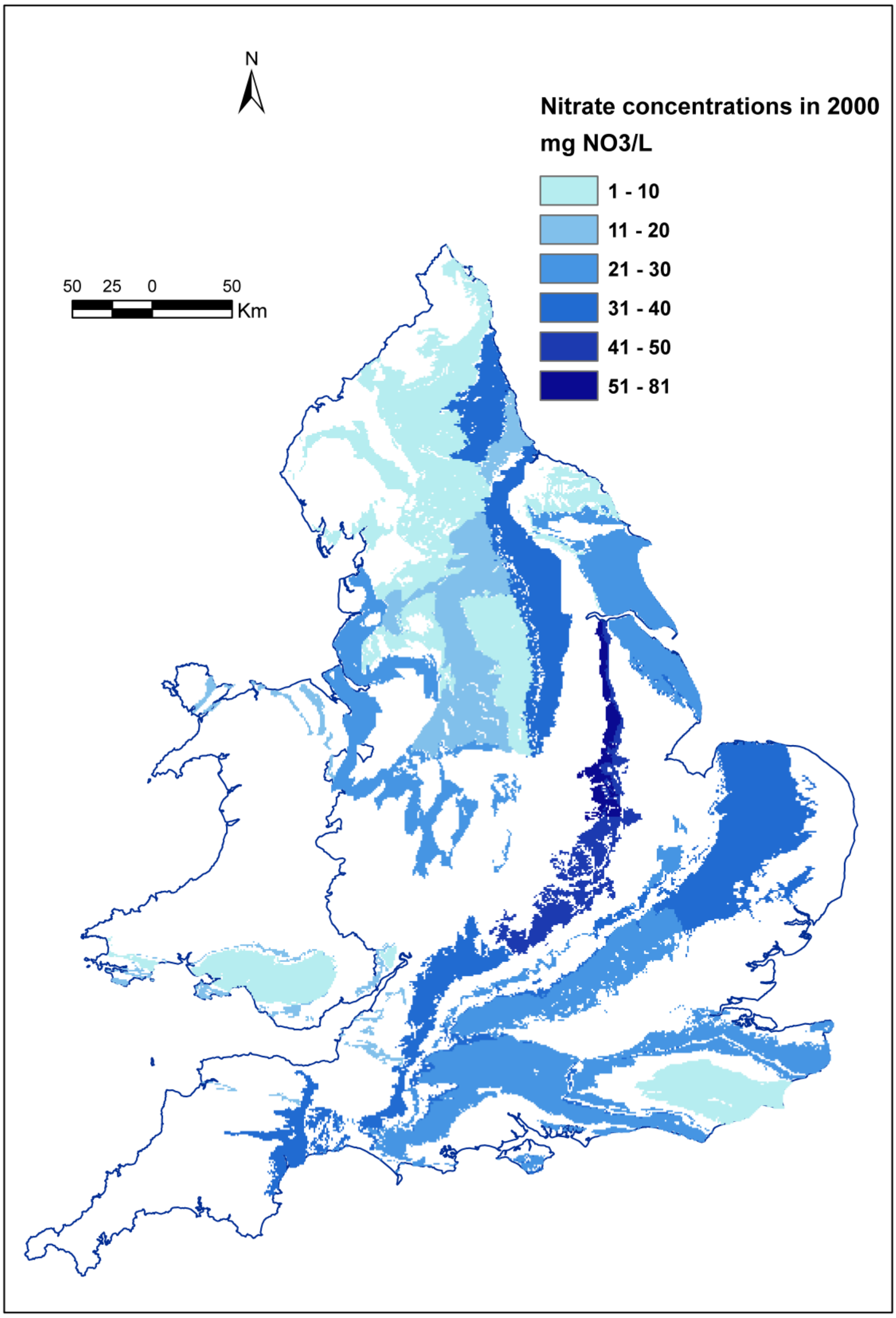

Figure 3.14. The estimated spatially distributed nitrate concentrations in the major aquifers of England and Wales in 2000.

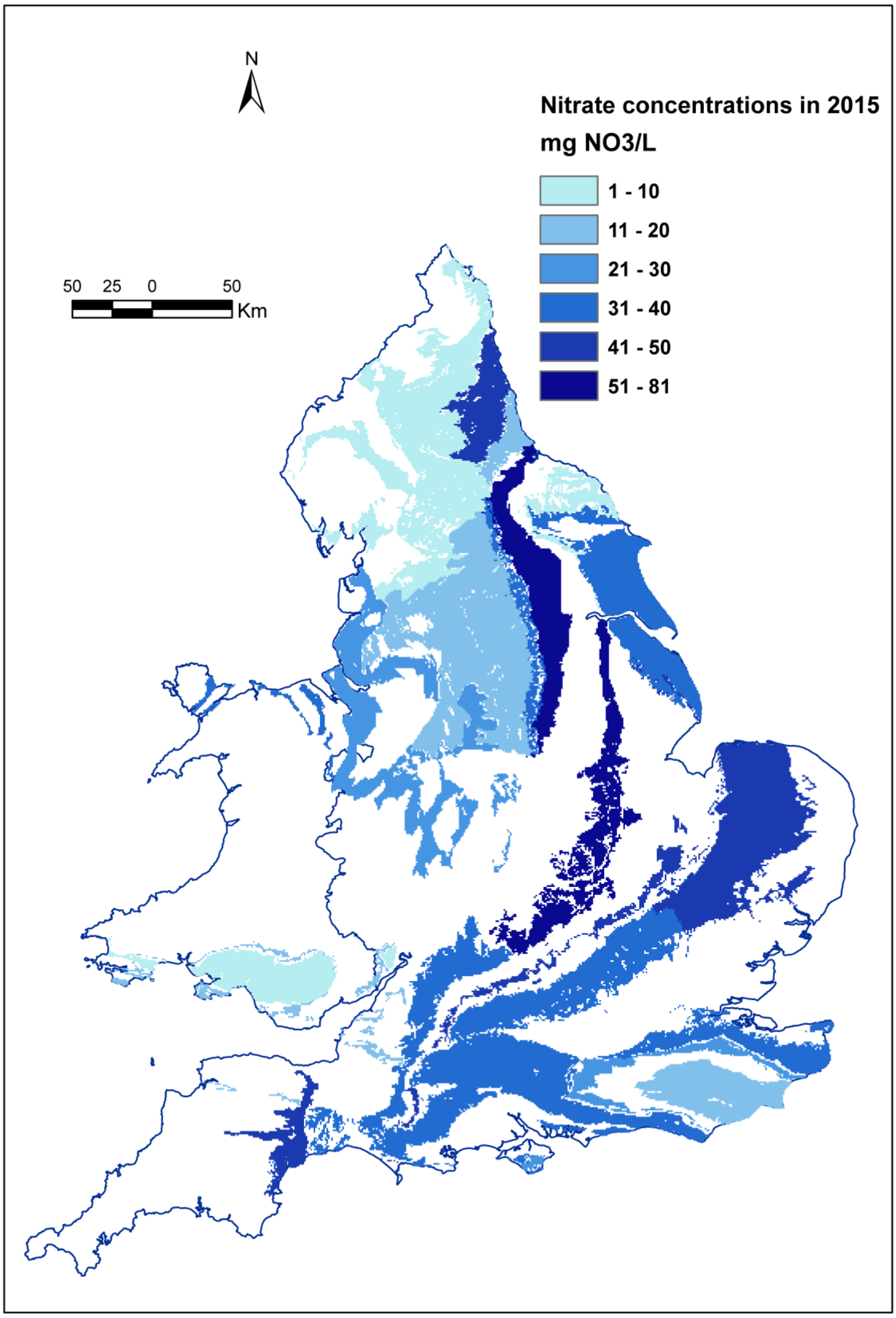

Figure 3.15. The estimated spatially distributed nitrate concentrations in the major aquifers of England and Wales in 2015.

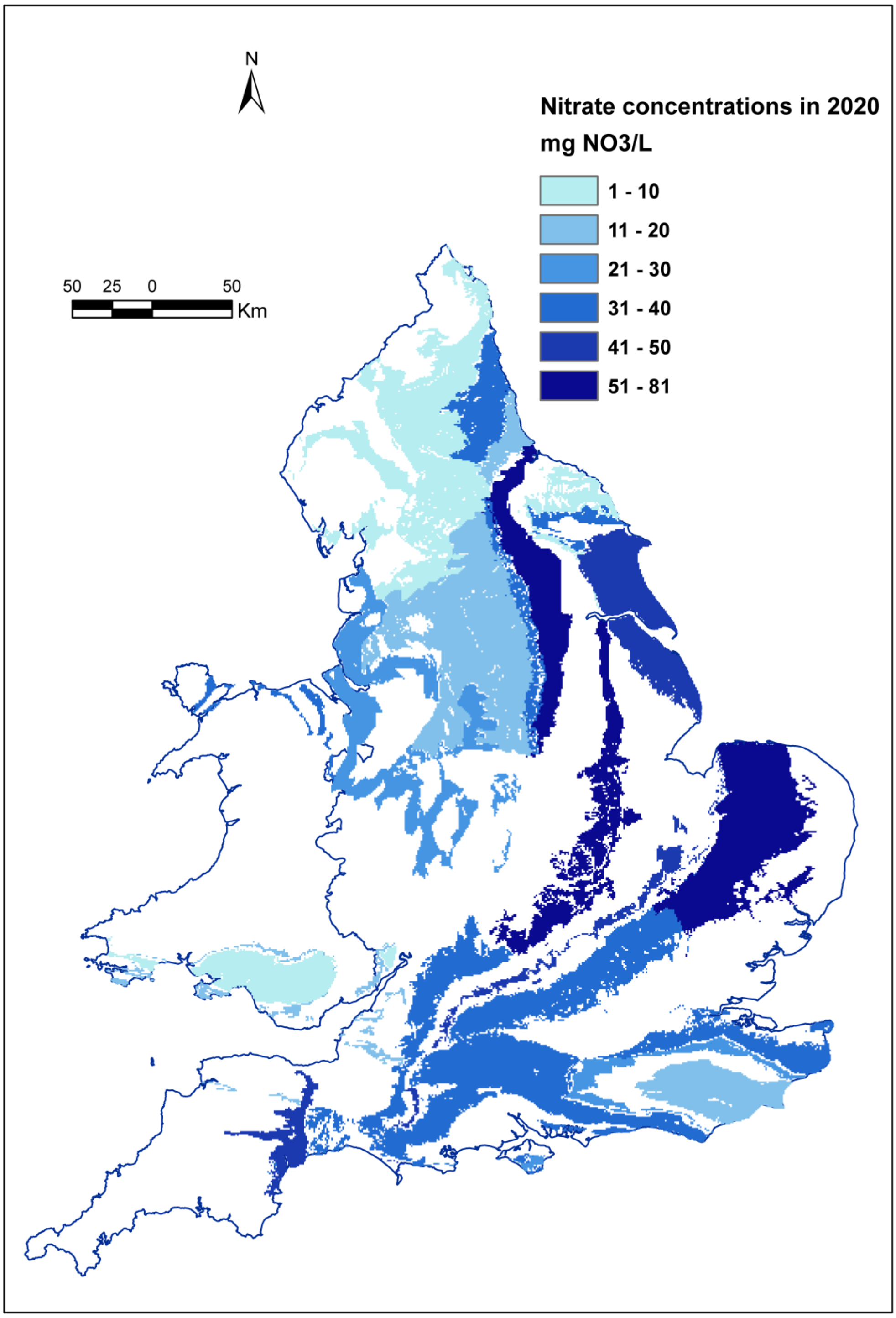

Figure 3.16. The projected spatially distributed nitrate concentrations in the major aquifers of England and Wales in 2020.

3.2.4 Outcomes of modelling

Groundwater is essential for maintaining the flow of many rivers in the form of baseflow. Therefore, the results in this case study can be used to study the impacts of the long-term groundwater nitrate concentration change on river quality, especially for rivers connected with high permeability aquifers. Since the aquifer zones selected in this study have baseflow index values of > 0.4, the nitrate held up in the groundwater system can greatly affect surface water quality where rivers are connected to these aquifers, and hence the ecological quality. On this basis, some of the outputs described herein have been incorporated into ongoing updates to the SEPARATE (SEctor Pollutant AppoRtionment for the AquaTic Environment) screening tool for England and Wales (see Zhang *et al.,* 2014 for version 1.0).

The Environment Agency in England and BGS have worked together to explore the possibility of incorporating the NTB model into the designation of nitrate vulnerable zones for England and Wales.

4 FRANCE

Laurence Gourcy, Stéphanie Pinson, Eline Malcuit, Nicolas Surdyk
BRGM, France

4.1 Introduction

For the territory of metropolitan France, two recent studies exist at the national level to assess and characterize the pressure-impact of nitrate and pesticide use:

- For nitrate: Gourcy et al, 2017 ;
- For pesticide: Auterives and Baran, 2017.

This work was complex to achieve as there is no geological and hydrogeological and agro-pedo-climatic homogeneity on the French metropolitan territory.

This chapter describes how to calculated nitrate transfer speed and estimated nitrate pressure. The nitrate pressure is an estimation of nitrogen load (in kg of N/ha) on the unsaturated zone.

4.2 Modelling approach

4.2.1 Overarching framework

Within the water framework directive the assessment of the impact on groundwater of the pressure from nitrate from agriculture origin is requested.

The principle of this modeling is to cross an input nitrate function with a delay function using GIS tools. The input function depends on the agricultural zone and the delay function depends on the hydrogeological zone characteristics. French department (Nuts3 scale) were select as a scale for work for the agricultural input function. A specific scale for work was developed for the hydrogeological zone since the current scale (the “water bodies”) is, in many cases, too large for a detailed analysis. In this study, the scale for work was developed by crossing different sources of spatial hydrogeological information using GIS tools. The spatial unit obtained is call “reference unit”.

The first step was the development of a national approach for the calculation of the nitrate pressure from agricultural sources on the unsaturated zone. A method based on the N Budget developed at the University of Tours was used (Poivert et al, 2017).

A delay function considering the transfer time in the unsaturated zone was calculated for the different lithologies where transfer time through the unsaturated zone was taken into account. To calculate the delay function, the thickness of each specific hydrogeological zone was combined with the nitrate transfer velocity in the dominant lithology of each specific hydrogeological zone.

The different information layers were combined to obtain an average transfer time for nitrate for each hydrogeological zone throughout metropolitan France. The spatial distribution of the nitrate recharge ages was calculated in order to relate the today’s impact to the original impact pressure.

The proposed approach gave an homogeneous national view of the pressure / impact approach for nitrate and highlighted the sectors where today’s pressure may lead to a degradation of groundwater quality and that will need local studies for the Water Manager to propose adequate program of measures (environmental and agricultural action plans).

4.2.2 Source term (i.e. flux from the base of the soil zone to the unsaturated zone)

Diffuse N pressure originating from agricultural systems can be found in Poivert et al (2017). Nitrogen surpluses were determined using a soil surface balance method (Oenema et al. 2003). The Surplus could be calculated such as

$$Surplus = N_{min} + N_{org} - N_Y + N_A + N_s \tag{4.1}$$

where N_{min}, N_{org}, N_Y, N_A and N_s refer to the N input form mineral fertiliser, N input form mineral organic fertilizer, N removed via crop yield, atmospheric N deposition, and symbiotic fixation respectively. The unit is kg N/ha/yr. Surplus refers to the N excesses (or deficit) at the spatial scale for work.

Soil surface balance was calculating by using statistical data available at the NUTS3 level (a spatial resolution, corresponding to the French departments). For each department, the soil surface balance quantifies N input such as manure and chemical fertilizers, atmospheric deposition and symbiotic fixation, and N output represented by harvested crops, including fruit, vegetables and grazing.
Agronomic information originated from two sources: the agronomical annual statistics of the SSP (Service de la Statistique et de la Prospective) and UNIFA (Union des Industries de la Fertilisation).
The SSP database provides yearly data for livestock numbers, crop yields (cash crop, fruit and vegetable) and agricultural areas for each department. Data for chemical fertilizers were obtained from the amounts delivered in each department, which were assumed to be equivalent to the quantity used in the same department.

Data for atmospheric N deposition were taken from the EMEP database (http://www.emep.int/mscw/index_mscw.html), which provided a 50 km × 50 km model of dry and humid N deposition.

Data for Symbiotic nitrogen fixation were taken from previous work already published (Anglade et al., 2016).

The annual pressure data calculated by the balance method was not used directly to represent the pressure transferring to the groundwater. A 5-year running average was used. The use of an average is justified by the fact that the sudden variations are linked to surface phenomena (good yields, increases in the price of fertilizers) which have a direct impact on soil concentrations but are buffered few meters below.

4.2.3 Unsaturated zone

Several methods can be used to estimate the time of arrival of nitrate at the saturated zone of aquifers. Two methods have been tested in France (Gourcy et al., 2017). This first tested method was initially developed for pesticides as described by Rao et al. (1985). The method is based on the "piston" model, taking into account a real recharge coupled with delaying factor. Yet, the results from this methods were discarded because there were different from experimental results.

Estimated the velocity of nitrate transfer in the unsaturated zone in this national study come essentially from experimental data found in published articles and from analyses of nitrate concentration profiles or from existing hydrogeological models. The data were collected according to the aquifer lithology and climate. Data collected in the literature for the French regions is presented in the table below (Table 4.1).

Table 4.1. Table of estimation data of velocity of nitrate transfer (in m/year) in unsaturated zone according to lithological contexts and French regions from the literature (according to Gourcy et al., 2017).

French regions	Lithology Chalk	Lœss	Silts	Altered area of granites / arenites	Old alluvial and glaciofluvial	Flint clay	**Bibliographic references**
Artois - Picardie	0.54 – 1.45		0.4 - 0.5				Surdyk et al., 2014 and 2016 ; Serhal et al., 2006 ; Serhal, 2006 ; Caous et al., 1984 .
Somme	0.5 - 0.7						Normand et al., 1999.
Alsace		0.2 - 0.3					Baran et al., 2005
Champagne - Ardenne	0.27 – 0.7						Kerbaul et al., 1979 ; Baran and Chabart, 2006 ; Landreau and Morisot, 1983 ; Ballif and Muller, 1983 : Seguin, 1986 ; Crampon et al., 1993 ; Philiipe, 2011.
Nord	1.25						Lacherez-Bastin, 2005
Nord-Pas-de Calais	0.5 - 1.95						Baillon et al., 2001
Bretagne				2 - 3			Limousin, 2007 ; Legout et al., 2007 ; Molenat et al., 2013
Normandie	0.35 - 0.64 to 2.5 (karst)						Arnaud et al., 2009 ; Crampon et al., 1993 ; Jauffret et al., 1984
Rhône-Alpes					4.7 - 6.5		Rousseau et al., 2016
Touraine	0.45					0.75	Landreau and Morisot, 1983.

The data from all the bibliographic source were combined to obtain a transfer velocity by lithology. Table 4.2 summarizes the transfer velocities used for each type of lithology. Even if there more lithology in France, only those presented below were more deeply analysed in the project because 1) enough data were available 2) concept of vertical flow modelling was applicable.

Table 4.2. Nitrate transfer velocity (in m/year) used for modelling vertical flow of nitrate transfer

Lithology	Transfer velocity (m/year) – field measurements
Limestone	1.5
Chalk	0.45 to 1.25
Sands	3
Sandstone	1.8
Regolith / granite	2.5

By combining the thickness of the unsaturated zone and the estimated nitrate transfer velocity (Table 4.2), a transfer time is obtained. For instance, if the nitrate transfer velocity is estimated around 1.25 m/year (typical case in chalk) and if the unsaturated zone is 10 m thick (several tens of meters is common in Paris Basin), the calculated transfer time is 12.5 years. The transfer time was obtained for 1613 units out of the 3631 covering the whole metropolitan territory.

The results of this calculation is a transfer time (in year) map (Figure 4.1). These transfer times only concern transport through the matrix and therefore neglects a transfer through crack / fractures which is faster.

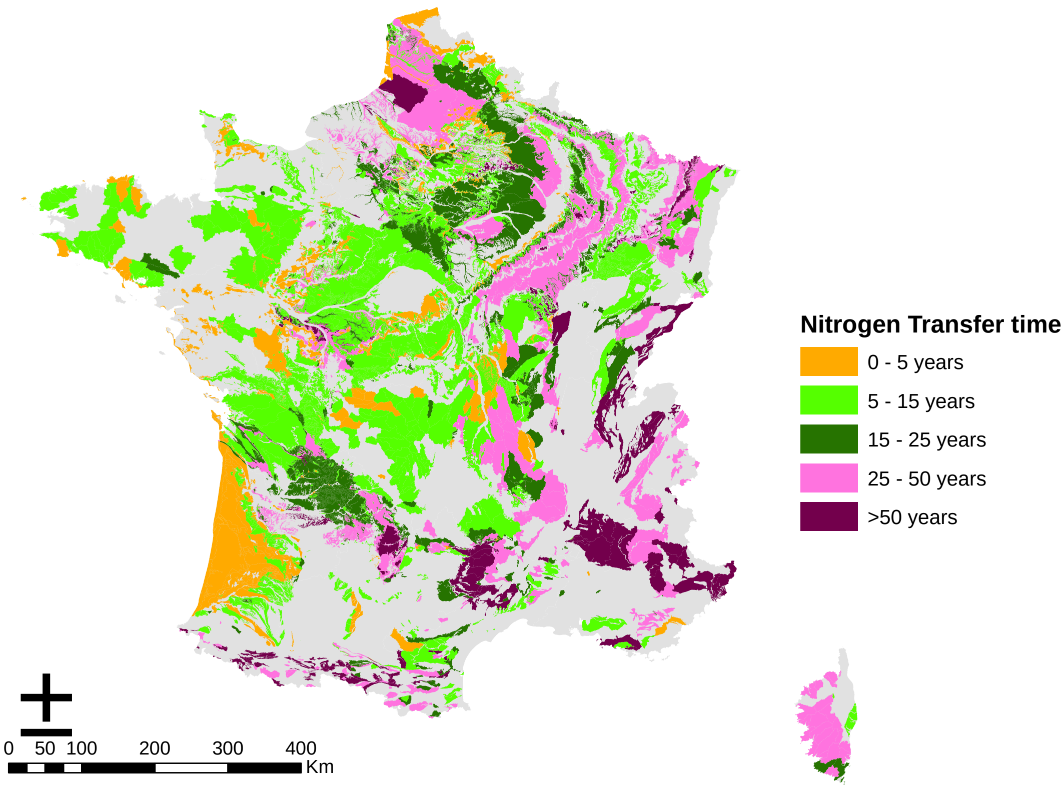

Figure 4.1. Nitrate transfer time (years) taking into account only the matrix porosity per “reference unit” (from Gourcy et al., 2017)

A year of reference was taken in order to recalculate the initial period of "pressure" for groundwater. The figure (Figure 4.2) presents the results for the year 2015 as the reference year. From the reference year and depending on the transfer time calculated for each “reference unit”, a simple subtraction was made to go back to the “year of NO_3 in the USZ”. The “year of NO3 in the USZ “could be defined as the approximated year of pressure causing nitrate concentrations in groundwater in 2015. Since the exact year is not known, an approximation is taken into account by gathering “year of NO3 in the USZ” into categories of roughly a decade.

On this map, the territory is divided into three zones: recent years for a large western half, the northeast quarter corresponds to intermediate years and the southeast quarter and the Pyrenees to older years

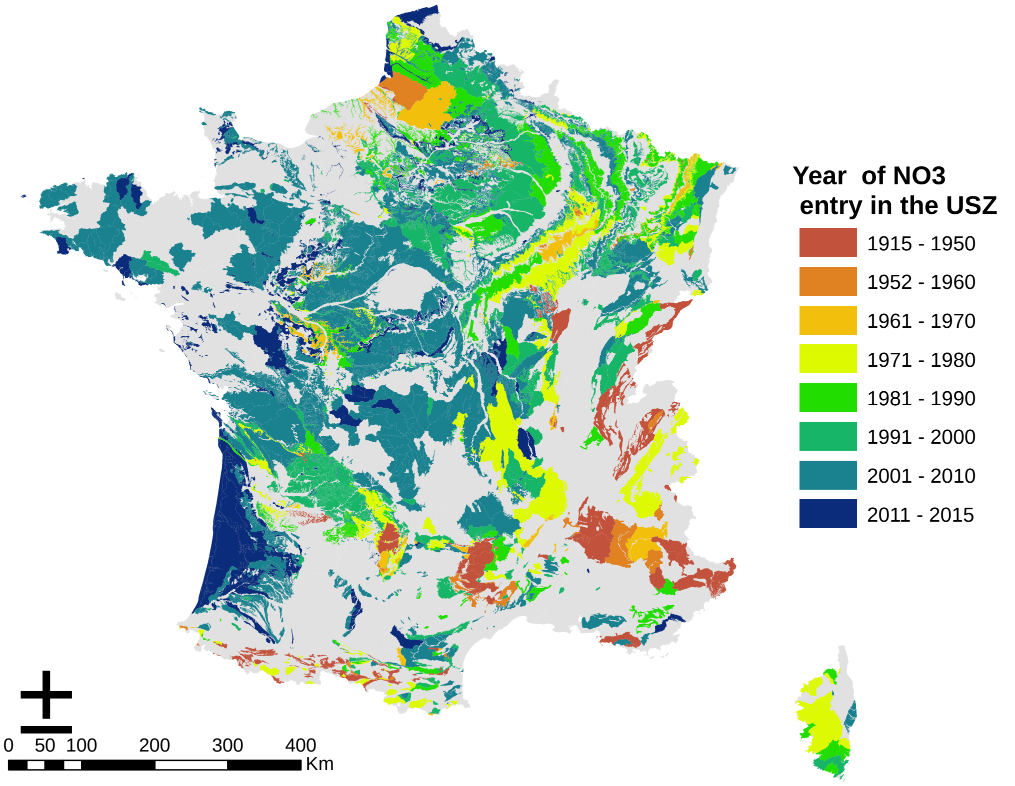

Figure 4.2. Map of “Year of NO_3 entry in the USZ” - Approximated year of pressure causing nitrate concentrations in groundwater in 2015

The pressure data calculated in paragraph 4.2.2 (as to say the Nitrogen Surplus) were crossed with the “Year of NO3 entry in the USZ” (Figure 4.2) to estimate the expected pressure on groundwater in 2015. A 5-year running average was used to calculate the expected pressure per reference nitrate concentration in 2015 (see 4.2.2). This expected pressure is called raw pressure.

The raw pressure was supposed to be the same than the surplus of the year of NO3 entry in the USZ. For instance, in the Ain department in South of France, the calculated transfer time was 9 years (USZ 11 m; transfer time 1,25 m/y). The year of NO3 entry in the USZ is 2006 (2015-9 years). The raw pressure in this reference unit is 44.1 Kg N/hal (Figure 4.3).

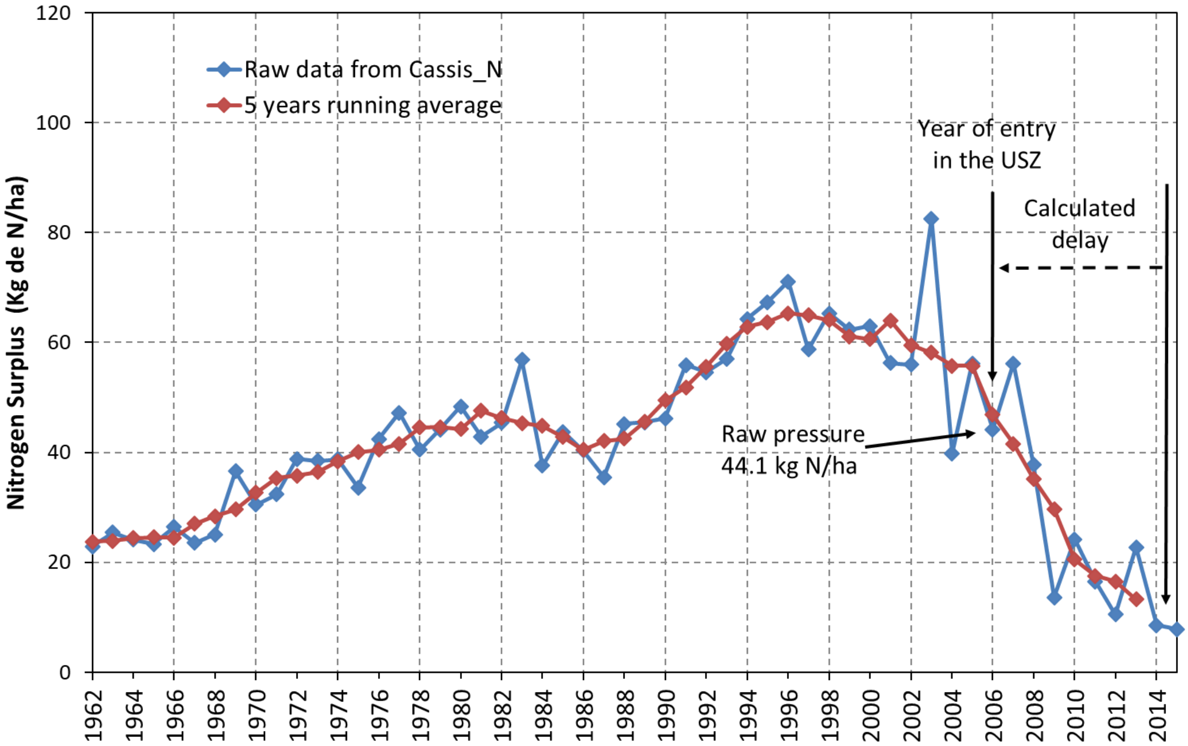

Figure 4.3. Annual data and running average over 5 years of nitrogen actual surplus for the department of Ain (kg NO3/ha) – year of initial pressure and resulting raw pressure of 2015

The map below (Figure 4.4) present the raw pressure for 2015 for France. The raw pressures were sorted in 6 classes to display an raw pressure for each French reference unit. Two additional classes are required to represent units with too fast (year of NO3 entry >2013) and too slow transfer velocity. (Year of NO_3 entry >1962).

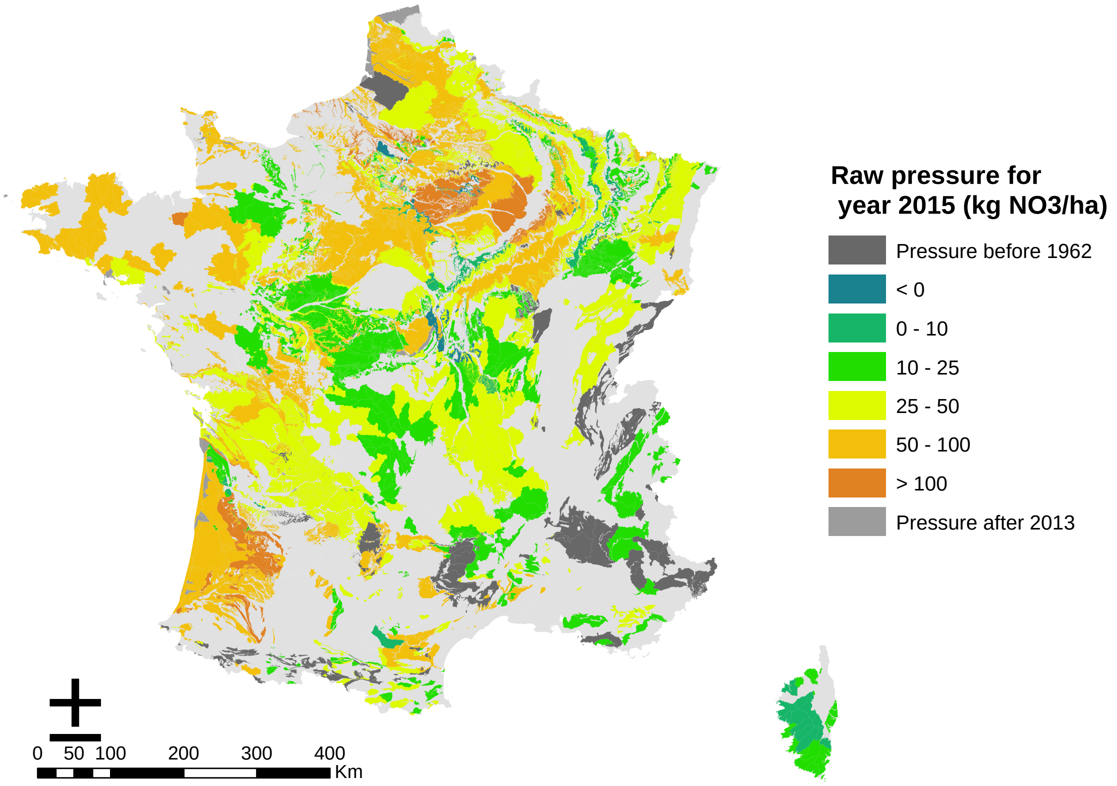

Figure 4.4. Expected Nitrogen raw pressure per reference unit in groundwater for year 2015

4.2.4 Saturated zone

This study focused on understanding and evaluating the transfer time in the unsaturated zone. The transfer time in saturated zone was not part of the calculation. However, data on the apparent water age and the transfer times in the saturated zone were collected throughout the French territory. This data collection aimed two objectives.

The first objective was to allow a comparison between the values resulting from the calculation by the transfer model in the unsaturated zone and the water age values. A good consistency was display between water ages in the saturated zone and transfer times in the unsaturated zone (It was not part of the study to make a detailed analysis of all the inconsistencies between transfer speeds and apparent water ages).

The second objective was to calculate a transfer speed in the unsaturated zone where the initial model (piston flow model) was not applicable (e.g. alluvions). Therefore, the transfer rates presented for alluvial type reference units in Figure 4.1 are not calculated with the model in the unsaturated zone but by using apparent water age data.

4.2.5 Representation of attenuation processes

In Gourcy et al., 2017, two attenuation processes were studied. The first one was the denitrification process, the second one was the dilution process

For denitrification, a method was applied for metropolitan France at the point scale. A classification-tree method has been developed, modified from Hinkle and Tesoriero, 2014. The following data has been taken into account: data extracted from the ADES database; physico-chemical parameters (dissolved oxygen content and redox potential); concentrations in elements sensitive to redox processes (Fe, Mn) and measured regularly in groundwater. The results indicate 1532 water points likely to denitrify on the French metropolitan territory. Although the calculation of denitrification could be performed at the point scale, no method were developed to use this data in order to calculate a denitrification at the scale of the reference work. The information collected for denitrification are punctual and upscaling works must be performed.

The important dilutions are generally located in the alluvial sectors where rivers can bring significant quantities of water having a different nitrate concentrations than the groundwater. No method was developed to take this phenomenon into account because the exchange zones between groundwater and rivers are local (partial part of reference units), and no evaluation of the volumes of water exchanged are known.

4.2.6 Model calibration and validation

The raw pressure for 2015 were compared with the concentrations observed in groundwater in 2015 (Figure 4.5). The monitoring networks use for the comparison are the RCS and RCO network. These monitoring were described in the previous report (5.2). The raw pressures were sorted in 5 classes (plus 2 non-pressure category) to make the comparison easier with concentrations.

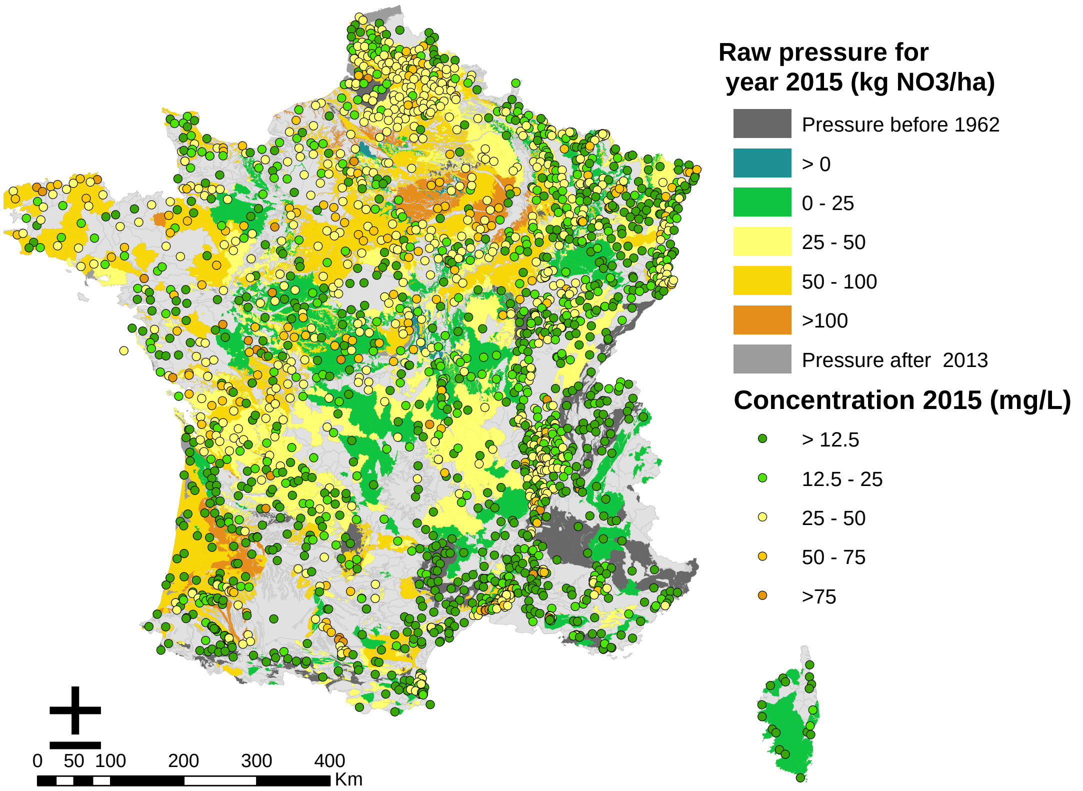

Figure 4.5. Comparison between observed concentration and Nitrogen raw pressure class

There is a good agreement between the concentrations observed and the raw pressures calculated. The highest pressure are measured regions with high agricultural activity around Paris. In central France, the expected and observed concentrations are lower.

However, due to the use of Cassis-N areas of inconsistency appear. Cassis-n uses a scale (Nuts 2) which is a bit large to represent the diversity of cultures and has a tendency to homogenize the data in one department. In some areas the distribution of crop is very heterogeneous and the calculated input does not reflect the activity of the whole area (Figure 4.6). In the Landes or in the Bas-Rhin, half of the area is occupied by a very agricultural area (mainly cultivated with corn) and the other half is occupied by a forest. The predicted concentrations are highly overestimated in the forest areas.

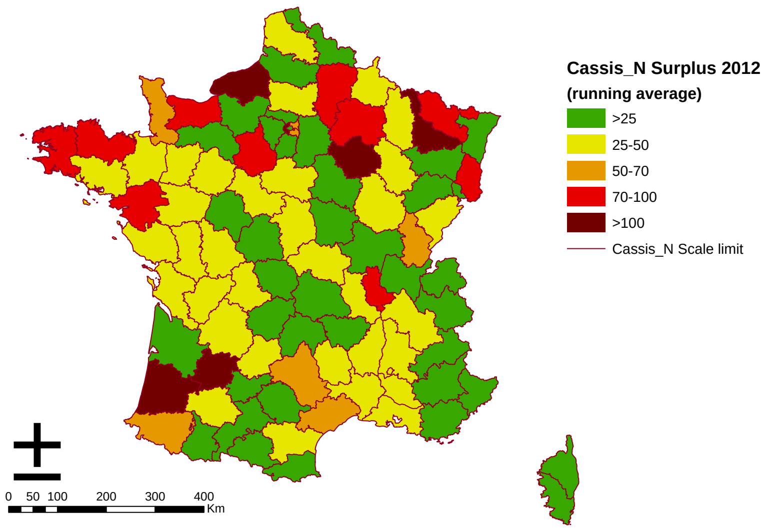

Figure 4.6. Surplus from Cassis N (Nut3 scale)

4.3 Key results

One of the main results of the project was to to gather the knowledge acquired on numerous independent sites across France on nitrate transfers through unsaturated zones. A database collected of apparent water age was also initiated. Thanks to all this data a map of transfer was made.

Nitrate transfer velocity could be estimated according to the lithology. In many regions the transfer speed is low (Table 4.2). Taking into account the thickness of the unsaturated zone (several tens of meters locally) and estimated low speed, the impacts of environmental actions on the water quality could be highly delayed. In lithologies where matrix transport is dominant, the impact of current practices would be visible in only several decades.

4.4 Outcomes of modelling

The Pressure-Impact study was used in European reporting as part of the water framework directive. These data have been used into each basin so that local stakeholders can take into account the specific features of their areas.

This work has shown the importance of transfer times in many areas. In certain sectors, this type of knowledge will make it possible to anticipate a need for agricultural action and the environment over the long term and to predict the absence of a short-term N concentration decrease after the application of an agricultural measure. This type of work, essentially for the use of stakeholders, allows to adjust decision-making and expectations.

5 NETHERLANDS

Hans Peter Broers, Mariëlle van Vliet (TNO), Gijs Janssen (Deltares)

5.1 Introduction

The science question that we address in the pilot study of the Netherlands are:

1. How useful are models to link measured nitrate and pesticides concentrations in groundwater to the application history of N and pesticides to farmlands?
2. Is it possible to use a national scale model to assess the travel times to small-size monitoring screens and link those to the measured concentrations?

For these aims we validated the outcomes of the Netherlands national groundwater flow model against measured tracer ages based on $^{3}H/^{3}He$ age dating. We evaluated whether the modelled time lags sufficiently mimicked the measured relations between recharge/application periods of a measured Nitrate or Pesticide concentration that were established by age dating methods.

5.2 Modelling approach

5.2.1 Overarching framework

Our work will focus on transfer times towards monitoring screens where we measure the development of concentrations of anthropogenic contaminants such as nitrate and pesticides (See HOVER deliverable D5.2 for an overview of transfer time approaches and definitions). The concept of transfer times that we distinguish for our chapter is illustrated in Figure 5.1; it mainly concerns the travel time through the saturated zone towards the monitoring screen. As water tables are shallow in our pilot study area, the delay in the unsaturated zone is short relatively to the transfer times through the saturated zone.

In section 5.2.2 we touch on the subject of these short unsaturated zone travel times, providing a map of estimates of the unsaturated travel time for the whole of the Netherlands. This work is mainly meant to enable a comparison with the work of other GeoERA HOVER partners on this subject. We report on this in section 5.2.2.

The remainder of the chapter on the Dutch pilot site (section 5.2.3 and further) is focused at the saturated zone travel times, which means the travel time towards monitoring screens and ultimately receptors such as springs or pumped wells (Figure 5.1). Therefore, our efforts were focused on age dating of the upper first 30 m of groundwater in order to obtain age-depth profiles and to relate concentrations of nitrate and eventually other solutes, such as pesticides and antibiotics, to the infiltration year of the groundwater (“infiltration year” approach; e.g. Visser et al. 2007; Hansen et al. 2010; Kivits et al. 2018). Using this infiltration year concept derived from the tracer based saturated zone travel times towards the monitoring screens, the leaching history of nitrate and pesticides could be related to the application history of nitrogen at farmlands. In principle, the same methodology is useful to study the transport of pesticides and emerging contaminants (see e.g. Kivits et al 2018), but care should be taken because of the pesticides being applied much more variable in space and time relative to nitrate, which promotes mixing and dispersion more than for nitrate.

Conceptually, one may argue that even the discrete age at a short monitoring screen may be regarded as an ‘age distribution’ (Weissmann et al., 2002), but for practical approaches this is often ignored without a loss of significant information (Visser et al., 2007; Hansen et al., 2010; Bohlke, 2002). Using a tracer-based approach, such mixing at the monitoring screen is sometimes recognizable, especially when applying the $^3H/^3He$ method which gives an idea of the initial 3H concentration, which can then be compared with the known ^3H in precipitation. Modelling may further help to reveal or confirm such mixing, which is one of the interesting issues in this deliverable.

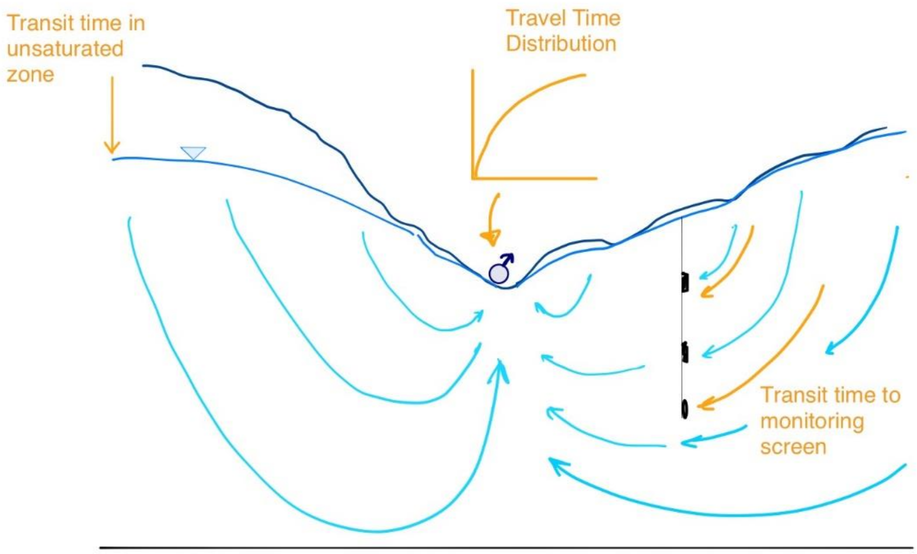

Figure 5.1 Concepts of transit times used in this report. The approach to the right has been followed in Denmark and the Netherlands, applying the "infiltration year" approach and is reported in the sections 5.2.3 and further. The approach to the left is followed in the UK and in France using unsaturated zone profiling and reported in section 5.2.2 in this report for the Netherlands.

Because the age dating approach is the concept that is presently used to serve stakeholders in the South of the Netherlands with information about infiltration periods of contaminants and their manifestation in groundwater, we first introduce the results of the tracer age dating in this chapter. Next, we compare those results with modelled ages using the national hydrological model, thus verifying and validating these model results. In subsequent deliverables, we will then combine these results with work on attenuation patterns, e.g. denitrification and pesticide degradation and sorption (Deliverables D5.4 and D5.5).

5.2.2 Modelling approach unsaturated zone

5.2.2.1 Map of unsaturated zone travel times

For the Netherlands, the thickness of the unsaturated zone is based on datasets of the average highest and lowest groundwater levels of version 3.4 of the LHM (Landelijk Hydrologisch Model, or National Hydrological Model), available to the public on the data portal of the NHI[1] (Nationaal Hydrologisch Instrumentarium). The datasets that are used include the GLG (Gemiddelde Laagste Grondwaterstand, or Average Lowest Groundwater level) and the GHG (Gemiddelde Hoogste Grondwaterstand, or

[1] https://data.nhi.nu/

Average Highest Groundwater level). Traditionally, groundwater levels in the Netherlands are measured twice a month on the 14th and the 28th. For each "hydrological year", starting on the 1st of April and ending on the 31st of March, the three highest and lowest groundwater levels are each averaged in a single value, and these are then averaged over a period of multiple years to arrive at the GHG and GLG. For this map, the years 1998-2006 are used.

The resolution of the LHM (250x250 m) was deemed too precise for the map of the unsaturated zone travel times. Therefore, the GLG and GHG raster's were upscaled to average values over 2x2 km grid cells. Next, the average thickness of the unsaturated zone for each of these 2x2 km cells was calculated by averaging the GHG and GLG. This results in a map of the unsaturated zone thickness, which was further used to give a rough estimate of the travel times in the unsaturated zones.

For the calculations of the travel times, different criteria were used based on the location and thickness of the unsaturated zone.

1. First, as a general rule for most of the Netherlands, an unsaturated zone water velocity of 1.5 m/yr. is used, based on the precipitation excess (recharge rate ~300 mm/yr.) and an assumed effective average saturated water content of 0.2 for the unsaturated zone.

2. Next to this general rule, two areas within the Netherlands are treated differently.
    a. areas with deep groundwater levels (>10 m) in the centre of the country, mostly located on the ice-pushed ridges of the Veluwe, originating from the Saalien land ice mass. In these sandy and tilted areas, preferential flow was found to be more important than in horizontally stratified strata. Chloride tracer experiments in the upper 10 m of the unsaturated zone estimated a soil water velocity (*v*) of 6.37 m/y in forested areas and 5.62 m/yr. in unforested areas following from *v* = Recharge rate (*R*)/ soil water content (Θ), with average recharge rates of 466 and 495 mm/yr. and average soil water contents of 0.072 and 0.089 in forested and unforested areas respectively (Gehrels, 1999). Because of the spatial resolution used (2x2 km), we assumed a general 6 m/yr. in the upper 10 m for the entire Veluwe area. For the unsaturated zone below 10 m, preferential transport is likely to be less important and although there are no precise measurements, we estimate unsaturated water velocity of 2 m/yr. in this deeper zone, assuming an average water soil water content of ~ 0.23-0.24. We have no data available to confirm this assumption as water velocity was never a parameter that was evaluated in the available groundwater models (e.g. Gehrels, 1999)
    b. the southernmost part of the Netherlands, which is dominated by limestones from the Cretaceous where unsaturated zone water velocities are generally also fast and probably governed by dual porosity flow. Here, unsaturated zone travel times were estimated on prior research on the ^{3}H-derived travel time distributions of the chalk springs, which include a piston flow assumption for unsaturated zone delay (Broers & van Vliet, 2018a, b). This earlier work constrains the maximum unsaturated zone delays to a maximum of ~20 years. For the unsaturated zone travel time maps, we distinguished four categories: an unsaturated zone travel time of 20 years for the highest parts of the area (groundwater levels >50 m), a travel time of 10 years for the unsaturated zones with thicknesses between 20-50 m, an unsaturated zone travel time

of 5 years for groundwater levels between 5-20 m, and an unsaturated zone soil water velocity of 1.5 m/yr. for all situations with more shallow groundwater levels.

For all areas, except for case 2b, the average values for the thickness of the unsaturated zone for each 2x2km grid cell were divided by the estimated unsaturated zone vertical water velocities described above, which eventually results in the map of the travel times in the unsaturated zone (Figure 5.2 and Figure 5.3).

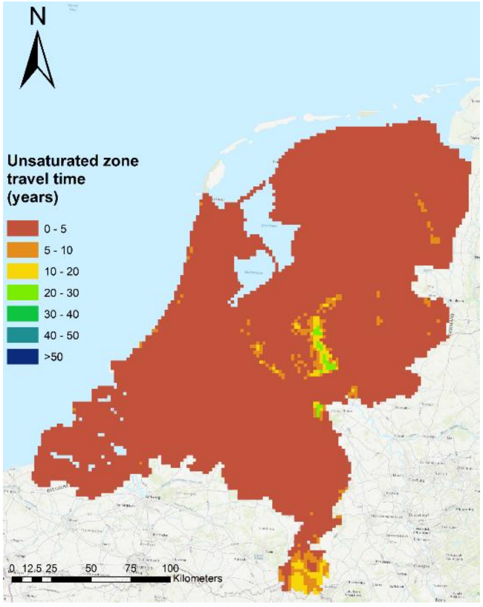

Figure 5.2. Map of travel time in the unsaturated zone in the Netherlands. Legend according to Figure 3.3 (UK)

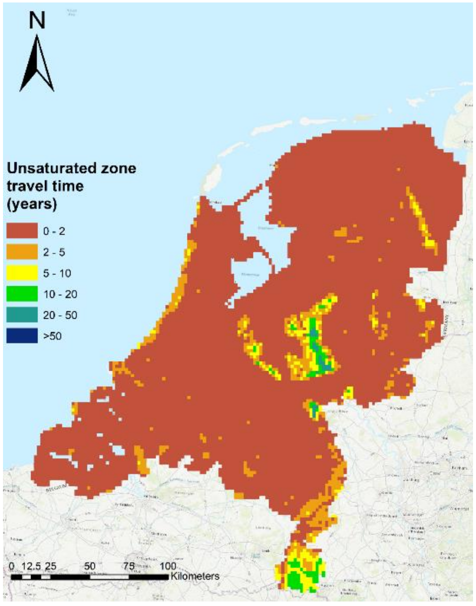

Figure 5.3. Map of travel time in the unsaturated zone in the Netherlands. Legend according to Figure 4.1.

Figure 5.2 and Figure 5.3 clearly show that unsaturated zone travel times in the largest part of the Netherlands are short (typically < 2 years) and mostly negligible relative to saturated zone travel times as discussed in sections 5.2.3 and further.

5.2.3 Modelling approach saturated zone

The model that we used to calculate travel times to monitoring screens is based on the National Hydrological Model of the Netherlands: LHM version 4.0, with adaptations for density driven flow and contaminant transport. The model runs for the whole of the Netherlands, integrating surface water and groundwater (Figure 5.4, Figure 5.6). The model has a grid discretisation of 250 x 250 m and for transport modelling runs in steady state using a combination of a surface water model, MetaSWAP for the unsaturated zone and MODFLOW-2005 for the saturated zone. For transport calculations, the model runs in stationary groundwater flow mode, using the long-term averaged groundwater recharge as was calculated from the transient MetaSWAP/MODFLOW model runs. Transport calculations for density driven groundwater flow are done with the 'NHI zoet-zout model' (or NHI fresh-saline model) that divides the subsoil in 39 layers (Figure 5.5). A further extended model was made by adding thin model layers in the top 30 metre of the subsoil to enable reliable transport calculations for water infiltrating in the subsurface from farmlands and infiltrating rivers. This 53-layer model was used for the calculations that are reported in this deliverable.

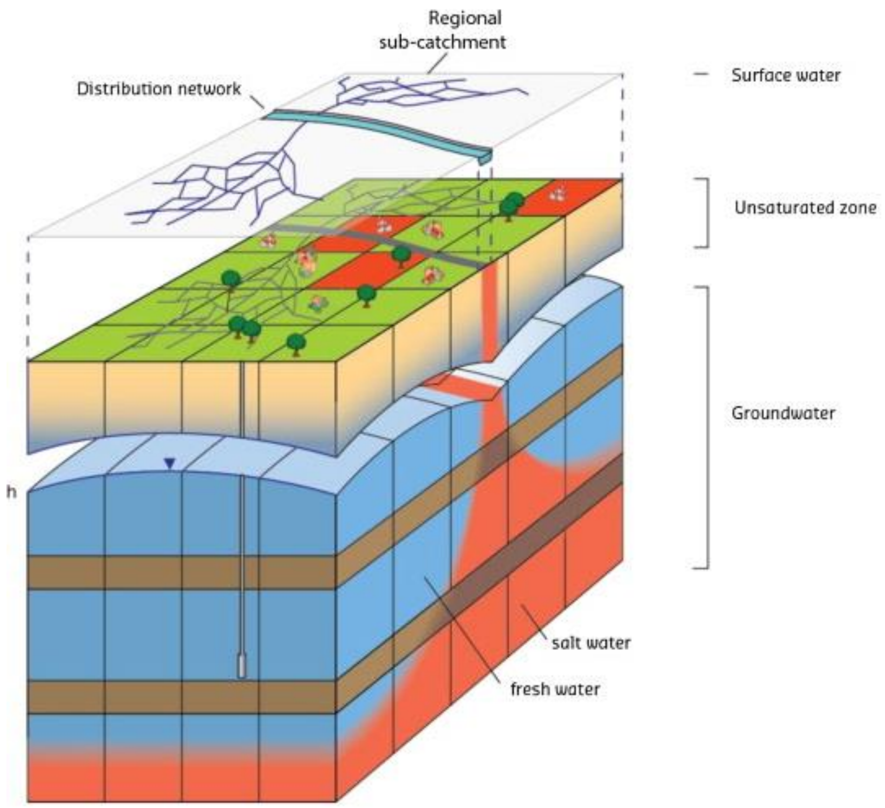

Figure 5.4. Concept of the National Hydrological Model (De Lange et al. 2014)

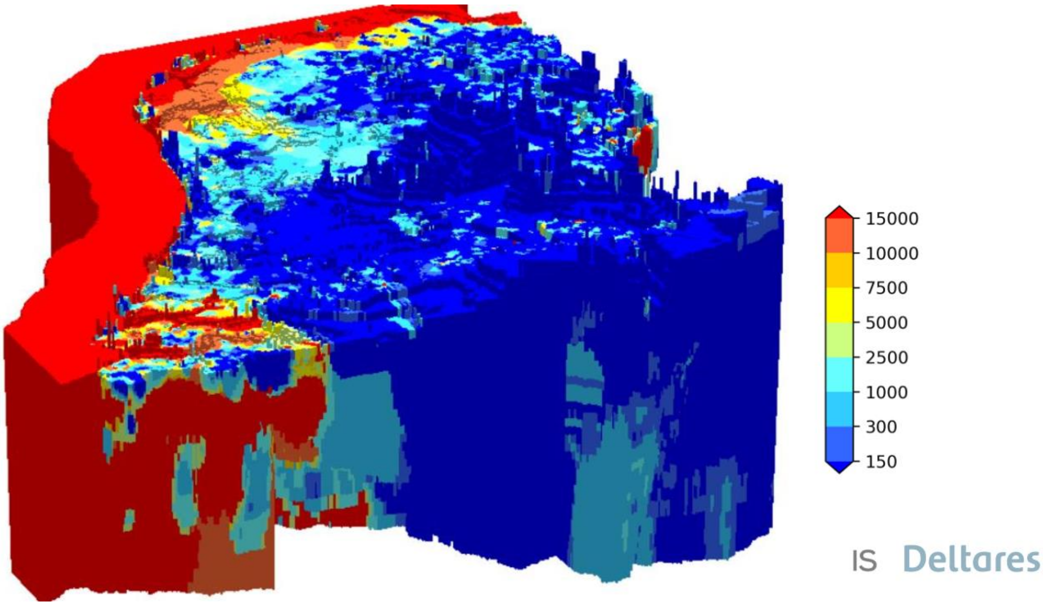

Figure 5.5. Illustration of the ‘LHM Zoet-Zout model’ (or fresh-saline model) covering the whole of the Netherlands, enabling calculations of density driven transport of fresh and saline water(source: Delsman et al. 2020a)

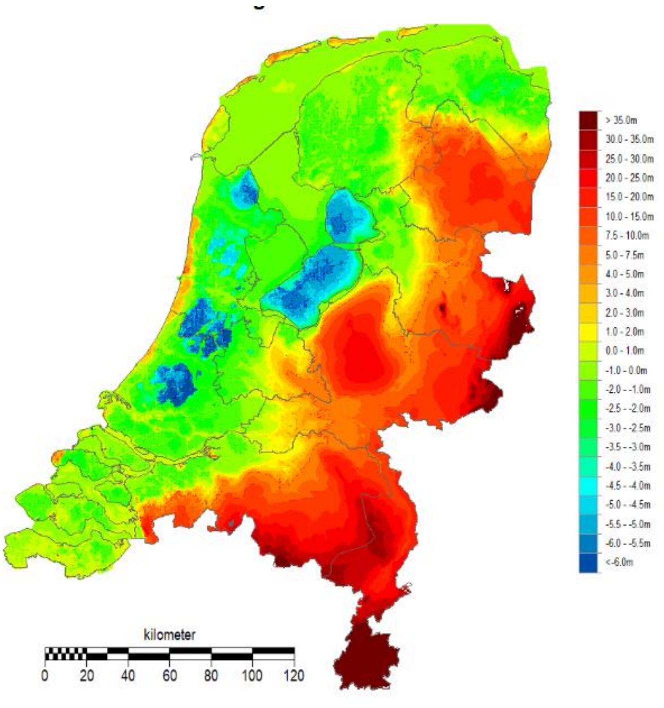

Figure 5.6. Results from the LHM 4.0 National Model: phreatic groundwater heads calculated with the NHI zoet-zout model (source: Delsman et al. 2020b)

Using the stationary groundwater flow model, the travel times were derived using the MODPATH code that is available in the iMOD version that is used by Deltares (Vermeulen et al., 2019).

Using MODPATH, per monitoring filter 160 particles were tracked backwards to find locations of infiltration and a travel time frequency distribution and median ages were derived for each of the monitoring screens.

MT3D calculations were performed in parallel mode in order to enable the efficient calculations necessary for such a large transport model using the TVD solving method (De Lange et al. 2014; Van Engelen et al. 2019). Average MT3D ages were derived for the complete cell for in which the monitoring screens is located. Because the model layers in the top of the system are quite thin, it is sometimes necessary to average the ages of a number of cells that together represent the 2m long monitoring screens. The MT3D age concept is effectively analogue to the concept of Goode (1996): a tracer with concentration zero was introduced in the top cell and left aging during transport.

Attenuation processes have not yet been introduced in the model, as our focus in on the validation of transit times. Attenuation of nitrate and pesticides are discussed in HOVER deliverable 5.4 and D5.5.

The LHM model suite is calibrated against measured groundwater heads, but not so much against transport parameters. The current deliverable effectively validates the calculated ages against measured ages by tracer methods. Key of the followed approach is that the modelled age distributions from MODPATH and MT3D are validated against measured tracer ages ($^3H/^3He$ ages). Subsequently, both modelled and measured travel times are used to elucidate the measured concentrations of nitrate and pesticides against the “recharge year” of the groundwater. As such, patterns reveal the mode of transport of nitrate and pesticides in the groundwater. Further relations between attenuation processes (degradation/sorption) and travel times are analysed in HOVER deliverables D5.4 and D5.5.

5.3 Tracer ages versus modelled ages

5.3.1 Tracer ages used as the reference dataset for our modelling work

In this pilot study data will be used from the Monitoring Network for the WFD in the Sand-Meuse region (Figure 5.7). This network consists of dedicated multi-level observation wells with standardized well completions and standard monitoring depths of 10, 15 and 25 m below surface level. The multi-level wells have screen lengths of 1 or 2 meters and a diameter of 2-inch that allows for sampling with submersible Grundfos pumps.

These wells have all been sampled for $^3H/^3He$ during campaigns in 2001, 2008/2009 and recently in 2017/2018. Until 2009, only wells under agricultural lands and sandy soils were age dated, whereas this dataset was complemented including wells in wetter sandy areas, in areas with clayey soils and in urban areas and nature reserves in 2017/2018 (Kivits et al, 2019). Using $^3H/^3He$ age dating, information is obtained about saturated zone travel times and groundwater ages, which enables the data produced to be used for forensics of past land use inputs. In this deliverable were refer to these ages as the “*tracer ages*”.

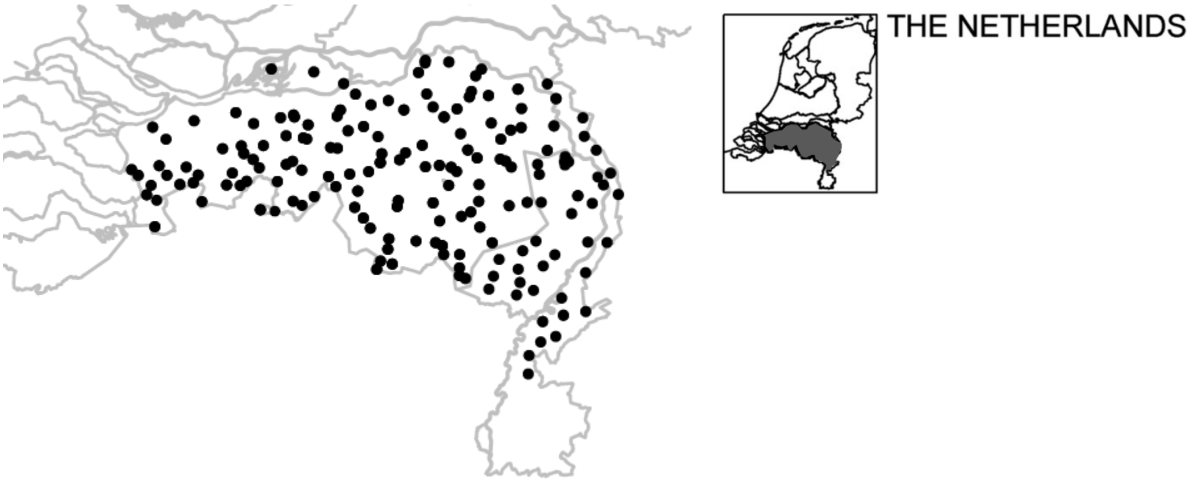

Figure 5.7. Monitoring wells for which “tracer ages” are available in the Dutch case study

Information about travel times in the saturated and unsaturated zones is derived from age dating using $^{3}H/^{3}He$ (Visser et al. 2007; Visser et al. 2009). Unsaturated zone travel times are typically short due to the shallow depths of the water tables in the region. Age-depth profiles are available for different types of land use and are used to facilitate trend detection and assessment of chemical status for these land uses. The design of the WFD monitoring network in the Meuse region distinguishes between specific combinations of land use and hydrological situations, which were called “homogeneous area types” (e.g. Broers 2004, Broers & Van der Grift, 2004). These combinations include: “farmlands on dry sandy soils”, “farmlands on wet sandy soils”, “farmlands on clay soils”, “nature reserves”, “urban areas” and “discharge areas in the sandy region”. The age dating results of a recent study helped to identify areas in which Meuse water recharges groundwater, and the wells that show signals of Meuse water recharge have been distinguished separately since (Kivits et al. 2019). Using the age dating results, age-depth relation was visualized for each of those area types (Figure 5.8).

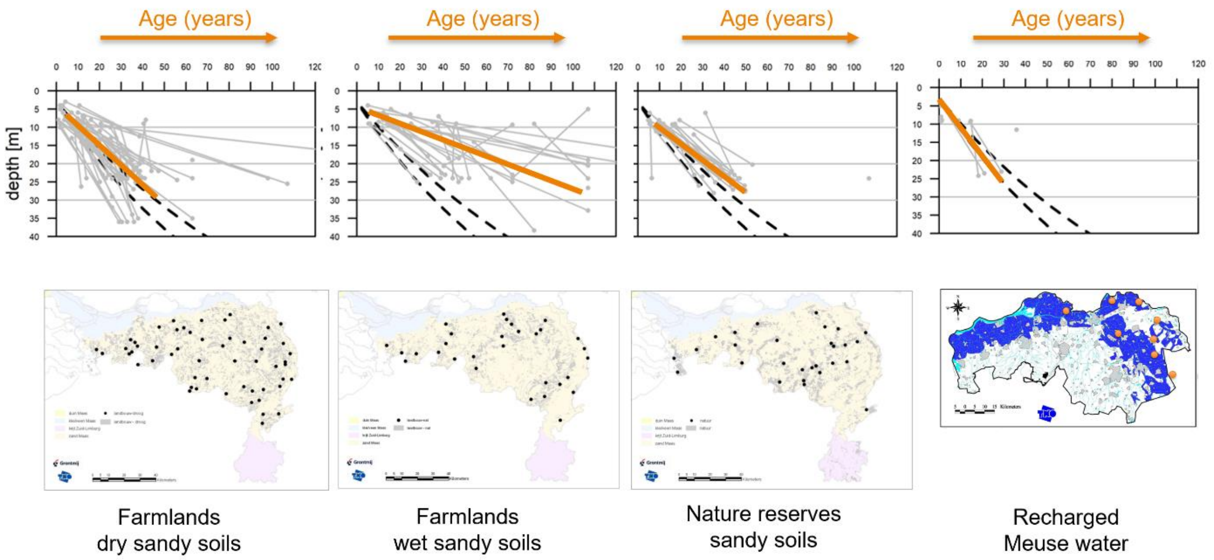

Figure 5.8. Age-depth profiles for different land use types in the pilot area. Grey lines connect shallower and deeper monitoring screens, visualizing the age-dept relation for the individual screens. The orange line suggests the median age-depth relation for the area type as a whole.

The age-depth relation for farmlands on dry sandy soils was established first (Visser et al. 2007, 2009). The average age-depth relation corresponds with recharge velocities in the order of 1 m per year in the upper parts of the saturated groundwater. The dashed line indicates estimate of the age-depth relation based on Vogel's model (Vogel 1967; Raats 1981) for a porosity of 0.35 and recharge rates of 250 and 320 mm yr^{-1}, respectively. The new age dating programs of 2017/2018 enable new interpretations for the other area types as well. Clearly, the overall age-depth pattern for farmlands on wet sandy soils is less steep and indicates much smaller overall vertical velocities as a result of shallow drainage of groundwater and associated mixing of water (Broers, 2004). Contrary, the measurements under nature reserves show age-depth profiles that are comparable to farmlands at dry sandy soils but indicating a somewhat smaller groundwater recharge rate, presumably induced by the higher evapotranspiration of forests as compared to cropland. The steepest age-depth gradient was found for the recharging Meuse water, which is logical because the downward flux of this water is not limited by the precipitation surplus, but dependent on the established surface water level regimes.

For many objectives, the age dating results are aggregated to age groups, which are summarized in Table 5.1. Samples that have a discrete apparent age from $^{3}H/^{3}He$ dating are labelled as "discrete age", whereas samples that suggest mixing of modern (post 1950) waters and pre-modern (pre-1950) waters have been distinguished separately, just as water with such low ^{3}H concentrations that they can be attributed to recharge before 1950. A special group with very old water was detected based on elevated ^{4}He concentrations.

Table 5.1. Proportion of the deeper screens (20-25 mbsl) of wells that agree with the 5 age groups Waters that have a discrete age are all modern, which is post-1950.

Area type	Discrete age	Mix modern - pre-1950	Mix mostly pre-1950	Pre-1950	Mix with old /old
Dry farmlands	59%	23%	6%	4%	2%
Wet farmlands	34%	20%	10%	27%	6%
Nature reserves	83%	13%		4%	
Urban	67%	17%			8%
Discharge	13%	13%	20%	47%	
Meuse river	100%				

The table shows that modern water with a discrete age has arrived at most of the deeper screens under dry farmlands, nature resources, urban areas and in areas where Meuse river water has recharged. Much less deep penetration of modern water is reported for wet farmlands and groundwater discharge areas in the sandy region, which is attributed to upward flow of older water and mixing between younger and older water in areas with converging flows (see Broers 2004). Knowledge of the age structure was of great help in identifying time lags and relating the application history of pesticides and nutrients to the occurrence in the monitoring wells (see section 4.4 and 4.5).

5.3.2 Validation of modelled travel times through comparison with tracer ages

5.3.2.1 MODPATH ages

The MODPATH calculated median ages were compared with the ages based on the $^3H/^3He$ ages. For monitoring screens that yielded a discrete $^3H/^3He$ age, the results of the comparison are presented in Figure 5.9. Clearly, a large part of the datasets shows reasonable, but certainly not perfect, fit for tracer age versus modelled age showing the same order of magnitude. However, at least 30 data points show much older median MODPATH ages than tracer ages, irrespective of the area types that were distinguished, which leaves a simple linear regression to an overall R^2 of only 0.10.

We attribute this to the rather coarse discretisation of the national model, with cell sizes of 250 x 250 m. As a result, monitoring screens that are in such a large cell are represented by only one vertical and horizontal flux, which makes the MODPATH calculation tricky. In reality, monitoring screens may be located at the boundary of such a cell, next to a recharge area and receive water from a specific direction and field.

Another part of the dataset consists of monitoring screens for which the tracer age could not be set to a specific year and were characterized to be pre-1950 or a mixed type (see Table 5.1). For these wells, we evaluated the MODPATH ages separately in Figure 5.10. Overall, the general pattern is well in line with the tracer ages with increasing MODPATH age with older tracer age. However, the spread around the MODPATH ages is considerable. Rather good results are listed for the classes mix pre-1950 modern, which has a median MODPATH age of around 50 years and a large spread around the year 1950, which corresponds with ~70-year-old on the Y-axis of the Figure. The same holds for the classes “mix mainly pre-1950”and “pre-1950” for which the majority of the MODPATH ages agree well. However, in the “very old” and “pre-1920” age classes, the spread around the median reveals that part of the MODPATH ages include water that is relatively young.

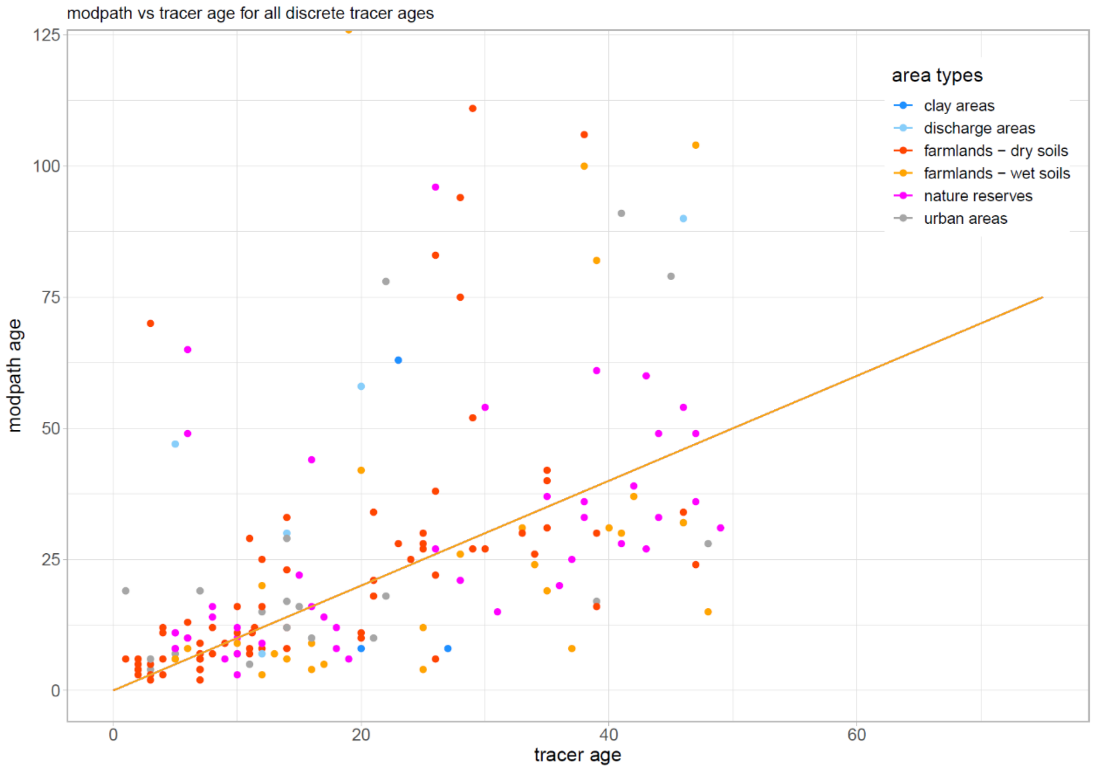

Figure 5.9. Scatter plot of MODPATH modelled age and $^3H/^3He$ tracer age for the monitoring screens for which a discrete tracer ages was available. Colours denoted the different area types. A number of 10 outliers of modelled age > 125 years are not shown.

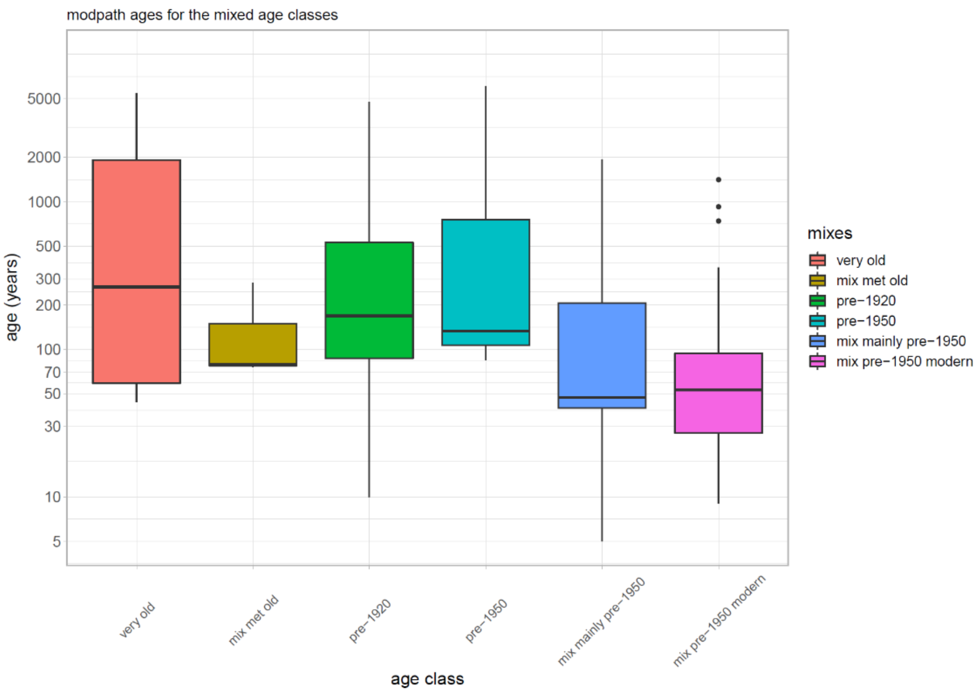

Figure 5.10. Comparison of MODPATH ages for the mixed tracer age classes

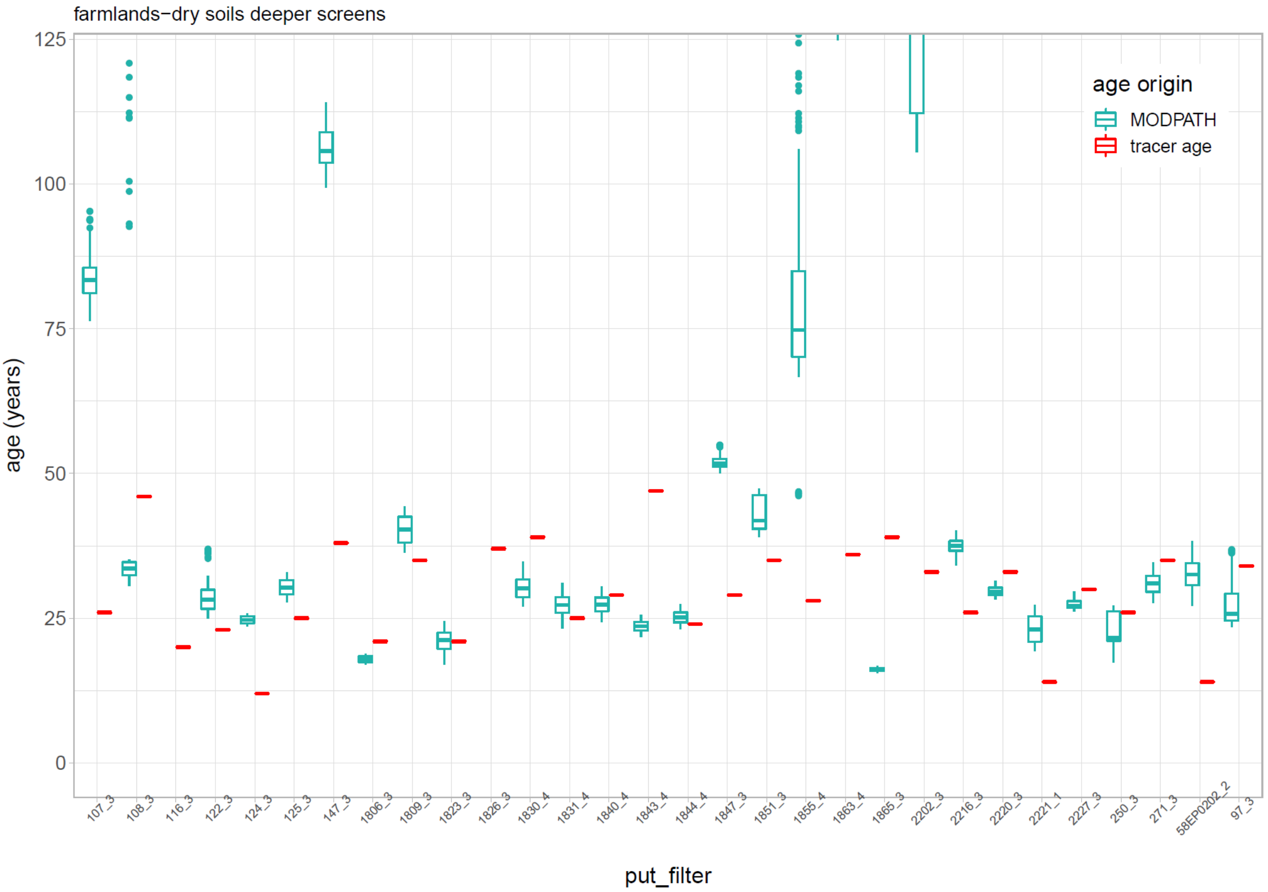

Figure 5.11. Illustration of the comparison between MODPATH ages and tracer ages for the deeper screens of the area type "farmlands-dry soils"

A further analysis at the scale of individual monitoring screens has been done, for which Figure 5.11 serves as an example. The boxplots reveal the travel time distributions as they are calculated from the MODPATH results of 160 tracked particles, the red bars represent the discrete tracer ages of the individual monitoring screens. Again, in general the pattern of MODPATH follows the pattern of tracer ages, but some monitoring screens show large deviations and sometime large spreads of the travel time distribution. Based on these individual evaluations all MODPATH ages have been evaluated, yielding three types of labels, that were consistent with the labels of the tracer ages:

- Infiltration periods 2010-2020, 2000-2010,1990-200,1980-1990,1970-1980 and 1950-1970 as based on the median MODPATH age for the year 2018, providing that the IQR (P75-P25) of the ages is less than 20 years
- Pre-1950 if the complete distribution of the MODPATH ages is above 68 years
- Very old if the complete distribution of the MODPATH ages is above 200 years
- Mixed if the spread of the MODPATH distribution (IQR) is too large to be distinguished from the period before 1950 and the period thereafter.

For the subsequent analysis of section 4.3.3, the mixed MODPATH ages were left out, as they would only lead to confusion.

5.3.2.2 MT3D ages

A comparison between MT3D ages and tracer ages has been made in Figure 5.12. Comparing Figure 5.12 with Figure 5.9, it is clear that MT3D ages are very similar to the MODPATH ages, showing the same deviations from the tracer ages for a number of the wells. The interesting feature of the MT3D age calculations is that MT3D would provide us with extrapolation options and mapping of groundwater ages over the whole of the Netherlands (See section 4.3.3 and Figure 5.13).

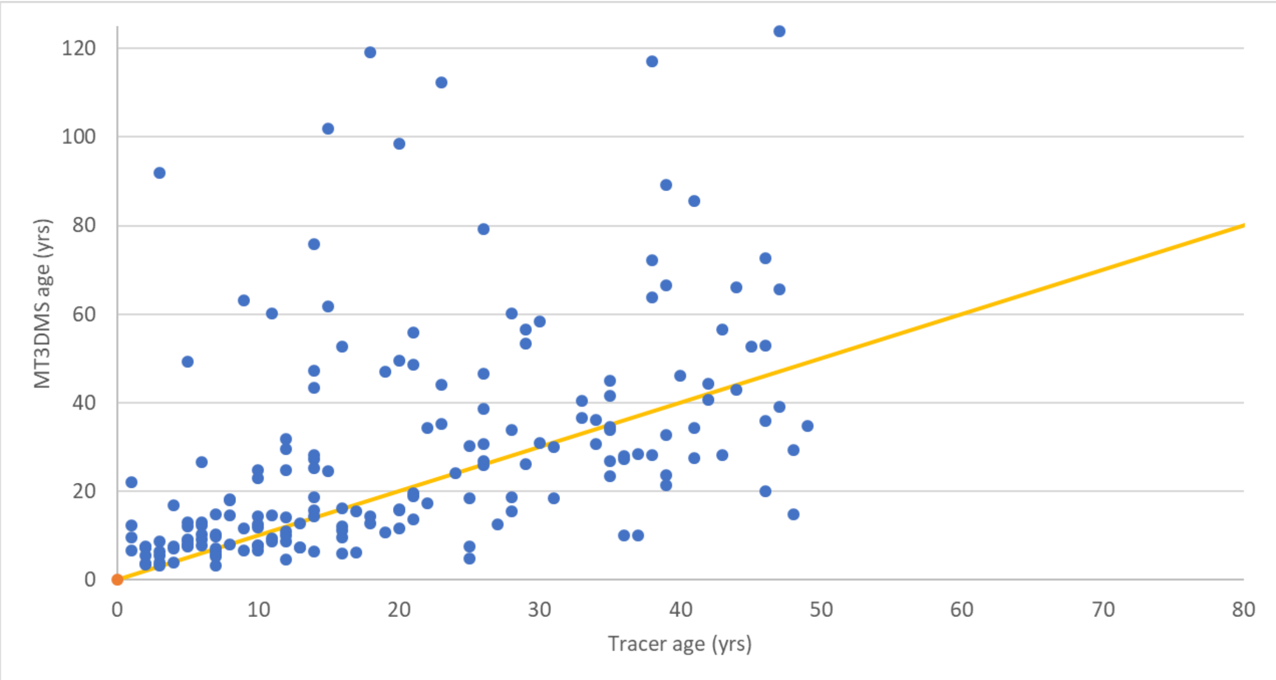

Figure 5.12. Comparison between discrete tracer ages and MT3D ages

5.3.3 Mapping groundwater travel times using MT3D

Figure 5.13 gives an illustration of the MT3DMS age model of the Netherlands. The idea is to set this model to evaluate the leaching of anthropogenic contaminants into the deeper Dutch subsurface. The current study helps to validate these kind of model results using tracer derived groundwater ages and helps to frame further research into the modelling approach. In order to further evaluate and validate the tracer and modelling approaches, we analyse patterns of known contamination with nitrate and pesticides in sections 4.4 and 4.5.

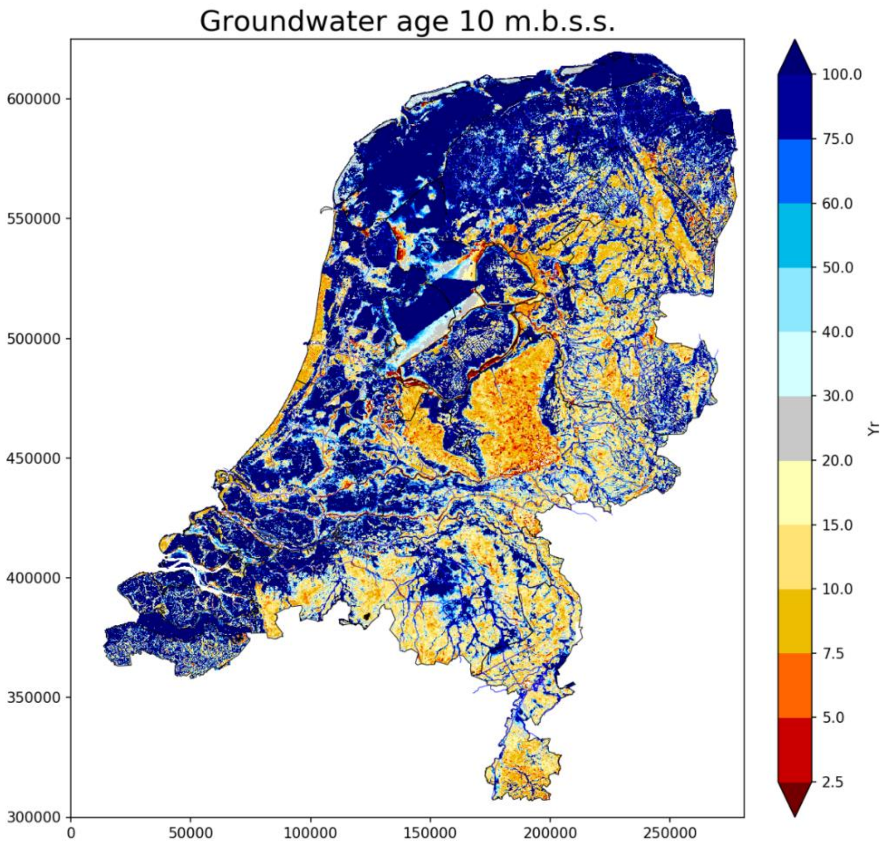

Figure 5.13. MT3DMS model result for the age distribution of Dutch groundwater at 10 m below surface level. Young ages up to 20 years mainly occur in the sandy regions of the Netherlands

5.4 Modelled and measured nitrate patterns

5.4.1 Introduction

For GeoERA HOVER an approach with jitters has been tested, in which nitrate, sulphate, oxidation capacity (OXC) and pesticide concentrations were related to classes of infiltration years. The advantage of jitter plots is that non-detects can be plotted at the concentration level of the detection limit itself, however pesticides "hits" can still be recognized. As a background, a boxplot is applied, which gives an immediate overview of the frequency distribution, indicating which concentrations should be regarded as outliers in the distribution.

The infiltration year is measured by subtracting the (tracer) age of the sample from the year of sampling itself. Then, these infiltration years are divided in eight classes: very old, pre-1950, 1950-1970, 1970-1980, 1980-1990, 1990-2000, 2000-2010 and 2010-2020.

We used the dataset of the province of Noord-Brabant and province of Limburg. The part of the dataset that is age dated was used for our analysis, which corresponds with the monitoring network described in section 4.3.1. In the analysis data were included from sampling years 2012, 2016 and 2019.

5.4.2 Measured patterns of nitrate based on tracer ages

5.4.2.1 Tracer age patterns of OXC, nitrate and sulphate in all areas

Figure 5.14, Figure 5.15, and Figure 5.16 shows on the x-axis the infiltration year classes and on the y-axis the concentration of oxidation capacity (OXC), nitrate or sulphate. The oxidation capacity (OXC) is defined as the weighted sum of molar concentrations of NO_3 and SO_4 as is our best performing indicator for overall agricultural contamination of groundwater. In the Netherlands, OXC is an efficient indicator for agricultural contamination of groundwater as it includes the reaction product sulphate which is formed by the reaction of denitrification coupled with pyrite oxidation.

Oxidation capacity

The jitter plots show that in all areas and in agriculture areas, the OXC concentrations are elevated since the 1960's and highest median concentrations between 1980 and 1990 (Figure 5.14). The shape of the curves nicely reflects the effects of reducing the N applications after the 1985 Manure Law which clearly led to overall decreasing concentrations in water that recharged since 1985. For comparison, in the nature reserves the concentrations are much lower which give conclusive evidence that the pattern under farmlands is related to N applications on land, and not to atmospheric deposition alone. Relatively high OXC concentrations are occasionally found in the younger water of the areas where Meuse river is infiltrating, which is probably related to sulphate inputs from the Meuse.

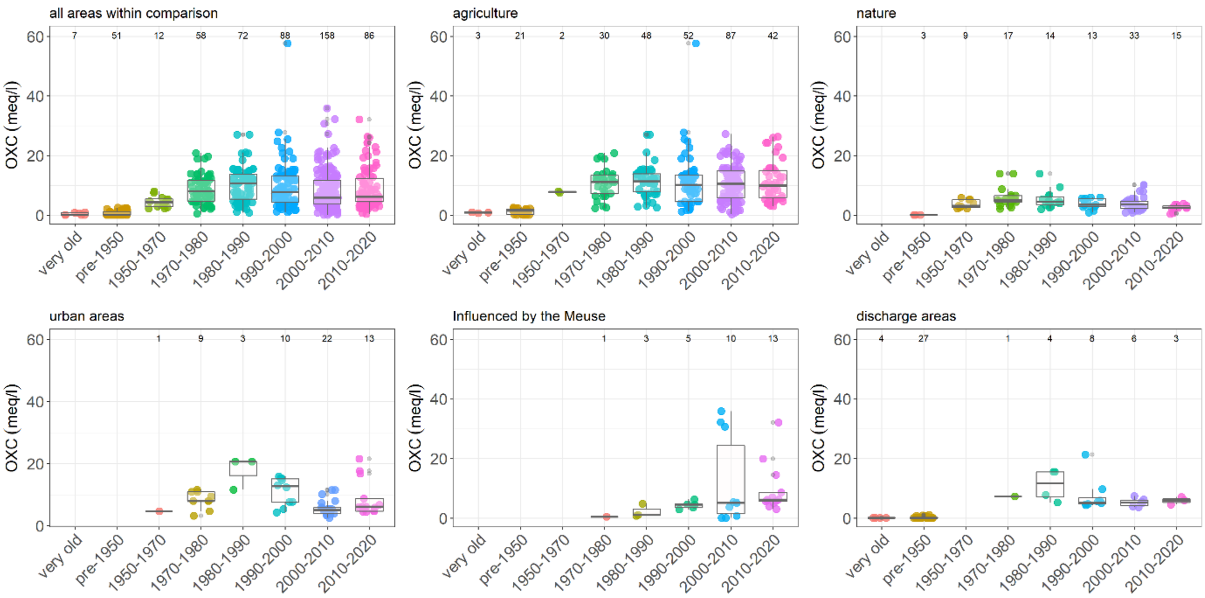

Figure 5.14. Jitters and boxplots of OXC (meq/l) per infiltration year class based on tracer ages for several land types: all areas within comparison, agriculture, nature, urban areas, areas influenced by the Meuse and discharge areas.

Nitrate

In all areas and agricultural areas, nitrate is particularly present in the infiltration year classes 1980-1990, 1990-2000, 2000-2010 and 2010-2020 (Figure 5.15). The absence of nitrate in water older than 1980 is completely determined by the process of denitrification. As expected, in nature areas the nitrate concentrations are much lower or absent. Remarkable are the high nitrate concentrations in infiltration year classes 2010-2020 and 2000-2010 in urban areas and in 2010-2020 in areas influenced by the Meuse.

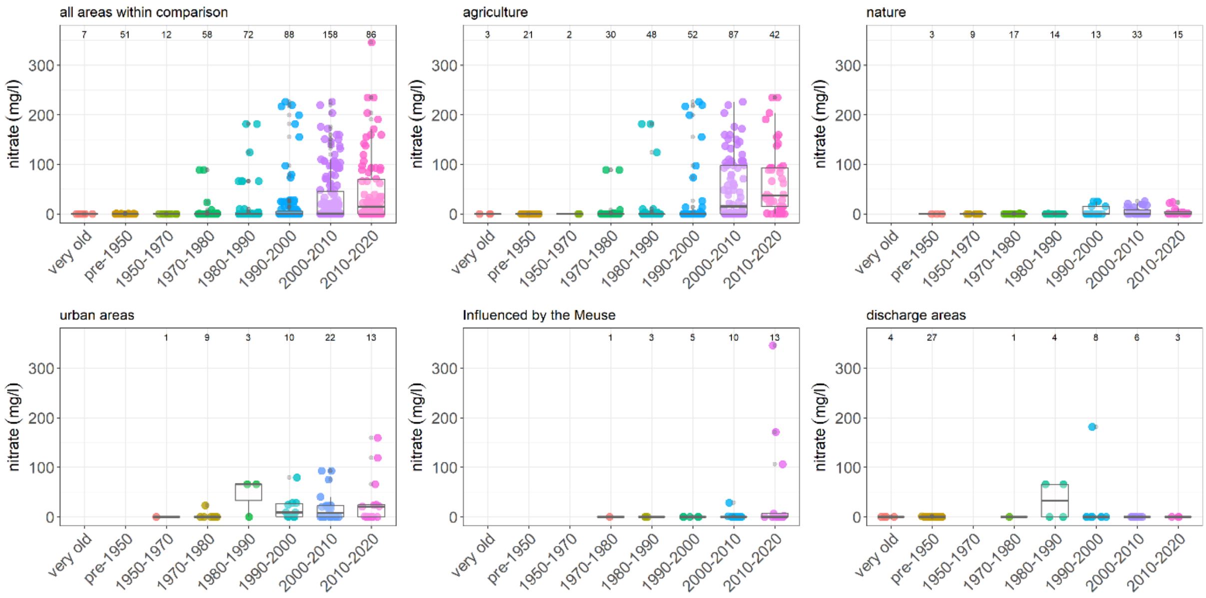

Figure 5.15. Jitters and boxplots of nitrate (mg/l) per infiltration year class based on tracer ages for several land types: all areas within comparison, agriculture, nature, urban areas, areas influenced by the Meuse and discharge areas.

Sulphate

Comparing the patterns of agriculture and nature shows that concentrations in agricultural areas are higher than in nature, but that they both peak around 1980 (Figure 5.16). Remarkable are the high sulphate concentrations in infiltration year 2000-2010 in areas influenced by the Meuse.

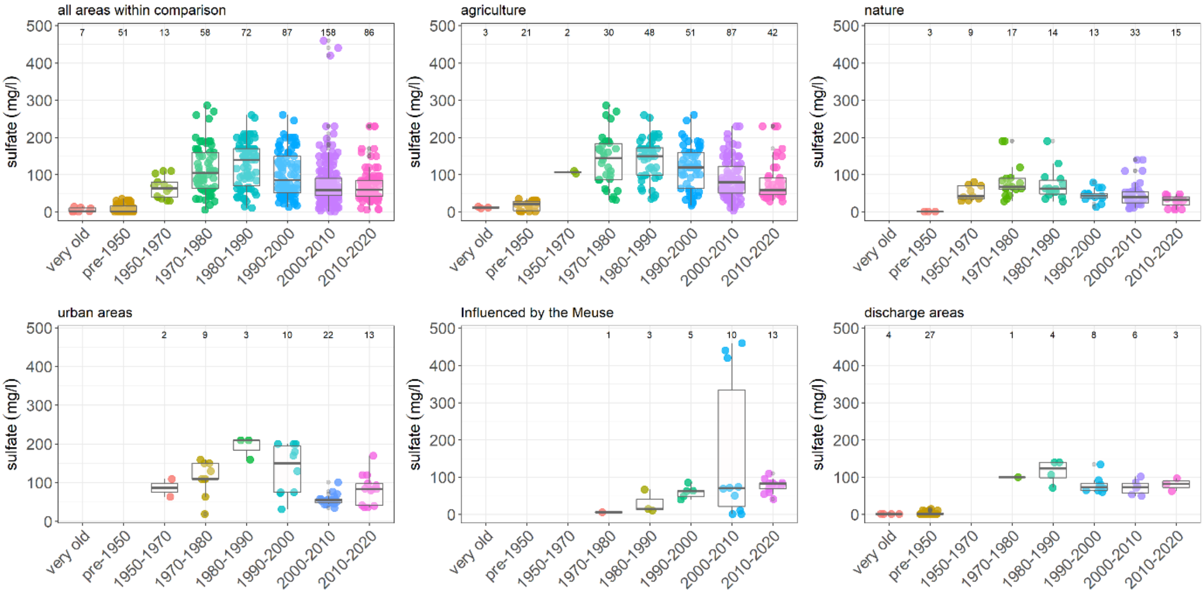

Figure 5.16. Jitters and boxplots of sulphate (mg/l) per infiltration year class based on tracer ages for several land types: all areas within comparison, agriculture, nature, urban areas, areas influenced by the Meuse and discharge areas.

Patterns in agriculture areas

Figure 5.17 shows areas the jitters and boxplots of nitrate, OXC, nitrate-nitrite ratio, iron, manganese and sulphate per infiltration year class based on tracer ages for the agriculture areas only. The orange line, which connects the medians of each boxplot, helps to recognize the patterns over time. The shape of the curves of OXC, iron, manganese and sulphate nicely reflects the effects of reducing the N applications after the Manure Law of 1985, which clearly led to overall decreasing concentrations in water that recharged since 1985. The curves of nitrate and nitrate-nitrite ratio have a different shape due to the absence of nitrate in water older than 1980. The absence is completely determined by the process of denitrification.

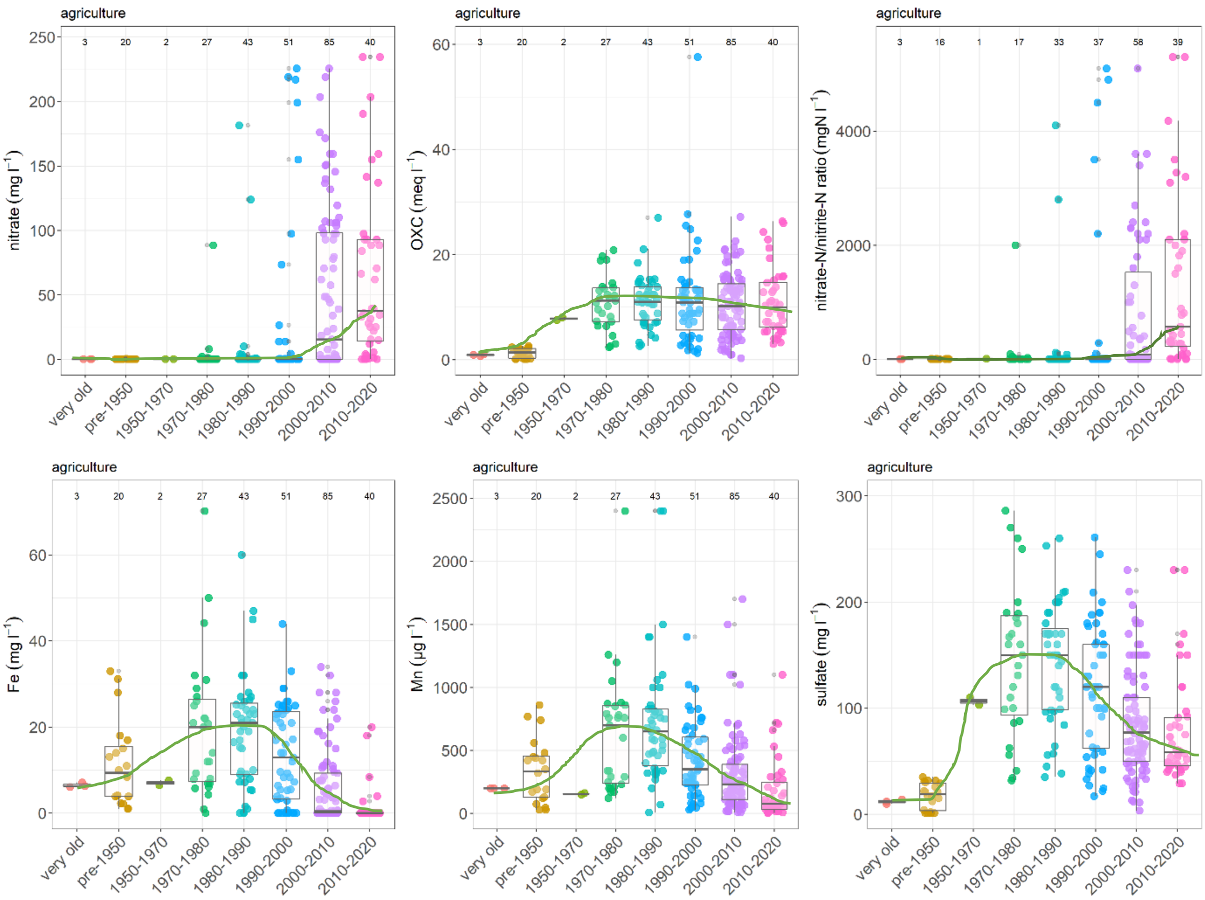

Figure 5.17. Jitters and boxplots of nitrate (mg/l), OXC (meq/l), nitrate-nitrite ratio (mgN/l), iron (mg/l), manganese (µg/l) and sulphate (mg/l) per infiltration year class based on tracer ages for agriculture areas. The orange line connects the medians of each boxplot to display the pattern over time.

5.4.3 Comparison of measured and modelled patterns of nitrate and major solutes

Figure 5.18, Figure 5.19 and Figure 5.20 show the same jitters and boxplots per infiltration year class not only based on tracer ages, but also as based on ages modelled by MODPATH and ages modelled by MT3D. In the left column the patterns are created by tracer ages, in the middle column by MODPATH ages and in the right column by MT3D ages. The jitters and boxplots are made for ‘all areas within comparison’ (i.e. agriculture, nature, urban areas, areas influenced by the Meuse and discharge areas), agriculture and areas influenced by the Meuse. The orange circles show the most important differences between tracer-MODPATH ages and between tracer-MT3D ages.

In Figure 5.18 the patterns of OXC based on tracer ages reflects the effects of reducing the N applications after 1985, which clearly led to overall decreasing concentrations in water that recharged since 1985. This pattern is visible in all areas and in agriculture areas. This pattern is less clear or even not visible in the figures of MODPATH and MT3D. This is because high concentrations occur in the infiltration year classes very old, pre-1950 and 1950-1970, where these concentrations in the tracer figures fall in the more likely younger infiltration years. In the figures of the Meuse the measurements in very old (MODPATH) and pre-1950 and 1950-1970 (MT3D) are striking. It is unlikely that groundwater in the areas influenced by the Meuse is that old.

The figures of nitrate (Figure 5.19) and sulphate (Figure 5.20) display comparable patterns. In deep older groundwater nitrate concentrations are not expected, because of denitrification processes or limited loading at that time (very old and pre-1950). However, nitrate concentrations are visible in old and deep groundwater according to MODPATH and MT3D.

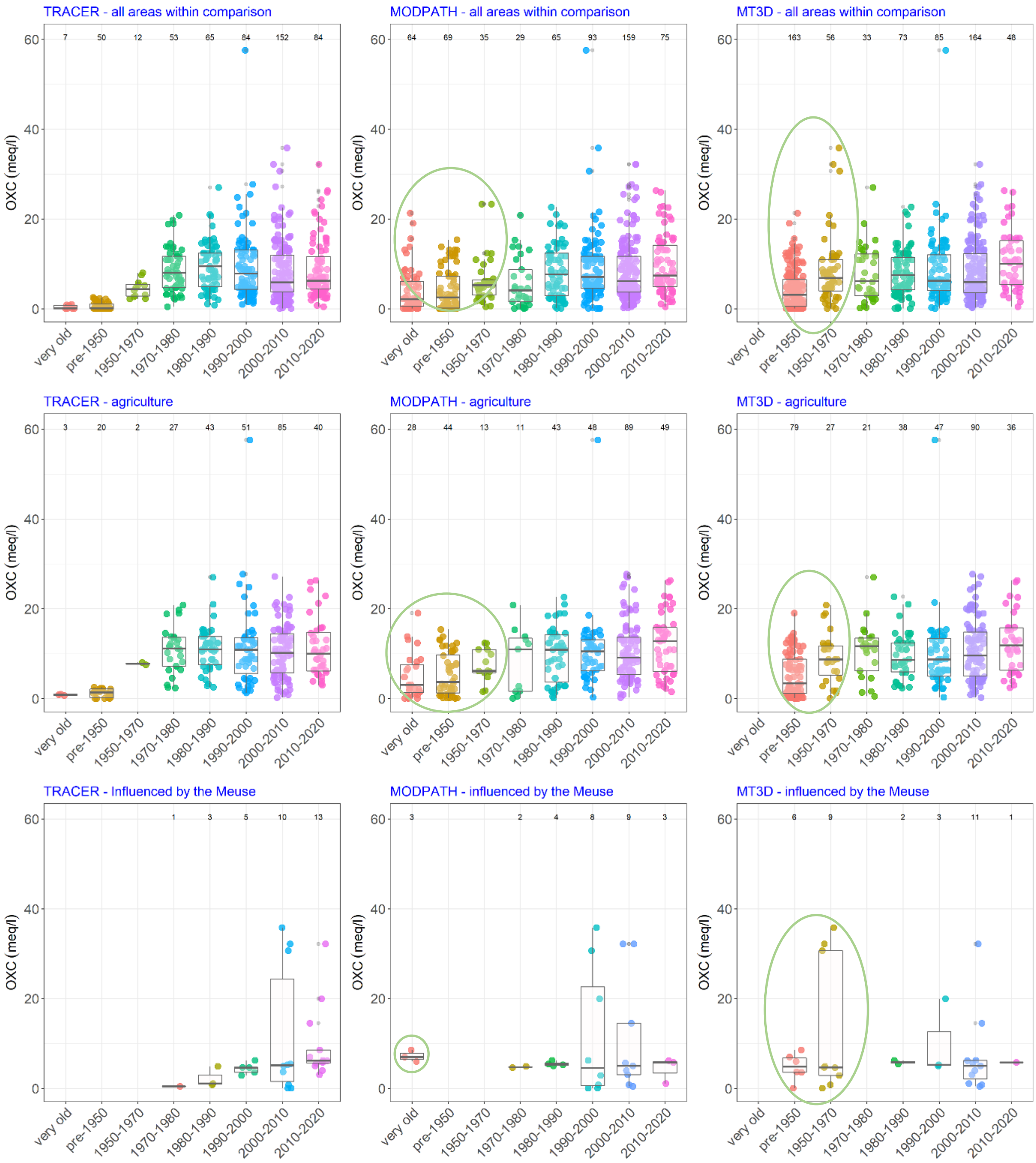

Figure 5.18. Jitters and boxplots of OXC (meq/l) per infiltration year class based on tracer ages (left column), MODPATH ages (middle column) and MT3D ages (right column) for all areas within comparison (upper row), agriculture (middle row), areas influenced by the Meuse (bottom row). The orange circles show the most important differences between tracer-MODPATH ages and between tracer-MT3D ages.

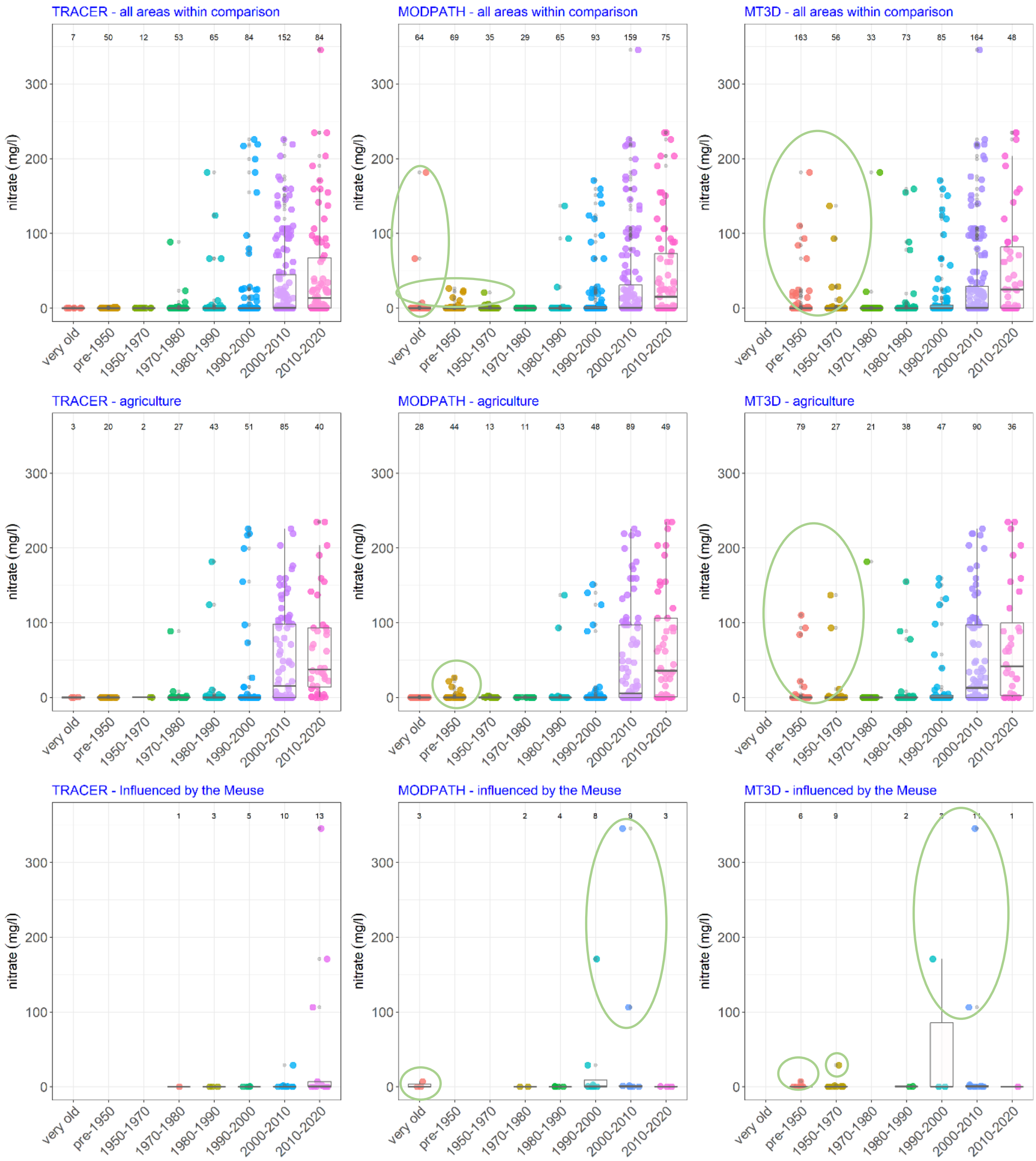

Figure 5.19. Jitters and boxplots of nitrate (mg/l) per infiltration year class based on tracer ages (left column), MODPATH ages (middle column) and MT3D ages (right column) for all areas within comparison (upper row), agriculture (middle row), areas influenced by the Meuse (bottom row). The orange circles show the most important differences between tracer-MODPATH ages and between tracer-MT3D ages.

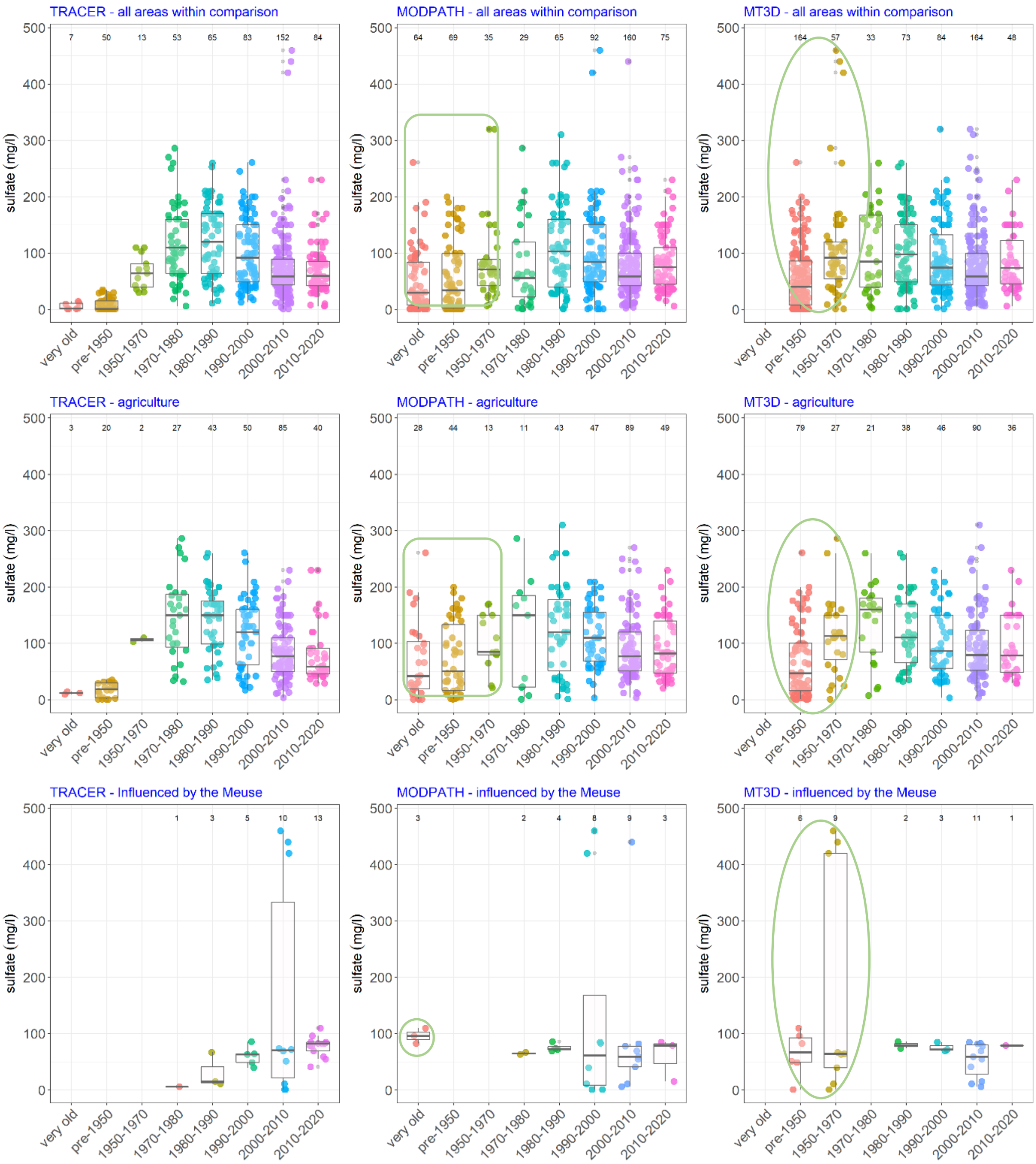

Figure 5.20. Jitters and boxplots of sulphate (mg/l) per infiltration year class based on tracer ages (left column), MODPATH ages (middle column) and MT3D ages (right column) for all areas within comparison (upper row), agriculture (middle row) and areas influenced by the Meuse (bottom row). The orange circles show the most important differences between tracer- MODPATH ages and between tracer-MT3D ages.

5.5 Modelled and measured pesticides patterns

5.5.1 Introduction

Most of the work TNO performed in the Netherlands, using the age dating results and transit time approaches, were focused on nutrients and macro-chemistry of the water. For GeoERA HOVER, this work has been extended to pesticides, using the measured groundwater ages as a forensic tool, evaluating pesticides patterns with age and relating it to the period when the specific pesticides were permitted. Therefore, again the $^{3}H/^{3}He$ recharge year ('infiltration year') has been calculated by subtracting the $^{3}H/^{3}He$ apparent age from the sample date and then group by infiltration year classes.

Organic contaminants typically occur in much lower concentration ranges and datasets of these substances are typically characterized by a large number of non-detects. This makes the general Infiltration Year approach and LOWESS smoothing less useful for signalling patterns of pesticides concentrations with age. For GeoERA HOVER an approach with jitters has been tested not only for nitrate, sulphate, oxidation capacity (OXC), but also for pesticide concentrations. As mentioned earlier, the advantage of jitter plots is that non-detects can be plotted at the concentration level of the detection limit itself, however pesticides "hits" can still be recognized. As a background, a boxplot is applied, which gives an immediate overview of the frequency distribution, indicating which concentrations should be regarded as outliers in the distribution.

We used the "broad screening" dataset of the province of Noord-Brabant and province of Limburg to evaluate the concentration of a number of pesticides for HOVER WP5. The part of the dataset that is age dated was used for our analysis, which corresponds with the monitoring network described in section 4.3.1. In the analysis data were included from sampling years 2012, 2016 and 2019.

5.5.2 Measured patterns of pesticides based on tracer ages

5.5.2.1 Tracer age patterns of 3 pesticides

Figure 5.21 shows jitters and boxplots of BAM (2,6-dichloorbenzamide) per infiltration year class based on tracer ages for several land types. BAM is a metabolite of dichlobenil. Dichlobenil has been permitted since the end of the 80's and has been banned since 2009. Concentrations of BAM above 0.5 µg/l were mainly observed in water that has infiltrated since 1990. Dichlobenil is typically absent water infiltrated before 1970 which corresponds to the known application period. Remarkable is that BAM is still present in water that has infiltrated since 2010, thus stemming from the period after the ban of dichlobenil. However, Van der Aa & Swartjes (2017) describe that BAM can also originate from the fungicide fluopicolide, which has been permitted since 2007. This could explain why BAM is still found in infiltration year classes 2010-2020. BAM is mainly found in agricultural and urban areas.

Figure 5.22 shows jitters and boxplots of desphenyl-chloridazon per infiltration year class based on tracer ages for several land types. Desphenyl-chloridazon is a metabolite of chloridazon. Chloridazon has been permitted in the Netherlands since the early 1990's and was found in the groundwater since then. Figure 5.22 shows that desphenyl-chloridazon was frequently found in agricultural areas in water from the infiltration periods 1990-2000, 2000-2010 and 2010-2020. Desphenyl-chloridazon is also regularly found in pumping wells used for drinking water production (Van der Aa & Swartjes, 2017). Another metabolite of chloridazon, methyl-desphenyl-chloridazon, was also regularly found in groundwater (see Table 5.2).

Bentazon is a pesticide (herbicide) and has been permitted under Dutch regulations since the end of the 80's but was applied and under EPA scrutiny since the early 80's. The bentazon jitter plot (see Figure 5.23) shows concentrations below detection limit for infiltration year classes older than 1980 and one detect in the class 1970-1980. Detections for bentazon are frequent in water under agricultural areas from the infiltration periods after 1980 and shows highest number of hits in the infiltration periods 1990-2000 and 2000-2010. All concentrations of bentazon in water aged before 1980 are below detection limits as should be expected from the application history. Overall, the pattern of bentazon is compatible with that of nitrate, and bentazon is clearly quite mobile in the Brabant subsurface.

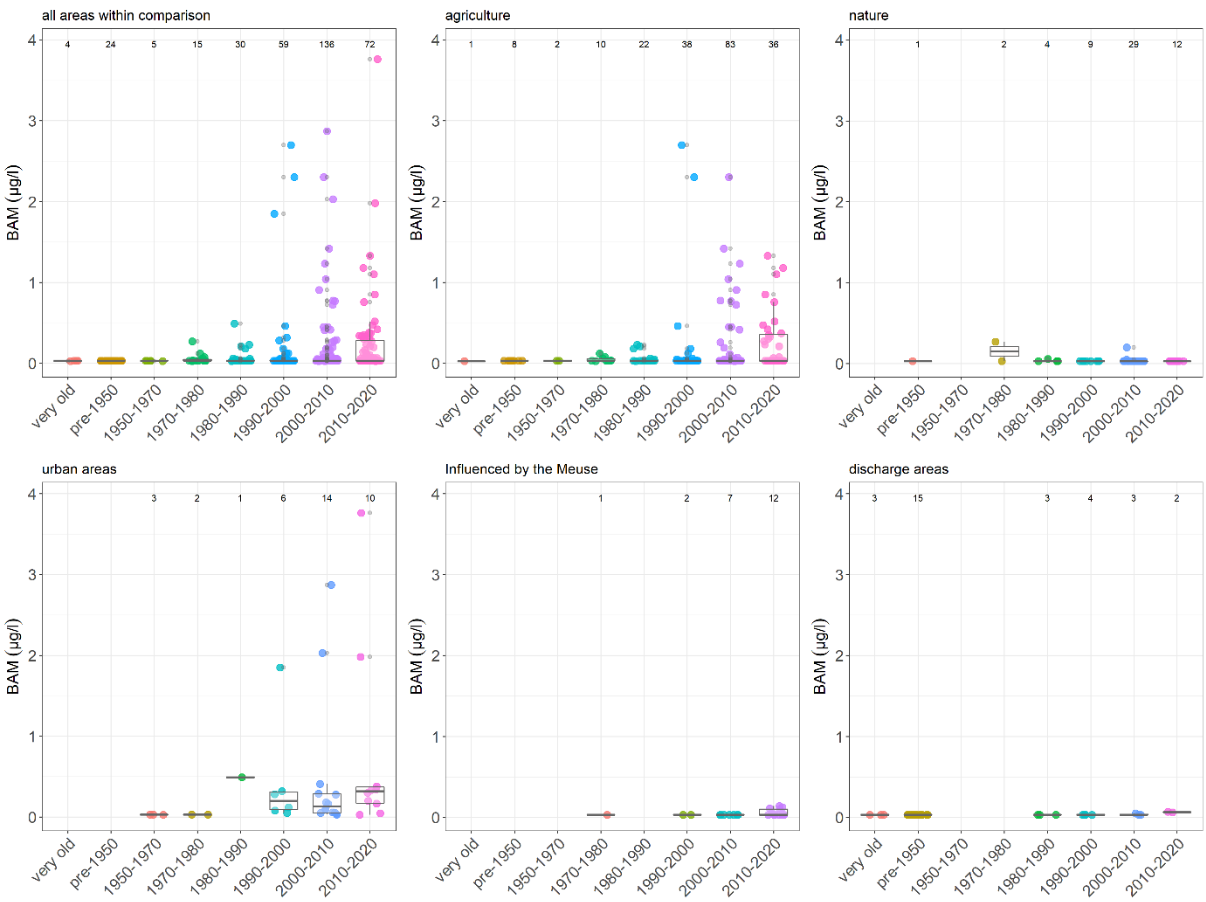

Figure 5.21. Jitters and boxplots of BAM (µq/l) per infiltration year class based on tracer ages for several land types: all areas within comparison, agriculture, nature, urban areas, areas influenced by the Meuse and discharge areas.

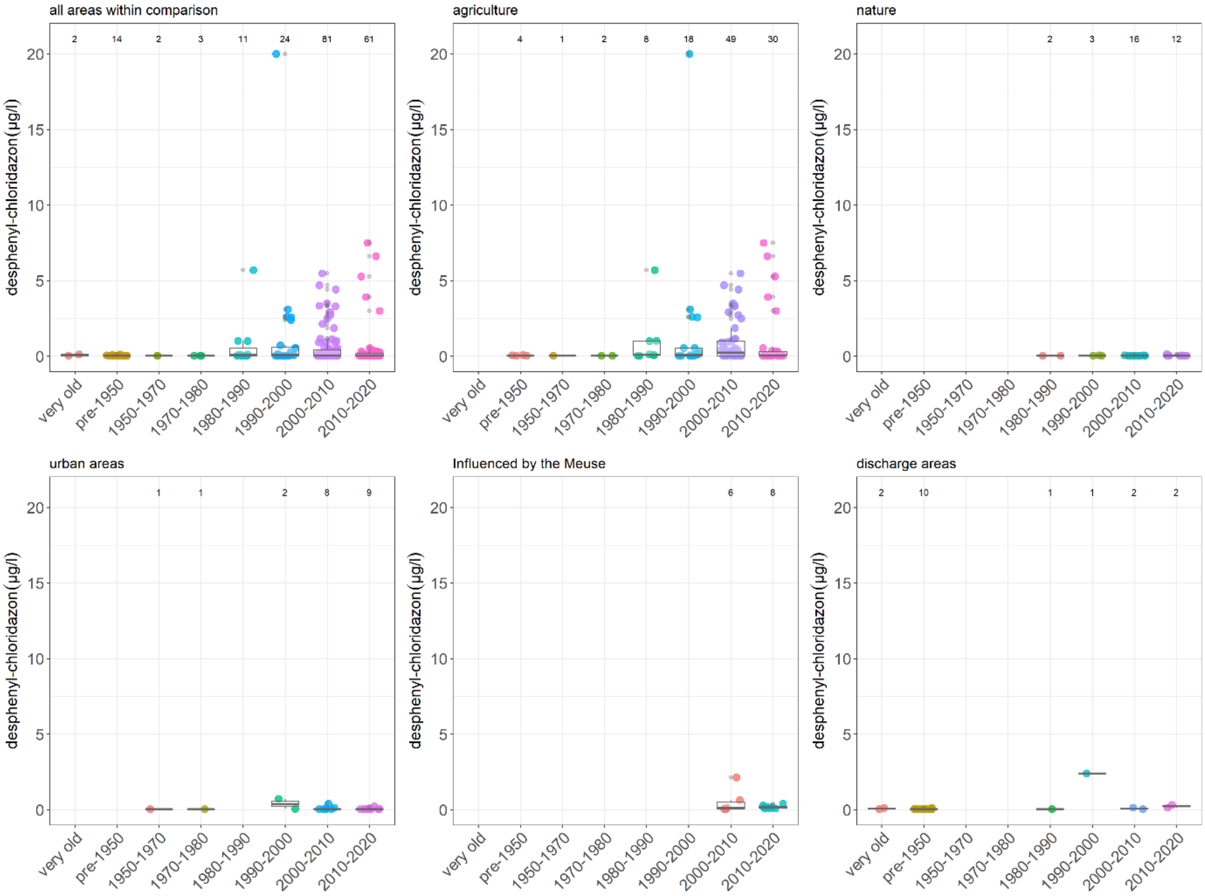

Figure 5.22. Jitters and boxplots of desphenyl-chloridazon (µq/l) per infiltration year class based on tracer ages for several land types: all areas within comparison, agriculture, nature, urban areas, areas influenced by the Meuse and discharge areas.

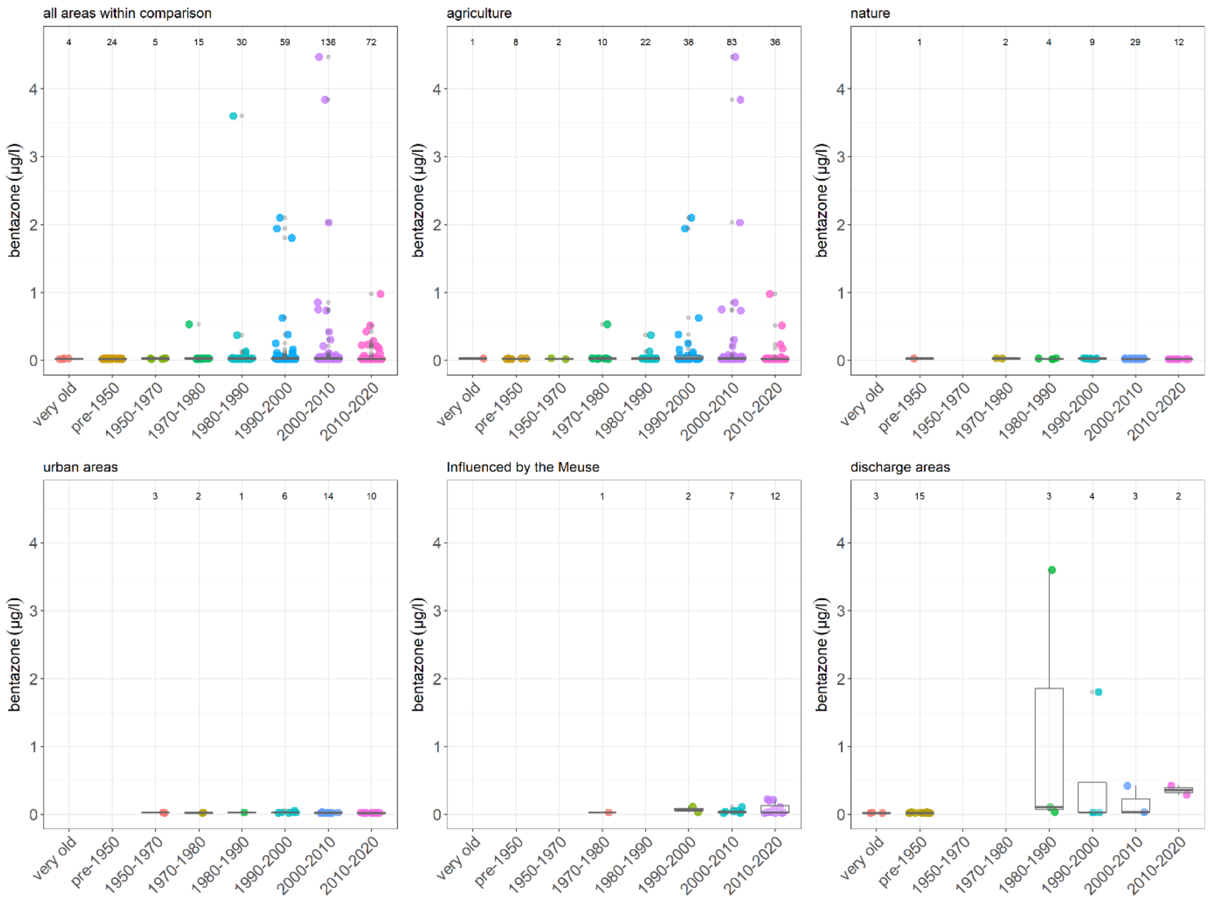

Figure 5.23. Jitters and boxplots of bentazon (µq/l) per infiltration year class based on tracer ages for several land types: all areas within comparison, agriculture, nature, urban areas, areas influenced by the Meuse and discharge areas.

5.5.2.2 Overview of tracer age patterns of pesticides

For 19 pesticides, their occurrence was related to the groundwater age tracer derived infiltration years and examined in relation to land use. Table 5.2 summarizes the results. The most frequent detected pesticides are on the top of the table, those found the least are at the bottom. The majority of pesticide hits were observed in the youngest infiltration year classes (2000-2010 and 2010-2020) and in agriculture areas. As we only related the pesticide hits to the advective flow using the infiltration year approach, we cannot rule out that degradation is partly responsible for the lower number of hits in water from the earlier infiltration periods. We will explore degradation further in HOVER Deliverable 5.4 using information on the redox status of the groundwater and possible attenuating reactions affecting the transport of pesticides and nutrients.

Table 5.2 Overview of the number of times parameters have been found per infiltration year class (based on tracer ages) and per land use.

Parameter	Remark	2010-2020	2000-2010	1990-2000	1980-1990	1970-1980	1950-1970	pre-1950	very old	Agriculture	Nature	Urban	Meuse	Discharge
BAM	dichlobenil metabolite	34	30	12	6	4				49	3	26	5	3
desphenyl-chloridazon	chloridazon metabolite	30	42	11	5			2	1	68	1	5	12	5
bentazone		13	30	14	5	1				43		1	10	9
methyl-desphenyl-chloridazon	chloridazon metabolite	11	27	2	2					37			5	
metalaxyl		4	2							6				
2-hydroxy-atrazine	atrazine metabolite	4	1							2			3	
2-methylthiobenzothiazole		3	5	1	2					5	4		1	1
ethofumesate		3											1	2
MCPP		2	10	7	1	1				18			3	
diuron		2											2	
metaldehyde		1	6							4			3	
N,N-diethyl-toluamide	metabolite tolylfluanide		2	2		1				4	1			
dinoterb			2							2				
glyphosate			1					1		1				1
glyphosate-ammonium			1										1	
AMPA	glyphosate metabolite			1				2		2				1
carbendazim					1					1				
chloridazon					1					1				
metalochlor														

5.5.3 Comparison of measured and modelled patterns of pesticides

As for oxidation capacity, nitrate and sulphate, the pesticide patterns were compared with infiltration year classes based on the tracer ages, Modpath ages and MT3D ages. The idea behind the comparison between was to see whether modelling may help to unravel pesticides transport patterns in case no tracer ages would be available (Figure 5.24, Figure 5.25 and Figure 5.26). The orange circles show the most important deviations between tracer- MODPATH ages and between tracer-MT3D ages.

In contrast to the tracer age evaluation (left graphs) the model evaluation shows significant numbers of pesticide hits for BAM, desphenyl-chloridazon and bentazon in the infiltration periods “very old”, “pre-1950” and “1950-1970”. This means that pesticide hits in groundwater are registered for periods for which leaching of the pesticides is not logical, given their production, application and authorisation history. For the patterns of the pesticides become disturbed and are wrongly associated with old groundwater and recharge before 1970. As sensible pesticide patterns were found using the tracer ages, we conclude that the problem arises from the overestimation of ages for a number of observation wells using the national model. We believe this is an inherent property of the spatial resolution of the model which uses 250x250 m grid cells. Observation wells that are not located in the centre of these grid cell may be characterized by downward groundwater flow indicating local recharge conditions, whereas the 250x250 ml grid cell may be characterized by an overall net discharge flux.

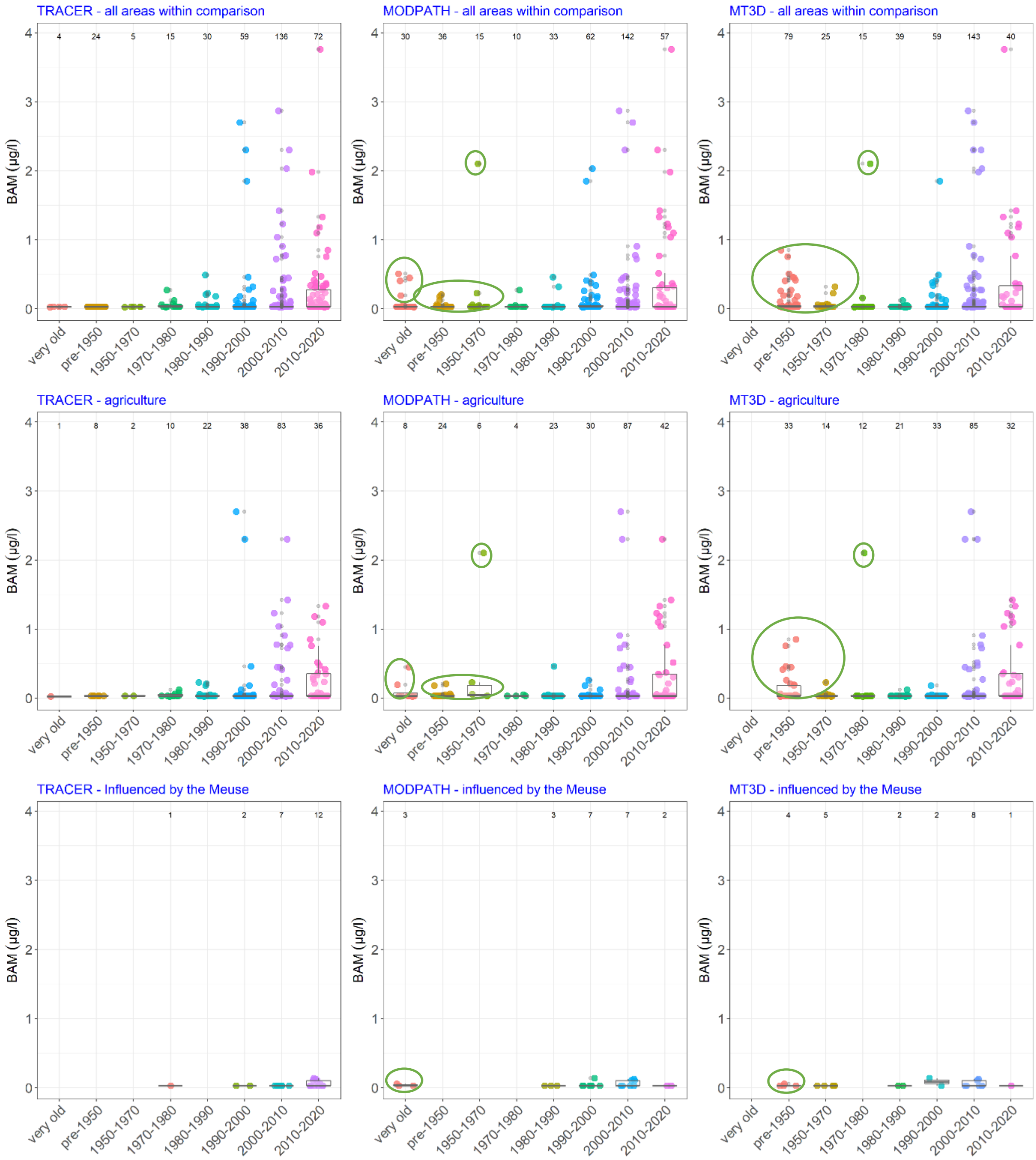

Figure 5.24. Jitters and boxplots of BAM (µg/l) per infiltration year class based on tracer ages (left column), MODPATH ages (middle column) and MT3D ages (right column) for all areas within comparison (upper row), agriculture (middle row), areas influenced by the Meuse (bottom row). The orange circles show the most important differences between tracer-MODPATH ages and between tracer-MT3D ages.

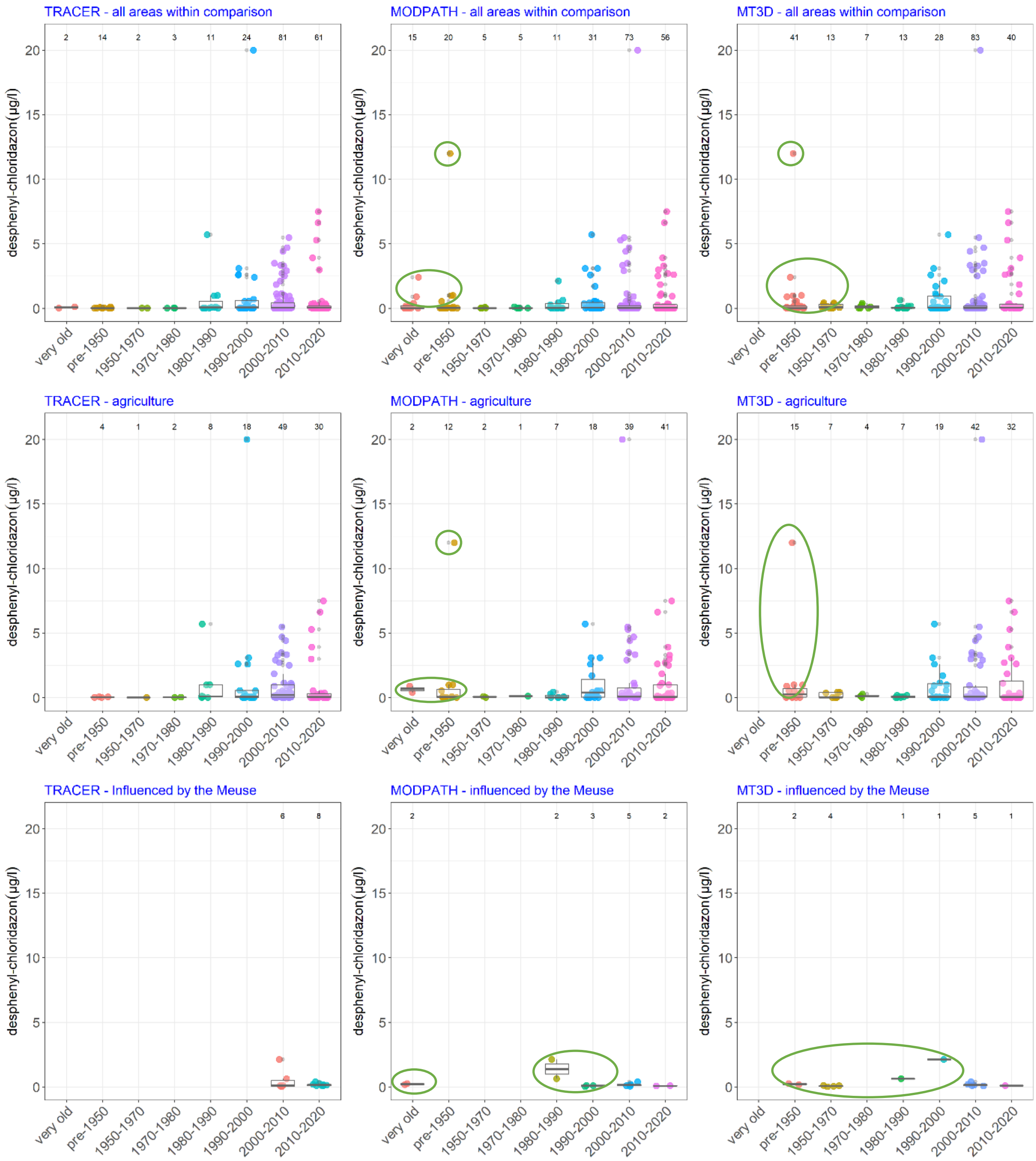

Figure 5.25. Jitters and boxplots of desphenyl-chloridazon (µg/l) per infiltration year class based on tracer ages (left column), MODPATH ages (middle column) and MT3D ages (right column) for all areas within comparison (upper row), agriculture (middle row), areas influenced by the Meuse (bottom row). The orange circles show the most important differences between tracer- MODPATH ages and between tracer-MT3D ages.

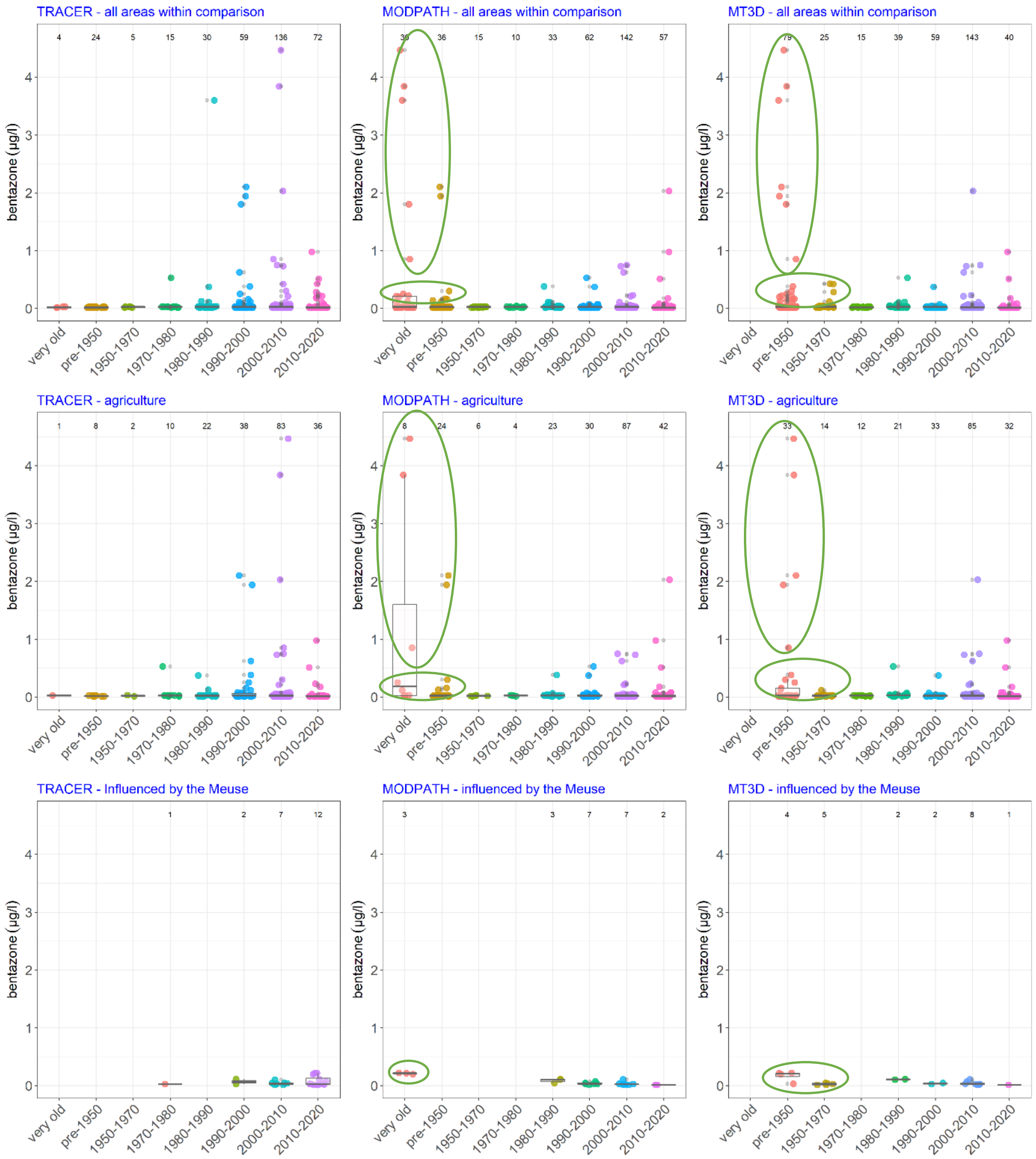

Figure 5.26. Jitters and boxplots of bentazon (µg/l) per infiltration year class based on tracer ages (left column), MODPATH ages (middle column) and MT3D ages (right column) for all areas within comparison (upper row), agriculture (middle row), areas influenced by the Meuse (bottom row). The orange circles show the most important differences between tracer-MODPATH ages and between tracer-MT3D ages.

5.6 Application of the outcomes for further application of modelling approaches

National models are useful to delineate overriding patterns of travel times and groundwater ages but fail to properly represent the travel times in specific short-screen multi-level monitoring wells. This is not completely unexpected as the coarse model discretisation of 250 x 250 of the national model cannot reflect the small scale hydrological variations which are mainly determined by the intensive drainage network which is present in the Netherlands (e.g. Broers, 2004). Though in general, a reasonable correlation exists between a large group of tracer and modelled ages, and similarities between measured and modelled ages appear for around 50% of the monitoring screens. However, a substantial proportion of monitoring wells show large deviations between measured and modelled ages. In 10-20% of the wells such a large deviation was observed leading to an overestimation of the amount of older water in the model (e.g. Figure 5.9 and Figure 5.12). As a result, patterns of nitrate and pesticides become disturbed and a number of pesticide hits and elevated nitrate concentrations are wrongly associated with old groundwater and recharge before 1970. Further works is obviously needed to start using modelled ages for evaluation of pesticides and nitrate trends. We see opportunities for pinpointing observation wells that wrongly receive too old model ages by including local information which can be subtracted from other national scale databases, such as the Local Altitude Model (AHN) or the distribution map of water resources as was applied earlier by Broers (2004). The current dataset remains valuable for validating such an approach.

5.7 Conclusions

For the Dutch HOVER pilot of the Sand-Meuse region, we evaluated the travel times for N and pesticides, using both tracer and modelling approaches. Firstly, we showed that the unsaturated zone travel times in our pilot region are typically between 0 and 2 years, which is relatively short relative to the saturated zone travel times in the region. For the saturated zone travel times, we evaluated the groundwater age as it has been determined using $^{3}H/^{3}He$ age dating. Based on these age determinations, we defined the infiltration year periods very old, pre-1950, 1950-1970, 1970-1980, 1990-2000, 2000-2010 and 2010-2020 for which we evaluated measured concentrations of nitrate, sulphate and chloride and 19 pesticides. We compared those tracer-based infiltration year patterns with model-based infiltration year patterns. For this purpose, we applied the National Hydrological Model to determine groundwater ages for each of the observation wells that were used in the tracer study, applying a particle tracking approach using MODPATH and a single solute transport approach using MT3DMS. Although the modelled patterns resemble the tracer patterns for the solutes and pesticides studied, we also observed that the spatial resolution of the model did not allow for a proper age determination of part of the wells, generally leading to an overestimation of the groundwater age in part of the wells. As a result, modelled pesticide hits and elevated nitrate concentrations were unjustly linked to infiltration periods before 1970. For future use of the models, a further investigation is foreseen for incorporating existing knowledge into better modelling practice, as the modelling approach would eventually enable us to extrapolate the findings of the pilot study to the larger country. In any cases, tracer sets such as available for Noord-Brabant and Limburg remain a prerequisite for validation of modelling approaches, and model may never be detailed enough to completely grasp the variability in groundwater ages which is strongly determining the transport of contaminants.

6 DENMARK

Klaus Hinsby, Annette Rosenbom, Sachin Karan
GEUS, Denmark

6.1 Nitrate transport modelling and monitoring in Denmark

6.1.1 Introduction

Nitrate transport and degradation in groundwater has been documented and modeled in several projects on nutrient transport in sandy aquifers in Denmark since environmental action plans and monitoring and strategic research programs were launched in the 1980s (Postma et al., 1991). Postma et al (1991) demonstrate leakage of nitrate from agricultural soils to groundwater aquifers and efficient degradation at the redox boundary at about 16 meter below the water table or 30 m below surface at the Rabis Creek test site in the central region of Jutland. This region has a relatively deep unsaturated zone and a relatively long travel time through the unsaturated zone for Danish conditions of 16 m and 4 years, respectively (Postma et al., 1991; Engesgaard et al., 2004).

The travel time in the saturated zone to the redox boundary at about 30 m below surface in the Rabis Creek test site where both nitrate (Postma et al., 1991) and CFC-gases (Hinsby et al., 2007) are degraded is simulated to 20-25 years based on tritium profiles (Engesgaard et al., 1996; Engesgaard and Molson, 1998). Postma et al. (1991) found that nitrate pollution from agriculture accelerated the downward migration of the redox boundary by a factor of five and that the estimated rate, which at the Rabis Creek site was controlled by the contents of pyrite, was a few centimeters a year.

Recognizing the nitrate threat to water supply wells and associated aquatic ecosystems several Danish action plans introduced mitigation measures that have reduced nitrate concentrations and nitrogen loadings to associated aquatic ecosystems (Blicher-Mathiesen et al., 2020; Hansen et al., 2011, 2019; Thorling et al., 2019). However, neither in groundwater nor in surface water the reduced loadings have been sufficient to comply with the groundwater quality criteria or good ecological status for all estuaries and coastal waters in many Danish regions (Hansen et. al 2019, Hinsby et al., 2008, 2012). Furthermore, the nitrogen concentrations and loadings recently stagnated or even increased in some areas (Blicher-Mathiesen, 2020; Thorling et al., 2019). Hence, groundwater chemical status in groundwater bodies in Denmark continues to be a significant challenge for water management in Denmark (Thorling et al., 2019; Henriksen et al., 2020; Hinsby et al. 2008, 2012) as in the rest of Europe (EEA, 2020) not the last considering recent findings about health effects of nitrate in drinking water (Schullehner et al., 2018) and that the major part of Danish coastal and transitional waters still do not comply with good status objects of the Water Framework Directive (Hinsby et al., 2012).

The studies by Postma et al. (1991) is believed to represent conditions in unconfined sandy aquifers of significant parts of Jutland similar to the conceptual model in Figure 6.1. Generally, travel times through the unsaturated zone and the oxic part of the aquifers are typically rather short in Denmark and with 50% being in the range of <5 and < 30 years and 98% being < 60 years in monitoring wells installed at depths between 1 and 110 meters below surface, respectively, for unconfined sandy aquifers (Figure 6.1). This is supported by recent modelling studies (Blicher-Mathiesen, 2020) and the fact that effects of mitigation measures of the action plans initiated in the late 1980’s has been observed in monitoring wells two decades later (Hansen et al., 2011). This observation was only possible due to dating of the monitoring wells, as the median travel time is around 30 years according to tracer estimated groundwater ages of groundwater monitoring wells (Thorling et al, 2019).

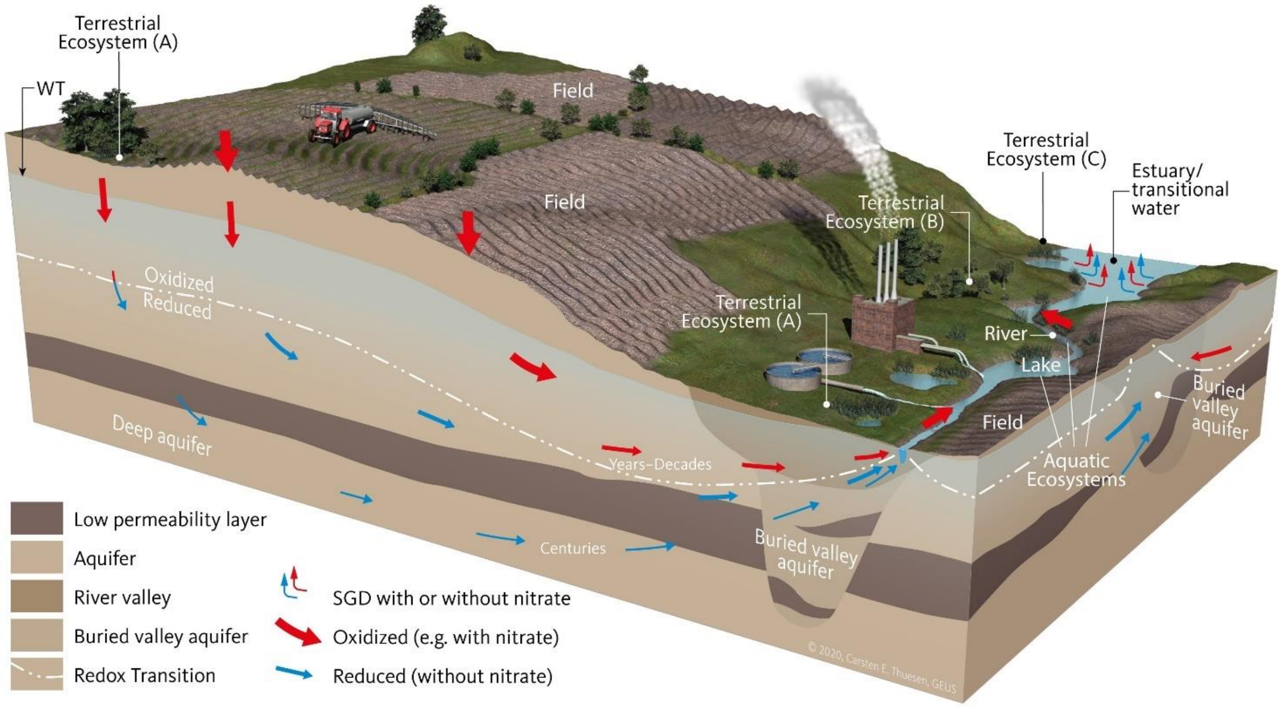

Figure 6.1 Conceptual model of nitrate transport and typical travel times in an unconfined sandy aquifer setting typical for mid-northern parts of Jutland – red-orange parts of Figure 6.4 – (modified after Hinsby et al. 2008, 2012).

Travel times from soils to streams in drained areas with confined and semi-confined aquifers systems in eastern Jutland and eastern Denmark in general is much shorter and typically between <<1 to < 5 years as illustrated in the conceptual model in Figure 6.2.

In areas with shallow redox boundaries (Figure 6.2) the nitrate leaching from the agricultural areas are primarily a threat to the groundwater associated aquatic ecosystems and less to water supply wells as the redox boundary is relatively close to the surface. This means that nitrate is typically reduced before it reaches the water supply wells in anoxic parts of the aquifers.

In drained areas on the other hand groundwater with high nitrate concentrations travels very fast to surface water via drain pipes (Figure 6.2). In such a system it is generally the total nitrogen loading to the associated aquatic ecosystem, which is of concern (Hinsby et al., 2008, 2012). Groundwater nitrate concentrations of 50 mg/l in such areas would typically breach maximum acceptable loadings to coastal ecosystems and require threshold values to be established below this concentration according to the Water Framework and Groundwater directives (Hinsby et al. 2008, 2012).

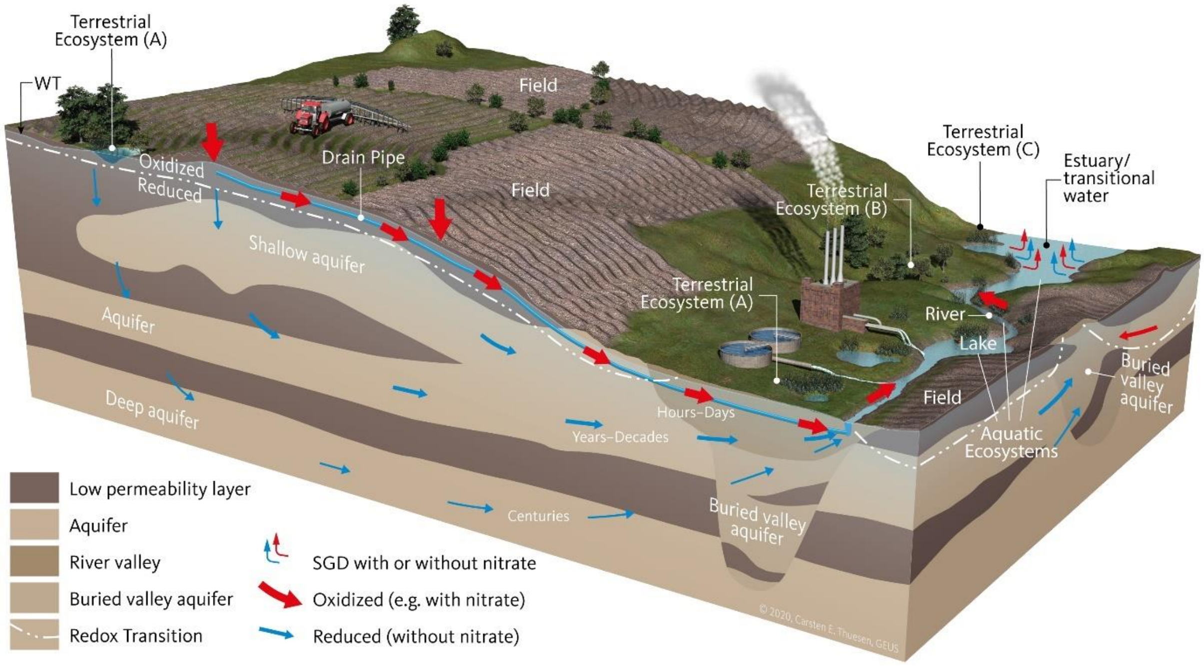

Figure 6.2 Conceptual model of nitrate transport and travel times in a typical aquifer system in eastern Denmark (modified after Hinsby et al. 2008., 2012).

Figure 6.3 below provides a brief overview of the evolution of nitrate concentrations in groundwater in Denmark as function of time (A) and depth (B) in intakes of the Danish groundwater monitoring program "GRUMO" (Thorling et al., 2019).

The upper panel of the Figure (A) demonstrate that the average groundwater concentrations were above the drinking water standard (DWS) of 50 mg/l of nitrate during approximately the first decade of the program 1990 -2000, at the DWS for about the next decade (2000-2010), and generally below the DWS for the latest decade 2010 – 2020. Recent studies, however, demonstrate that a significant part of the monitoring intakes again exhibits increasing trends (Hansen et al., 2019; Blicher-Mathiesen et al., 2020).

The lower panel of the Figure (B) illustrate that approximately 25% of the monitoring intakes have nitrate concentrations above the DWS in groundwater in the upper 20 meters of the subsurface, while no nitrate is found at a depth of more than 80 meters primarily because nitrate has been reduced at the redox boundary (Figure 6.6).

A.

B.

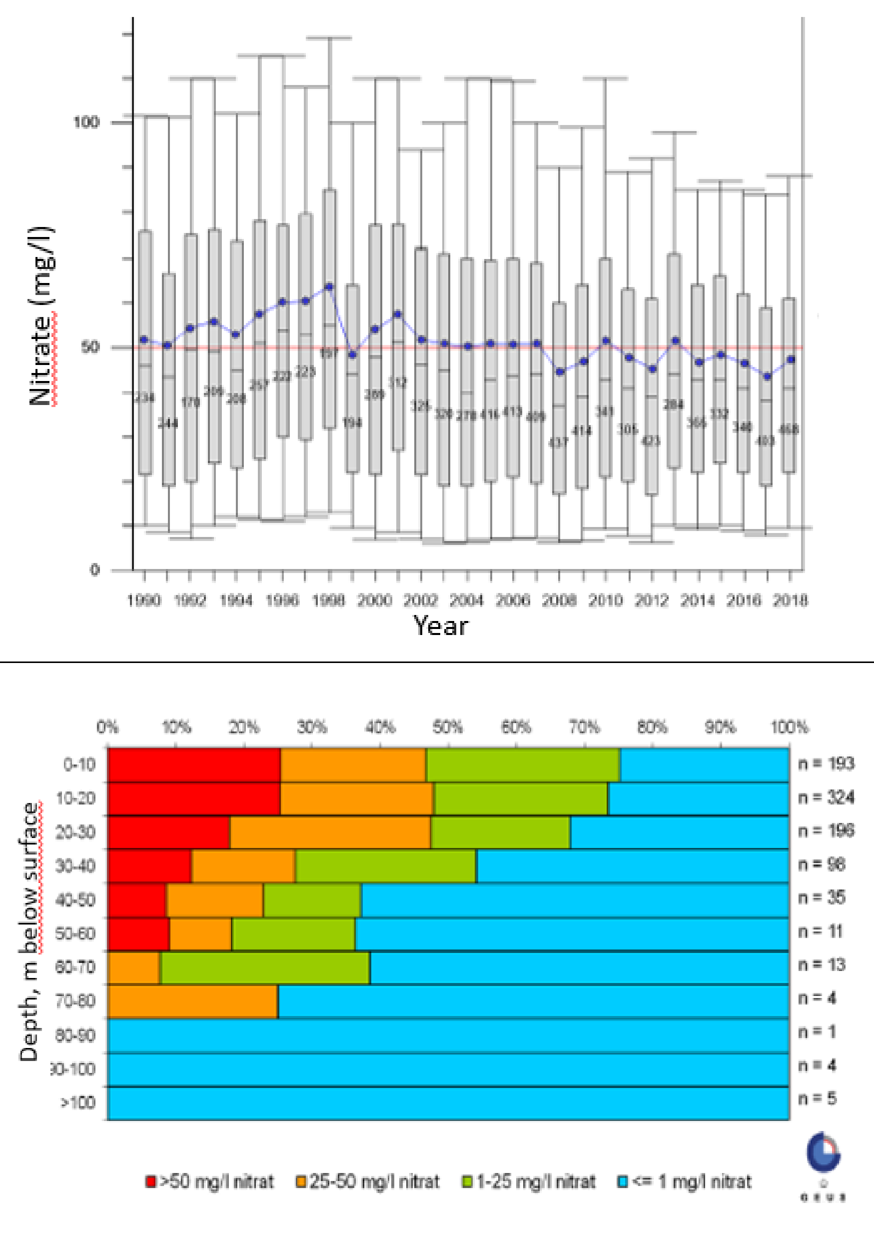

Figure 6.3 Distribution of nitrate concentrations in intakes of the Danish groundwater monitoring program – A) Mean, median and 10, 25, 75 and 90 % fractiles of nitrate concentrations in intakes from 1990 -2018; B) Percentages within the defined concentration intervals at different depth intervals. (Thorling et al., 2019)

The distribution of nitrate in Danish monitoring and water supply wells can be further assessed at public GEUS web services (GEUS, 2020).

The Danish National Water Resources Model and especially the Danish Nitrogen Model used for simulating the fate and retention of nitrate in groundwater and surface water, nitrogen loadings to groundwater associated aquatic ecosystems as well as nitrate travel times from soils to groundwater, streams, lakes and the sea are briefly described in the following.

6.1.2 Introduction to the Danish National Water Resources Model (the DK-model)

The DK-model is a mechanistically, transient and spatially distributed groundwater-surface water model developed by the Geological Survey of Denmark and Greenland (GEUS) in MIKE SHE (Henriksen et al. 2003, 2008, Højberg et al., 2013). MIKE SHE model code are coupled physics-based models for overland flow, unsaturated flow, groundwater flow, and fully dynamic channel flow, including all their complex feedbacks and interactions. MIKE SHE also includes processes such as vegetation-based evapotranspiration, irrigation, snowmelt and water quality (DHI, 2020).

The DK-model includes a 3D hydrogeological description of the entire 43.000 km2 in Denmark in seven sub-models initially in 1 km x 1 km resolution and based on a national interpretation by GEUS, but gradually updated e.g. on data from regional water authorities and lately based on data from the national groundwater mapping program. By continuously incorporating new knowledge, the model is kept up to date ensuring a common framework for assessments at various scales by different authorities, consultants and reseachers. Recently a 500 x 500 m model was released (Stisen et al., 2019) as the latest development and used for groundwater quantitative and chemical status assessments (Troldborg et al., 2020, Thorling et al., 2020).

The hydrogeological interpretation has been utilised in a 3D georeferenced delineation of groundwater bodies and aquifers for the entire country. Linking the model to the national database on groundwater extraction and chemical analysis, assessments of groundwater quantitative and chemical status at the groundwater body level, required for the implementation of the WFD, have been made possible (Troldborg et al., 2020; Thorling et al., 2020).

Since the first application of the DK-model in 2003 to assess the national exploitable groundwater resource, the model has constituted an essential tool in the assessment of the quantitative and chemical status of Danish groundwater at national (Højberg et al., regional and local levels (e.g well fields). Utilising predicted climate changes the model has further been applied to estimate future changes in groundwater levels and recharge at national scale. These results have been used by local authorities in a screening phase for formulating climate change adaption strategies. Combining the DK-model with supplementary models on nitrogen leaching and retention in surface water systems, the DK-model is the backbone of national model on nitrogen transport, supporting the national regulation on nitrogen.

6.1.3 Nitrate transport modelling with the National Nitrogen Model (NNM)

The National Nitrogen Model (NNM, Hojberg et al. 2015) is developed in a collaboration between Geological Survey of Denmark and Greenland (GEUS) and the University of Aarhus (AU) based on the DK-model developed by GEUS and the NLES4 model an empirical model estimating N-loss from the root zone and a statistical model estimating nitrogen retention in surface water (stream, lakes and wetlands) developed by AU.

The DK-model / NNM enables simulation of nitrate travel times through the unsaturated and saturated zones as well as nitrate or total nitrogen loadings to surface waters and ecosystems e.g. Lakes and estuaries (coastal and transitional waters) including effects of climate change (Sonnenborg et al., 2012) and assessments of criteria and threshold values according to EU policy and guidance (Hinsby et al., 2012). Besides applying the model for simulation of nitrate transport in large regional simulations in the seven sub-models of NNM, the model may also be used for establishing boundary conditions for model simulations in a higher resolution at much smaller scale (e.g. Hinsby et al., 2012, Hinsby et al., in prep.).

Figure 6.4 shows that the thickness of the unsaturated zone in major parts of Denmark is below 2 meters, but that thicknesses above 10 meters (with travel times more than a few years, Figure 6.5) exist especially in the central and northern part of Jutland e.g. at the Rabis Creek site (Postma et al., 1991, Engesgaard et al., 2004; Hinsby et al. 2007). Travel times through the unsaturated zone (up to more than 20 years) computed by the DK-model is shown in Figure 6.5. The conceptual setting in the major parts of the red areas in Figure 6.4 corresponds to the situation described by Figure 6.1, while the major parts of the blue areas corresponds to the situation described by Figure 6.2.

Nitrate transport through the unsaturated zone

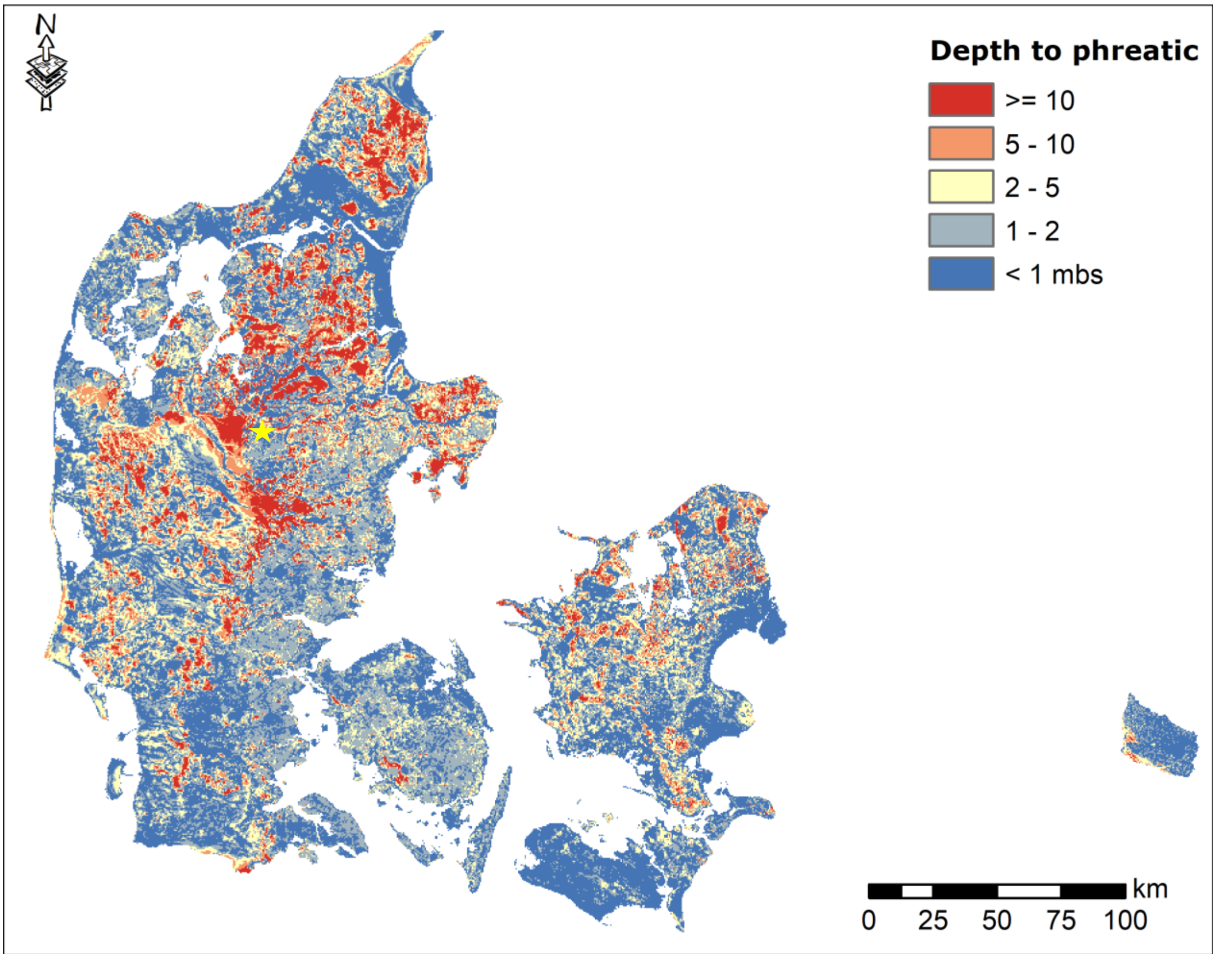

Figure 6.4 Depth to phreatic water tables in Denmark as simulated by the DK-model (Hojberg et al., 2013). Yellow Star in central Jutland indicates location of the Rabis Creek test site (Postma et al., 1991; Engesgaard et a., 1996, 2004; Hinsby et al., 2007).

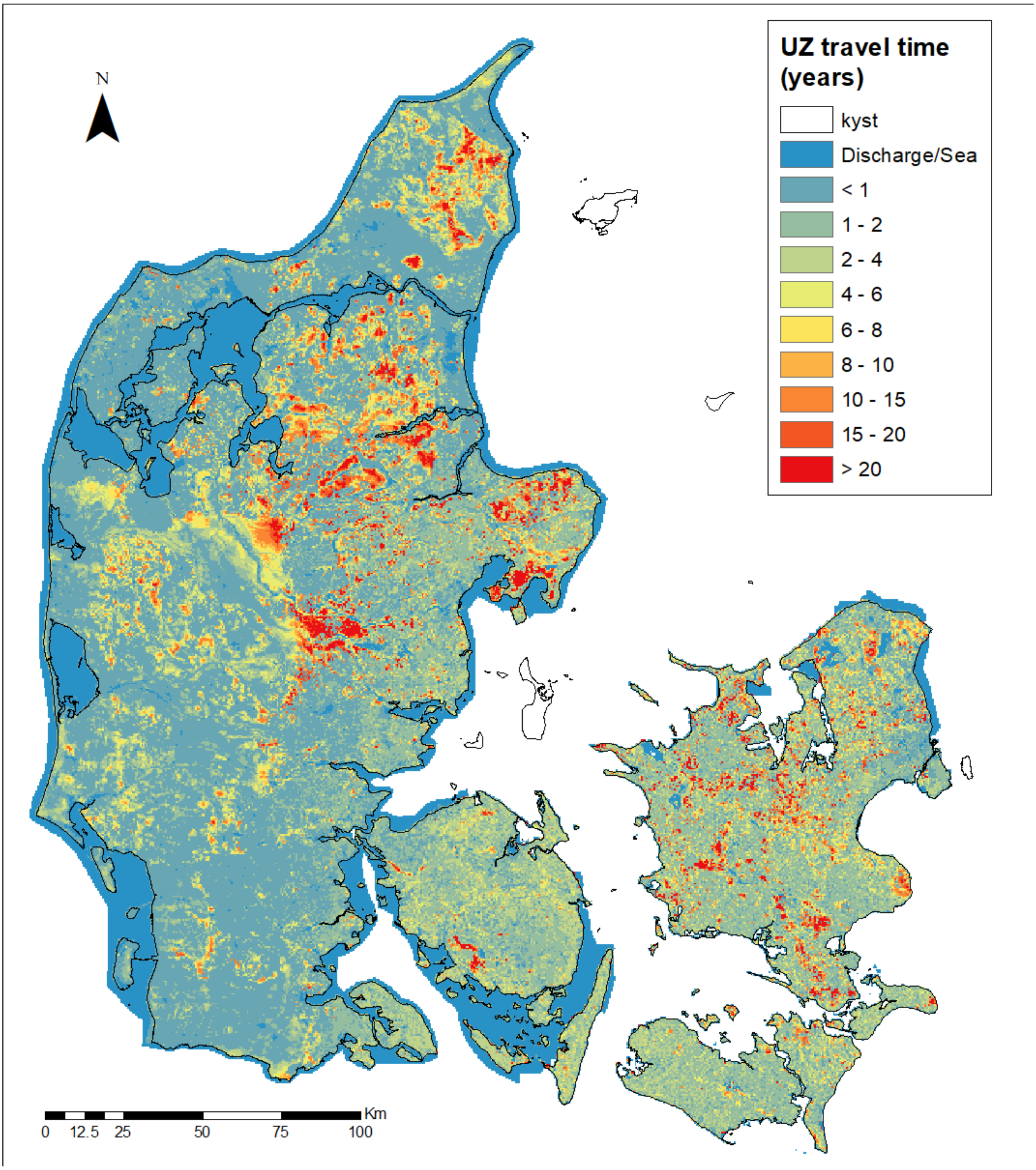

Figure 6.5 Travel times through the unsaturated zone in Denmark computed by the DK-model (unpublished data).

Nitrate transport in the saturated zone

Nitrate is found to depth of up to 80 meters below surface (Figure 6.3) or even more in some rare situations typically in areas described by the conceptual model in Figure 6.1. In contrast the redox boundary or transition zone in drained clay till areas is typically found within the upper five meter of the surface as shown by Figure 6.2. In these areas the nitrate is transported by tile drain systems to streams. Hence, leaking nitrate from agricultural soils primarily threatens water supply wells in areas described by the conceptual model in Figure 6.1 to which the travel time is typically 3-4 decades, while it primarily threatens groundwater associated aquatic ecosystems in areas described by the conceptual model in Figure 6.2, where the travel time in the saturated zone e.g. through tile drain systems is days to a few years.

One of the most important factors for nitrate transport through the saturated zone is the location of the redox boundary (Figure 6.1 and Figure 6.2). This was recently mapped and modelled by Koch et al. (2019) at national level (Figure 6.6) and by Kim et al. (2019) at local level. The information on the location of the redox boundary is needed in order to be able to estimate 1) Nitrate travel times in the oxic zone (Figure 6.7), 2) nitrate retention in groundwater (Figure 6.8) as well as total nitrate retention in groundwater and surface water between soils and the coast (Figure 6.9).

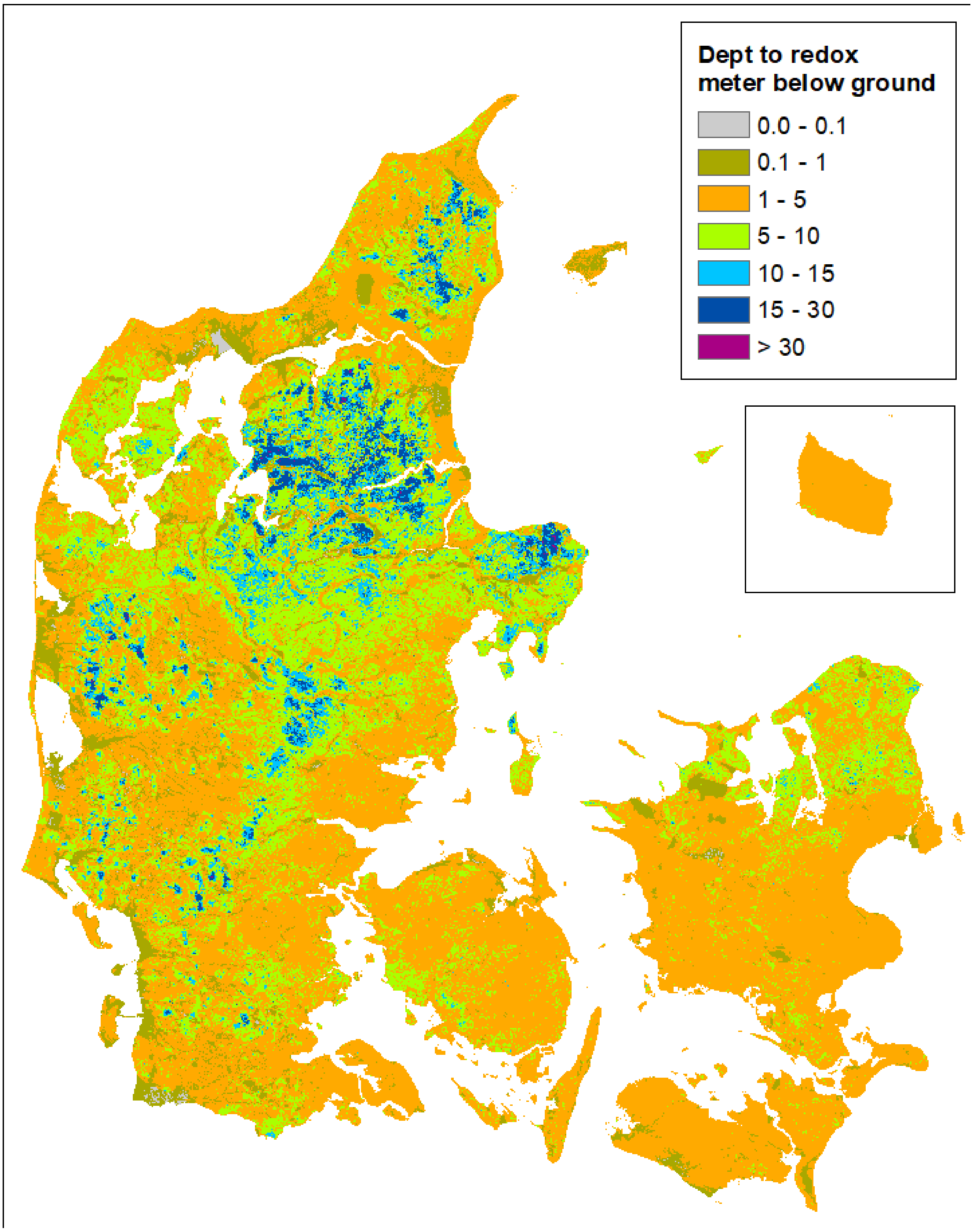

Figure 6.6 Depth to the redox boundary (transition zone) based on geological information in the borehole database of GEUS, expert knowledge and Machine Learning (Koch et al., 2019).

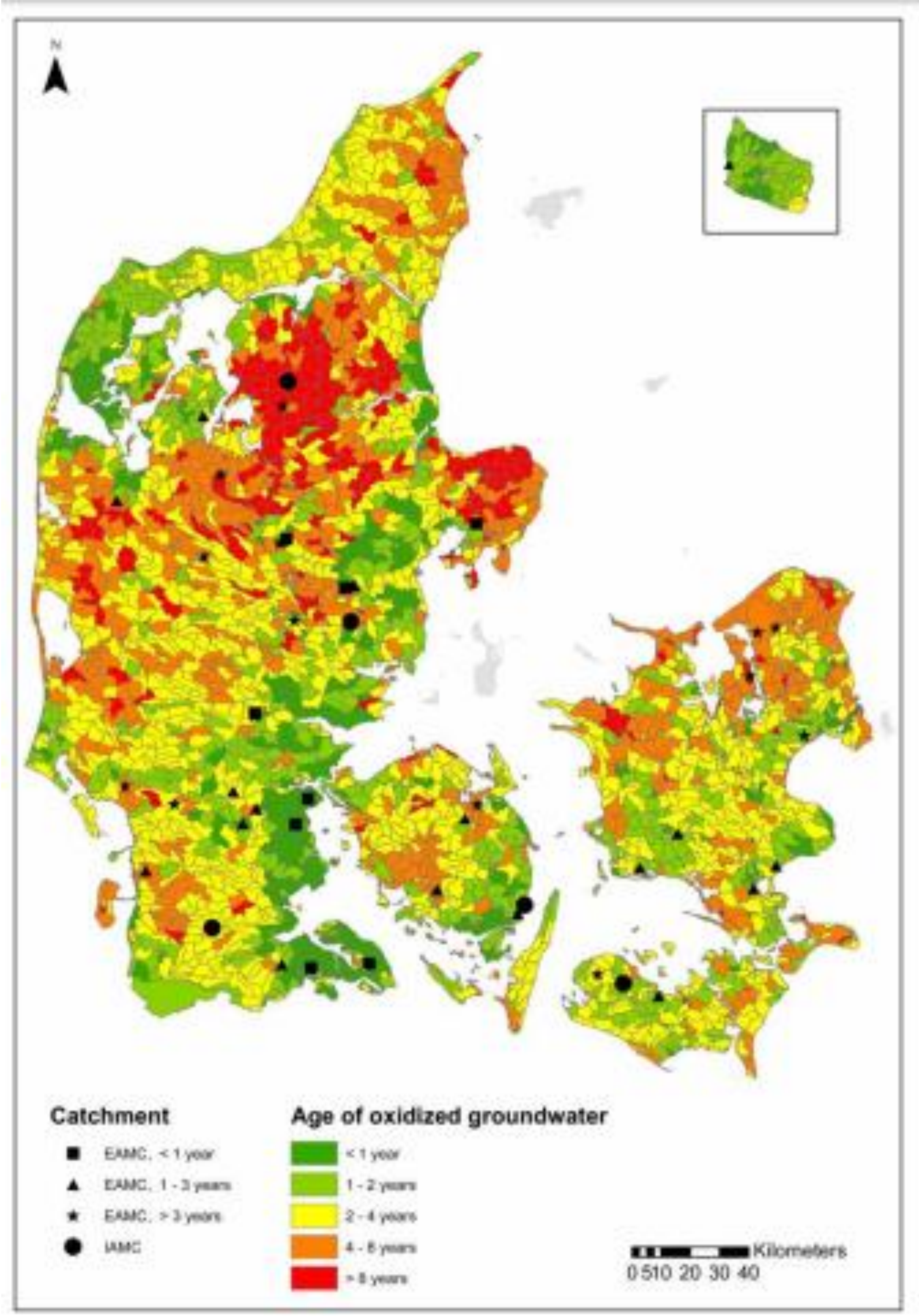

Figure 6.7 Age of oxic groundwater as simulated by NNM.

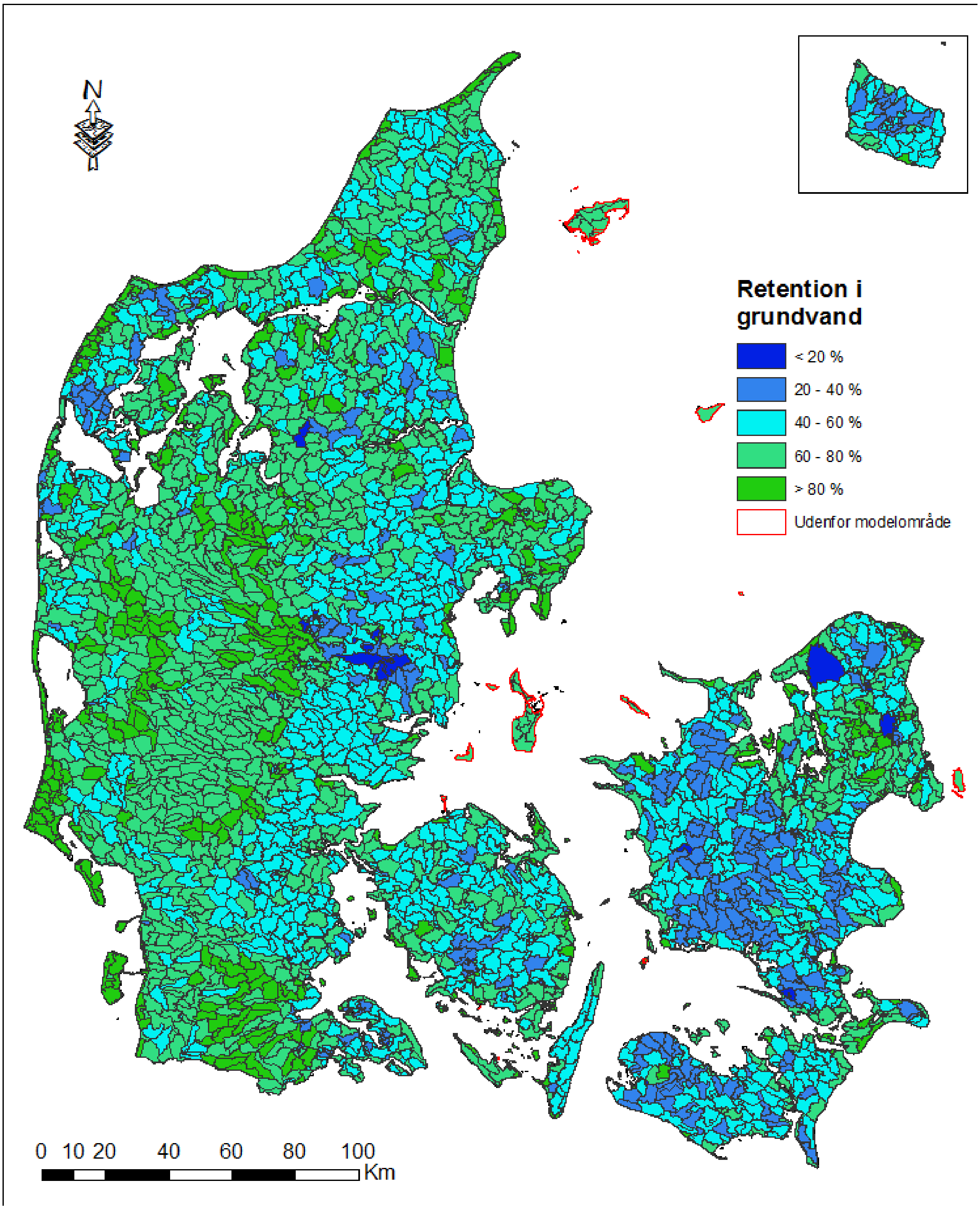

Figure 6.8 Nitrate retention in groundwater (Højberg et al., 2015).

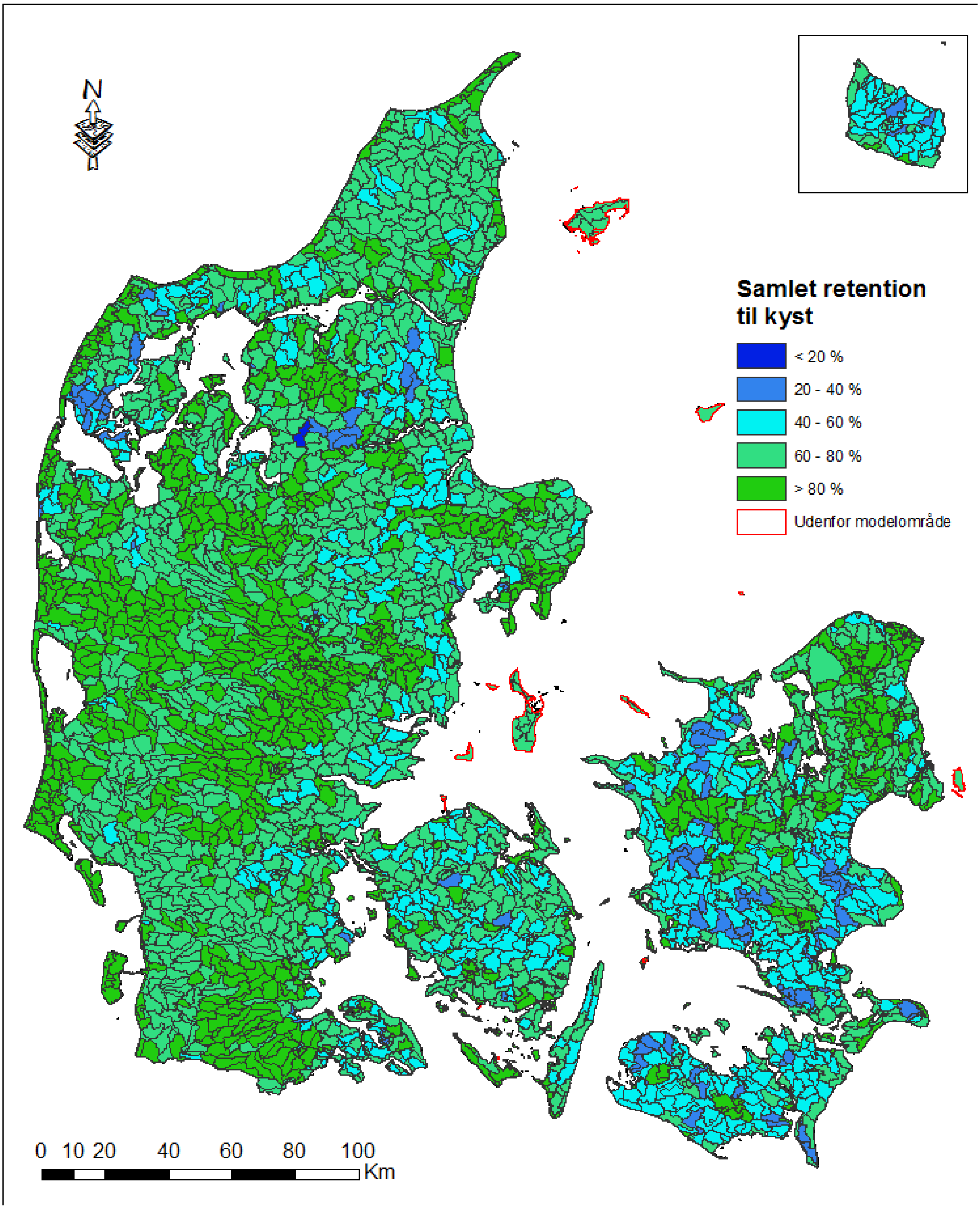

Figure 6.9 Total nitrate retention in groundwater and surface water between soils and the coasts (Højberg et al., 2015).

Figure 6.10 show travel times from the water table to streams in Denmark as simulated by the National Nitrogen Model excluding the transport through the unsaturated zone. Total transport times from soils to streams can be assessed by combining information shown in Figure 6.4, 6.5 and 6.10 assuming groundwater travel times to streams in drained areas are less than a year.

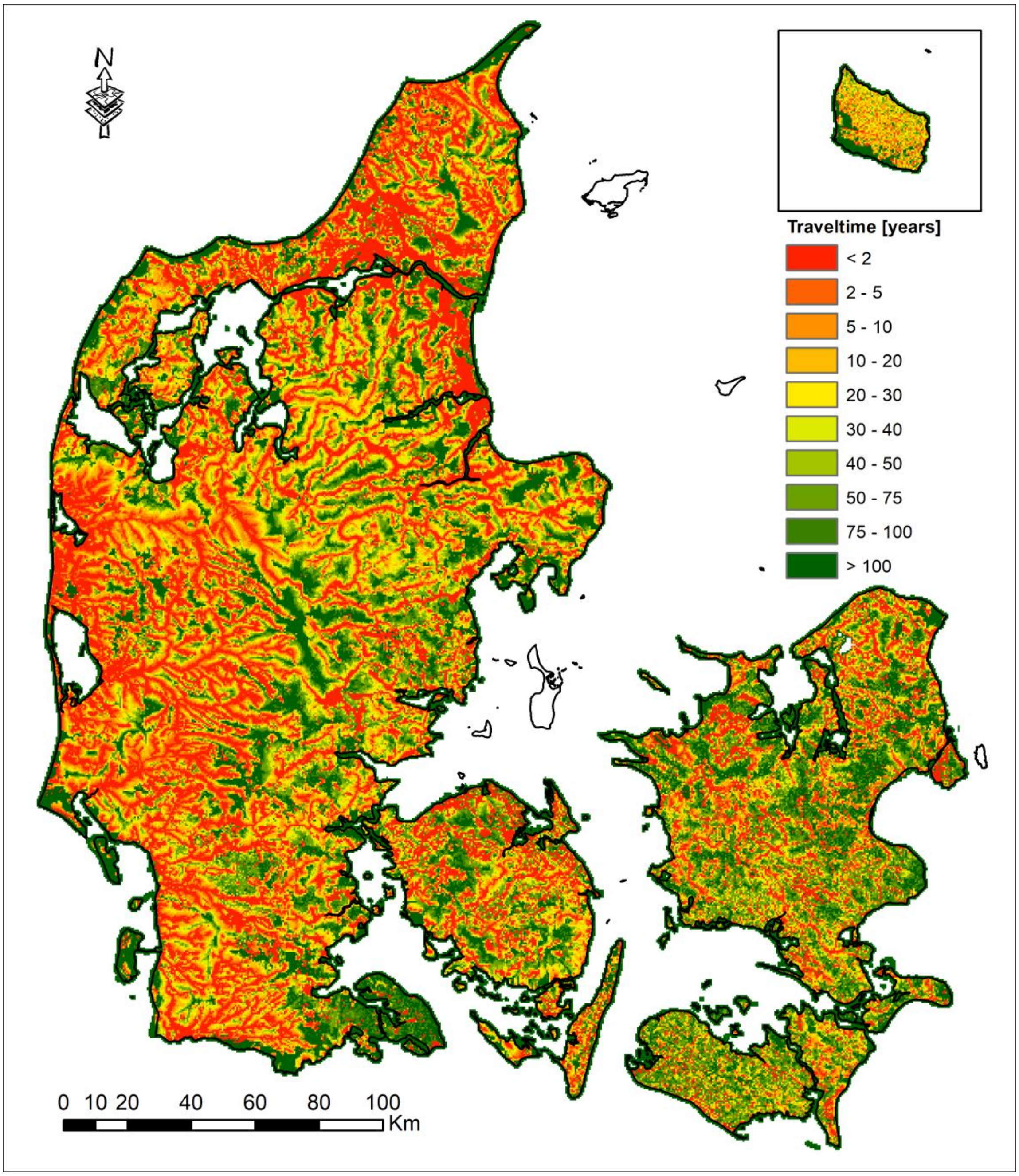

Fig. 6.10 Travel times from the groundwater table to streams as simulated by the NNM.

6.2 Lessons learnt from field-scale modelling of pesticide and nitrate leaching as monitored in the Danish Pesticide Leaching Assessment Programme

6.2.1 Introduction

Based on the detailed hydrogeological characterisation of the agricultural fields (two sand; four clayey tills) included in the Danish Pesticides Leaching Assessment Programme, PLAP, a variety of modelling studies have been conducted. The basis for the model studies is the PLAP data with comprehensive monitoring data on agricultural practices, water balance and presence of contaminants (e.g. pesticides, the degradation products of pesticides and nitrate; Rosenbom *et al.*, 2015, and Ernstsen *et al.*, 2015) in water at 1 m depth and the groundwater underneath the fields. The studies presented include:

A. Long-term leaching of degradation products of pesticide applied to potatoes on **sandy field** (Rosenbom *et al.*, 2009)
B. Spatial degradation potential of pesticide in the plough layer of a **clayey till field** (Rosenbom *et al.*, 2014)
C. Impact of lower boundary conditions and presence of worm burrows on the assessment of leaching risk of pesticides through a **clayey till field** (Karan *et al.*, in submission; Rosenbom *et al.*, 2020)
D. Impact of soil domain specific hydraulic and retardation processes on pesticide leaching through a macroporous **clayey till field** (Johnsen *et al.*, 2020)
E. Assessing the degree of preferential nitrate leaching through **clayey till field** (Nagy *et al.*, 2020)
F. Quantifying the degree of preferential flow through three different geological **clayey till** tile drained settings (Study is ongoing).

Common for these studies is that they evaluate the ability of the numerical models to capture the monitored leaching from the soil surface of the field into the upper part of the groundwater zone. This include the models used in regulation of pesticides (FOCUS-models; FOCUS 2000) and nitrate (empirical model NLES4-model applying the crop-database of the mechanistic Daisy-model), which primarily consider the unsaturated zone as isolated from the saturated zone.

6.2.2 Modelling approach

6.2.2.1 Overarching framework

All the modelling studies listed above are based on a holistic model approach in regard to the water movement through the soil profile of the field. This is conducted by applying the Richard's equation and hence avoid splitting the profile up in an unsaturated and a saturated part. By doing so, it is possible to account for the measured dynamics in the water balance given by the highly variable climate conditions and fluctuating groundwater table shown in PLAP to vary between 1 to 5 metres. The monitoring results from the fields reveal:

- a piston-like flow through the **sandy fields**, where certain solutes are exposed to kinetic sorption.
- a flow and solute transport through the low-permeable **clayey till fields** that is controlled by the presence of hydraulic active and well-connected burrow and fractures.

Therefore, to cope with the presence of kinetic sorption and a dominating preferential flow and solute transport through the variably-saturated zone, it requires models that can handle such highly nonlinear systems. The following models have been used:

A. The **one-dimensional**, process oriented, dual-permeability **MACRO** model 5.1 (Larsbo *et al.*, 2005) for water flow and reactive solute transport in soil. MACRO is included in the European regulation of pesticides for surface water and groundwater (FOCUS DG SANTE). In the model, the soil pore space is divided into a micropore and a macropore domain characterized by different flow rates and thus solute concentrations. For the micropore domain water flow is governed by Richards' equation and solute transport by the convection-dispersion equation. For the macropore domain water flow is gravity driven applying the kinematic wave and the solute transport assumed to be solely convective. The lateral exchange of water and solutes between pore domains is calculated using approximate, physically based, first-order expressions. Additional model assumptions include first-order kinetics for degradation in each of four "pools" of pesticide in the soil (micro- and macropores, solid and liquid phases), together with instantaneous or kinetic sorption.
B. The numerical code, **COMSOL Multiphysics** (COMSOL Inc., Stockholm, Sweden). It was used for **three-dimensional** finite element simulations considering the spatial mineralization data from the variably-saturated upper meter of a clayey till. The following interfaces were applied as governing equations: (i) Richard's Equation Interface for the variably-saturated water flow, (ii) the Solute Transport Interface accounting for biodegradation, and iii) Coefficient Form PDE (Partial Differential Equation) Interface for the growth in biomass described by Monod-kinetics.
C. The **one-dimensional**, process oriented, dual-permeability, public domain, **HYDRUS-1D** software package version 4.17 (Šimůnek et al., 2018). It was used to simulate transient flow and pesticide transport through a one-meter soil columns based on PLAP-data from a clayey till field with and without a macropore. Opposed to MACRO where the flow in the macropore domain is solved with a kinematic wave equation assuming gravity driven flow, HYDRUS numerically solves flow in both micro- and macropore domains with the Richards' equation.
D. As in B. **COMSOL Multiphysics** was applied for a **three-dimensional** finite element simulation for i) representing the hydraulics and sorption isotherms of eight different domains in a five-meter clay till profile, ii) incorporating the fluctuating groundwater table and the mapped burrows and fractures, and iii) applying coherent realistic variations in net precipitation and depth to the groundwater table.
E. The **one-dimensional**, process oriented, dual-permeability model **Daisy**. It is a Soil-Plant-Atmosphere system model, which incorporates modules describing plant water uptake and plant growth, C-N turnover, heat and N-dynamics in the soil. Like the MACRO model, a macropore module is included in Daisy and described by Mollerup (2010) (https:/daisy.ku.dk/publications). The macropore module is tested as described in a technical report prepared for and published by the Danish Environmental Protection Agency (Hansen *et al.*, 2010a, b and 2012). Unlike MACRO, the macropore is a vertically oriented discrete feature, and not a domain, and is characterized by physical properties, such as length and diameter.
F. As in A. the **one-dimensional MACRO**-model version 5.2 was applied. **PEST** (Doherty, 2015) was applied to optimize the MACRO-model-setups for three clayey tile-drained PLAP-fields reported by Barlebo *et al.* (2007).

6.2.2.2 Source Term

The modelling study A-D focus on describing the leaching of pesticides and/or their degradation products:
A. The degradation product diketometribuzin of the herbicide metribuzin, which was applied to potato plants on two sandy fields.
B. The herbicide MCPA applied to clayey till directly.

C. The fungicide tebuconazole applied to greens and the herbicide MCPA applied to fairways situated on clayey till.
D. The fungicide tebuconazole applied to spring barley on a clay till field, where after glyphosate was applied.

whereas the study E and F focus on the leaching of:
E. Nitrate as an outcome of 10-years nitrogen applications (slurry, manure and fertilizers) on a clayey till field based on detailed agricultural management data.
F. Bromide as an outcome of 2-4 bromide applications (30 kg ha^{-1} KBr) during approximately 20-years at three different clayey till fields.

All studies except study C attempt to capture the leaching caused by actual applications conducted on PLAP-fields.

6.2.3 Key results / Outcome of modelling

The key results of the modelling study A-F are as follows:

A. The ability of regulatory models to accurately simulate leaching of pesticides has been evaluated, but little is known about model's ability to accurately simulate long-term leaching of degradation products (Rosenbom *et al.,* 2009). A PLAP study on the dissipation and sorption of metribuzin, involving both monitoring and batch experiments, concluded that desorption and degradation of metribuzin and leaching of its primary degradation product, diketometribuzin, continued 5-6 years after application, and thus posing a risk of groundwater contamination. Based on this study, the ability of the numerical regulatory model MACRO (FOCUS, 2000) to accurately simulate long-term leaching of metribuzin and diketometribuzin was evaluated. When calibrated and evaluated with respect to both water and bromide balances and applied assuming equilibrium sorption and first-order degradation kinetics as recommended in EU pesticide authorization procedure, MACRO was unable to accurately simulate the long-term leaching of metribuzin and diketometribuzin. In fact, the concentrations in the soil were underestimated by up to six orders of magnitude. By introducing alternative kinetics, it was possible to capture the observed leaching, thus underlining the necessity of accounting for long-term sorption and dissipation characteristics when using models to predict the risk of groundwater contamination.

B. The potential for pesticide degradation varies greatly at centimetre-scale in agricultural soils (Gonod *et al.*, 2006). The study in B aimed to answer if such small-scale spatial heterogeneity affects the leaching of the biodegradable pesticide 2-methyl-4-chlorophenoxyacetic acid (MCPA) in the upper meter of a variably-saturated clayey till? A realistic spatial variation in degradation potential was extracted from data from a PLAP-similar clayey till where 420 mineralization curves over five depths were measured (Badawi *et al.*, 2013). Monod kinetics was fitted to the individual curves to derive initial degrader biomass values, which were incorporated in a reactive transport model to simulate heterogeneous biodegradation. Six scenarios were set up using COMSOL Multiphysics to evaluate the difference between models having different degrader biomass distributions (homogeneous, heterogeneous, or no biomass) and either matrix flow or preferential flow through a soil matrix with a worm burrow. The study revealed that MCPA leached only when degrader biomass was absent and preferential flow occurred. Thus, based on degradation potential measured from the clay till PLAP fields, the small-scale spatial heterogeneity in initial degrader biomass within each measured soil matrix layer had little effect on the leaching.

C. The EU regulatory model scenarios do not represent realistic hydrogeological settings with preferential flow pathways and fluctuating groundwater levels, nor do they account for fate properties of pesticides in commercial products. To assess the consequence of this measured fate properties of tebuconazole (Badawi *et al.*, 2016) and MCPA as pesticides and in commercial products were implemented in simulations with realistic hydrogeological conceptualizations. The mobile MCPA leached in higher concentration with fluctuating groundwater levels compared to fixed groundwater levels, whereas tebuconazole (TBZ) did not leach due to stronger sorption in the upper 30 cm for this type of soil setting (K_d up to 93.5 L Kg^{-1}). MCPA was simulated with preferential flow pathways incorporated and showed substantial increase in leaching even for scenarios where MCPA was not leaching without the pathways. Additionally, with preferential flow pathways, the increase in leached concentrations going from fixed groundwater levels to fluctuating groundwater levels was further enhanced. This demonstrated that it is imperative in leaching risk assessments of pesticides to groundwater to account for the impact of formulation on pesticides fate properties, apply realistic soil and boundary condition including fluctuating groundwater levels, and incorporate preferential flow pathways where it is pertinent (Karan *et al.*, in submission).

D. The soil profile of a clayey till encompass many domains (i.e., different soil matrix and discontinuities with coating such as worm burrows and fractures) with different hydraulic- and pesticide fate properties. Since such knowledge of domain properties is not applied in the current regulation of pesticides (FOCUS, 2000), a study was conducted to investigate the impact on future leaching risk assessments. Based on a field-to-lab study by Albers *et al.* (2019) a profile of a clayey till together with its domains and their sorption of TBZ and glyphosate was built into a model incorporating realistic climate and groundwater table data. The simulations showed distinct leaching of TBZ caused by low sorption (K_d =2.4 L Kg^{-1}) and degradation in all the investigated domains combined with a highly fluctuating water table in clayey till. Glyphosate also leached to 1 meter's depth in spite of the strongly sorbing soil domains, and also to 4.5 meters depth in scenarios with reduced sorption and no degradation. The leached concentrations of glyphosate were, however, much lower compared to that of TBZ and caused by the low sorption and the fast water flow in the worm burrow and the fracture. This study shows that leaching of sorbing pesticides to the upper groundwater, may be caused by a combination of fast flow in macropores to the upper groundwater due to strong precipitation incidents and a fluctuating water table, low sorption in mineral soil horizons. The findings reveal a need for addressing the different hydraulics and pesticides fate properties of domains in clayey tills, when assessing the leaching risk of pesticides.

E. Numerous numerical model concepts have been developed in order to describe nitrate leaching and possible routes of nitrogen at field scale, often without being evaluated in regard to their ability to account for dominant preferential transport as measured through clayey tills (Ernstsen et al., 2015) and the coherent lack of denitrification in the macropore domain. Hence, do future leaching risk assessments need to account for preferential transport of nitrate? A model concept, including macropores, capable of capturing the water and bromide balance of a clayey till PLAP field within a 10-years' timeframe, was able to predict water transport to drainage, dry matter and N-yield of the harvested crops. While the same model concept was unable, with the standard default denitrification abiotic water reduction factor, to predict dynamics and quantity of N-loss to drainage. Modification to the water reduction function affecting denitrification was hence conducted to reduce the denitrification with approximately 50 % from a seasonal average of 75 kg N ha^{-1} to 35 kg N ha^{-1} while 48 % to 80 % of the total N-loss to drainage had to be preferentially transported from the plow layer. This study, therefore, reveals that, by not accounting for preferential transport and coherent denitrification, there is a high risk of underestimating leaching of nitrate to surface waters and groundwater.

F. As written by Nimmo (2020) *Current science places unequal emphasis on the two main unsaturated flow modes, with a longstanding tradition of relegating preferential flow to a secondary or negligible role. In reality, however, preferential flow is a normal unsaturated zone occurrence almost everywhere*. This comply with that many models used in leaching risk assessments are based on piston flow assumptions. To highlight the necessity of accounting for preferential flow, this study (ongoing with the aim of being published in early 2021) focus on quantifying the degree of preferential flow of water through different clayey tills.

To predict leaching of pesticides, their degradation products, and nitrate observed in the monitoring of the PLAP-fields, the model studies show:

- that **sandy fields** assuming piston flow (chromatographic flow) in the model can to some extent be acceptable. When predicting solute transport through the sandy media it is though imperative to be aware of compounds having long-term sorption and dissipation characteristics when using models to predict the risk of groundwater contamination. Long-term leaching of degradation products from pesticides applied on potatoes plants can be predicted applying the MACRO-model with non-validated lab or field kinetic fate parameters. These parameters are not possible to obtain in the lab where realistic conditions for soil are not possible to be obtain in the long-term. Hence, models cannot correctly simulate long-term leaching given the lack of obtaining parameters for fate representing the long-term – here new methods are needed.
- that in **clayey till fields** preferential transport through macropores like burrows and fractures is more the rule than the exception like described by Nimmo (2020) and hence piston flow cannot be assumed. Knowledge from model studies such as the mentioned, followed by methods to parameterize models accordingly (Moeys et al., 2012), have not yet been incorporated in the regulation of:
    - pesticides why only one of the nine FOCUS groundwater scenarios (Chateaudun; FOCUS, 2000) accounts for preferential transport.
    - nitrogen/nitrate.

The above findings extracted from the extensive monitored PLAP-fields seems to indicate in general that fate processes control the leaching through sandy fields with high effective porosity, while it seems to be the preferential transport and hence the hydrogeological setting that is decisive for the leaching through clay till fields with low effective porosity. Due to the dynamic hydrogeological regime of preferential leaching and groundwater table fluctuations occurring at especially the clayey till fields, the models for such soils need to include realistic upper and lower boundary conditions by applying coherent climate and hydrological data. If these representative hydrogeological conditions are not applied in current models for regulation of pesticides and nitrogen there is a high risk of underestimating the real leaching of pesticides, degradation products and nitrate to groundwater and surface water. These field-scale model studies of leaching through the variably-saturated zone to the drainage and groundwater elucidate the necessity of being able to account for dominating transport pathways of contaminants from the source at the soil surface to the groundwater and surface waters when conducting large scale modelling.

7 CROATIA (DRAVA)

Ozren Larva, Željka Brkić
HGI-CGS, Croatia

7.1 Introduction

The study area is located in the northwestern part of Croatia along the borders with Slovenia and Hungary (Figure 7.1). It is a lowland area with developed hydrographic network. It belongs to Central and Eastern Europe region and covers 2500 km^2 (Figure 7.1).

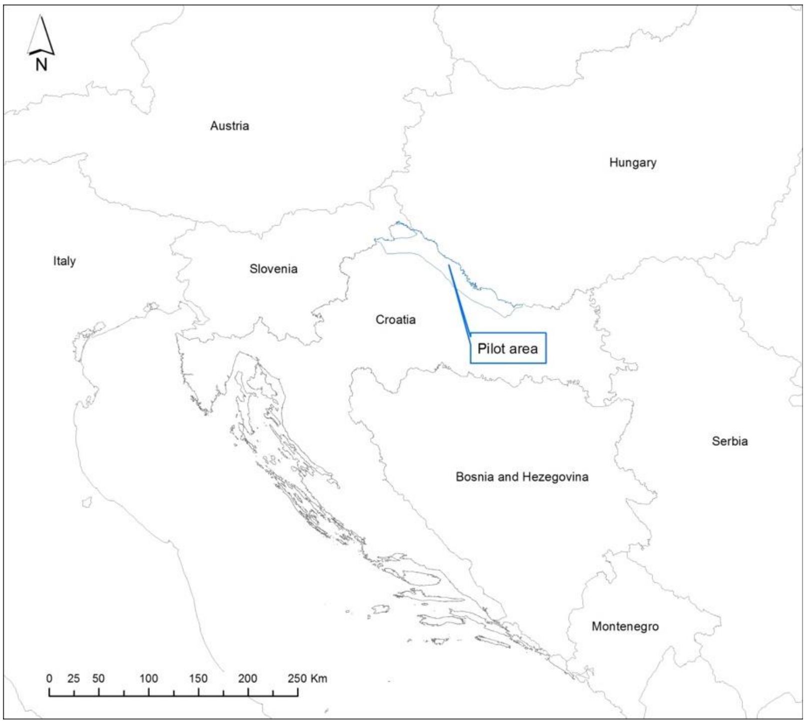

Figure 7.1. Location of the pilot area

Four groundwater bodies are, partly or completely, within the pilot domain – two of them entirely (Varaždinsko podurčje and Novo Virje), whereas the other two (Međimuirje and Legrad-Slatina) participate only with the parts where alluvial aquifer is developed (Figure 7.2, Table 7.1).

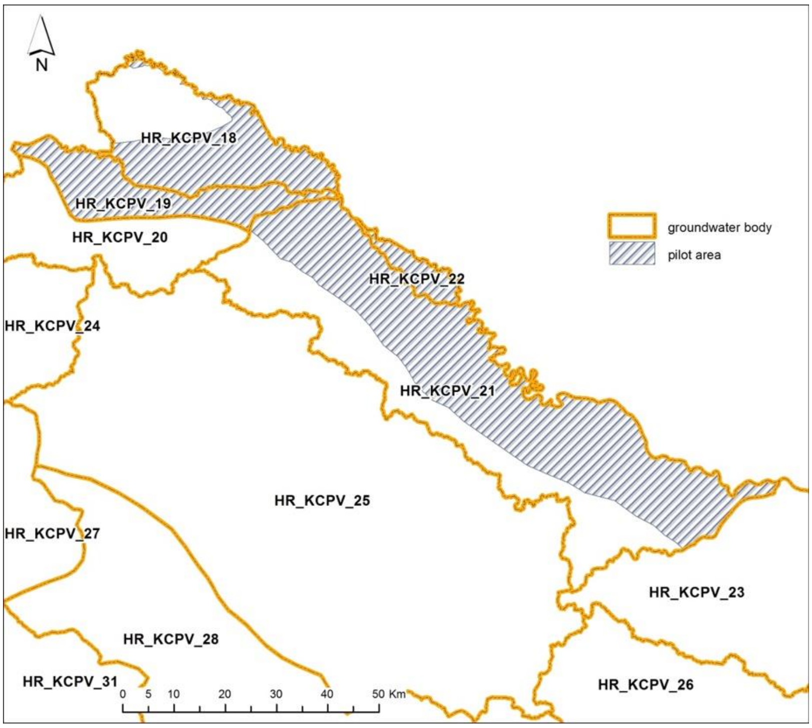

Figure 7.2. Pilot area and groundwater bodies

Table 7.1. Groundwater bodies within pilot area

Name	Code	GWB total area [km^2]	GWB area within the pilot area [km^2]
Međimurje	HR_KCPV_18	747	455
Varaždinsko područje	HR_KCPV_19	392	392
Novo Virje	HR_KCPV_22	97	97
Legrad-Slatina	HR_KCPV_21	2364	1516

The Drava aquifer is a transboundary alluvial aquifer spreading over Slovenian and Croatian territory. It is an important source of groundwater, mainly for public water supply, but also for irrigation and industry water supply purposes. Besides, there are a number of groundwater dependent ecosystems (GWDEs) and Natura 2000 protected areas, mostly spread along river banks of the Drava river. Over the years, high concentrations of nitrate in groundwater have become a main concern for both public water supply and GWDEs, especially in the western part of the alluvial aquifer in Croatia. Consequently, Varaždinsko područje is a groundwater body with bad chemical status according to the requirements of Water framework directive (WFD).

Over the years, the behaviour of nitrate in both unsaturated and saturated zones of the Drava alluvial aquifer has been investigated in several studies with the aim to increase understanding of their fate in aquifer systems (Karlović et al., 2019; Brkić et al., 2019; Marković et al., 2018; Marković et al., 2015; Larva, 2008; Marković, 2007). This section reports the research approach focused on estimation of travel times in USZ, and evolution of NO_3 concentrations in groundwater.

7.1.1 *Hydrogeology*

The Drava aquifer system is formed during Pleistocene and Holocene as a consequence of neotectonic activity and sedimentation of material which was transported mainly from the Alps by the Drava river. It is stretched parallel to the Drava river (Figure 7.3). There are three types of sediments at the ground surface that are all of Quaternary age: Pleistocene loess, Holocene Aeolian sands and Holocene alluvial deposits which cover the majority of the pilot area.

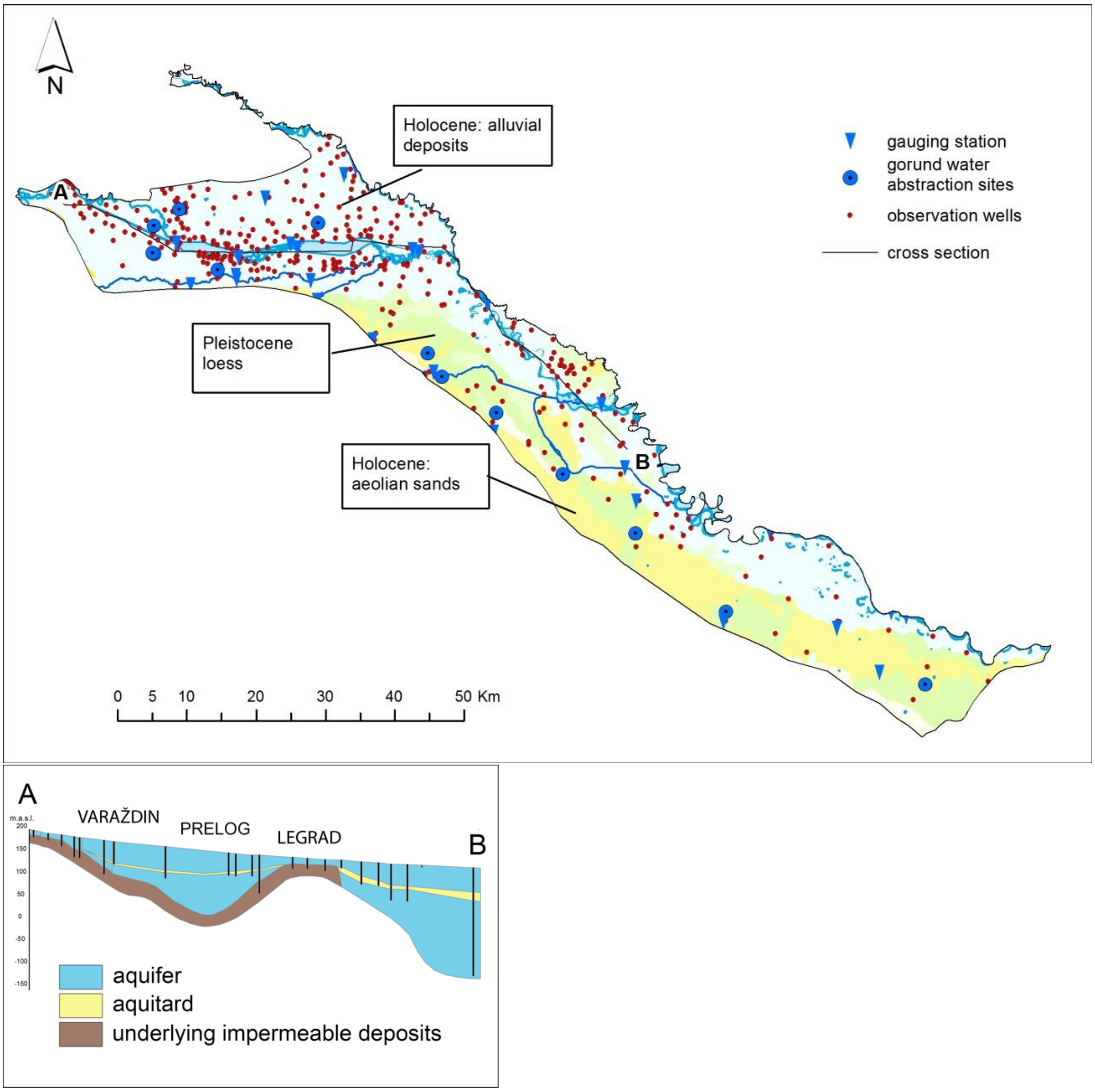

Figure 7.3. Geological map (HGI, 2009) and hydrogeological cross section

Gravel and sand prevail in the lithological composition of the aquifer, with small shares of silt and clay (Babić, et.al., 1978; Urumović, 1971; Urumović, et.al., 1990). The thickness of the aquifer system increases in the southeast direction. It is around 10 m at the utmost western part of the pilot area (Figure 7.4). Further on downstream, it gets gradually thicker, reaching 150 m near Prelog (Urumović,

1990) and 250-300 m in the central and eastern parts of investigated area (Figure 7.3). In the same direction the average grain size decreases as a consequence of energy loss of the Drava river.

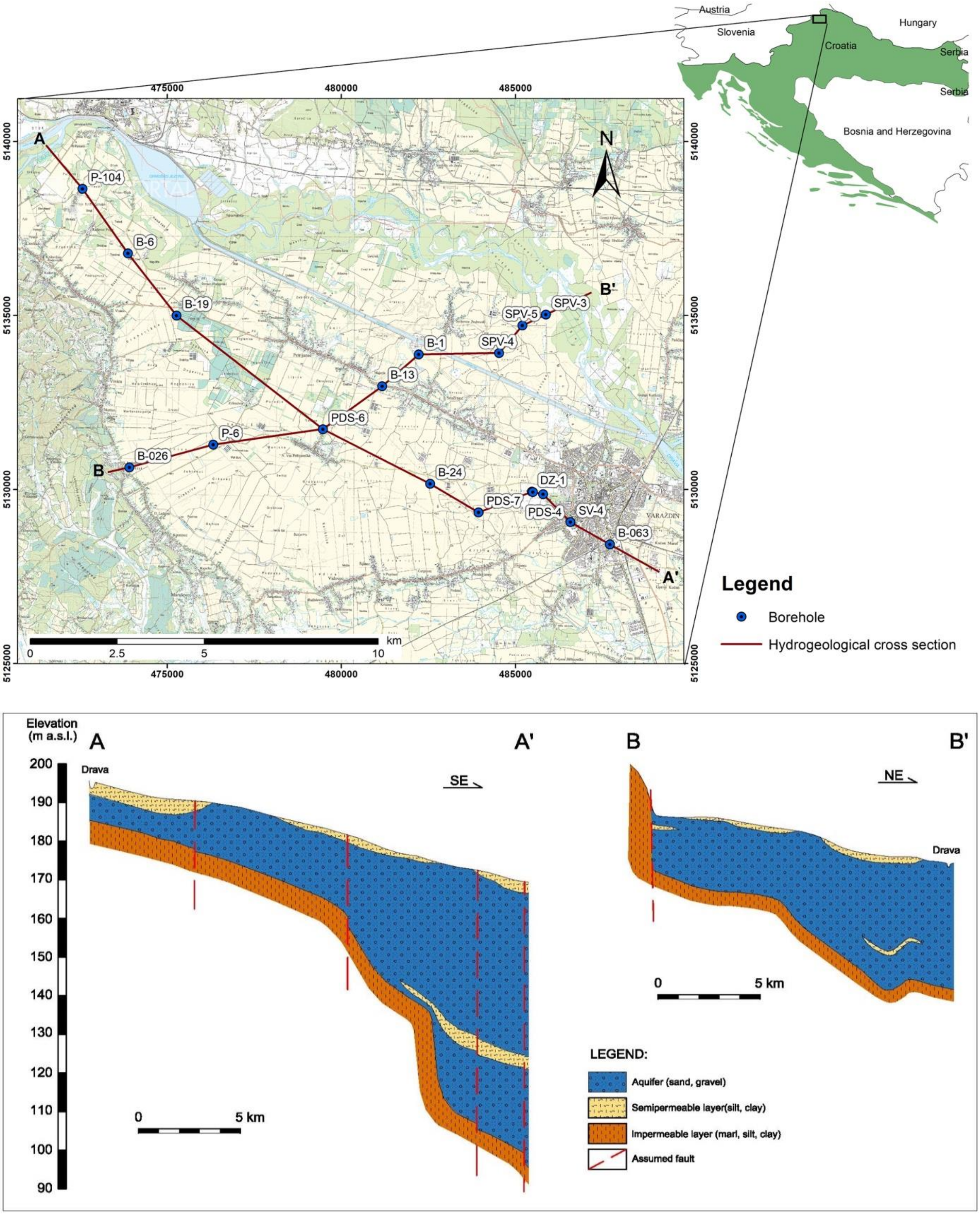

Figure 7.4. Schematic hydrogeological cross sections across Varaždin aquifer (modified according to Larva, 2008)

There is a covering aquitard at the top of the aquifer composed of various shares of silt, clay and sand. In the westernmost area its thickness is generally low (< 1m), and in many places there is no cover at all. Further on downstream the thickness generally increases.

The general groundwater flow direction is toward the Drava river, apart from the western area where seepage from hydropower plants reservoirs (accumulation lakes) takes place. The aquifer is mostly unconfined in the western part of the pilot area. It is recharged by infiltration of precipitation and, only during high water levels, there is a seepage from the Drava river bed into the aquifer. The recharge rates are relatively high and, depending on thickness and permeability of covering layer and type of land use, range from 15 to 30% of annual precipitation (Urumović et al, 1981; Patrčević, 1995; Brkić, 1999). Such hydrogeological conditions are favourable from groundwater utilisation perspective but, at the same time, are the cause of high aquifer vulnerability (Larva, 2008).

Groundwater quality deterioration over the past 2-3 decades is the evidence of aquifer vulnerability and different pressures among which agricultural production with intensive application of fertilizers and manure has an important role. As a result, nitrate concentration has been gradually increasing in the groundwater since 1970s. For instance, it exceeds 100 mg NO_3/L in the catchment area of Varaždin pumping site, albeit the trend reversal has been achieved in the last several years (Figure 7.5).

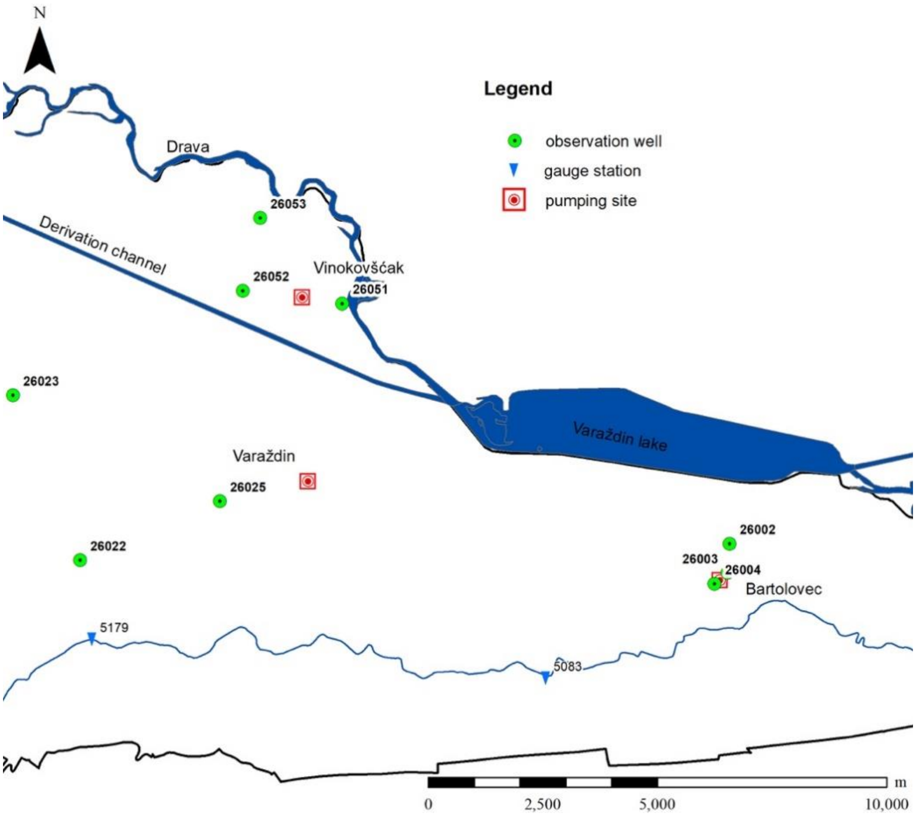

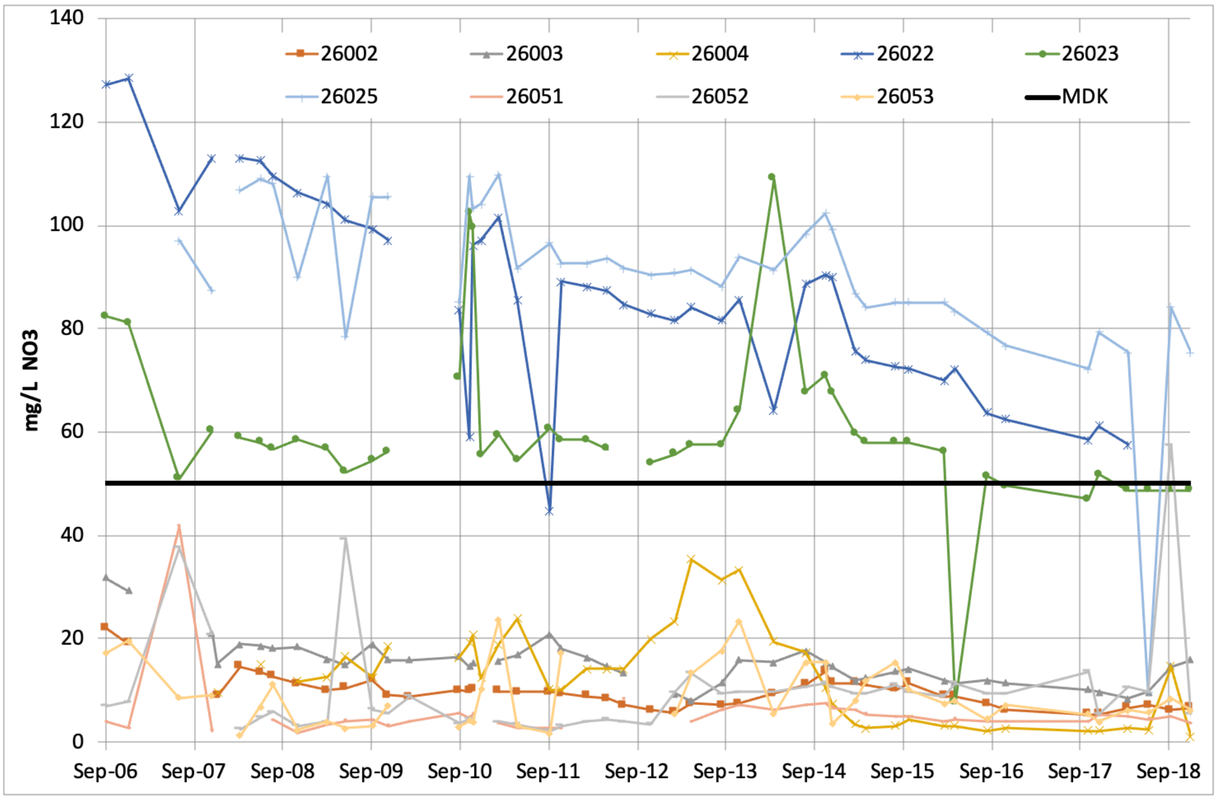

Figure 7.5. Nitrate concentration in groundwater from observation wells included in National monitoring network of groundwater quality in Varaždin pumping sites catchment area

7.2 Modelling approach

In order to evaluate nitrates behaviour in the aquifer system a relatively simple conceptual model has been developed (Figure 7.6).

The factors influencing nitrate travel lag in unsaturated zone involve its thickness and nitrate unsaturated zone velocity, whereby the unsaturated zone thickness is retrieved from calibrated groundwater flow model. Mean velocities in the unsaturated zone, as well as nitrates excess leaving the soil zone and reaching groundwater table were derived from results of investigations performed in the Slovenian study area, including lysimeter field laboratory – lysimeter in Selniška dobrova. Since the majority of study area generally has similar hydrogeological conditions, these data together with land use information and census data on fertilizer application enabled estimate of nitrate input at groundwater table for the pilot area. The evolution of nitrate concentration in groundwater was simulated by numerical model of solute transport in saturated zone of aquifer.

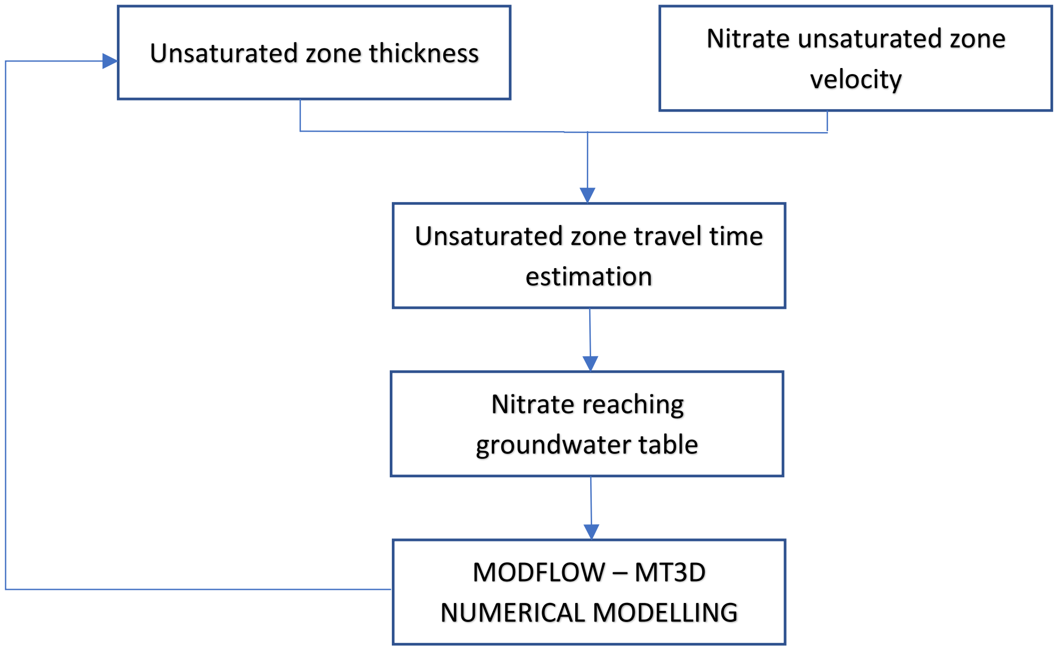

Figure 7.6. Flow chart of the modelling framework

7.2.1 Groundwater flow and nitrate transport in saturated zone of aquifer

Nitrate transport modelling in saturated zone of aquifer included two steps. First, the steady state groundwater flow model was developed and then, in the second step, the numerical model of nitrate transport was established.

7.2.1.1 Numerical model of groundwater flow

Numerical modelling of groundwater flow was carried out with MODFLOW 2005 code (Harbaugh et al., 2017) using GMS graphic user interface. The horizontal discretization of model domain was performed by grid size 500 m x 500 m. Vertical discretization was obtained by four layers representing covering layer, upper aquifer, aquitard and lower aquifer.

There are different natural boundaries to groundwater flow in the study area for which appropriate mathematical description was applied. In the south and south-west, groundwater flow boundaries include hills and mountains along which there is inflow into modelling domain that is simulated as specified flow boundary. The northern model boundary is the Mura and Drava rivers, which are modelled as a head-dependent boundary. Besides, there are several power plant reservoirs with a strong influence on the groundwater flow net, which are also simulated as a head-dependent boundary. The same boundary condition was employed for rivers and drainage channels, while Neumann boundary condition was applied for recharge, which was estimated according to previous studies (Patrčević, 1995; Brkić, 1999; Urumović et al., 1981) in the range from 20 to 30% of mean annual precipitation (Figure 7.7), and groundwater abstraction at pumping sites.

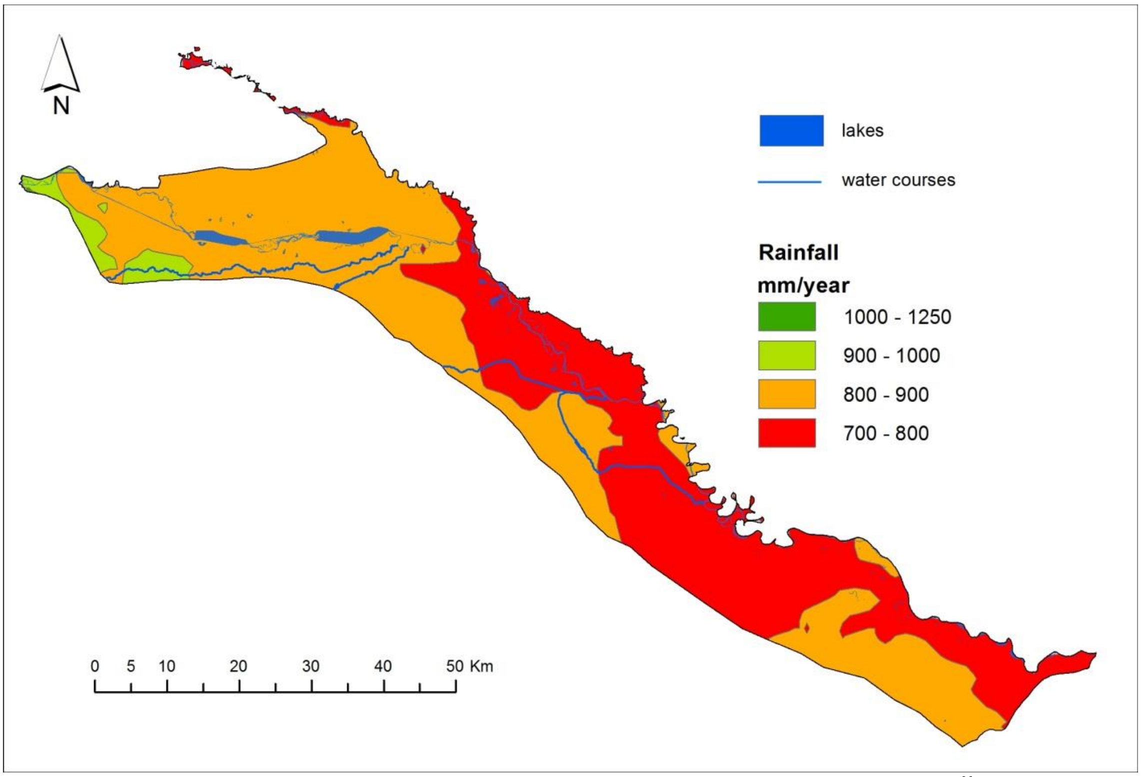

Figure 7.7. Spatial distribution of mean annual precipitation, 1961-1990 (Gajić-Čapka et al., 2003)

Model parameters were initially assigned according to the results of pumping tests carried out mostly for the purpose of pumping sites development, and were subsequently adjusted during calibration process. Calibrated horizontal hydraulic conductivity values range from 40 to 250 m/day in the central part of the upper aquifer. Vertical anisotropy factor (Kh/Kz) is 10, while effective porosity is 0,23.

The 3D groundwater flow was simulated in steady-state (Figure 7.8). Accordingly, all boundary condition data were prepared in order to adequately represent average hydrological conditions.

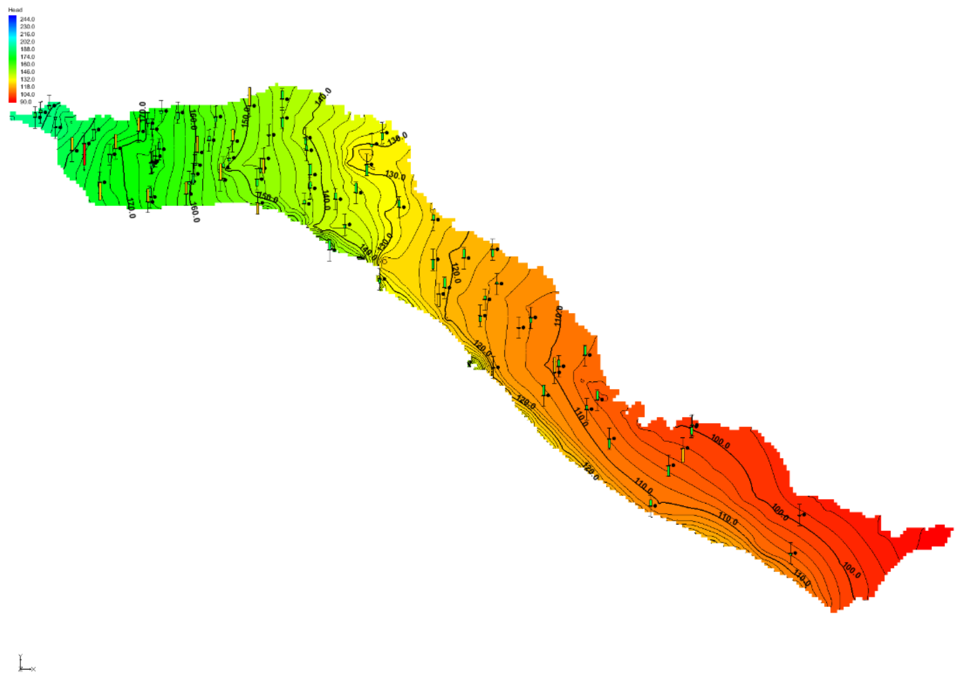

Figure 7.8. Simulated hydraulic head in the upper aquifer

Model was calibrated against observed groundwater heads obtained from the network of observation wells (Figure 7.3, Figure 7.9). For calibration purpose, the parameter estimation tool PEST was used (Doherty, 2015). In accordance with parsimony principle (Hill, 2006), the model was kept as simple as possible, and the complexity was added in the process of calibration when necessary. The calibration error statistics were calculated in order to evaluate the model performance. The goodness of fit between simulated and observed heads was evaluated using mean absolute residual (MAR), root mean squared residual (RMS) and normalised root mean squared residual (NRMS) (Table 7.2).

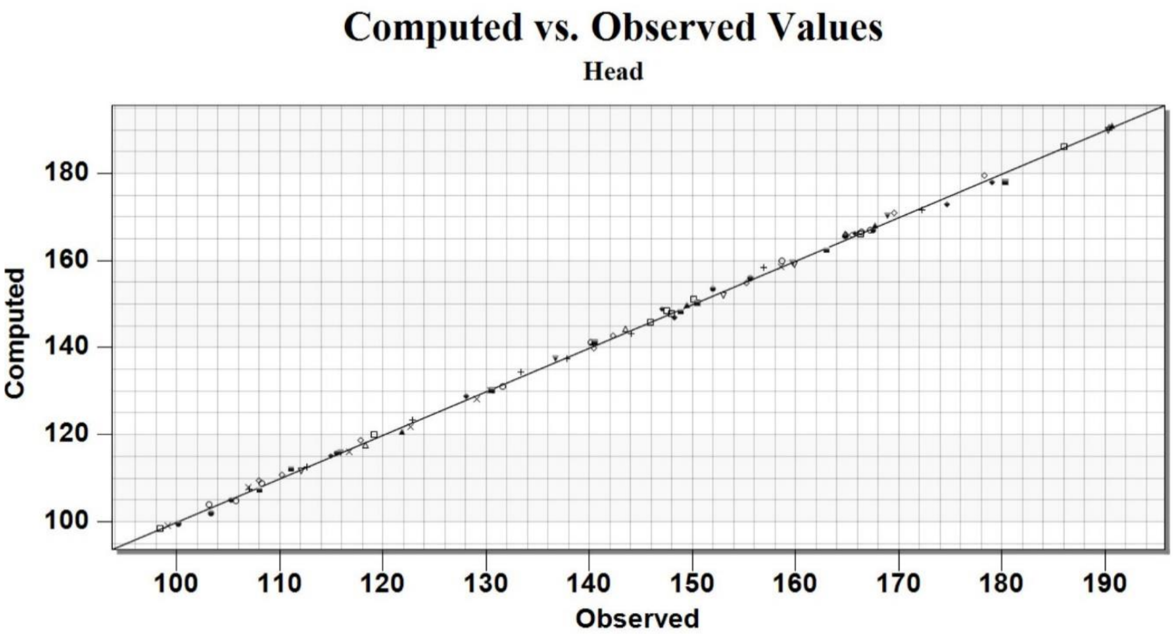

Figure 7.9. Calculated vs. observed heads for steady state simulation

Table 7.2. Calibration error statistics

MAR	0.70 m
RMS	0.83
NRMS	0.90%

7.2.1.2 Travel times in the unsaturated zone

The modelling approach for definition of nitrate travel times in unsaturated zone consists of determination of the groundwater table depth and groundwater velocities in the vadose zone. Then, the nitrate travel time was calculated for each 500 m x 500 m grid cell as a quotient of the unsaturated zone thickness and flow velocity. It was applied only in areas with unconfined aquifer (Figure 7.10). Nitrate was assumed to be conservative in the unsaturated zone and move predominantly vertically and at the same speed as groundwater.

The depth to groundwater table for average hydrological condition was retrieved from numerical model of groundwater flow (Figure 7.10). It ranges from less than 1m in the central part of the pilot area and close to the Drava river to over 50 m along the southern boundary of the aquifer with Bilogora Mt. However, groundwater is mostly shallow below the ground, rarely exceeding 7,5 m. It leads to the occurrence of semi-confined conditions, especially in the central and eastern parts of the pilot area, although the thickness of the covering aquitard rarely exceeds 10 m.

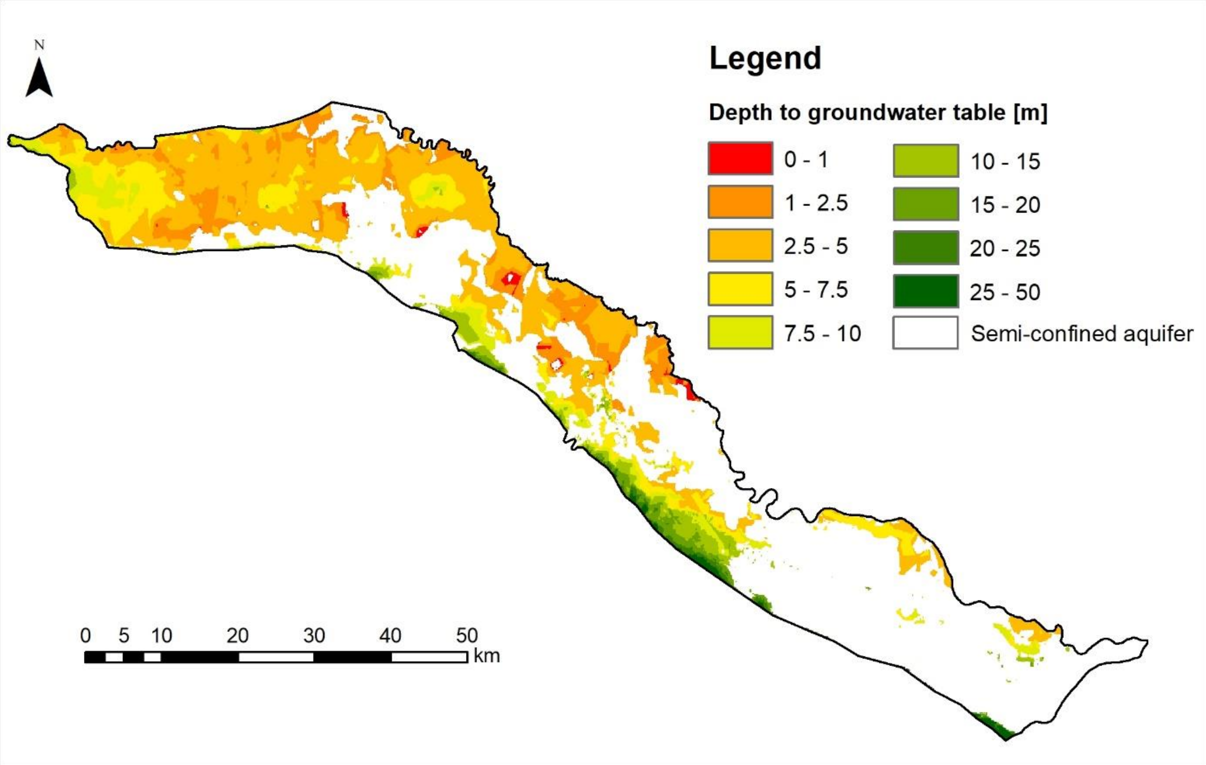

Figure 7.10. Depth to groundwater table

The covering aquitard is made of clay, silt and sand. Its thickness ranges from 0 m in the western part to over 15 m in the central and eastern parts of the pilot area. The lithological composition is heterogeneous as a result of sedimentation conditions leading to lateral and vertical changes in the proportion of individual lithological components. Due to similarities of hydrogeological properties of the Drava alluvial aquifer in Slovenian and Croatian pilots, the average flow velocities in the unsaturated zone consisting mainly of: i) coarse grained deposits and ii) fine grained deposits were obtained from the results of the research performed on the Drava alluvial aquifer in Slovenia (Koroša et al., 2020; Mali & Koroša, 2015). The flow velocity of 0,013 m/day was applied in the areas where the thickness of covering aquitard is less than 2 m, whereas the flow velocities of 0,003 m/day, characteristic of clayey fluival deposits, was applied in areas with the thickness of covering aquitard exceeding 2 m.

The nitrate travel time in the unsaturated zone is predominantly less than 2,5 years in the western part of the pilot, as a consequence of the shallow groundwater table and thin or even non-existent covering aquitard. In central part and especially in the southern, marginal parts of the aquifer, the travel time exceeds 5 years and locally is more than 25 years.

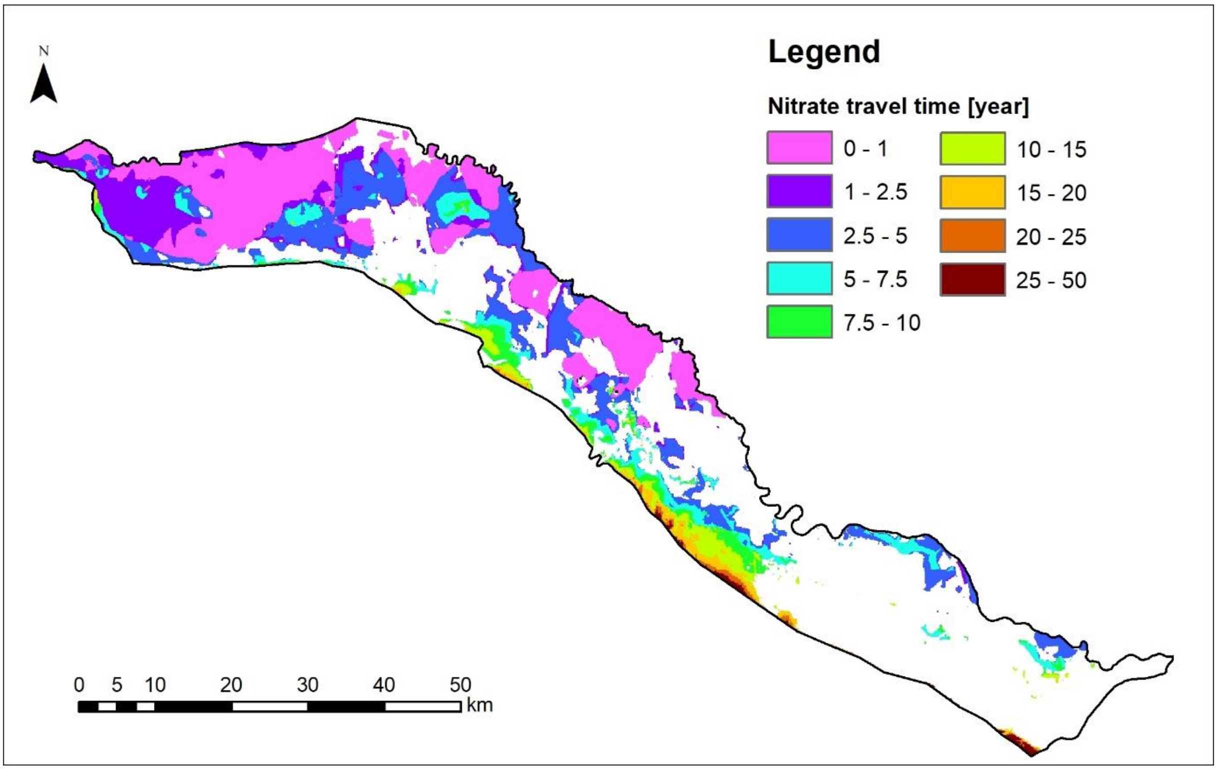

Figure 7.11. Nitrate travel times in the unsaturated zone of the Drava alluvial aquifer

7.2.1.3 Numerical model of nitrate transport in saturated zone

The numerical model of transport of nitrate in the saturated zone of aquifer was established for the western and central parts of the study area where oxic condition in aquifer prevails (Figure 7.11). Downstream, the hydrochemical conditions change with anoxic conditions, as result of sedimentation environment, gradually becoming dominant and leading to denitrification processes, which were outside the scope of research activities reported here.

Numerical simulation of 3D transport of nitrate was made using the MT3D-USGS code (Bedekar et al., 2016), which is an upgrade to the groundwater flow solution from MODFLOW code and has capability to route solute through dry cells that may occur in the Newton-Raphson formulation of MODFLOW (Niswonger et al., 2011) applied in groundwater flow simulation at the pilot area. The simulation does not consider processes that affect the retardation and decomposition of nitrates, but only the advection-dispersion transport. For the purposes of quantifying the effect of three-dimensional dispersion, it is necessary to determine the values of transverse and vertical dispersivity in addition to longitudinal dispersivity. It is common practice that the assigned value of transverse dispersivity is 10 times, and that of vertical 100 times less than longitudinal dispersivity.

Definition of dispersivity values is problematic, primarily because they depend on the scale, i.e. the distance between the entry of pollutants into the system and the receptor - the well, the observation point, etc. Determination is further complicated in case of non-point (diffuse) sources of contamination. Most researchers and agencies agree on the dependence of dispersivity on the scale, such as USEPA (Wiedemeier et al., 1998; Aziz et al., 2000), however, there is no agreement on the nature of this relationship.

Assessment of dispersivity can be performed by laboratory methods, by inverse modelling or by using one of the empirical expressions. Gjetvaj (1990) investigated the dispersivity at the catchment area of the Varaždin pumping site by monitoring the migration of NaCl solution in a radial flow towards well. Taking into account the results of this study, the value of longitudinal dispersivity of 100, transverse of 10 and vertical dispersivity of 1 was used for modelling nitrate transport in the pilot area.

Initial concentrations of nitrate in groundwater in 2006 were derived from National monitoring of groundwater quality datasets (Figure 7.5, Figure 7.12 , Figure 7.13). Nitrate concentration values were then interpolated and extrapolated in areas without information about groundwater quality.

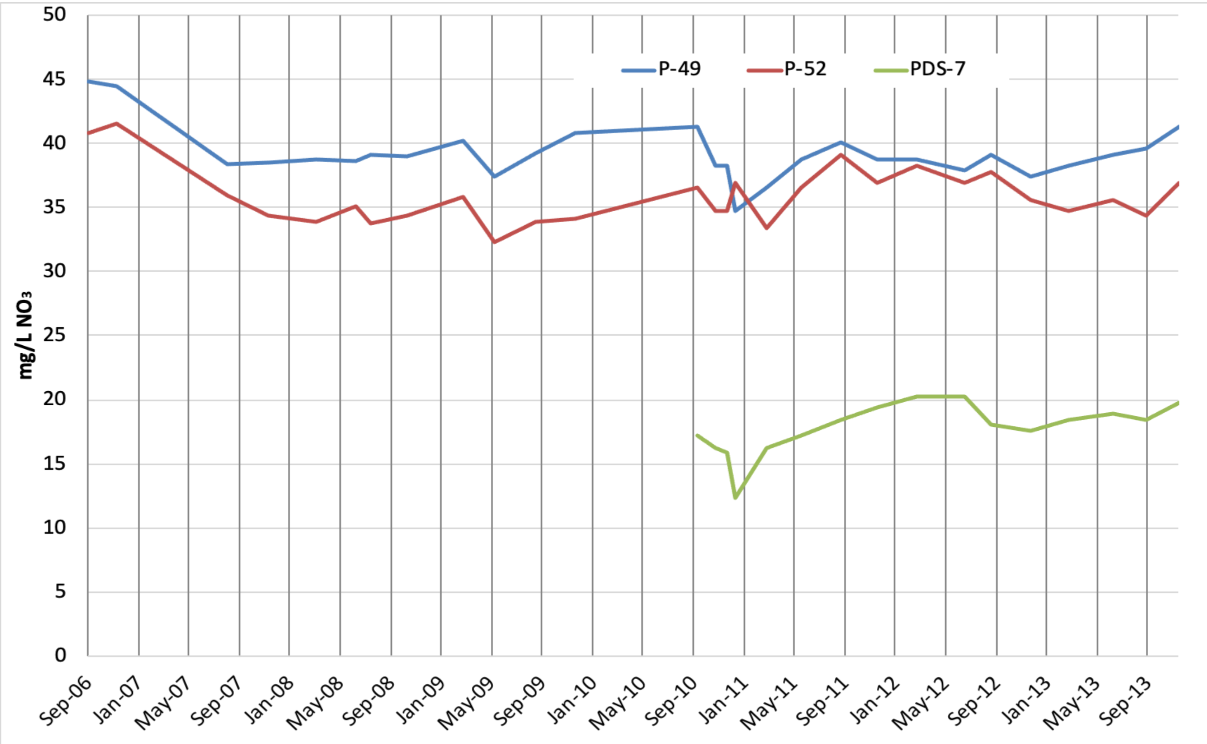

Figure 7.12. Nitrate concentration in groundwater from observation wells included in National monitoring network of groundwater quality in Prelog pumping site catchment area

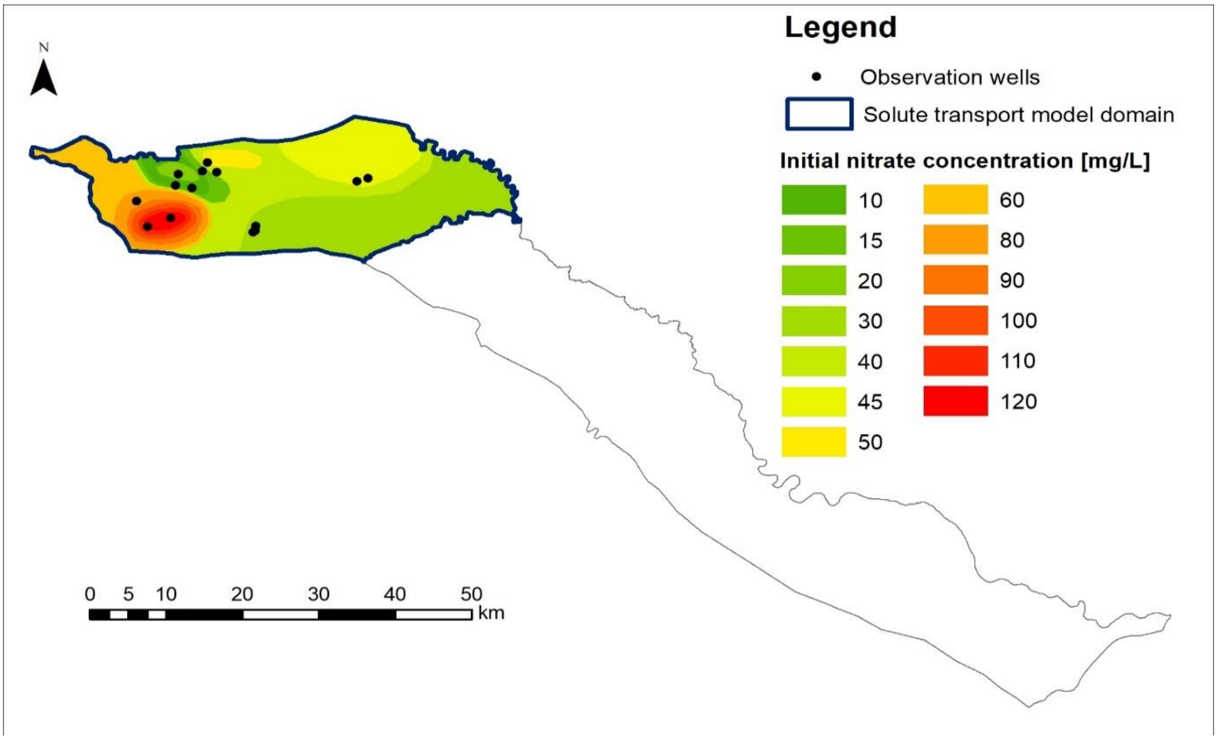

Figure 7.13. Spatial distribution of initial concentrations of nitrate in groundwater in the upper aquifer

Nitrate input at the model boundaries was simulated by the Neumann and Cauchy boundary condition. For leachate from areas where a zero inflow of nitrate is assumed the Neumann boundary condition was applied:

$$\frac{\partial C}{\partial x_i} = 0 \tag{7.1}$$

The Cauchy boundary condition was applied for the nitrate flux at the boundaries with watercourses and lakes, and from agricultural land identified as the sources of NO_3 in groundwater.

$$F_x = \eta_e v_x C - \eta_e D_x \frac{\partial C}{\partial x} \tag{7.2}$$

Agricultural land occupies the majority of the pilot area and was identified as the main source of nitrate (Figure 7.14). Other sources, except for surface water courses, were not taken into consideration.

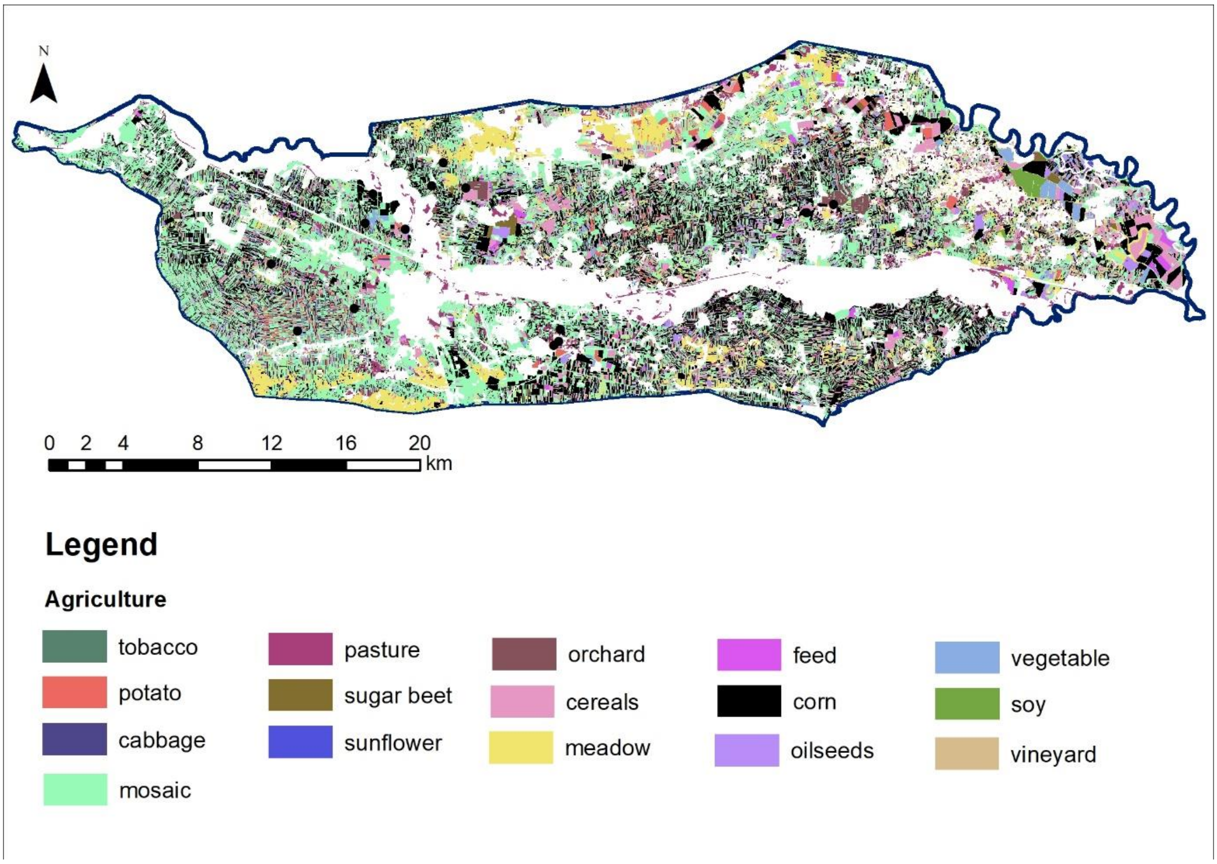

Figure 7.14. Map of agricultural land (Romić et al., 2015)

There is no data on nitrate concentrations in unsaturated zone of the aquifer in the pilot area. Hence, the results of research carried out in similar hydrogeological setting in Slovenia (Urbanc et al., 2014) were used in order to determine the nitrate surplus reaching the groundwater from different agricultural lands. For this purpose, different classes of agricultural lands were merged based on similar amount of nitrate surplus. Mosaic represents the zones where different crops occupy small areas. Additional class was created to account for the increased application of manure on agricultural land in the vicinity of numerous farms. Manure accumulated over time in farm premises is subsequently spread on agricultural land, and the nearest plots are most often used for this purpose. In total, five classes were identified with nitrate surplus ranging from 7,8 to 81,3 mg/L NO_3 (Table 7.3, Figure 7.15).

Table 7.3. Agricultural lands and nitrate concentrations

Crop	Nitrate concentration in infiltrating water [mg/L NO_3]
Tobacco	7.8
Cereals, corn, sugar beet, soy, oilseeds, potato, vineyards, meadows, pastures, sunflower	24.4
Mosaic	42.0
Feed, vegetables, cabbage, orchards,	56.9
Agricultural land in vicinity of farms	81.3

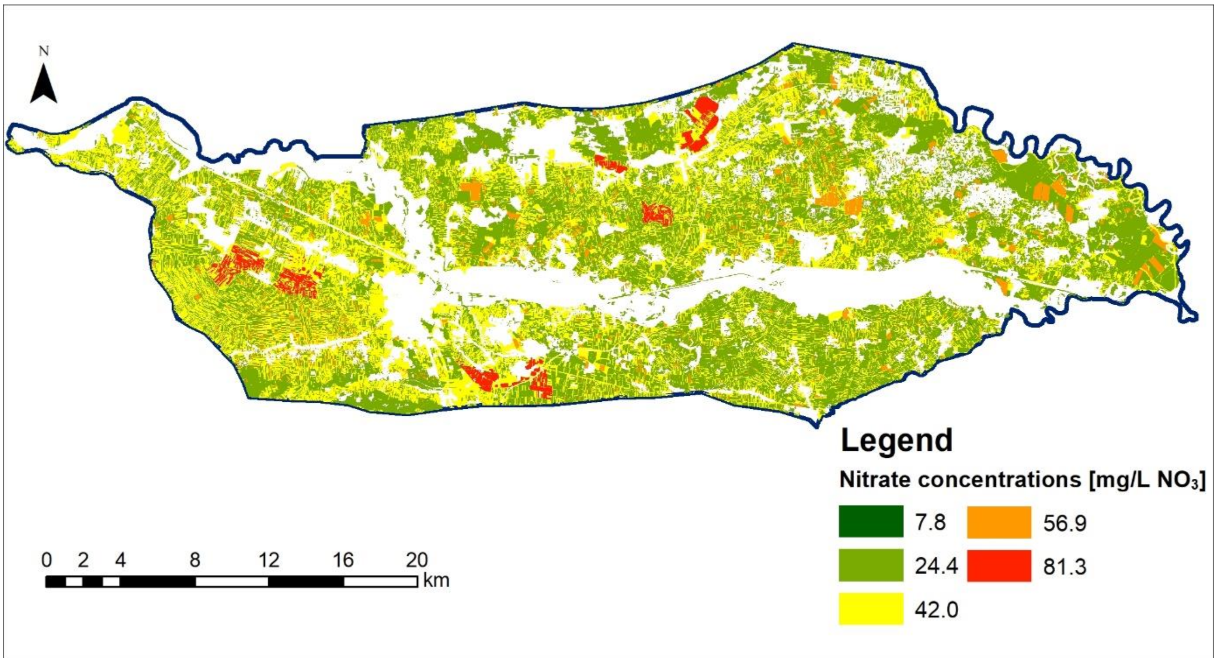

Figure 7.15. Spatial distribution of modelled nitrate concentrations in infiltrating water

The calibrated steady-state groundwater flow model was used together with MT3D-USGS for simulation of nitrate transport in the saturated zone of the aquifer. The transport simulation was performed for the period from 2006 to 2026, over which the constant input from the sources of nitrates in groundwater was assumed. The applied approach provided for validation of the model performance in the period from 2006 to 2018, and prediction of nitrate evolution in groundwater for the period from 2018 to 2026.

7.3 Model validation

The model performance and its ability to make reliable prediction were evaluated by comparing the simulated and observed nitrate concentrations in groundwater samples from different locations included in National monitoring of groundwater quality (Figure 7.16).

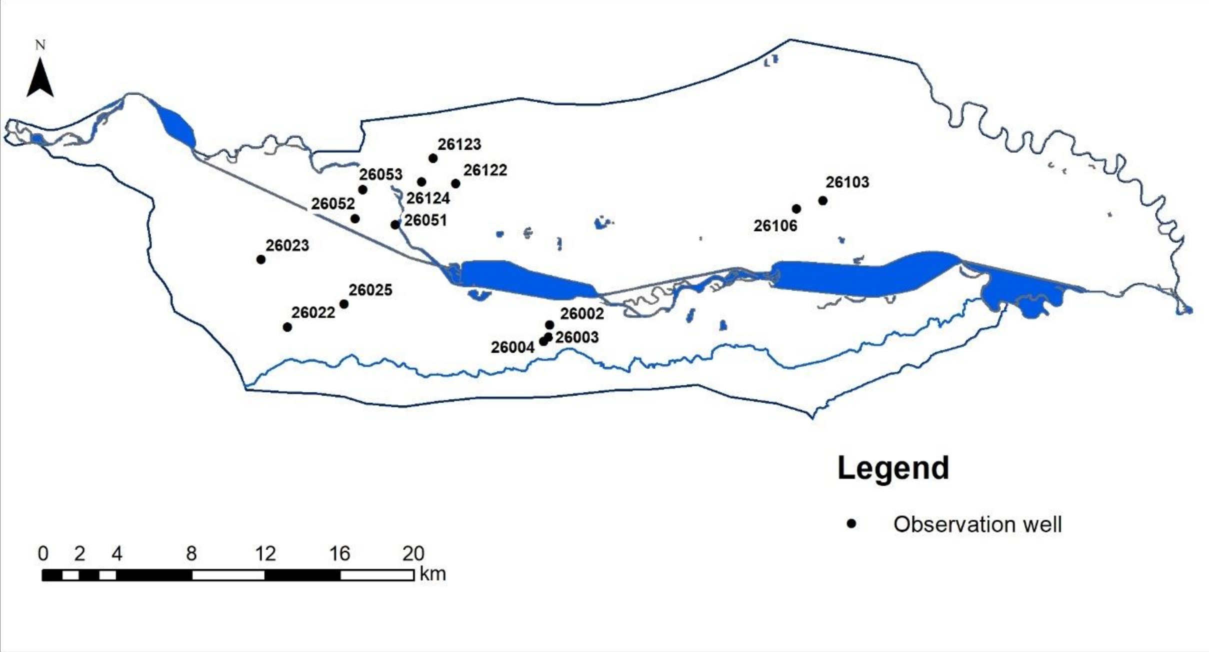

Figure 7.16. Location map of observation wells

In the western part of the model domain, where the starting concentrations were the highest, simulated nitrate concentrations fit well with observations (Figure 7.17, Figure 7.18). The residuals are somewhat higher for the observation well 26023, but the decreasing trend is reproduced well for both wells despite relatively high nitrate inputs upstream of the observation wells due to numerous farms and, consequently increased application of manure on agricultural land.

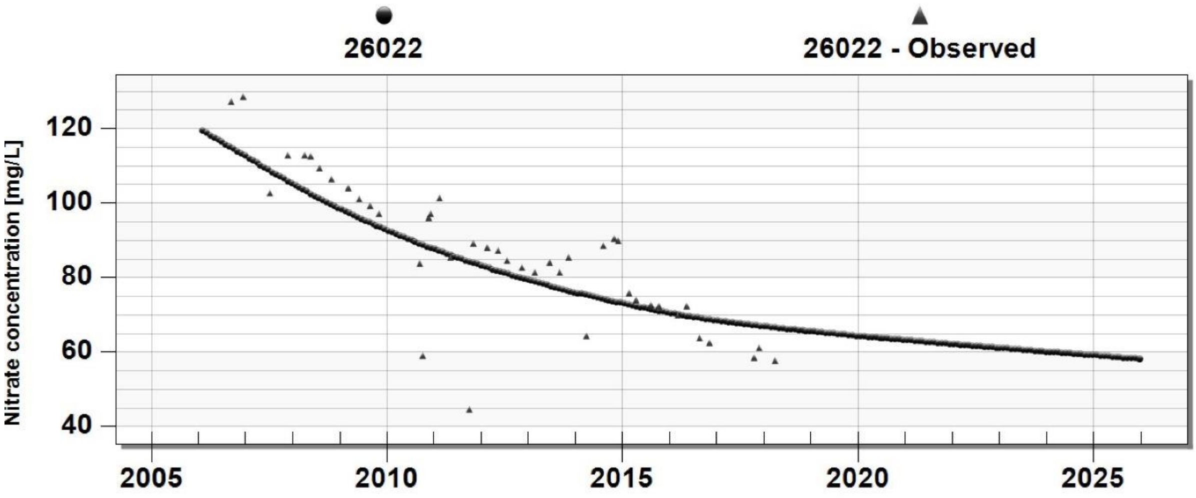

Figure 7.17. Simulated versus observed nitrate concentrations at observation well 26022

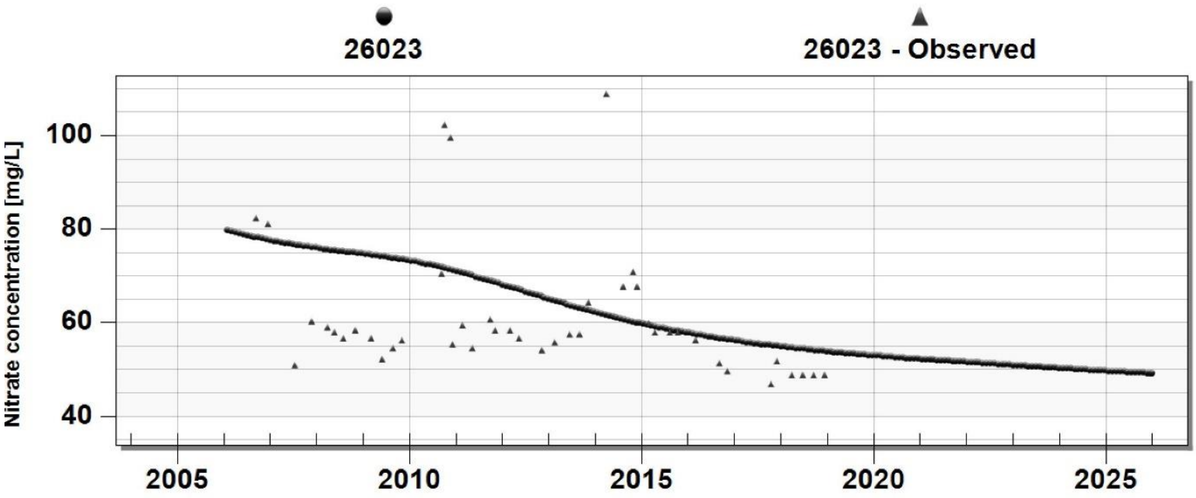

Figure 7.18. Simulated versus observed nitrate concentrations at observation well 26023

North, close to the Drava river the starting concentration in all observation wells were lower – below 60 mg/L NO_3. This is mainly due to groundwater mixing with infiltrated water from the Drava river, which contains only 8 mg/L NO_3 on average. The model performed well in this region, on both banks of the Drava river (Figure 7.19, Figure 7.20, Figure 7.21). At the beginning of simulation, the trend differs depending on the starting concentrations and nitrate inputs in the catchment area of the specific wells. After 2010, observed and simulated values show no significant trend.

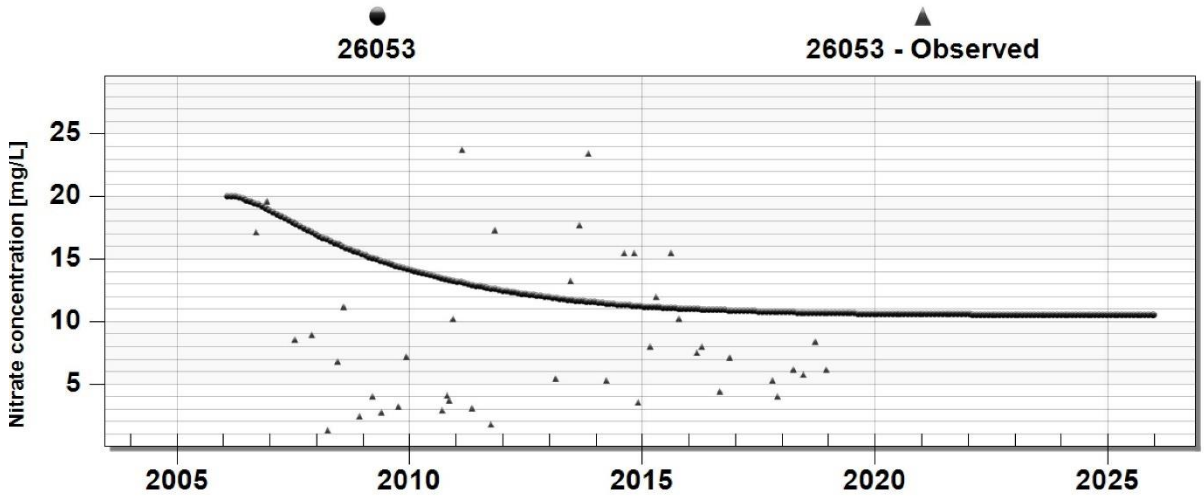

Figure 7.19. Simulated versus observed nitrate concentrations at observation well 26053

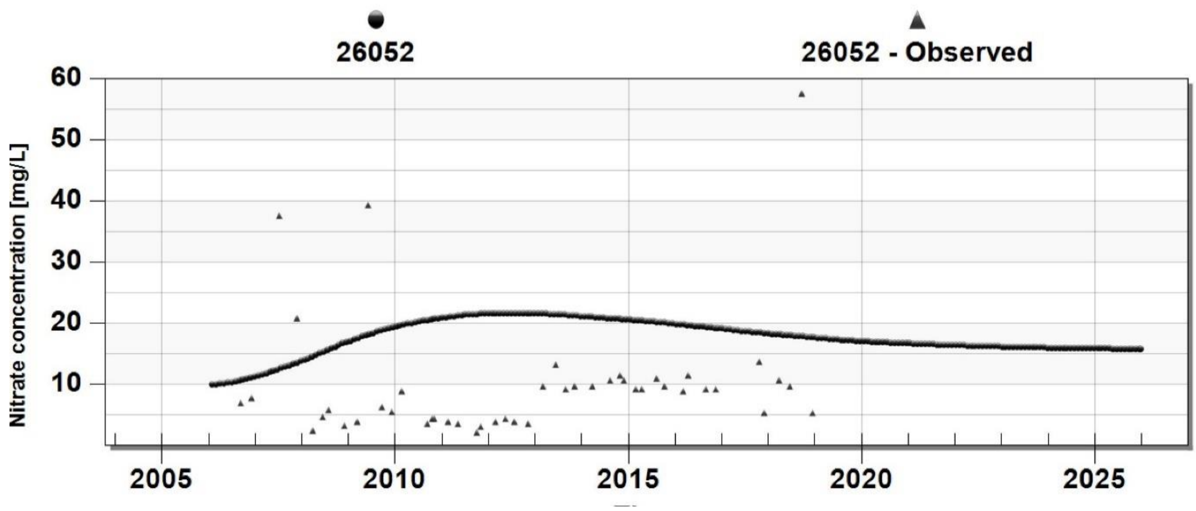

Figure 7.20. Simulated versus observed nitrate concentrations at observation well 26052

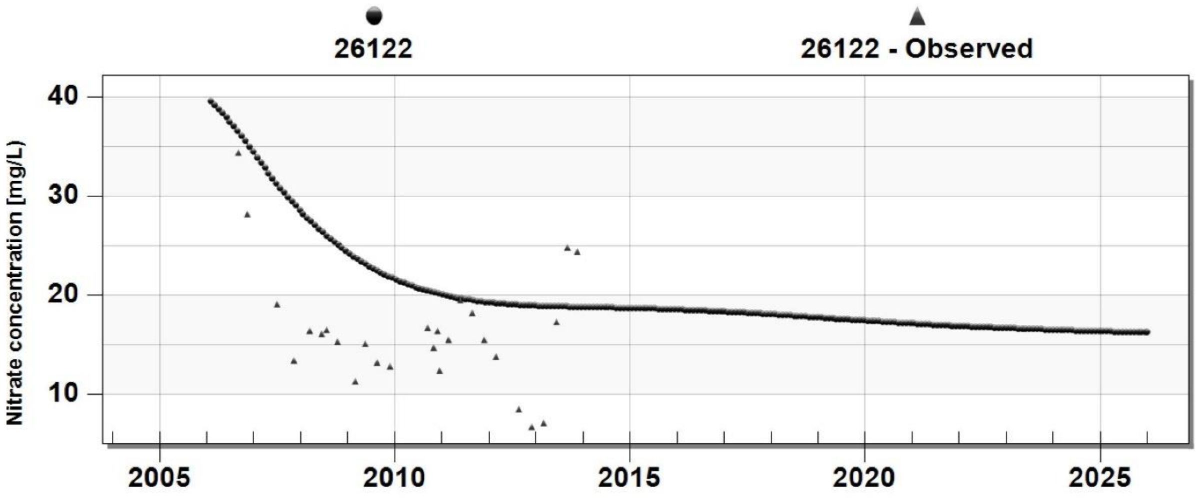

Figure 7.21. Simulated versus observed nitrate concentrations at observation well 26122

Downstream, in the area between the hydropower plant accumulation lake and the Plitvica river the simulated values are higher than observations (Figure 7.22, Figure 7.23). In the first five years of simulation there is an upward trend of simulated values, which is in contrast with observed concentrations. The reason for that may be overestimation of the initial values of nitrate concentration immediately upstream of the observation wells. In the period between 2011 and the end of observation in 2018, there is no trend in both observed and simulated values. However, the simulated values remain above the observed ones due to too high calculated concentrations in the first few years of the simulation.

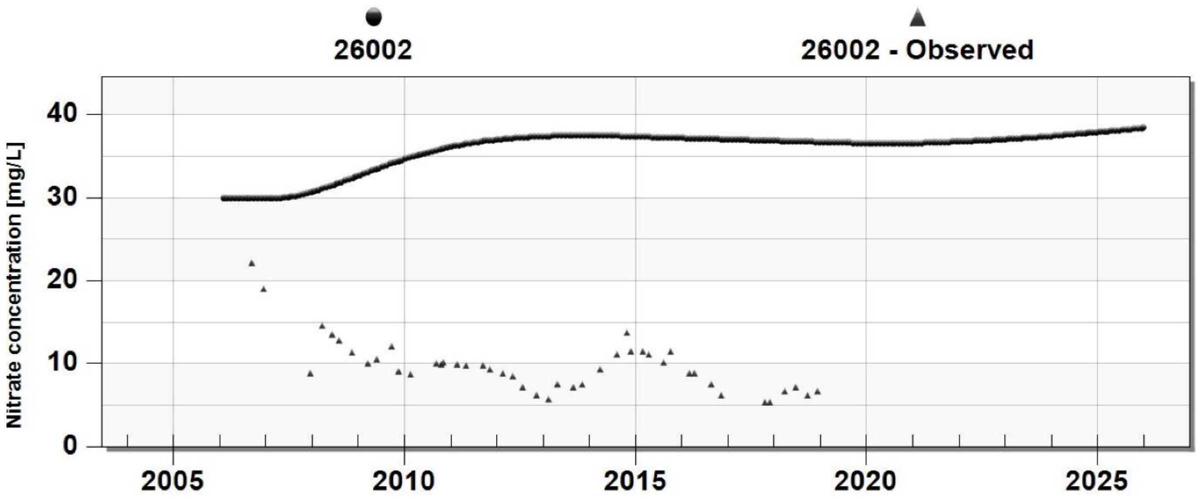

Figure 7.22. Simulated versus observed nitrate concentrations at observation well 26002

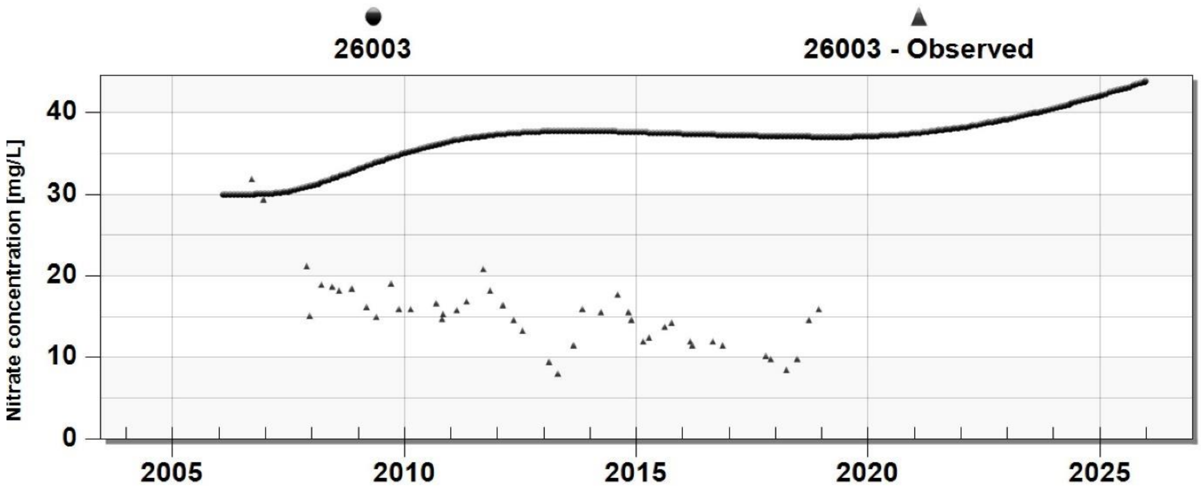

Figure 7.23. Simulated versus observed nitrate concentrations at observation well 26003

The starting nitrate concentrations in the eastern part of the study area were below 50 mg/L NO_3. The simulated values match well the observations in both upper (Figure 7.24) and lower aquifer (Figure 7.25). It is difficult to determine the trend of observations due to relatively short observation period, especially for the observation well 26106. However, simulation results point to a downward trend in the upper aquifer and a slight upward trend of nitrate concentrations in the lower aquifer.

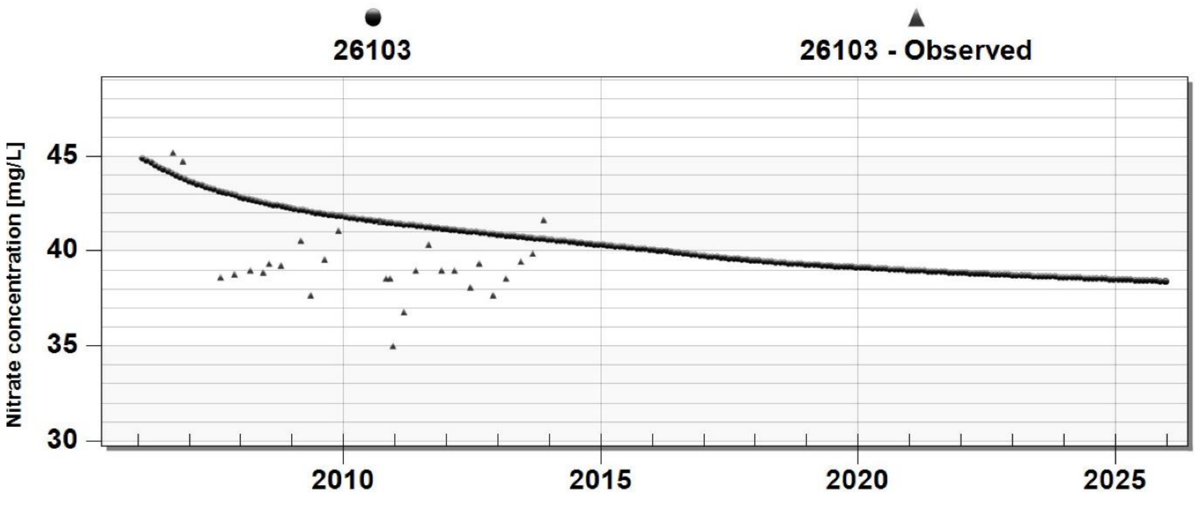

Figure 7.24. Simulated versus observed nitrate concentrations at observation well 26103

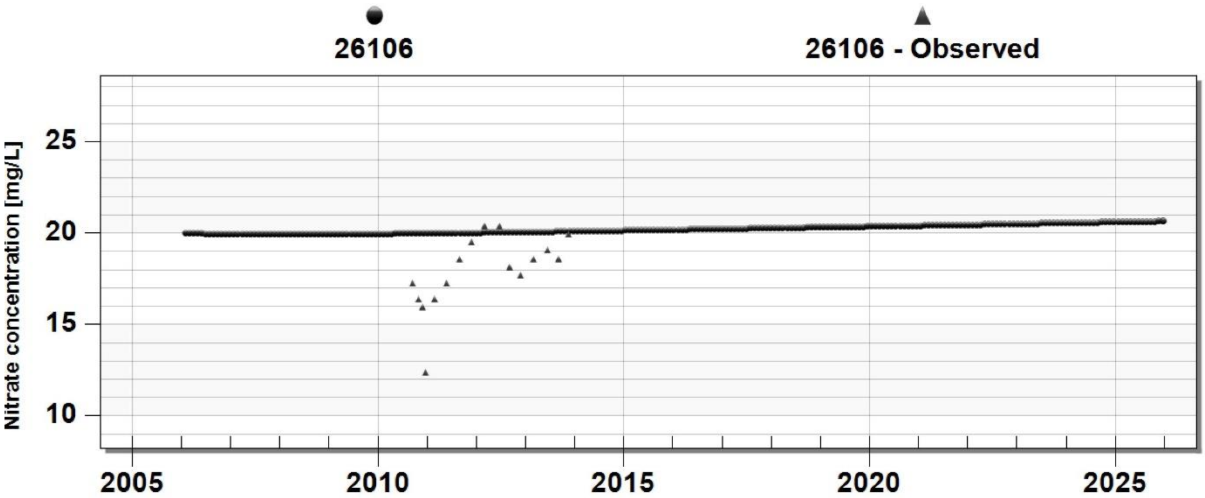

Figure 7.25. Simulated versus observed nitrate concentrations at observation well 26106

Overall, the results of validation are satisfactory, bearing in mind that it is a steady-state model with 500 m by 500 m spatial discretization. Due to model limitations, it was not possible to reproduce seasonal changes in nitrate concentrations in groundwater resulting from changes in boundary conditions of groundwater flow and nitrate transport models. However, the trend in nitrate concentrations in saturated zone of both upper and lower aquifers is simulated well and consequently, the model is deemed suitable for making prediction on evolution of nitrates in groundwater.

7.4 Key results

The pilot area is characterized by elevated nitrate concentrations in groundwater in the upper aquifer, while the situation in lower aquifer is mostly satisfactory. This led to a bad chemical status qualification of a groundwater body Varaždinsko područje.

Nitrate travel times in the unsaturated zone of the aquifer in the study area are relatively short. This is the result of high groundwater table and relatively high permeability of the unsaturated zone. Due to high groundwater heads semi-confined aquifer occupies large areas.

The results show that nitrate travel times in the unsaturated zone in the western parts of the model is dominantly under 2,5 years, while a significant portion is less than one year (Figure 7.11). The travel times above 5 years are characteristic of marginal areas, e.g. along the western aquifer boundary with Bilogora Mt.

Relatively short residence time of groundwater in the unsaturated zone implies that any changes in land use management and application of nitrogen on the ground surface are relatively quickly reflected in the quality of groundwater reaching the saturated zone. However, the quality of groundwater at any particular point in the saturated zone of aquifer is the result of complex processes which were simulated by numerical model of nitrate transport.

The simulation of evolution of nitrate concentration in groundwater was performed for the period 2006-2026, assuming a steady state conditions for both groundwater flow and nitrate transport model. It covers validation period form 2006-2018 and projection until 2026.

The initial concentrations vary from 10 to over 100 mg NO_3/L (Figure 7.13). The simulation results show different trends in the modelling domain. A significant downward trend is characteristic of western part of the model (Figure 7.17, Figure 7.18, Figure 7.26) with historically high application of fertilizers and manure on agricultural land. To the north and close to the Sava river the starting concentrations are significantly lower, and after approximately 5 years of simulation the curve of calculated values stabilizes showing almost no trend, which is in line with observations (Figure 7.19, Figure 7.20, Figure 7.21) Downstream, simulated values are somewhat higher than observed, but the absence of the trend in calculated values from 2011-2018 is supported by observations (Figure 7.22, Figure 7.23, Figure 7.26). In the eastern part of domain, the nitrate concentrations are below 50 mg/L. Historic concentrations are matched well with calculated values, which show clear downward trend (Figure 7.24, Figure 7.26).

Projection of evolution of nitrate concentration for the period 2018-2026 shows that existing trends will be mostly sustained under the assumption of the constant boundary conditions. Nitrate concentrations will keep decreasing, e.g. from 125 mg/L in 2006 to under 65 mg/L in 2026 in observation well 26022 (Figure 7.17). However, the opposite trend is evident in observation wells 26002 (Figure 7.22), and especially 26003 (Figure 7.23), where calculated values start increasing from 2020 as a consequence of contamination plume spreading from the upstream contaminated area.

Overall, the simulation results point to the conclusion that the groundwater quality will notably improve by 2026 in the regions with historically high nitrate concentrations, while the plume movement will not significantly deteriorate the groundwater quality downstream.

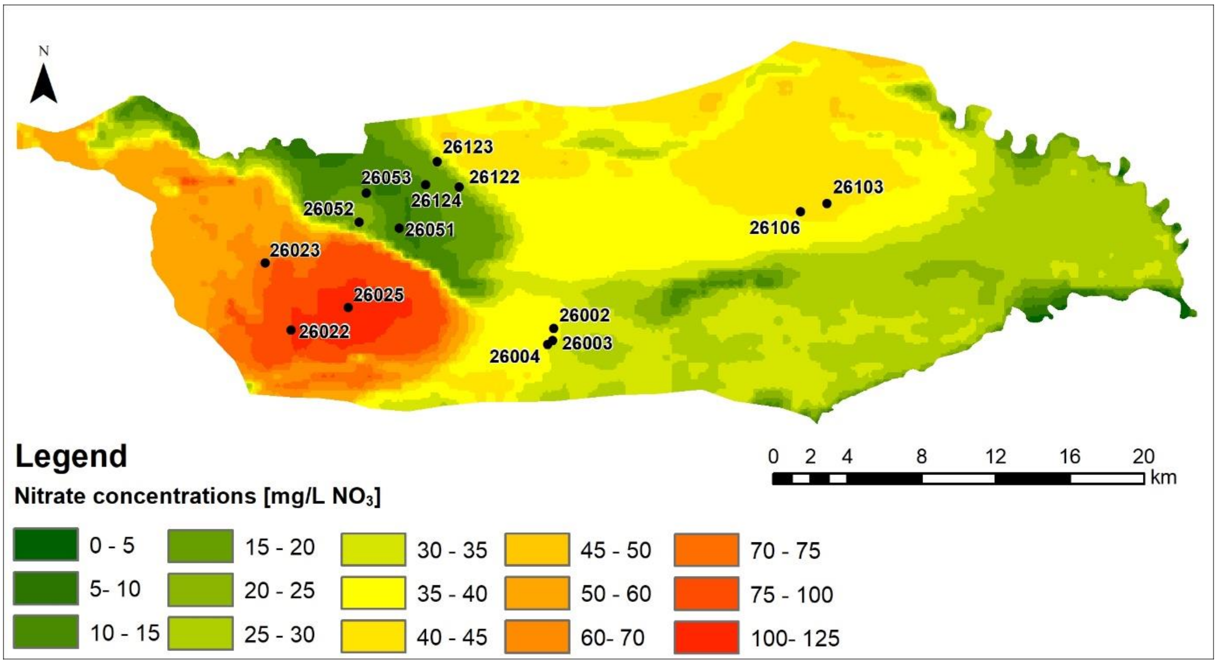

a)

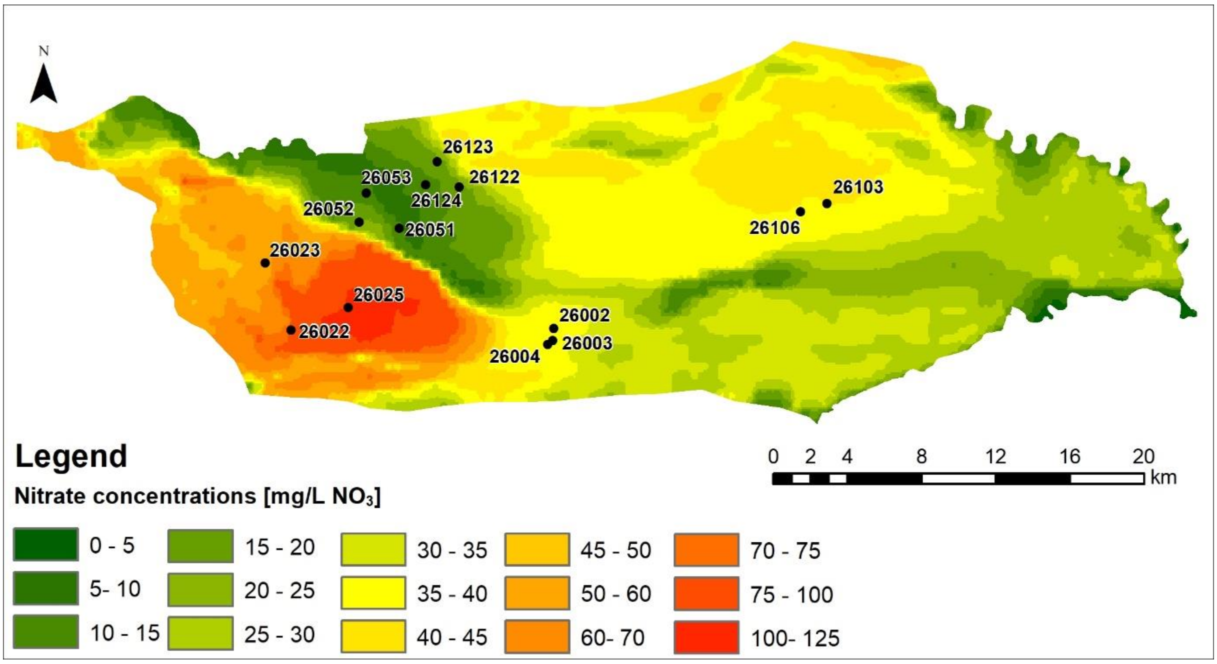
N
26123
26053
26122
26124
26052
26051
26023
26025
26022
26002
26003
26004
26103
26106
Legend
Nitrate concentrations [mg/L NO3]
0 - 5
5- 10
10 - 15
15 - 20
20 - 25
25 - 30
30 - 35
35 - 40
40 - 45
45 - 50
50 - 60
60- 70
70 - 75
75 - 100
100- 125
0 2 4 8 12 16 20
km

b)

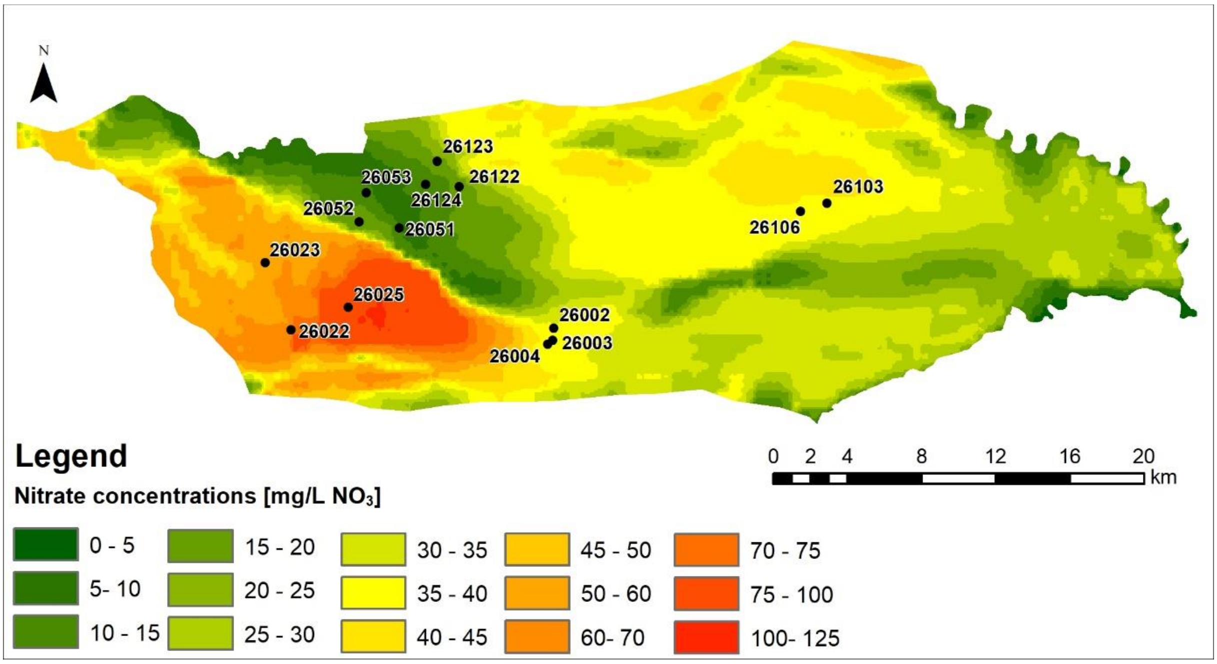
N
26123
26053
26122
26124
26052
26051
26023
26025
26022
26002
26003
26004
26103
26106
Legend
Nitrate concentrations [mg/L NO3]
0 - 5
5- 10
10 - 15
15 - 20
20 - 25
25 - 30
30 - 35
35 - 40
40 - 45
45 - 50
50 - 60
60- 70
70 - 75
75 - 100
100- 125
0 2 4 8 12 16 20
km

c)

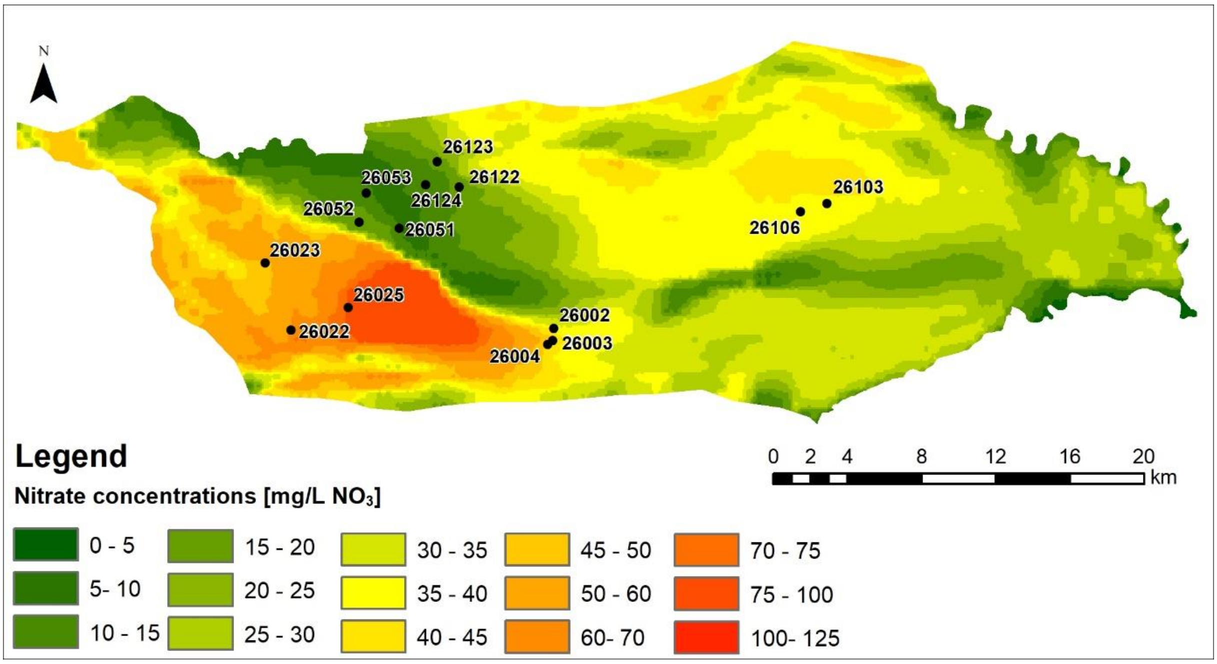

d)

Figure 7.26. Distribution of nitrate concentrations: a) after 5 years, b) 10 years, c) 15 years and d) 20 years of simulation

8 SLOVENIA (DRAVA)

Janko Urbanc
GeoZS, Slovenia

8.1 Geography of Drava Pilot Area – Slovenian Part

Slovenian part of Drava pilot area is part of groundwater body (GWB) Dravska kotlina (. GWB is situated on alluvial gravel deposits between Selnica ob Dravi and Ormož all the way to Središče ob Dravi at the Croatian border. Drava pilot area consist of three aquifers: Dravsko polje, Ptujsko polje and Ormoško polje.

Figure 8.1. Groundwater body Dravska kotlina

Dravsko polje aquifer is situated on right bank of Drava river. In general, it is shaped as triangle between Maribor, Ptuj and Pragersko. On west it is bounded with Pohorje hills, on north-east with Slovenske Gorice hills on south with Haloze and Dravinjske Gorice. Parallel to Drava river a conductive channel is built for hydroelectric power plant Zlatoličje. In Ptuj city river Drava transitions into artificial lake Ptuj from which river continues its way. Areal extend of Dravsko polje aquifer is approximately 293 km^2.

Ptujsko polje is situated on the left bank of Drava, stretching between Ptuj and Ormož city. It is bounded with Dravsko polje aquifer on west boundary and with Ormoško polje aquifer on east boundary. On north it is bounded with Slovenske Gorice hills and on south with Drava river. It has a shape of stretched triangle with areal extent approximately 91 km^2. Surface is slightly tilted towards east.

When hydroelectric power plant Formin was built, Ptujsko polje aquifer was divided by 8.5 km long conducting channel between Markovci and Formin and 8 km long conducting channel between Formin and Ormož city (Žlebnik, 1991).

8.2 Hydrogeology

Groundwater body Dravska kotlina is typically built of alluvial quaternary gravel, sand, silt and clay predominate. However, on surface predominate carbonate and silicate rocks with intergranular porosity (ARSO, 2008).

GWB contains three typical aquifers. We are going to discuss only the first, upper most one. This alluvial quaternary aquifer with intergranular porosity is composed of gravely sand deposited by Drava river. Important recharge boundary present surface streams from Pohorje hills between village Ruše and river Polskava. At the NW margin of Dravsko polje field these streams infiltrate as soon as the flow reaches the alluvial aquifer. Bottom base of Quaternary aquifer consists of Tertiary layers. Drava river is the dominating surface stream on the area. More importantly it is an important hydrodynamic boundary of alluvial aquifer. Furthermore, river acts for most part as a drain. Along the river stream groundwater springs are found. However, on the northern part of the Dravsko polje aquifer river recharges the aquifer (ARSO, 2018). This recharge is estimated to approximately 0.5 m^3/s (Brilly, 1994). Gravel aquifer of Dravsko polje aquifer is not uniform. Furthermore, differences in the way it is being recharged are so great it has been divided into three hydrogeological units as described by Žlebnik, 1984. Each of these units have separate precipitation outskirt and significant regime of how groundwater is being recharged and discharged.

First unit is covering NW part of the field which is mainly urbanized. It contains the outskirts from Pohorje hills of Radvanjski and Razvanjski stream. On south it is bounded by the surface Razvanjski stream ridgeline and by the underground ridgeline from Bohova to Dogoše. On this unit groundwater flow is quite small since the precipitation catchment area is small as well and most importantly the aquifer layer on this part is very thin.

Second hydrogeological unit covers a part of Dravsko polje aquifer between Bohova and Dogoše on the north and Hotinja vas, Dravski Dvor and Starše on the south part of Dravsko polje aquifer. Moreover, it covers hilly outskirts of Pivolski, Hočki and Polanski stream. Groundwater is being recharged by the infiltration of these streams from Pohorje hills and with infiltration of the precipitation. Groundwater recharge from the second unit of Dravsko polje aquifer is drained towards the Miklavž spring and in Drava river.

Third and the biggest hydrogeological unit is covering the hilly outskirts of Rančki stream and middle part of the Dravsko polje aquifer field from the Pohorje boundary at west all the way to the Drava river on the NE and Polskava river on the south. Groundwater is discharging from Pohorje towards the channel Zlatoličje and Hajdina and Pobreš spring (Žlebnik, 1984). Main part of the recharge is represented by infiltration of precipitation. One third of whole yearly average amount is being infiltrated and discharged towards Drava river. Average annual precipitation amount is between 800 and 1000 mm/a (ARSO, 2018). Long term mean annual groundwater recharge is estimated to 300-450

mm/a including the evapotranspiration (ARSO, 2018). River Polskava have no influence on the groundwater (Žlebnik, 1984).
Recharge rate of the Quaternary aquifer is estimated to 3 m^3/s (Turnšek, 2016) thereof groundwater discharge present 2 m^3/s, and direct recharge 0.8 m3/s. The smallest amount is presented with surface runoff and approximately 41% is presented by infiltration from precipitation (27-47%) (Turnšek, 2016). Generally, Dravsko polje aquifer has good hydraulic conductivity. Hydraulic conductivity span from approximately $7.9x10^{-4}$ to $0.91x10^{-3}$ m/s (Žlebnik, 1982).

Ptujsko polje aquifer is filled with Quaternary gravel deposits with thickness varying from 4 m and up to 22 m. The Tertiary base of the Quaternary aquifer consists of conglomerate sand, clay and marl, with very low permeability. Nearby the Ptuj lake at west boundary Ljutomer fault is stretching in direction from SW to NE. Between Ptuj and Ljutomer fault base of the Quarternary aquifer consist of Pliocene sediments. Rest of the area in east direction from the fault base consist of lower Pliocene and Miocene sediments. Tertiary base is highly undulate (Žlebnik, 1991).

Main watercourse on Ptujsko polje aquifer is Drava river. It has a flow along south margin of Ptujsko polje aquifer all the way to Ormož. When Formin hydroelectric power plant was constructed between Markovci and Ptuj town, 5 km long and 1.2 km wide lake Ptuj appeared. Along this artifical lake a rampart was built all around it to prevent the flooding with surface waters from the lake.

Ptujsko polje aquifer is mainly being recharged from precipitation and partly from Drava river. Groundwater is discharging to numerous springs called Zvirenčine on foot of the high Quaternary gravel terrace. The Ormož town is supplied with drinking water from the wells on the eastern part of Ptujsko polje aquifer. The conducting channel that belongs to Formin hydroelectric power plant affected the underground water in a very low extent, because all necessary interventions were made for the underground water protection. This channel is sealed all the way down to Tertiary base only on the eastern side of Ptujsko polje aquifer from Formin 6 km towards Ormož city. However, last 2 km are permeable so the underground water can discharge into Drava river.

Infiltration of Pesnica river and its inflows is negligible since its bottom is mostly formed of clay (Žlebnik, 1991). On west part of the Ptujsko polje aquifer groundwater flows in NW to SE direction between lake Ptuj and Formin village. Flow is uniform in the west part. Influence on groundwater oscillation is mainly caused by precipitation and partly by natural flow of Drava river. Groundwater is discharging into river Drava and springs along the Drava river. Discharging of groundwater into Drava is significant for part after Dravinja flows into Drava river. However, before Dravinja flows into Drava equilibrium is reached between river and groundwater, so it is not being drained, neither recharged (Brenčič, 2002).

On east part between Formin village and Ormož city groundwater flow is not uniform anymore because conducting channel Formin is sealed all the way to non-permeable Tertiary base. Therefore, groundwater flow is divided into two parts; south and north from the channel Formin. On northern part groundwater flow direction is from W-E and is discharging into Drava river where last 2 km of the channel are permeable again. Only precipitation has the influence on the groundwater oscillation. On this part water is being tapped for fresh water supply of the Ormož city. On the south part of the conducting channel both precipitation and Drava river have the influence on the groundwater oscillation.

Main part of the recharge is represented by the infiltration of precipitation. One third of the whole yearly average amount is being infiltrated and discharged towards Drava river. Average yearly precipitation amount is between 800 and 1000 mm (ARSO, 2018). Long term mean annual groundwater recharge is estimated to 300-450 mm including the evapotranspiration (ARSO, 2018).

8.3 Water and Nitrate Transport in an Unsaturated Zone

8.3.1 Introduction

Water and nitrate pollution transport in the unsaturated zone (UZ) was studied in a field laboratory – lysimeter in Selniška dobrava (Figure 8.2). Transport parameters were estimated by a combined tracer experiment with deuterated water and $Ca(NO_3)_2$. Deuterium was used as a conservative tracer of water movement, and $Ca(NO_3)_2$was used as a nitrate tracer in a high-permeable coarse gravel UZ. One of the aims of research (Koroša & Mali, 2015) was to specified parameters of nitrate transport in coarse gravel UZ which will allow to model nitrate transport in other aquifers with similar hydrogeological characteristics, such as for example Dravsko polje aquifer, which was declared as a water body at risk due to the presence of nitrate.

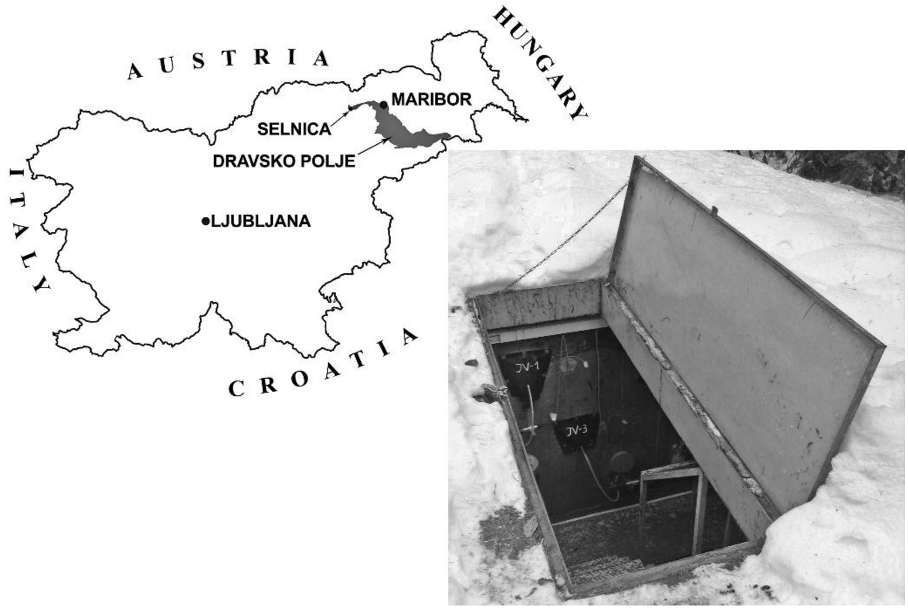

Figure 8.2. Area of lysimeter location and lysimeter cross-section

8.3.2 Area Description

The Selniška dobrava aquifer (Figure 8.2) is situated in the north-east of Slovenia and is part of Dravska kotlina groundwater body (GWB). The 15 km^2 area is bordered by the Drava in the south and with the hilly area in the north (Mali et al., 2005). The main aquifer Selniška dobrava can be classified as an intergranular aquifer of good permeability. The old riverbed, which presents the principal aquifer, runs along the present stream of the Drava River. The aquifer is recharged from the Drava, by the infiltration of precipitation and by seepage from the upper terrace aquifer. The thickest coarse gravel deposit is estimated to about 50 m. Groundwater table is at a depth of 25 to 37 m in the average, thus the thickness of the saturated layer along the aquifer axis is estimated to 7-14 m, and even more in the deepest sections (Mali, 2006; Mali et al., 2005). The hydraulic conductivity of the coarse gravel aquifer is estimated to 5x10^{-3} m/s (Mali & Janža, 2005). The area has the moderate continental climate of central Slovenia with a typical continental precipitation regime and an average annual rainfall between 1200 and 1300 mm. The average yearly air temperature lies between 8 and 12 °C (Mali & Janža, 2005).

The lysimeter is located (Figure 8.2) in the area of the principal aquifer of Selniška dobrava. The larger area of the lower aquifer is covered by mixed forest. The soil at lysimeter location was defined as distric cambisol. The hydraulic conductivity of the soil was estimated to 1.5-4.5x10^{-5} m/s by double ring method (Mali, 2006). The thickness of the gravel deposit in this area is 37.5 m, the water table is at 27.5 m, and the saturated layer is 10 m thick. The gravel at lysimeter location consists of metamorphic rock and carbonates (limestone, marble-sandstone, marble and agglutinated carbonate gravel). Here and there the gravel is incrusted by calcite. Based on granulometric analyses the hydraulic conductivity of the coarse gravel was estimated to 2.9x10^{-3}-6.9x10^{-2} m/s (Mali, 2006).

8.3.3 Experimental Set-Up

The lysimeter (Figure 8.3) was designed as a concrete box, measuring 2x2 m, 5 m deep, with walls 0.2 m thick. There are 10 sampling and measuring points at different depths (from JV-1 to JV-10). Sampling point positions are random with approximately equal distances by depth. For sampling groundwater in the UZ drainage samplers were installed. The stainless-steel drains are 10x10 cm profiles, 1.7 m long, with inverse inner perforated profiles (5x5 cm), and with a collection system at the end. The steel drains were inserted horizontally into the undisturbed wall using a hydraulic press. Each sampling point was equipped with a water collection system. The closed system was made up of one 400ml glass bottle and collecting containers. A measurer of precipitation with access for the collection and sampling of precipitation is positioned at the lysimeter (Koroša et al., 2019).

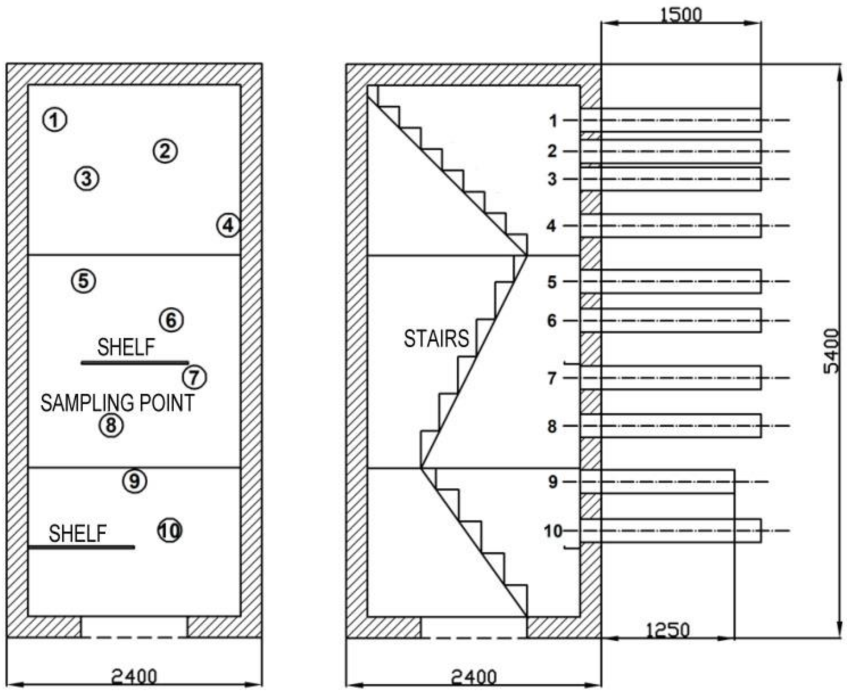

Figure 8.3. Lysimeter cross-section

8.3.4 *Deuterium and Nitrate Tracer Experiment*

A tracer experiment was performed in April (2006) after the period of intensive snow melting. Water and nitrate transport processes were estimated by a combined tracing experiment with deuterated water and $Ca(NO_3)_2$. Deuterium was used as a conservative tracer of water movement, and NO_3-N was used as a tracer of nitrate in an UZ. Before tracer injection, irrigation with groundwater was performed to reach good field capacity. 1.2 kg of $Ca(NO_3)_2$ and 1000 ml of D_2O (70%) were dissolved in 50 l of groundwater and injected by sprinkler irrigation. After injection the tracer was again splashed by irrigated groundwater. The area of irrigation was 9.5 m^2 big. The distribution of the artificial rainfall was controlled by 10 precipitation measuring points. The average amount of irrigated water was 50 mm (Mali & Koroša, 2015).

8.3.5 *Methods*

Evaluation of breakthrough curves from tracer experiment was done with two different approaches. First is with program TRACI'95 (1998) where best-fit method was used. Second is using the HYDRUS-1D software package (Šimunek et al., 2010) where water in the UZ was simulated by numerically solving the Richards equation. Transport in UZ was calculated using the advection-dispersion equation without retention, which assumes a single porous medium, and is the most widely used model to predict solute transport in soils under field conditions (Vanderborght and Vereecken, 2007).

8.4 Results and Discussion

8.4.1 *Numerical Model – Hydrus 1-D*

The aims of tracer experiment were also to determine the UZ hydraulic properties of coarse gravel UZ and specify the flow of nitrate in coarse gravel UZ under real environmental conditions. Physical parameters of Mualem-van Genuchten model were estimated for each drain and was applied for the parametrization of water retention (*ϑ*) and unsaturated hydraulic conductivity (*K*) (van Genuchten, 1980; Mualem, 1976):

$$\theta(h) = \begin{cases} \theta_r + \dfrac{\theta_s - \theta_r}{[1+[1+|ah|^n]^m]} \ h < 0 \\ \theta_s \quad h \geq 0 \end{cases} \tag{8.1}$$

$$\mathrm{K}(h) = K_s S_e \left[1 - \left(1 - S_e^{\frac{1}{m}}\right)^m\right]^2 \tag{8.2}$$

$$\mathrm{m} = 1 - \frac{1}{\mathrm{n}}, \mathrm{n} > 1 \tag{8.3}$$

These are specified according to residual and saturated volumetric water content (ϑ_r and ϑ_s), inverse of capillary fringe thickness (α), two shape parameters n and m (where $m = 1-1/n$), with the saturated hydraulic conductivity (K_s) and tortuosity parameter (l) set to 0.5 in order to reduce the number of free parameters, while S_e represents effective saturation (Mualem, 1976). Nash-Sutcliffe efficiency (NSE) was used to model efficiency (Nash and Sutcliffe, 1970):

$$NSE = 1 - \frac{\sum(y_0 - y_p)^2}{\sum(y_0 - \overline{y_0})^2} \tag{8.4}$$

where y_0 and y_p are the observed and simulated values at a given time t, and $\overline{y_0}$ is the mean observed value over the entire observation period. An efficiency of 1 (NSE = 1) corresponds to a perfect match of the modelled values to the observed data. An efficiency of 0 (NSE = 0) indicates that the model predictions are as accurate as the mean of the observed data, whereas an efficiency of less than zero (NSE < 0) occurs when the observed mean proves a better predictor than the model. The matching of simulated data was determined by comparing observed and simulated values for each sampling point.

Longitudinal dispersivity (αL) in the model was determined for each sampling point using the equation αL = 1.75d50 (Xu and Eckstein, 1997). Data for average particle size (d50) was obtained from a previous analysis of grain size (Mali, 2006). The upper boundary condition was determined using the variable atmospheric condition “atmospheric boundary condition with surface runoff”, and “free drainage” was used as the lower boundary condition for water flow and solutes (Šimunek, 2010).

All long-term precipitation data used for the models is taken from the Maribor - Tabor measurement station (Slovenian Environmental Agency, 2017). Evapotranspiration data was estimated by the Slovenian Environmental Agency (2017) based on the Penman-Monteith equation (Allan et al., 1998).

The inversely estimated soil hydraulic and transport values based on the modelling deuterium breakthrough curves are as follows: θs is 0.38–0.51, α is 0.03–0.038 1/cm, n is 1.3–1.39, Ks is 4.00×10^{-4} – 5.7×10^{-3} m/s, and longitudinal dispersivity α_L is 8 to 52 cm. For model optimization NSE is set between 76 % and 98 %. According to the properties of the coarse gravel UZ θr was set to zero to reduce the number of optimized parameters; at the same time, it has no significant influence on transport.

A more detailed description of this method is given by Koroša et al. (2020).

Modelled parameters were used as the basis for the characterization of the transport processes of nitrate in the UZ with analytical model.

8.4.2 Analytical Model - TRACI’95

For evaluation of breakthrough curves from a tracer experiment a best-fit method of the computer program TRACI’95 (1998) was used. TRACI’95 was used to estimate the mean flow velocity and vertical dispersion. For analytical solution, the one-dimensional convection–dispersion model with standardizing values for single porosity was chosen.

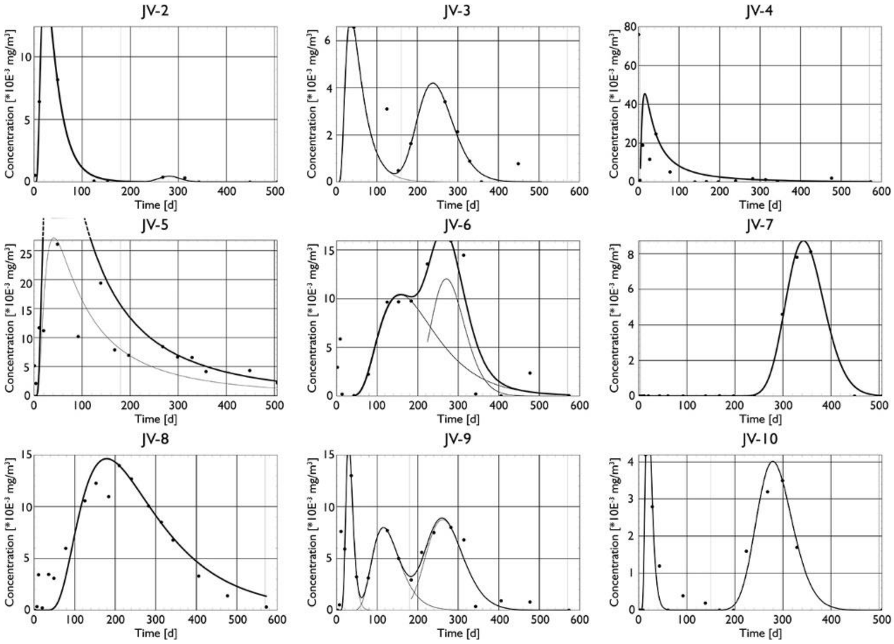

Figure 8.4. Best fit curves for nitrate concentrations (10-3 mg/m^3)

The mean flow velocities based on nitrate concentration breakthrough curves were estimated by analytical best-fit method (Figure 8.4). For JV-2, JV-3, JV-5, JV-6, JV-9, and JV-10 the Multi-Peak-Modus model was used. Up to the depth of 1.08 m (JV-2, JV-3) the mean flow velocities are estimated at 0.003-0.019 m/d, on average 0.011 m/d. In JV-4 the mean flow velocity is 0.016 m/s. From sampling point JV-5 to JV-8 the mean flow velocities range between 0.008-0.12 m/d, on average 0.010 m/d. The highest mean flow velocities were calculated in the lower part of the lysimeter at JV-9 and JV-10. Concentrations are moving between 0.014-0.197 m/d. Not considering the highest estimated mean flow velocities at JV-9 and JV-10, the average mean flow velocity is estimated at 0.013 m/d.

Table 8.1. Fastest, dominant (dom.) and mean flow velocities (m/s) of nitrate (Mali & Koroša, 2015)

		JV-2	*JV-3*	*JV-4*	*JV-5*	*JV-6*	*JV-7*	*JV-8*	*JV-9*	*JV-10*
Distance	m	0.82	1.08	1.58	2.04	2.41	2.95	3.4	3.93	4.39
Fastest f.	m/d	-	-	0.19	0.255	0.301	0.369	0.425	0.491	0.549
Dom. f.	m/d	0.02	0.026	0.036	0.032	0.009	0.009	0.015	0.028	0.023
Mean f.-1	m/d	0.019	0.019	0.016	0.01	0.011	0.008	0.012	0.117	0.197
Mean f.-2	m/d	0.003	0.004	-	0.01	0.009	-	-	0.03	0.015
Mean f.-3	m/d	-	-	-	-	-	-	-	0.014	
Dispersion-1	m2/s	0.003	0.003	0.024	0.016	0.003	0,000	0.006	0.019	0.051
Dispersion-2	m2/s	0.000	0.000	-	0.016	0.000	-	-	0.005	0.001
Dispersion-3	m2/s	-	-	-	-	-	-	-	0.001	-

The thickness of the UZ on lysimeter location reaches 27.5 m. If it is assumed that the ground water level is 27.5, average first speed of nitrate is 0.369 m/d the first contamination can reach the water in 74 days. Based on the average dominant flow velocity (0.022 m/d) the percolation time is 3.42 years. When the estimated mean flow velocity is 0.013 m/d, the time of pollution arrival is estimated at 5.80 years.

8.5 Travel Times of Nitrate in Fluvial Deposits

Travel times are calculated as ration between thickness of unsaturated zone and flow velocity of pollutant (NO_3). Flow velocity is calculated for two materials: coarse gravel fluvial deposits and clayey fluvial deposits with lower permeability (Mali & Koroša, 2015) shown on Figure 8.5. It is calculated with Van Genucht parameters (Table 8.2) (Koroša et al., 2020). Fluvial deposits have average flow velocity 0,013 m/day based on depth of unsaturated zone 7,4 m and average modelled hydraulic conductivity 5×10^{-3} m/s. Clayey fluvial deposits flow velocity have a range between 0,003 and 0,019 m/day. For the case study we used flow velocity 0,003 m/day and average hydraulic conductivity 9.65×10^{-4} m/s (Koroša et al., 2020).

Table 8.2. Physical van Genuchten parameters for two different types of fluvial deposits

	Θs	***α* [cm^{-1}]**	**n**	**Ks [m/s]**	**α_L [cm]**	**Average hydraulic conductivity [m/s]**
Coarse gravel fluvial deposits	0.38 – 0.51	0.027 – 0.03	1.25 -1.38	4.03×10^{-4} – 5.9×10^{-3}	4 - 52	5×10^{-3}
Clayey fluvial deposits with lower permeability	0.3891	0.0443	1.839			9.65×10^{-4}

Notation: θs - saturated volumetric water content, α - inverse of capillary fringe thickness, *n* a shape parameter, Ks - saturated hydraulic conductivity, α_L - longitudinal dispersity.

On Figure 6 are shown travel times in unsaturated zone on Drava pilot area. Average travel time of nitrate in fluvial deposits with lower permeability is 1701 days, minimal travel time is 4 days and maximal travel time is 5731 days or 15.7 years. Average time of nitrate in coarse gravel fluvial deposits is 544 days, minimal travel time 0.5 day and maximal 3752 days or 10.3 years.

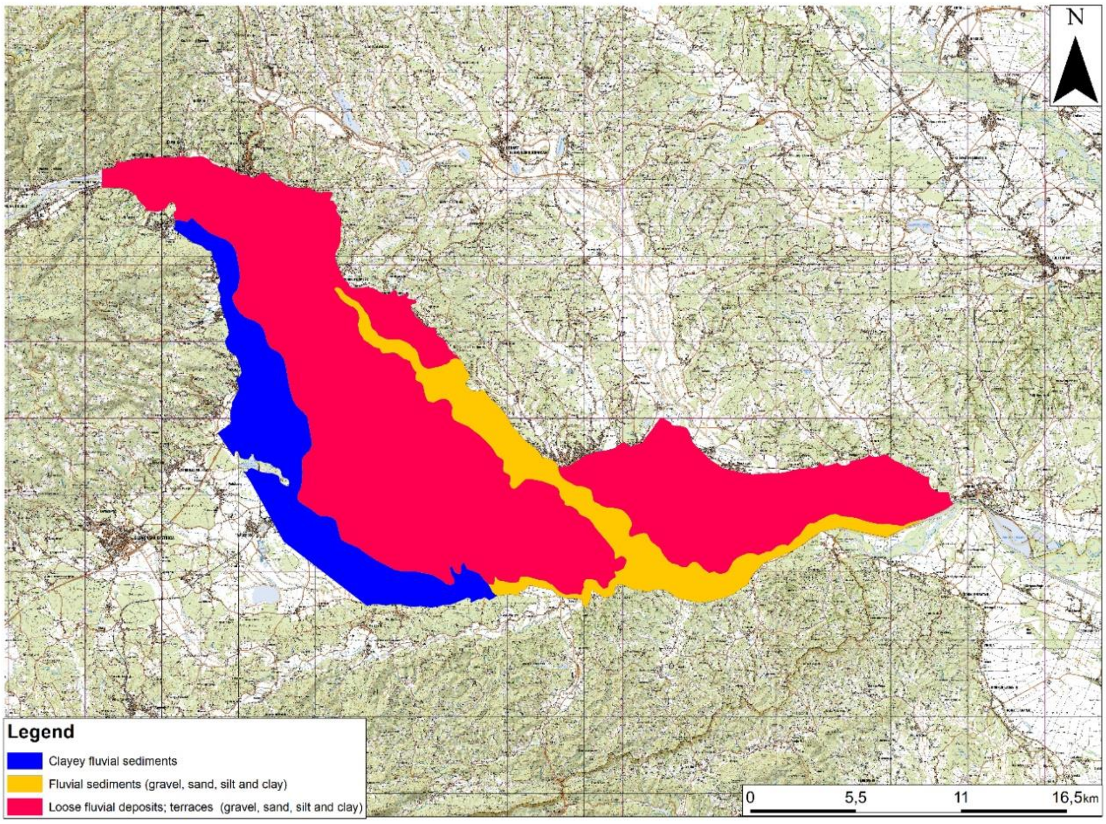

Figure 8.5. Lithology on investigated area for different flow velocity

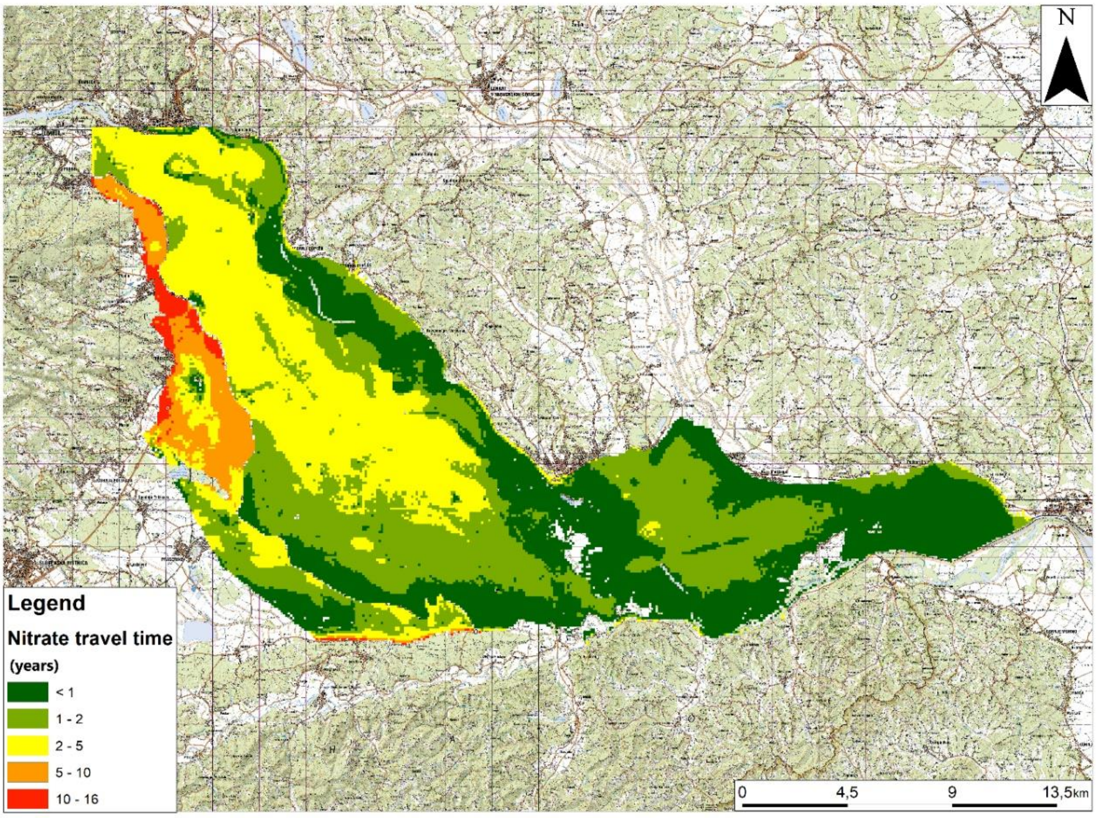

Figure 8.6. Travel times of NO_3 in unsaturated zone on Dravsko and Ptujsko polje aquifer

8.6 MODELING WATER AND NITRATE TRANSPORT IN SATURATED ZONE

8.6.1 Methodology

Models of Dravsko polje and Ptujsko polje aquifers were both designed separately. At first conceptual models were built for each field, afterwards two numerical models with Modflow-2000 were designed.

8.6.1.1 GMS

For numerical models GMS 10.1.3 was used (Groundwater Modelling System) from Aquaveo. It is a graphic user interference with number of analysis codes such as MODFLOW and MT3DMS for preforming groundwater simulations. For groundwater simulation Modflow-2000 was used.

8.6.1.2 MODFLOW

Units that describe flow between cells are L which represents length unit and T for time unit. Groundwater flow in the model is calculated using Darcy's law.

The three-dimensional movement of groundwater of constant density through porous earth material may be described by the partial-differential equation:

$$\frac{\partial}{\partial x}\left(K_{xx}\frac{\partial h}{\partial x}\right)+\frac{\partial}{\partial y}\left(K_{yy}\frac{\partial h}{\partial y}\right)+\frac{\partial}{\partial z}\left(K_{zz}\frac{\partial h}{\partial z}\right)+q=S_s\frac{\partial h}{\partial t} \tag{8.5}$$

where:
K_{xx}, K_{yy}, K_{zz} – values of hydraulic conductivity along x, y and z coordinate axes, which are assumed to be parallel to the major axes of hydraulic conductivity $[L/T]$,
h – hydraulic head $[L]$,
q – volumetric flux per unit volume representing sources and sinks of water, with q<0 for flow out of the ground-water system, and q>0 for flow into the system $[T^{-1}]$,
S_s – is the specific storage of the porous media $[L^{-1}]$,
t – time $[T]$.
In general S_s, K_{xx}, K_{yy} and K_{zz} are functions of space and q is a function of space and time.

Equation 1 describes ground-water flow, under non-equilibrium conditions in a heterogeneous and anisotropic medium. Principal axes of hydraulic conductivity are aligned with the coordinate directions. Except if system is very simple analytical solution is possible, but usually numerical methods must be employed to solve this equation. One approach is the finite-difference method, where space is described with elements that have prescribed head values at the centre point of each element. The solution yields the values of head at specific points and times (Harbaugh, 2005).

8.6.1.3 PEST

The purpose of PEST (parameter estimation) is to assist in data interpretation, model calibration and predictive analysis.

In our model we used PEST for calibration of hydraulic conductivity and hydraulic heads between measured and modeled data.

8.7 CONCEPTUAL MODELS AND BOUNDARY CONDITIONS

Groundwater levels (GWL) and model top and bottom layers were made together for both models. First, we will discuss the methodology how layers were made. Afterwards, we will explain situation of conceptual models separately for Dravsko polje and Ptujsko polje aquifers.

Based on measured groundwater heads on Dravasko polje aquifer (Figure 8.7) with 206 boreholes and Ptujsko polje aquifer (Figure 8.8) with 90 boreholes groundwater level map was made in ArcGis software. Its purpose is to be able to compare the modelled groundwater head to modelled results.

For Dravsko polje aquifer most data is available from 21th and 25th November 2012. High water state is significant for this time. For Ptujsko polje aquifer most data is available for 20th March 2015. Intermediate water state is significant for this time.

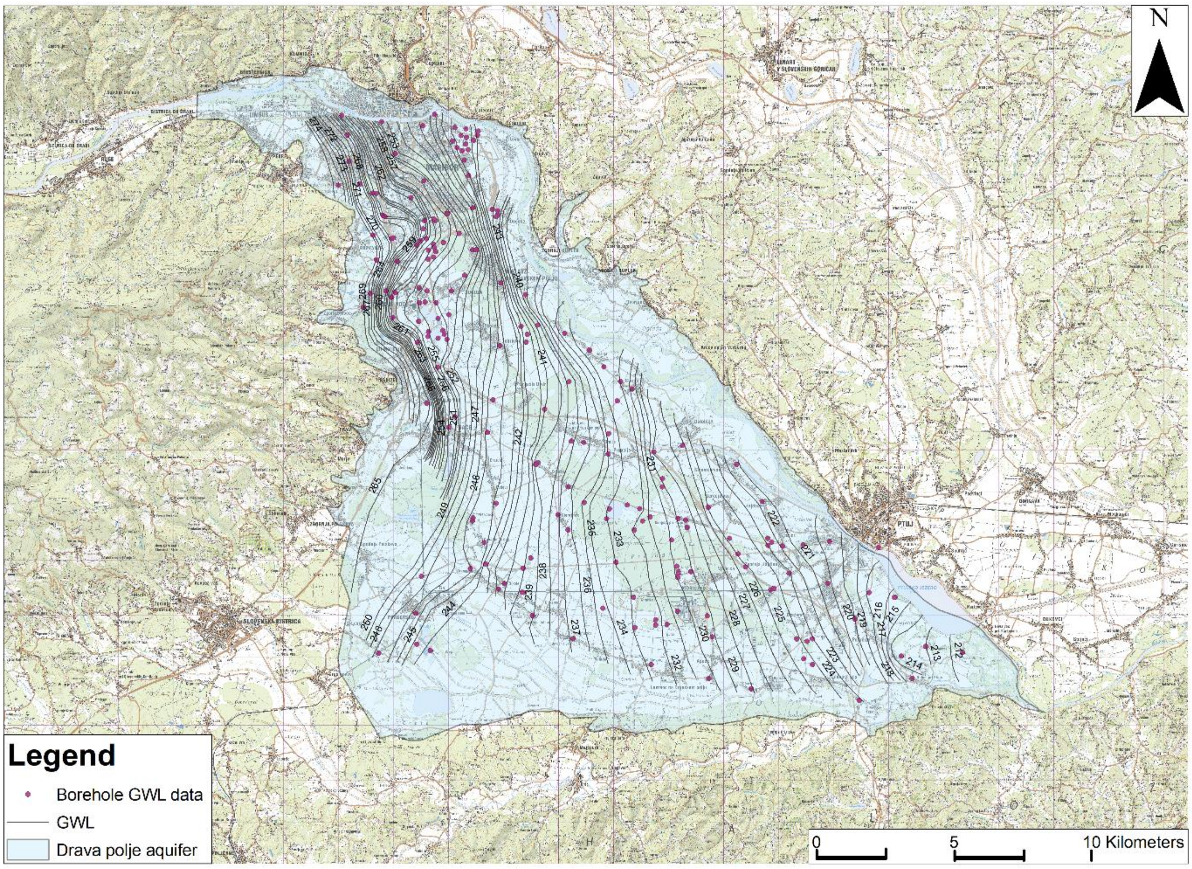

Figure 8.7. Groundwater level map for Dravsko polje aquifer

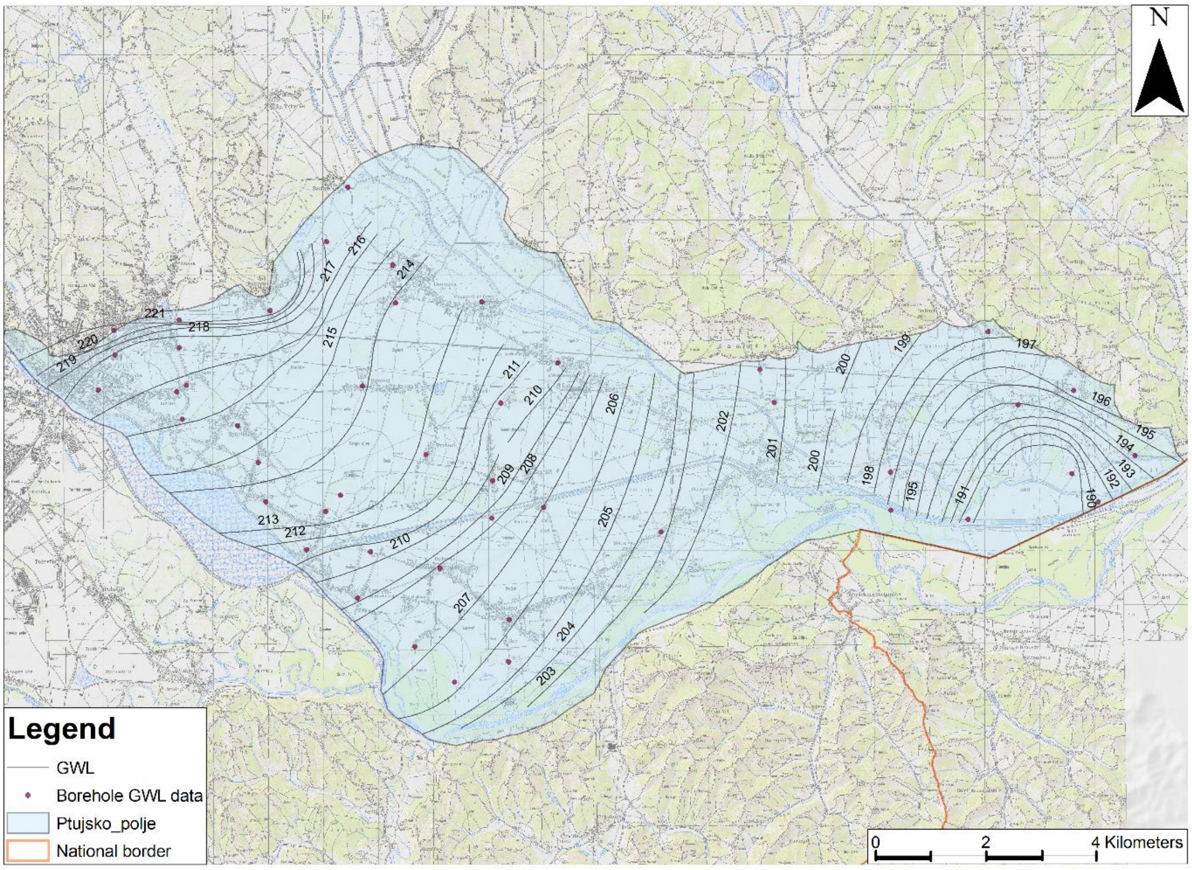

Figure 8.8. Groundwater level for Ptujsko polje aquifer

Same as GWL layer, Quaternary aquifer bottom layer was constructed in ArcGis with data from boreholes. Bottom layer of the Quaternary aquifer was designed in 2013. It was updated in year 2020 with new data from 1710 boreholes on Dravsko polje aquifer and on Ptujsko polje aquifer from 822 boreholes (Figure 8.9). For surface layer LIDAR data was used. All Lidar data in Slovenia is available for free. Models are set to cells with size 100 x 100 m. The porosity value 0.15 is used in both models (Veselič, 1984).

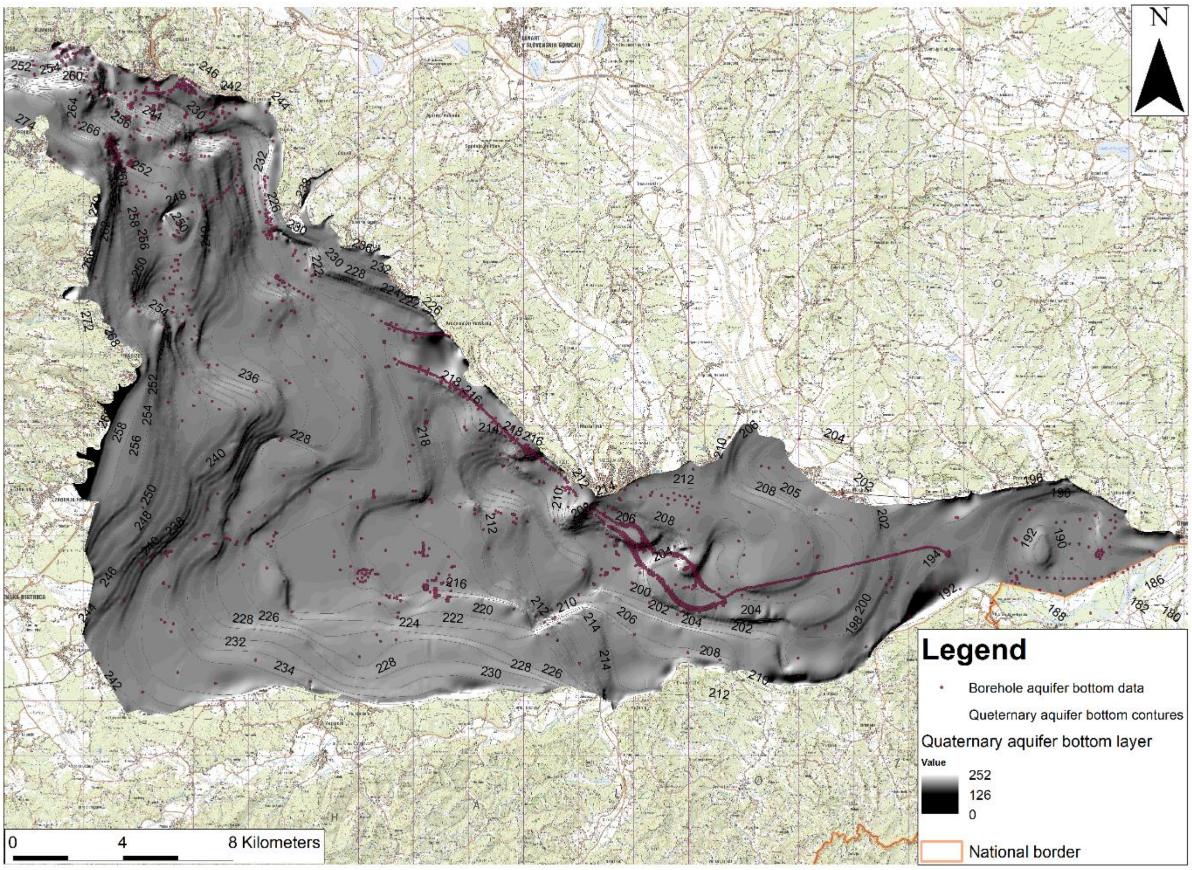

Figure 8.9. Bottom layer of Quaternary aquifer

8.7.1 Modelling Dravsko Polje Aqufier

West side of the Dravsko polje aquifer model is bounded by BC 'Specified head'. This boundary allows constant flow from Pohorje hills to Dravsko polje aquifer. Along the west margin constant head is divided into three sections as shown on

Figure 8.10. Each cell with constant head has prescribed head stage based on GWL map.

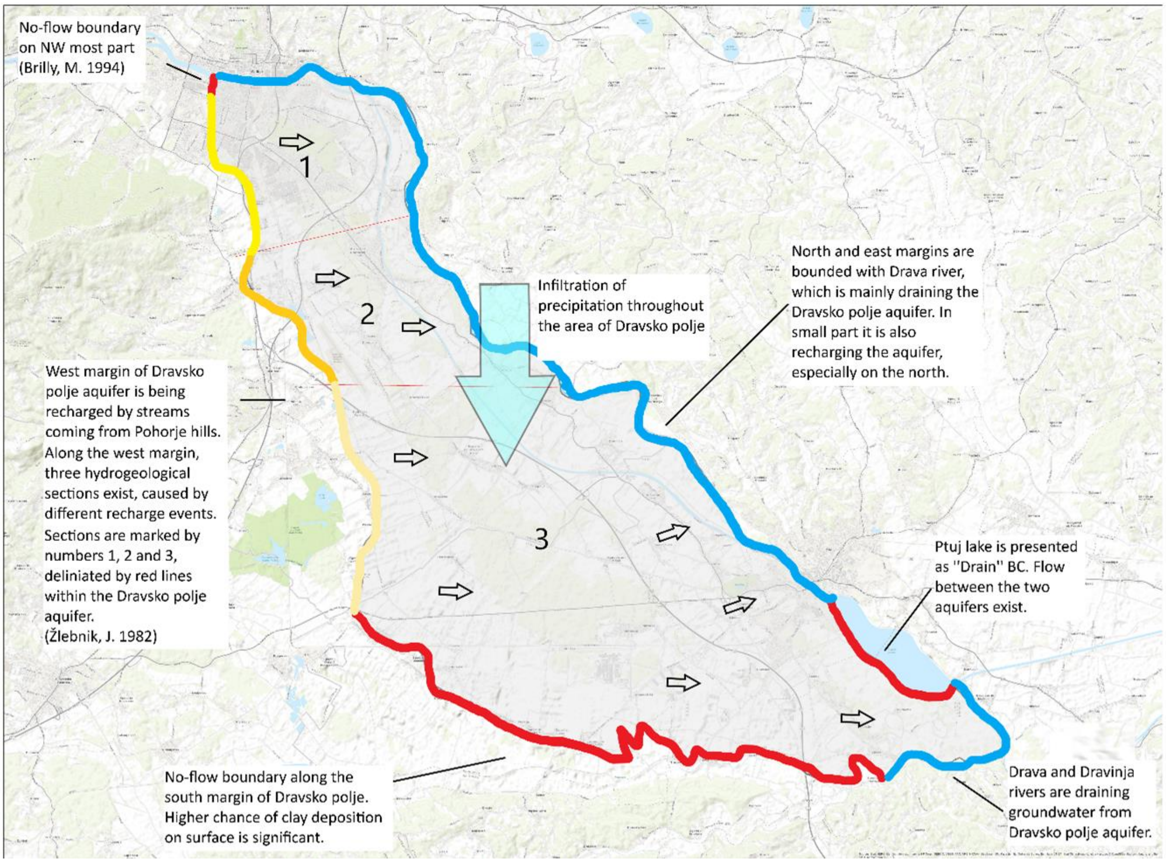

Figure 8.10. Conceptual model Dravsko polje aquifer

On east margin BC 'Drain' is set for lake Ptuj. Head stage values equals bottom layer of the lake where groundwater is higher than the lake bottom layer (Figure 8.11). This is the indicator that the flow under the lake between Tertiary bottom and lake bottom exist. Lake bottom layer is shown on Figure 8.12. It was adapted after Veršič, 2007, where image of the bottom layer is attached. We redraw it in ArcMap.

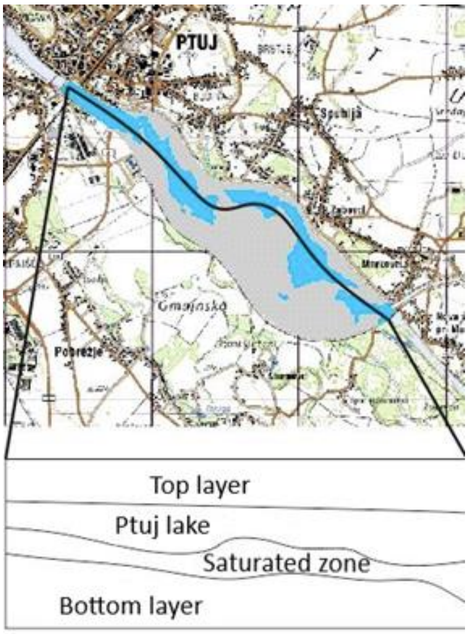

Figure 8.11. Groundwater level above the lake bottom layer (blue coloured part). Indicator that Quaternary gravel deposits are fully saturated and the groundwater flow between Tertiary base and lake bottom exists

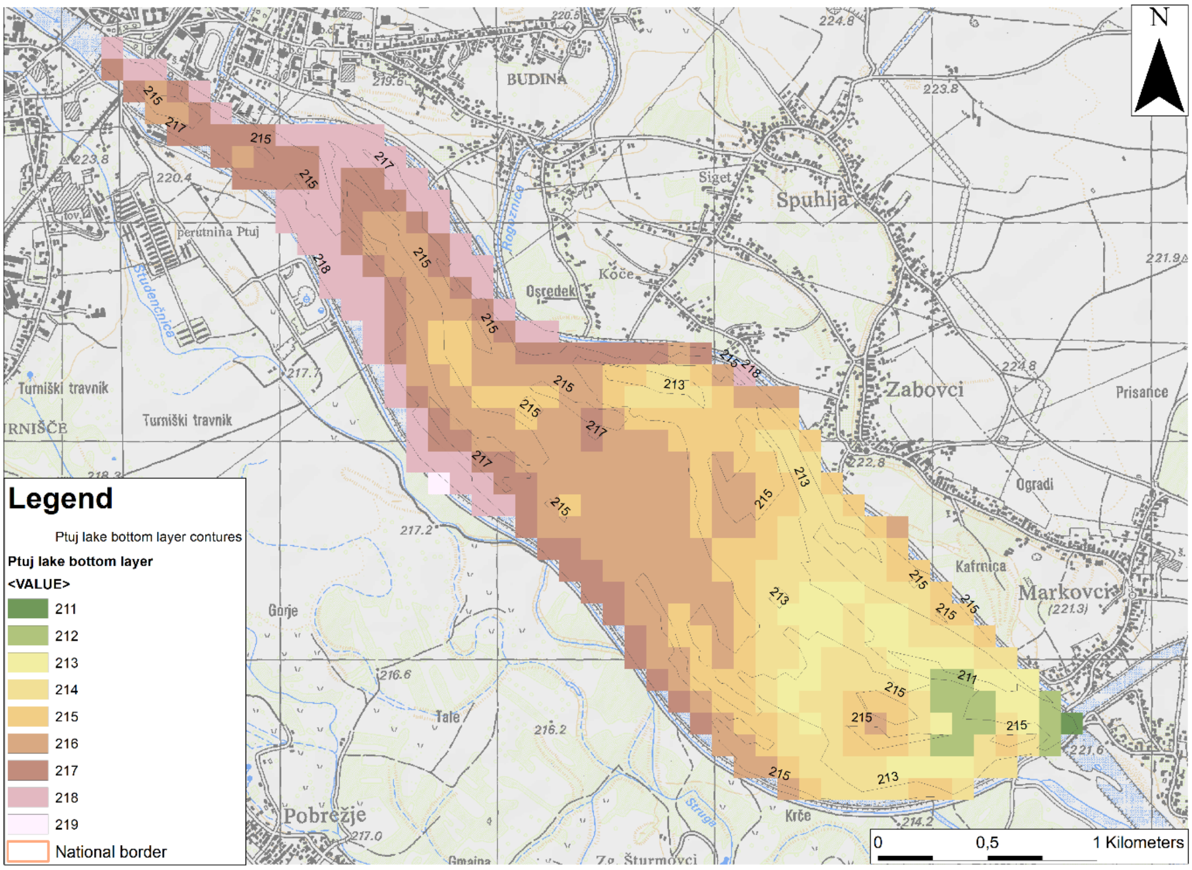

Figure 8.12. Ptuj lake bottom layer (adapted after Veršič, 2007)

Groundwater flow under the lake bottom is calculated based on Darcy's flow for unconfined aquifer with equation as follows:

$$Q = -K \times A \times \frac{h_2 - h_1}{L} \tag{8.6}$$

h_1, h_2 – groundwater head
L – length
K – hydraulic conductivity
A - area
Q – groundwater flow

North and east margins are bounded by Drava river and at the bottom by Dravinja river. Drava and Dravinja are mainly draining groundwater. Some leakage from Drava is significant for north most part of the river. The same as for the boundary condition constant head, groundwater level is prescribed to each cell of the river boundary based on the map from the year 2020. Riverbed elevation is calculated based on the top elevation which is subtracted by 2.5 m at each point of the river. However, some elevations were corrected if they were below the bottom elevation of the aquifer or groundwater head was below the riverbed elevation.

No-flow boundary condition is set along south margin of the model between river Dravinja on SE and Pohorje on west.

Whole area of Dravsko polje aquifer field has infiltration from precipitation. Based on GROWA model calculations (Growa, 2018) infiltration is between 300 and 450 mm/a. In year 2012 annual precipitation was 900 mm/a. Infiltration of precipitation on Dravsko polje aquifer is one third of the total amount which is 300 mm/a. Daily average precipitation is 0.00082 m/day and is prescribed to each cell as a recharge.

Near east margin in the middle and on SE are two drains, draining some part of the groundwater. Bottom elevation of drains is deepened for 0.5 m from the top elevation.

Model includes 7 pumping fields, in total 10 wells. Total pumping rate is 528.5 m^3/day (Table 8.3).

Table 8.3. Pumping rates on Dravsko polje aquifer

Pumping field	**Pumping rate** (m^3/day)
Betnava	40
Dobrovce	60
Šikole	44.5
Skorba	135.5
Kidričevo	183
Lancova vas	15.5
Bohova	50

Porosity of the whole model is 0.15. In

Table 8.4 are presented approximate values for water balance on Dravsko polje, estimated based on literature.

Table 8.4. Estimated groundwater flow values for Dravsko polje aqufier

	Wells	River	Recharge from precipitation	Recharge from west boundary (Pohorje)	Lake Ptuj
Flow in [m^3/s]	0	50.000 (Brilly, 1994)	106.272 (Arso, 2018)	259.200 (Turnšek, 2016)	0
Flow out [m^3/s]	528.5	app. 400.000 (groundwater is mainly discharging into river)	0	0	50.000 (calculated based on Darcy's flow)
TOTAL in-out [m^3/s]	**415.472**				

8.7.2 Modelling Ptujsko Polje Aquifer

Ptujsko polje aquifer is mainly recharged by the infiltration from precipitation including the evapotranspiration. Whole annual precipitation amount is being infiltrated into the groundwater. Based on the data from ARSO this value vary between 300 and 450 mm per year. In the model mean annual daily precipitation infiltration was used 0.00082 m/day for each cell.

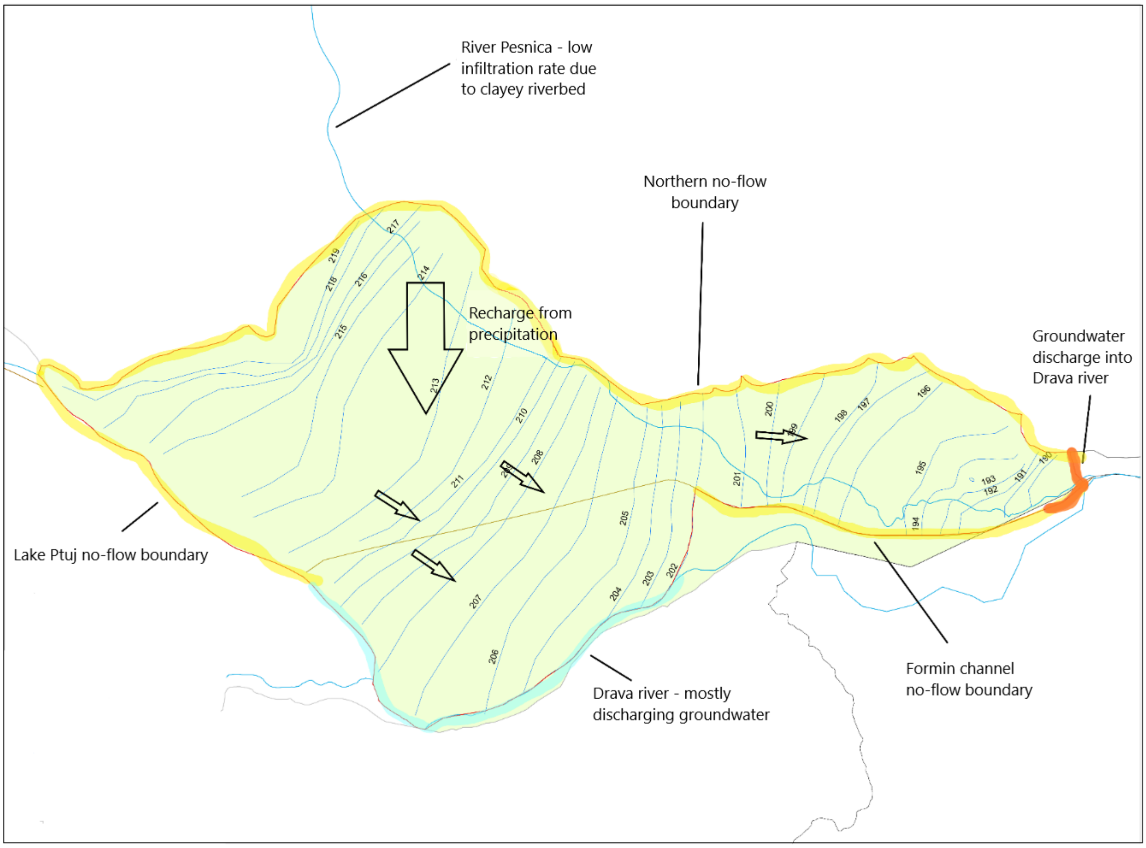

Figure 8.13. Conceptual model for Ptujsko polje aquifer

From Slovenjske Gorice hills on the north margin of Ptujsko polje aquifer very low amount of surface water from the streams is infiltrated. Therefore, north boundary is set to no-flow boundary due to simplification of the model. Conceptual model for Ptujsko polje aquifer is shown on Figure 8.13.

On east part between Formin village and Ormož city conducting channel for hydroelectric power plant Formin present impermeable boundary since it is sealed to the impermeable Tertiary base of the Quaternary aquifer. However, last 2 km of this channel is permeable to provide discharge of the groundwater into Drava river. The most eastern part of the Ptujsko polje aquifer is permeable as well, where it is connected with Ormožko polje aquifer. Therefore, conducting channel between Formin village and Ormož town presents no-flow boundary condition, except the last two kilometers and the eastern most part of the Ptujsko polje aquifert, where groundwater is being discharged. This boundary condition is set to drain BC and has prescribed head stages.

On west site groundwater is mainly discharging into the Drava river. However, in small part Drava river is also recharging the groundwater. Drava river is bounding the model from Ptuj town to Formin village. Head stage of the river boundary condition is set to groundwater level based on the GWL map. Riverbed elevation is calculated based on the top elevation which is subtracted by 2.5 m at each point of the river. However, some elevations were corrected if they were below the bottom elevation of the aquifer or groundwater head was below the riverbed elevation.

On west side between Ptuj and Markovci artifical Ptuj lake presents another boundary condition. In a model it is presented as specified flow boundary condition. Recharge rate is the same to one computed for Dravsko polje aquifer, since the same amount of water should be flowing from Dravsko towards Ptujsko polje aquifer under the lake. With specified flow boundary condition the same amount is provided.

Pesnica river that has a stream from Slovenjske Gorice hills and flows on Ptujsko polje aquifer towards Ormož town was neglected, since the amount of water infiltrating into the gorundwater is low due to clay deposits at the bottom of riverbed.

On east part of the Ptujsko polje aquifer a pumping site Sejanica pri Mihovcih is located to provide fresh water for Ormož town. Water is tapped from 16 pumping wells. However, to avoid depletion of the aquifer groundwater is being replenished by 5 infiltration fields where surface water from the conducting channel is infiltrated into the groundwater. Recharge rates are shown in Table 8.5 and pumping rates in Table 8.6.

Table 8.5. Recharge rates from infiltration fields on Ptujsko polje aquifer

Infiltration field	**Recharge rate (m^3/day)**
1	347.87
2	581.73
3	0
4	233.37
5	65.03

Table 8.6. Pumping rates on east side of Ptujsko polje aquifer

Pumping well	**Pumping rate (m^3/day)**
1	255.07
2	0

3	158.97
4	246.73
5	58.83
6	218.37
7	117.50
8	262.57
9	303.77
10	271.37
11	308.87
12	140.67
13	321.10
15	167.33
16	46.57
17	73.43

In Table 8.7 are presented acceptable values for water balance on Ptujsko polje, estimated based on literature.

Table 8.7. Estimated groundwater flow values for Ptujsko polje aquifer

	Wells	Infiltration fields (m^3/day)	Recharge from precipitation (m^3/day)	Recharge from west boundary lake Ptuj
Flow in	0	1228	77.433	15.000 (approximated based on result from numerical model Dravsko polje aquifer)
Flow out	2951.15	0	0	0
TOTAL in-out	**93.661**			

8.8 RESULTS

Both numerical models were successfully modeled. Below are presented results for both models for Dravsko and Ptujsko polje aquifer.

8.8.1 Dravsko Polje Aquifer

Hydraulic heads are well aligned between computed and observed values (Figure 8.14). Computed direction of flow is as expected from W-E direction in northern part and slightly to SE in southern part. Modeled hydraulic heads met the expectations of estimated hydraulic heads from the conceptual model. As seen from Figure 8.15 most hydraulic heads reached the deviation below 0.25 m (green boxes).

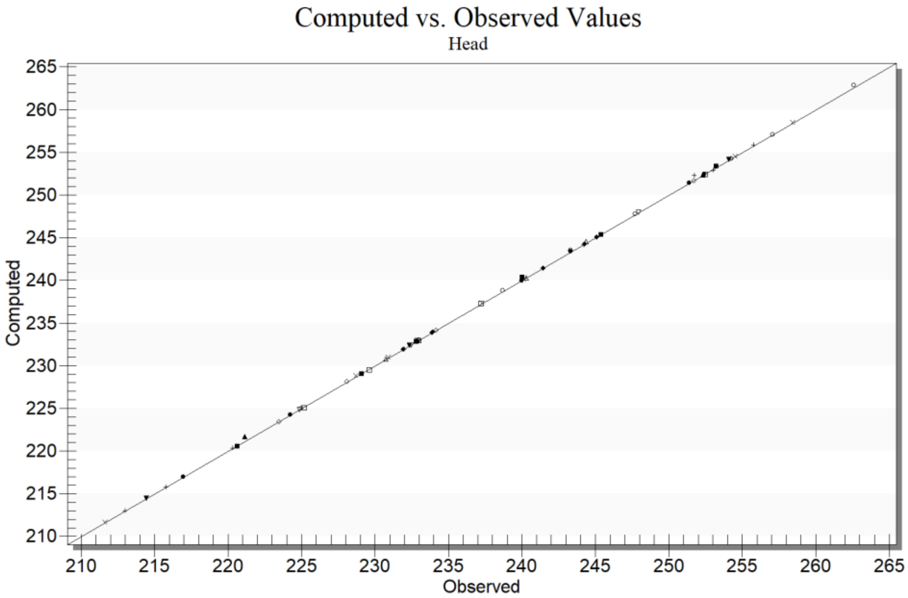

Figure 8.14. Comparison between computed and observed hydraulic heads on Dravsko polje aquifer

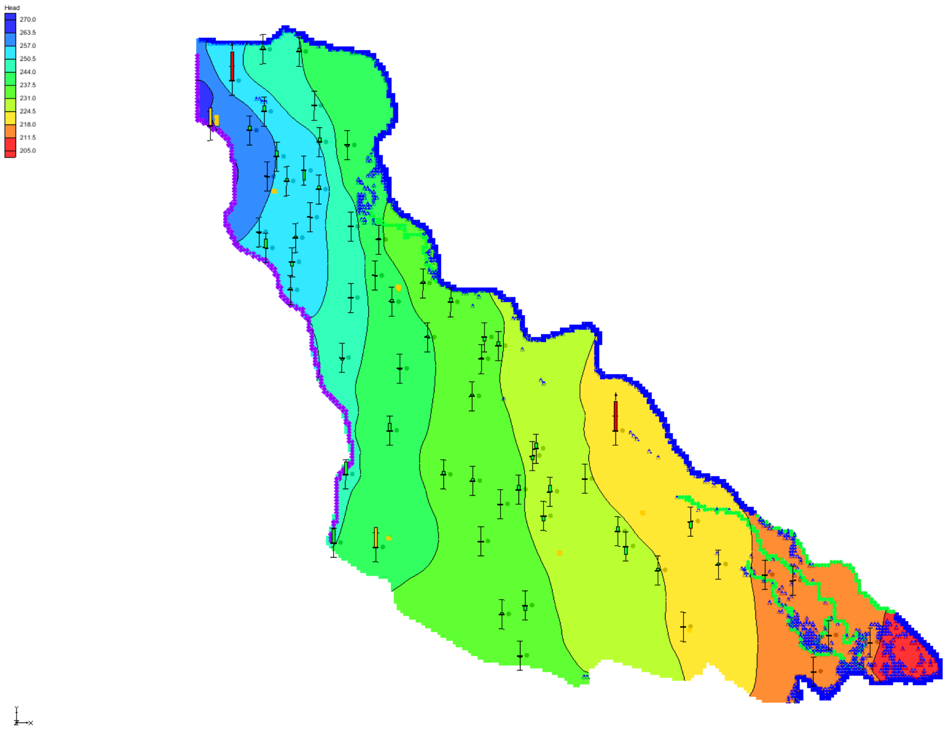

Figure 8.15. Computed hydraulic heads on Dravsko polje aquifer

Hydraulic coefficient span from 0.1 m3/day up to 2500 m^3/day. Values between 500 and 250 m/day predominate which is a very good result based on measured hydraulic conductivity values (Žlebnik, 1982). The distribution of hydraulic conductivity is shown on Figure 8.16.

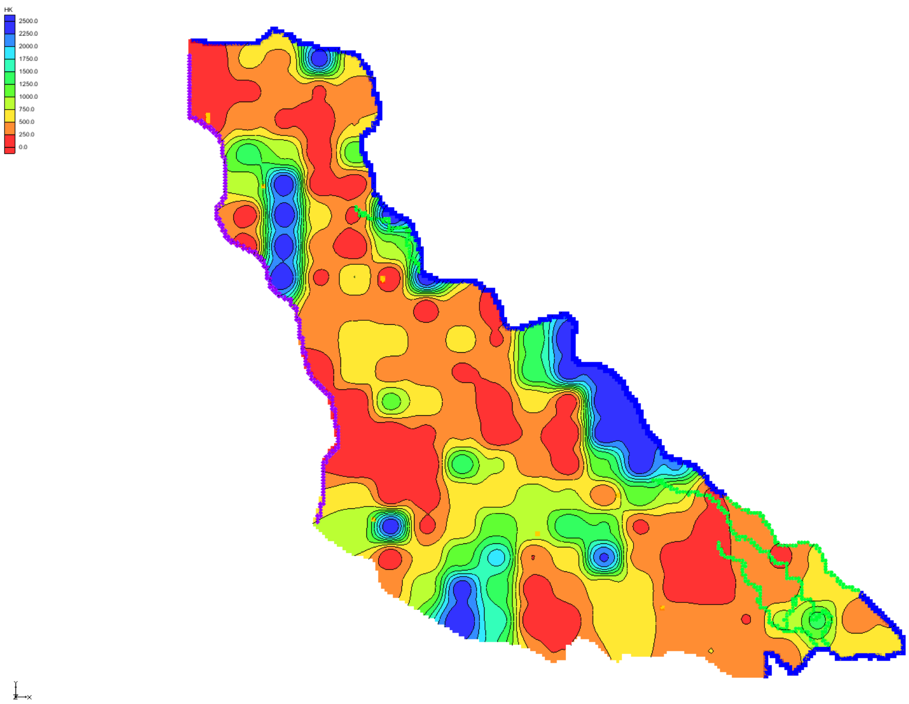

Figure 8.16: Hydraulic conductivity on Dravsko polje aquifer

Computed flow budget results are good (Table 8.8). Total in and out flow is higher than predicted flow but still adequate. Majority of groundwater is discharging to Drava river and the rest goes to drains. Lake Ptuj discharge is lower than computed discharge which was estimated to 50.000 m^3/s and computed discharge is approximately 14.000 m^3/s.

Table 8.8. Model flow budget results for Dravsko polje aquifer

	Flow in (m^3/day)	**Flow out (m^3/day)**
Wells		528,5
Drains		42.984
Lake Ptuj		13.632
River leakage	105.479	482.762
Constant head (Pohorje)	299.119	27.617
Recharge (Precipitation)	162.997	
Total in-out	**567.595**	**567.539**

Along the west margin as desribed before general head boundary is divided into three hydrogeological sections 1, 2 and 3 as described by Žlebnik, 1982. In

Table 8.9 are given flow rates for 1, 2 and 3 section.

Table 8.9: Flow rate for west margin of Dravsko polje aquifer.

Constant head section	**Flow rate (m^3/day)**
1 section	101.631
2 section	87.947
3 section	81.922

Where Dravsko polje aquifer is connecting with Ptujsko polje aquifer discharge from Lake Ptuj should be unified (Figure 8.17). Therefore, it is important to get similar values between the two fields. River values should vary, since it is not necessary to have the same conditions on left and right bank of the river. From Dravsko polje aquifer lake is discharging approximately 14.000 m^3/day. River discharges 18.000 m^3/day.

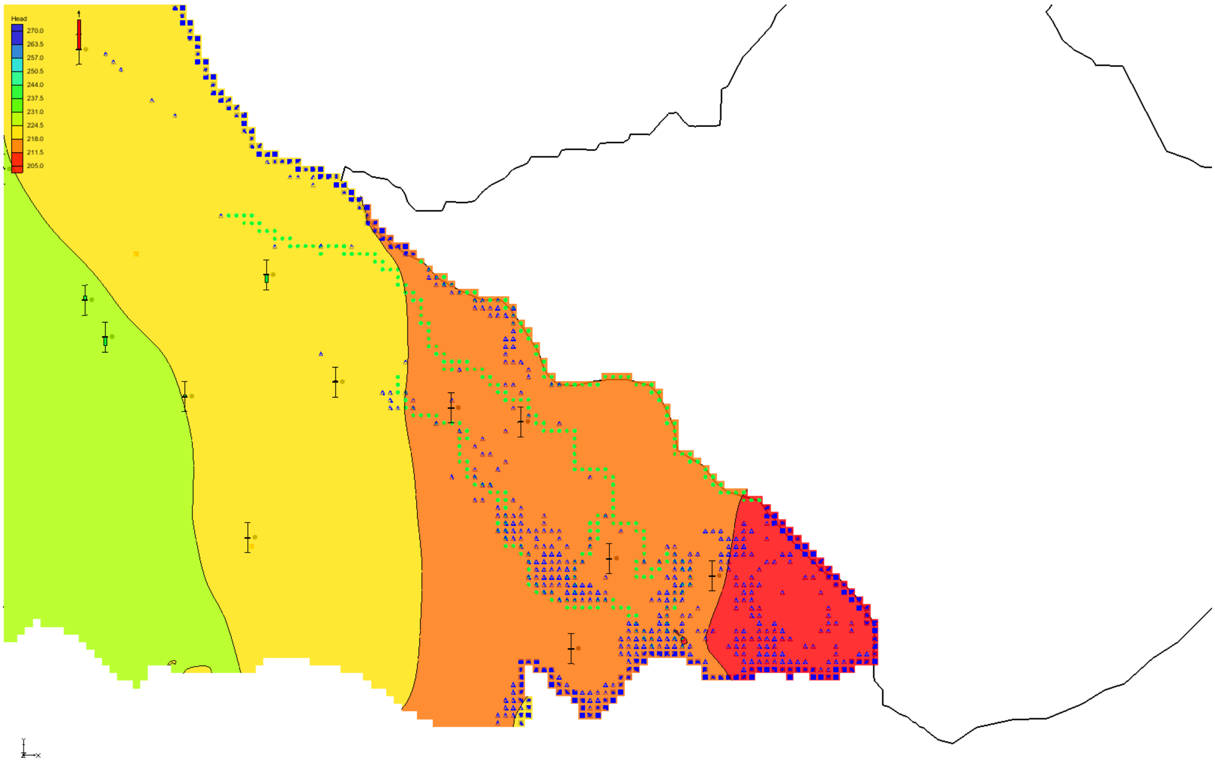

Figure 8.17. Interecting part between Dravsko and Ptujsko polje aquifer

Flow budget with intersecting part between Ptuj and Dravsko polje aquifer is given in Table 8.10.

Table 8.10. Flow budget for intersecting part between Dravsko-Ptujsko polje aquifer

	Flow in (m^3/day)	Flow out (m^3/day)
Lake Ptuj		13.632
River leakage	2.982	17.492
Total in-out	**2.982**	**31.124**

8.8.2 Ptujsko Polje Aquifer

Development of computed hydraulic head elevation shows flow direction as expected (Figure 8.18); in western part it has a direction from NW to SE and in eastern part parallel to conductive channel or Drava river with W-E direction. Based on observed groundwater level data computed hydraulic heads are well aligned with observed elevations (Figure 8.19).

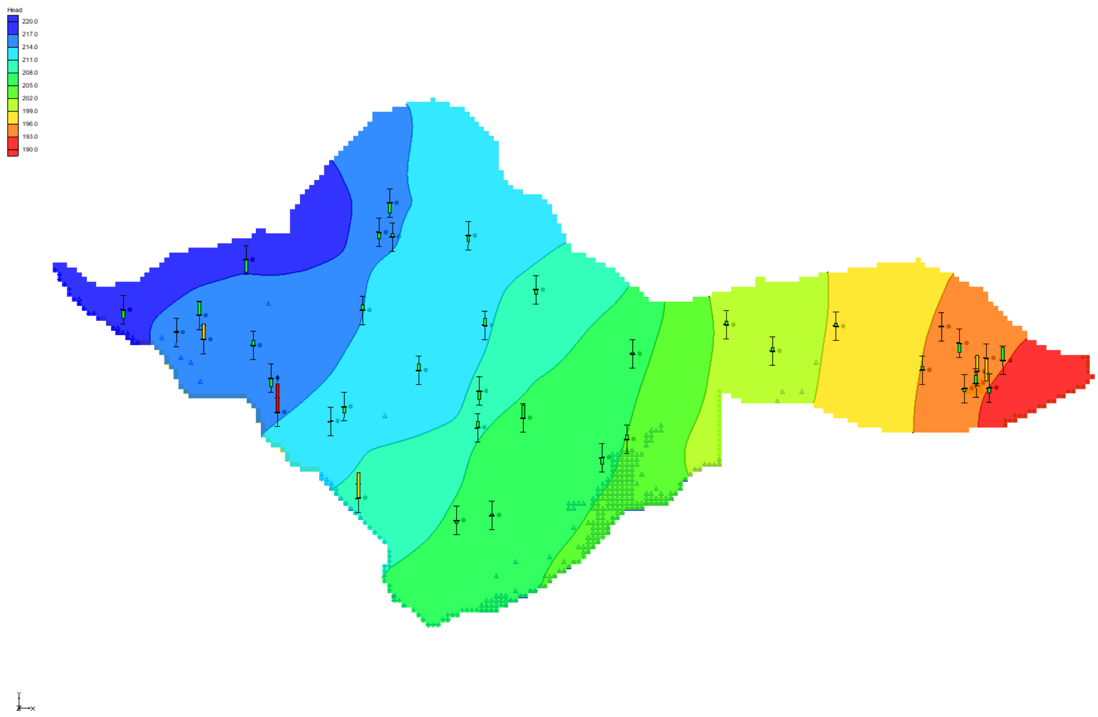

Figure 8.18. Caluclated hydraulic head on Ptujsko polje aquifer

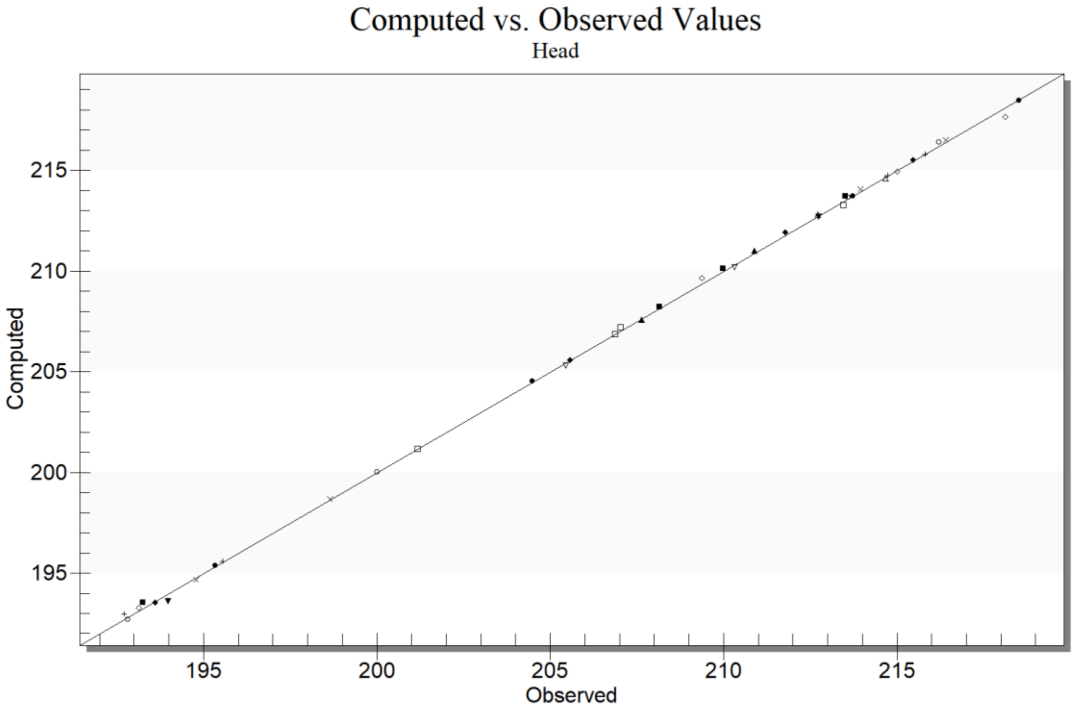

Figure 8.19. Deviation between computed vs observed values

Hydraulic conductivity has a range between 0.8 to 1500 m/day. Based on measured GWL data hydraulic conductivity is calculated as shown on Figure 8.20.

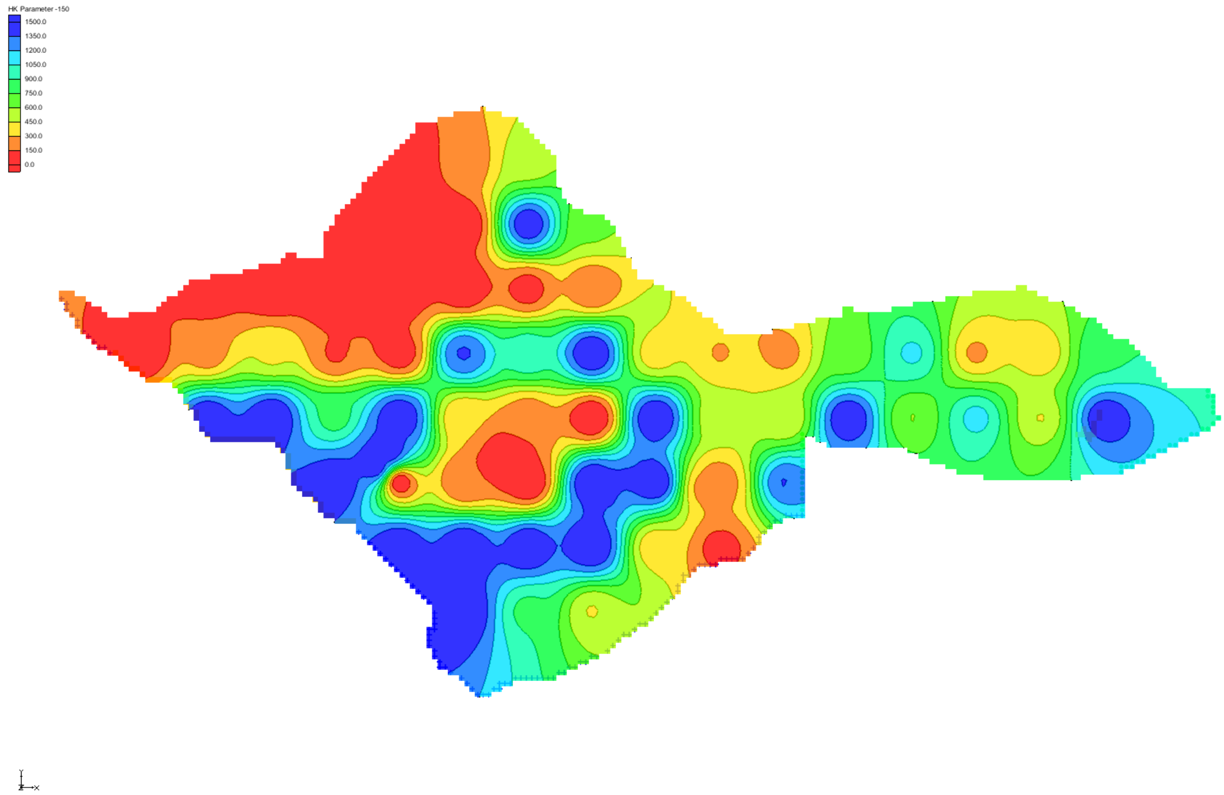

Figure 8.20. Calculated hydraulic conductivity on Ptujsko polje aquifer

In Table 8.11 are written modelled water budget results.

Table 8.11: Flow budget result for Ptujsko polje aquifer

	Wells	Infiltration fields	Lake	River	Drains	Precipitation
Flow in	0	1228	9.765	7.457	0	76.205
Flow out	2.951	0	0	51.619	40.065	0
TOTAL in-out	**94.656-94.635**					

Flow budget at intersection with Dravsko polje aquifer at west boundary is shown in Table 8.12.

Table 8.12. Flow budget result for intersecting part Ptujsko-Dravsko polje aquifer

	Lake (m^3/day)	River (m^3/day)
Flow in	9.765	4.095
Flow out	0	14.525
TOTAL in-out	**13.860-14.525**	

From modelled water budget total in-out budget is very close to estimated one. The result is considered as very good. Majority of groundwater is discharging into Drava river and the rest goes to drains.

8.9 MODELING NITRATE DISTRIBUTION AND TRANSPORT IN SATURATED ZONE OF DRAVA PILOT AREA

This chapter consist of two parts: in the first part we analytically calculated nitrate concentrations over the whole Drava pilot area, which mainly depend on land use characteristics. In the second part we used these raster data sets of nitrate concentrations to numerically calculate distribution of nitrate concentrations over a seven year time frame.

8.9.1 Analytical Calculation of Nitrate Concentrations over the Drava Pilot Area

Within the project Hover we made a nitrate concentration development map for Drava pilot area, which consist of three fields followed from the biggest to smallest: Dravsko, Ptujsko and Ormoško polje aquifers.

Nitrate infiltrates into the aquifer from various sources:

- Feces from local sewage system
- Animal waste from farms; pigs, cattle, chicken, small cattle
- Mineral fertilizers
- Nitrate from precipitation
- Recharge of small streams from outskirts

All input nitrate concentrations were computed for hydrochemistry model made in 2014 (Urbanc, J., et al., 2014). Data was computed based on potential infiltration causes of nitrate such as animal and human annual nitrate production, agriculture nitrate contribution and infiltration of nitrate with precipitation.

Different nitrate concentrations were assigned to different layers based on their land use purpose.
Only one part of nitrate infiltrates into groundwater from surface. Nitrate concentration in groundwater decreases by various causes:

- Nitrate plant consumption
- Nitrate loses by conversion into manure, ammonia evaporation, weathering of manure
- Denitrification processes in unsaturated zone

8.9.2 Methods

This section is divided into three parts; land use, nitrate concentration and sewage/cesspit nitrate contribution. When all of the data was collected for each part, together they form a nitrate concentration development map of Drava pilot area.

8.9.2.1 LAND USE

Layers for land use were collected from Ministry of Agriculture, Forestry and Food (MKGP, 2020). All land use layers covering Drava basin area were categorized into six land use categories. Layers we used in spatial nitrate analysis are presented and categorized in Table 8.13.

Table 8.13. Categorization of land use layers on Drava pilot area

LAND USE	LAND USE ID	LAND USE CATEGORY
Fields and garden	1100	1
Hop garden	1160	1
Agricultural land- Permanent crops	1180	1
Greenhouse	1190	2
Vineyard	1211	2
Intensive orchard	1221	2
Extensive orchard	1222	2
Other permanent plantation	1240	2
Permanent meadows	1300	2
Land in overgrow	1410	3
Plantation of forrest trees	1420	3
Forest trees and bush	1500	3
farmland overgrown with forrest trees	1800	3
Uncultivated farmland	1600	4
Forrest	2000	5
Urbanised land	3000	6

Land use category explanation:

1 – area with higher potential of fertilizers and agents for plant protection in soil (field and garden, hop garden and permanent plants on field),
2 – area with lower potential of fertilizers and agents for plant protection in the soil (temporary meadow, green houses, vineyard, intensive and extensive orchard, olive tree plantation, other permanent plantation, permanent meadows and moor meadows),
3 – non-intensive farmland use (mountain pasture, land in overgrow, plantation of forest trees and bush, farmland overgrown with forest trees),
4 – uncultivated farmland
5 - forest,
6- urbanized land

As described these layers were processed and divided into each category from 1 to 6 in ArcMap.

8.9.2.2 NITRATE CONCENTRATION

Nitrogen surface infiltration amount [kgN/ha] calculated for Dravsko polje aquifer (Urbanc, J., et al., 2014) was used to assign nitrate infiltration on Dravsko, Ptujsko and Ormoško polje aquifer. Therefore, the same nitrate amount proposed for Dravsko polje aquifer per hectare was used for Ptujsko and Ormožko polje aquifer. This is acceptable since all three fields have similar hydrological parameters and farm land prevail.

Nitrate concentration were primary assigned to surface layer. As found in previous project, 41 percent of all amount is held in unsaturated zone and does not go into the groundwater. The rest 59 percent infiltrate into the groundwater.

8.9.2.3 SEWAGE/CESSPIT NITRATE CONTRIBUTION

Annual nitrate infiltration into the groundwater from sewage systems was computed based on amount of population intersecting with sewage system.

Spatial layers for sewage systems and house numbers with number of registered households are found online on site of Ministry of the environment and spatial planning (MOP, 2020). At each point where the two layers intersect amount of infiltrated nitrate is multiplied with number of households with annual human nitrate contribution. At sections where house numbers are not intersected by sewage system it is assumed cesspit is in use.

It is assumed that sewage systems average leakage is 50% (Prestor et al., 2014). This depends on sewage system material and age; older it gets, higher the leakage amount. Where sewage system is not available and population is registered, most probably cesspits are in use. Leakage of cesspit is assumed to be higher, therefor we prescribe it 70%.

Nitrogen infiltration N_2 from sewage system and cesspit but with higher leakage factor was calculated with equation

$$I_N = \frac{(k_{lpč} \times n) * 0{,}5}{A} \left[\frac{kgN}{ha}\right] \tag{8.7}$$

I_N – infiltration of N_2 (kgN/ha)
k_{aN} – annual N_2 infiltration per human (kgN/a)
n – people count
A – area (ha)

This equation gives us nitrate concentration from sewage and cesspit on surface layer. This amount present 100 percent of nitrate concentration on surface layer. As found in previous project 41 percent of all amount is held in unsaturated zone and does not go into the groundwater. The rest 59 percent infiltrate into the groundwater.

8.9.3 Results

Final result of nitrate concentration development is a sum of the two rasters one with prescribed nitrate concentration for different land use and the second nitrate concentration from sewage and cesspit.

At first we made a map with 6 land use categories as described in Table 8.13. Land use categories for Drava basin are shown on Figure 21.

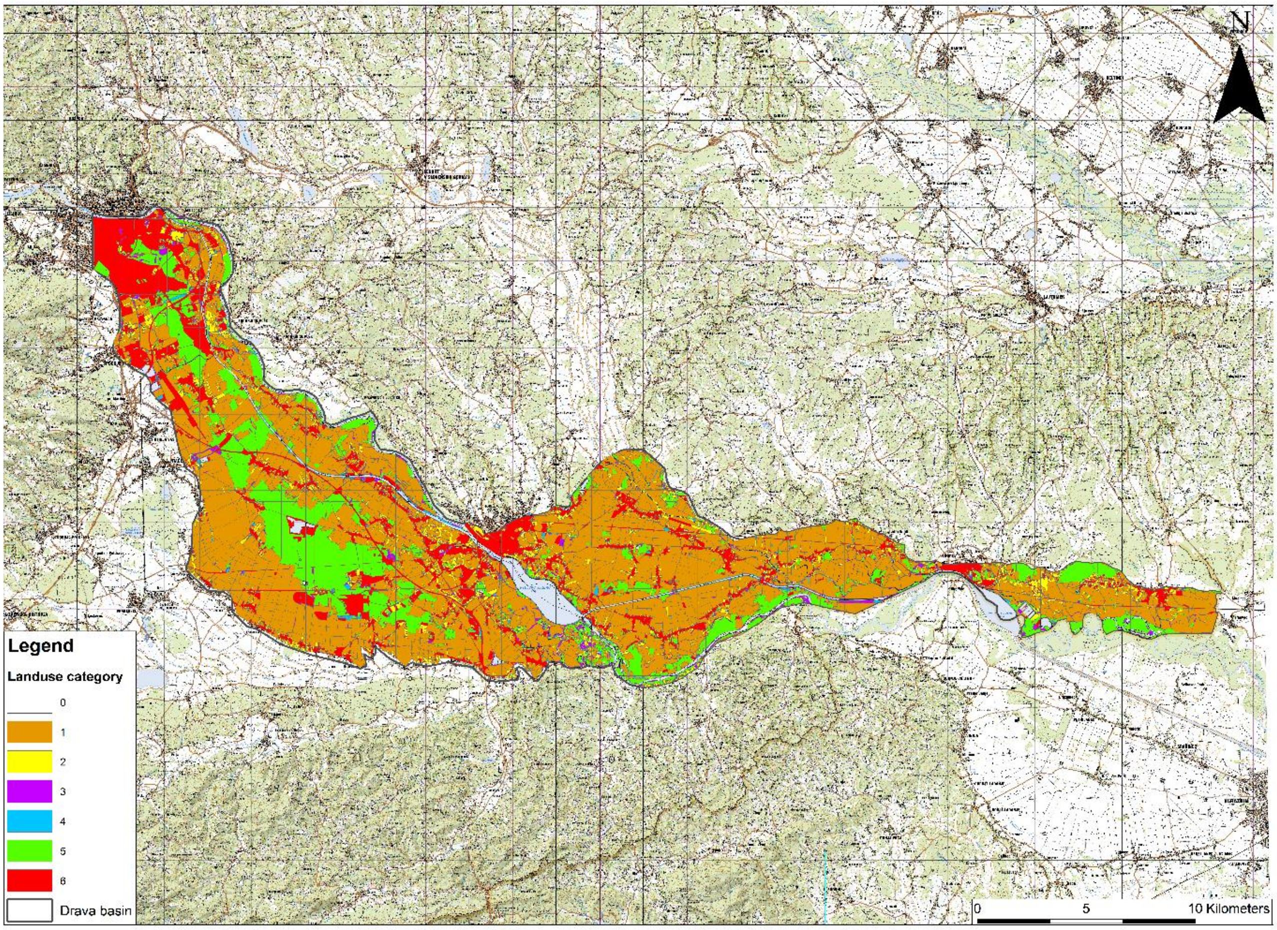

Figure 8.21. Land use categories on Drava pilot area

Table 8.14 presents areal extent for each field in Drava pilot area separately and for each category. Finally, all three areas are summed to show total extend of Dravsko polje aquifer.

Table 8.14. Areal extent of Drava pilot area

DRAVA PILOT AREA	Areal extend of category [ha]						
	TOTAL	**1**	**2**	**3**	**4**	**5**	**6**
Dravsko polje	19 442.59	9 166.80	1 138.50	460.30	570.76	3 841.70	3 572.40
Ptujsko polje	10 202.90	6 478.10	608.60	214.30	195.90	1 005.50	1 235.10
Ormoško polje	3 031.00	1 443.65	271.82	77.17	49.22	607.04	363.91
TOTAL [ha]	**32 676.49**	**17 088.55**	**2018.92**	**751.77**	**815.88**	**5 454.24**	**2 171.41**
TOTAL [%]	**100**	**52.30**	**6.18**	**2.30**	**2.50**	**16.69**	**15.83**

Below are presented nitrate concentrations for different land uses on Drava basin, presenting surface total infiltration (

Table 8.15), 41% of actual infiltration into the groundwater (Table 8.16) and 59% of nitrate that stay in unsaturated zone (Table 8.17).

Table 8.15. Nitrate surface concentrations for different land use on Drava pilot area

100 % INFILTRATION OF SURFACE NO3 – DRAVA PILOT AREA			CATEGORY
Annual production of nitrate per human $k_{lpč}$	4.85kgN/a		
Precipitation deposition		13.18 $mgNO_3/l$	
Uncultivated land and forest		4.98 $mgNO_3/l$	4 + 5
Nitrate on farmland (extensive and intensive use)		137.75 $mgNO_3/l$	1 + 2
Extensive land use		41.33 $mgNO_3/l$	2
Intensive land use		96.43 $mgNO_3/l$	1
Non-intensive land use		13.18 $mgNO_3/l$	3
Urbanized land		13.18 $mgNO_3/l$	6

Table 8.16. Concentration of nitrate surplus

59 % SURPLUS OF NO3– DRAVA PILOT AREA			CATEGORY
Annual production of nitrate per human $k_{lpč}$	4.85kgN/a		
Precipitation deposition		7.77 $mgNO_3/l$	
Uncultivated land and forest		2.94 $mgNO_3/l$	4 + 5
Nitrate on farmland (extensive and intensive use)		81.28 $mgNO_3/l$	1 + 2
Extensive land use		24.38 $mgNO_3/l$	2
Intensive land use		56.89 $mgNO_3/l$	1
Non-intensive land use		7.77 $mgNO_3/l$	3
Urbanized land		7.77 $mgNO_3/l$	6

Table 8.17:. Concentration of nitrate loses

41 % LOSES OF NO3 – DRAVA PILOT AREA			CATEGORY
Annual production of nitrate per human $k_{lpč}$	4.85kgN/a		
Precipitation deposition		5.40 $mgNO_3/l$	
Uncultivated land and forest		2.04 $mgNO_3/l$	4 + 5
Nitrate on farmland (extensive and intensive use)		56.48 $mgNO_3/l$	1 + 2
Extensive land use		16.94 $mgNO_3/l$	2
Intensive land use		39.54 $mgNO_3/l$	1
Non-intensive land use		5.40 $mgNO_3/l$	3
Urbanized land		5.40 $mgNO_3/l$	6

When all land use layers were categorized, nitrate infiltration amounts were prescribed to each land use as described above. Furthermore, these layers were transformed into raster.

Uncultivated land and forest have nitrate concentration computed for joint area. The same amount is prescribed to category 4 and 5.
Farmland jointly cover area of extensively and intensively use, considering both mineral and animal fertilizers. Amount of nitrate for intensive use is prescribed to category 1 and for extensively use to category 2. Extensive use presents 30% of intensive use nitrate amount.

For non-intensive land use amount of nitrate is consumed from precipitation deposition proportional to areal extend of non-intensive land use on both fields.

Uncultivated land and forest have nitrate infiltration computed for joint area. This amount is prescribed to category 4 and 5.

Farmland jointly cover area of extensively and intensively use, considering both mineral and animal fertilizers. Amount of nitrate intensive farm use is prescribed to category 1 and for extensively use to category 2. Extensively use present 30% of nitrate from intensive use.

For non-intensive land and urban areas prescribed amount of nitrate is from precipitation deposition. Length of the total sewage system is calculated from spatial layers in ArcMap. Total length of the sewage system on Drava pilot area is 1 238 838.6 m. It is assumed that average width of the sewage system is 1 m. Therefore, total area covered by sewage system is 123.8 ha. Afterwards, in ArcMap sewage system is divided into two sections, where it is covered by houses and where houses do not intersect with sewage system. Each house has a number of households. Intersecting and non-intersecting layers are imported into Excel spreadsheet, where total amount of nitrate is calculated for each house with equation 3.1.

Nitrate concentrations from cesspit are the highest (red spots) around bigger cities Maribor and Ptuj. Other locations have lower amount of nitrate leakage from sewage and cesspit.

Infiltration of precipitation on investigated field is 378 l/m^2/a.

Finally, raster presenting nitrate concentrations of sewage system and separate raster presenting land use were summed up where they were intersecting. On Figure 8.22 are resented nitrate ranges on Drava pilot area. All this was made for total surface infiltration (Figure 8.23), 59 % of surplus nitrate concentration (Figure 8.24) and 41 % of loss nitrate concentration (Figure 8.25).

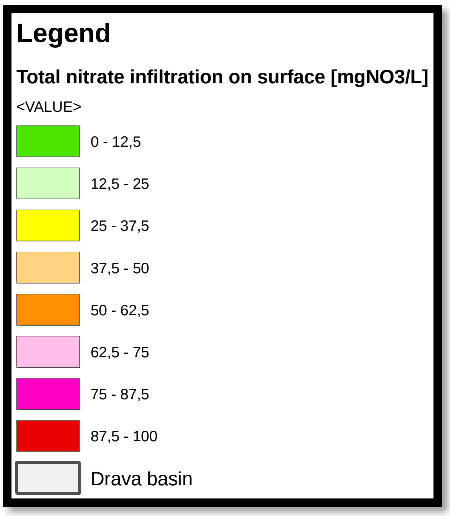

Figure 8.22. Nitrate concentrations range

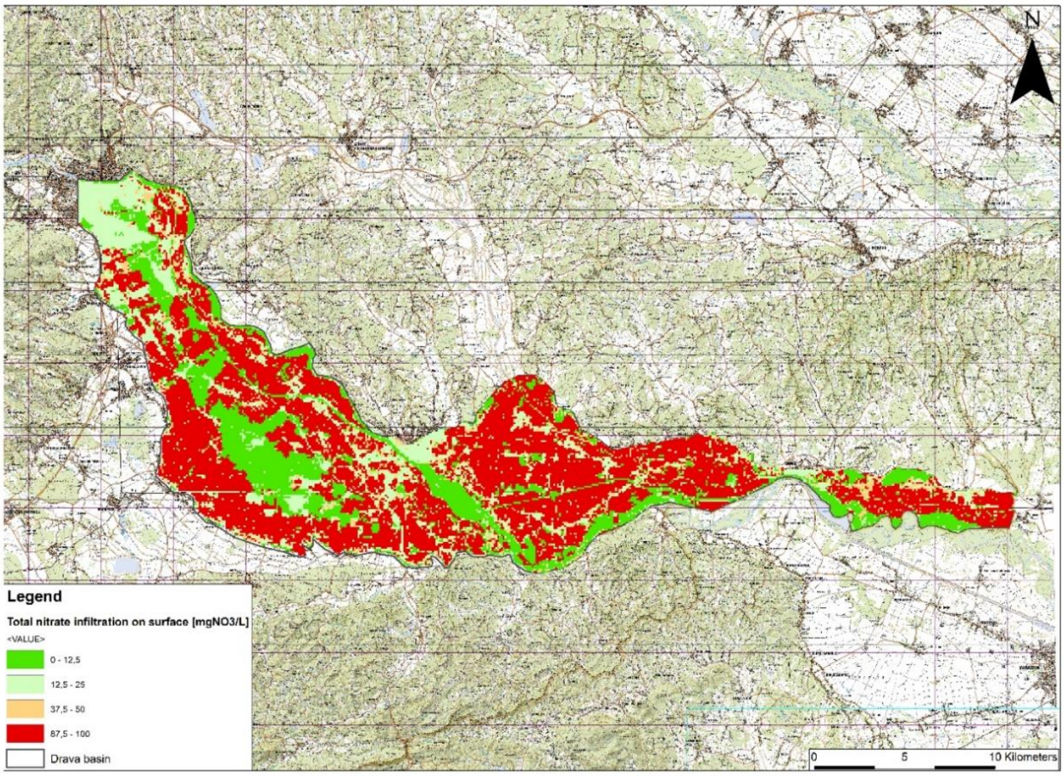

Figure 8.23. Raster with different nitrate values for different land-use

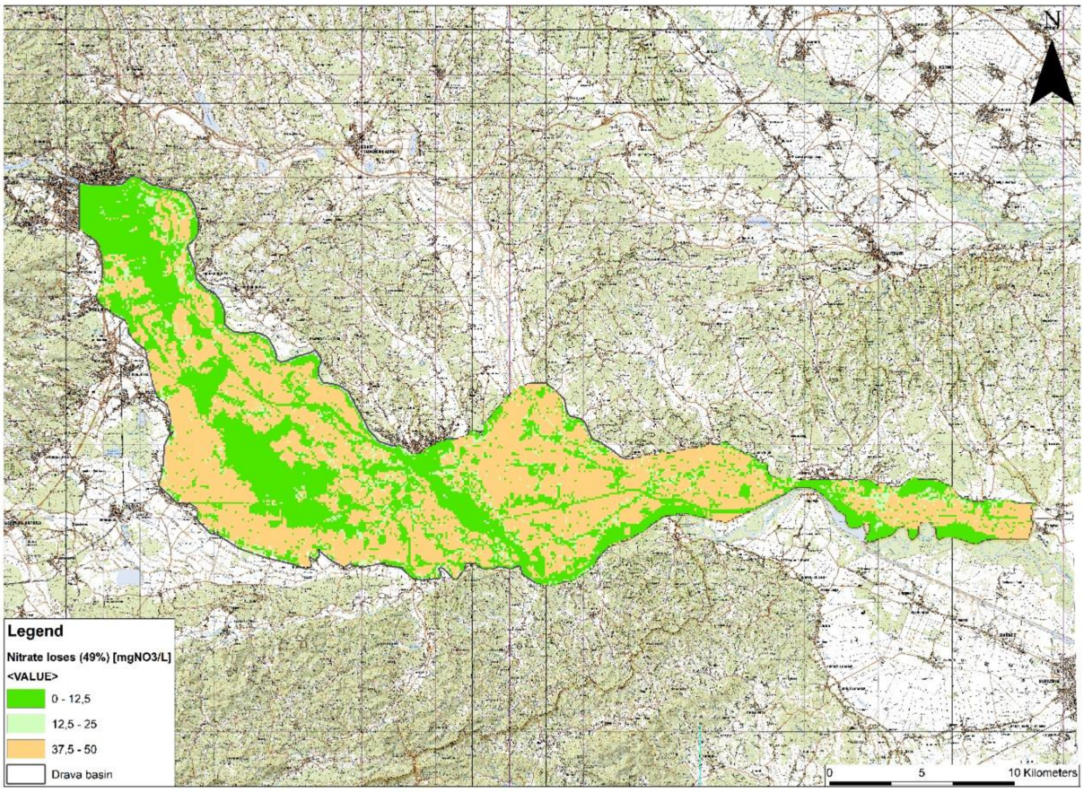

Figure 8.24. Nitrate loses on Drava depression

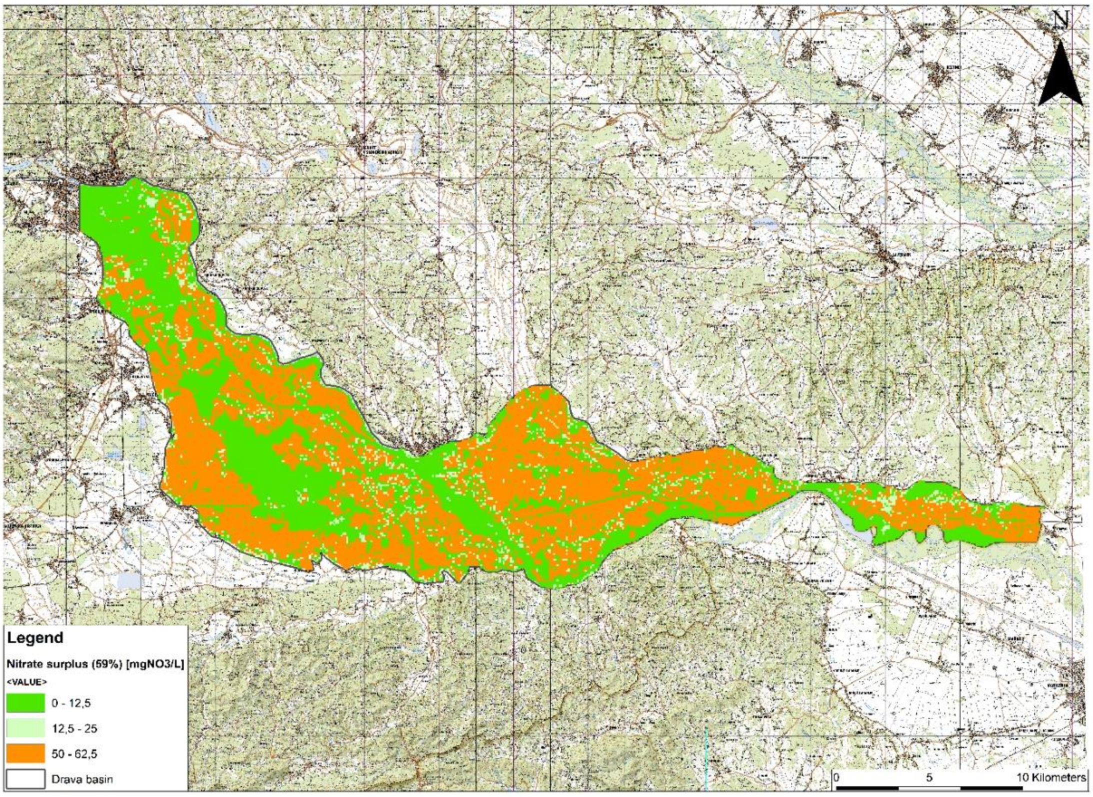

Figure 8.25. Nitrate surplus on Drava depression

8.10 NUMERICAL NITRATE CONCENTRATION TRANSPORT MODEL OVER THE DRAVA PILOT AREA

8.10.1 Methodology

For nitrate concentration modelling starting concentration and annual recharge concentrations were used. Starting concentrations for Drava and Ptuj polje aquifer were computed in year 2013 (Cerar, S., et al., 2016). Annual nitrate concentration for both aquifers were calculated as described above. As yearly nitrate concentration input we used nitrate surplus shown in Table 8.16. For both models nitrate concentrations were modelled for time period of 7 years, starting in year 2013. Results were compared with observation nitrate concentration in year 2019 (Arso, 2019).

8.10.1.1 MT3DMS

MT3DMS is groundwater solute transport simulation for MODFLOW. It supports simulation of transport using MODFLOW flow solution in saturated zone. Therefore we used it to simulate a nitrate concentration over a time period of 7 years.

8.10.2 Results

8.10.2.1 DRAVA POLJE AQUIFER

Results of modelled nitrate concentrations [mg/l per year] on Drava field are presented on Figure 8.26, Figure 8.27, Figure 8.28.

On Figure 8.26 are presented starting concentrations and annual nitrate recharge concentrations at the beginning of simulation. Maximum concentration is 130 mg/l per year and minimum 20 mg/l per year. Nitrate concentrations depend mainly on landuse.

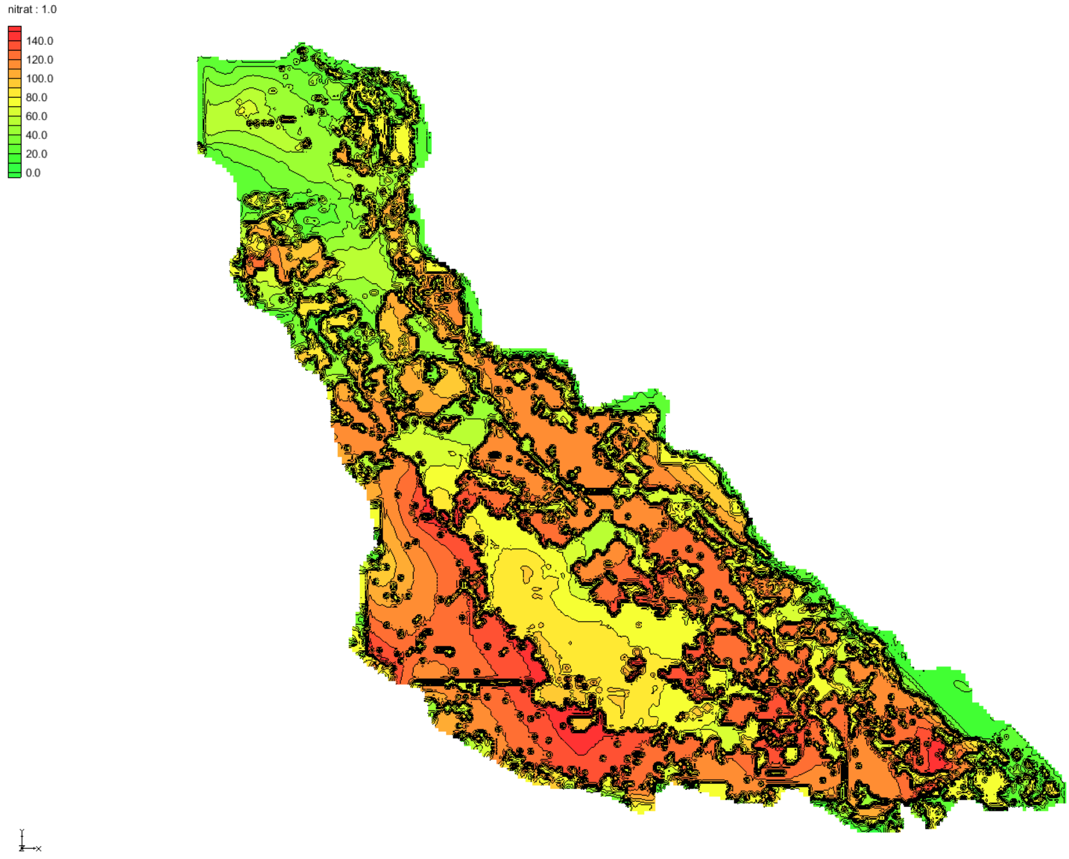

Figure 8.26. Starting concentrations and annual nitrate recharge t_0 for year 2013

On Figure 8.27 are presented nitrate concentrations after 1 year (2013-2014).

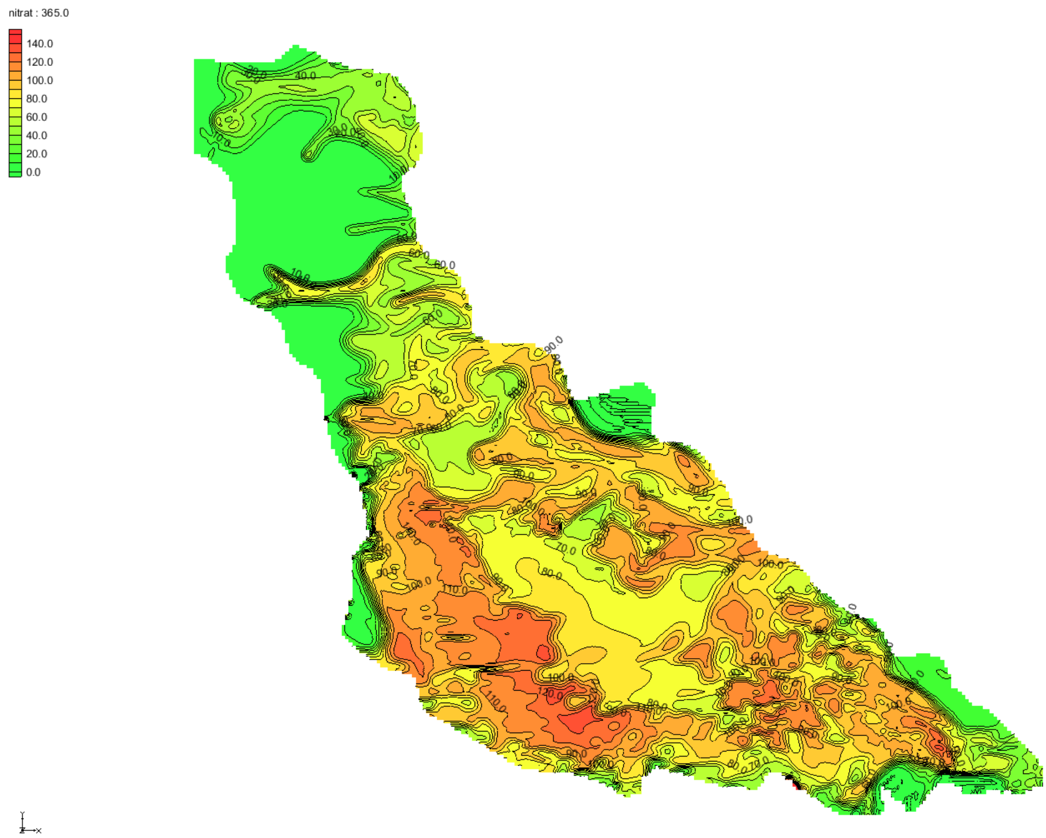

Figure 8.27. Nitrate concentrations after t_0+365 days with starting concentration from year 2013-2014

Figure 8.28 presents nitrate concentrations after 7 years (2013-2019). Values are compared with observation values shown in Table 8.17. Three observation points have large discrepancies; Šikole which is at the SW model margin, therefor this point could be excluded from observation, while Kidričevo and V-5 observation points are in the centre of the bottom area. At this area the largest nitrate concentrations are expected whilst the nature of groundwater flow from NW towards SE where area is wider and less influenced by the outskirt groundwater recharge. Other observation points give acceptable results.

From modelled concentrations after 7 years nitrate concentrations dilute over time, which means groundwater volume is large enough to be able to dilute the annual recharge concentrations triggered mainly by landuse. As expected nitrate concentrations are higher at the bottom part of the modelled area and lower at north most part. Reason for this is in recharge from outskirts at NW, diluting the nitrate and concentrating it in lower parts where groundwater is recharged only from precipitation for most of the time, meaning nitrate concentration dilution is decreased.

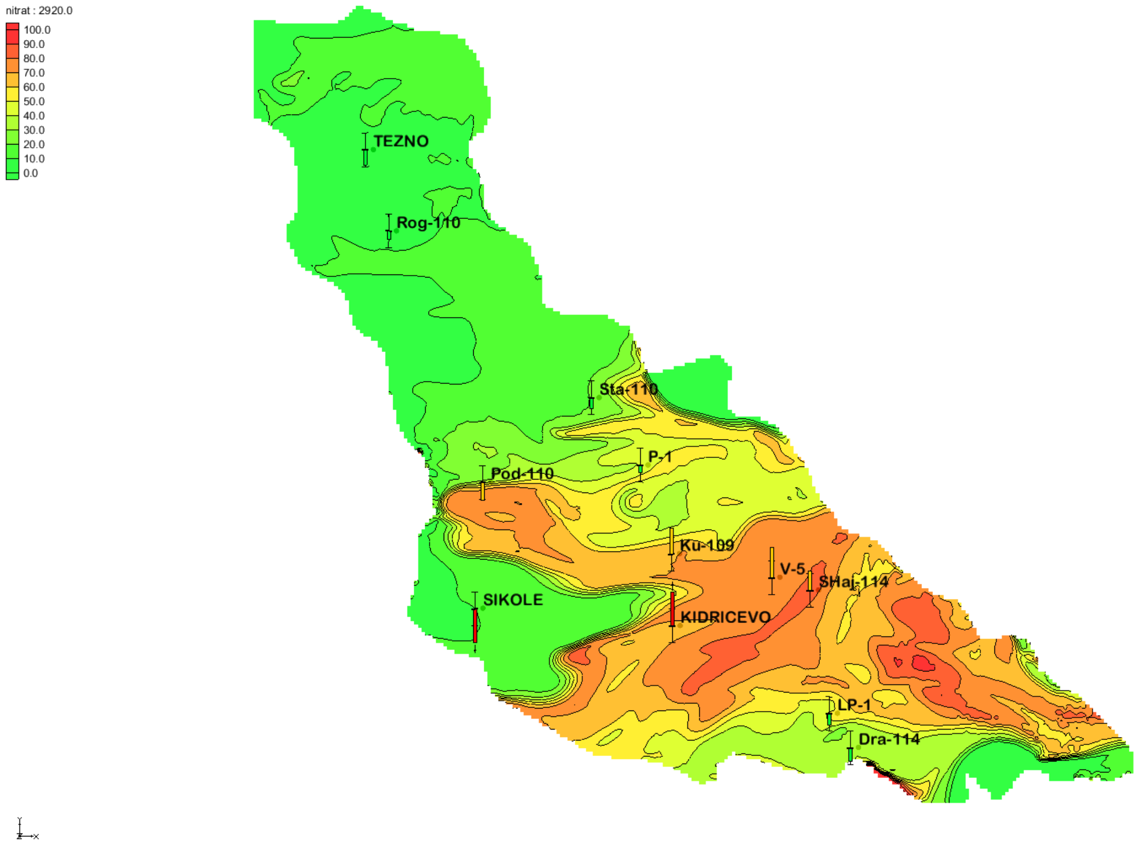

Figure 8.28. Nitrate dispersion in t_0+2555 days with starting concentrations from year 2013

Table 8.18: Drava polje aquifer nitrate concentration comparison between observed and modelled values

OBSERVATION POINT	GKX	GKY	OBSERVED CONCENTRATION [mg/l]	MODELLED CONCENTRATION [mg/l]	RESIDUAL
ŠIKOLE	141064	555339	58	10.5	**47.5**
KIDRIČEVO	140588	560737	8.9	65.9	**57**
V-5	141914	563466	37	72.9	**35.9**
SHaj-1/14	141564	564525	58	82.1	24.1
LP-1	138182	565043	66	51.4	14.6
Dra-1/14	137246	565620	53	37.2	15.8
TEZNO	153642	552340	26	7.9	18.1
Sta-1/10	146841	558520	35	22.2	12.8
PREPOLJE P-1	144992	559858	53	45.8	7.2
Pod-1/10	144526	555552	62	33.2	28.8
Rog-1/10	151412	552973	19	9.9	9.1
Ku-1/09	142561	560722	39	68.9	29.9

8.10.2.2 PTUJ POLJE AQUIFER

Results of modelled nitrate concentrations [mg/l per year] on Ptuj field are presented on Figure 8.29, Figure 8.30, Figure 8.31.

On Figure 8.29 are presented starting concentrations and annual nitrate recharge concentrations at the beginning of simulation. Maximum concentration is 130 mg/l per year and minimum 40 mg/l per year.

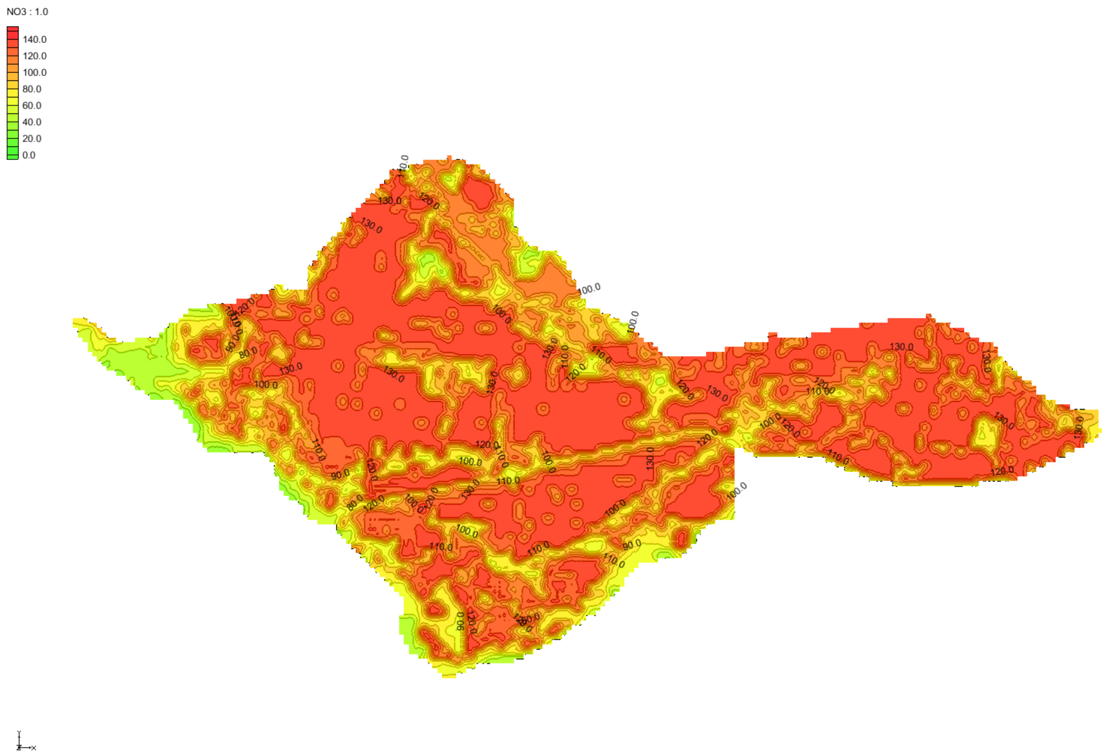

Figure 8.29. Starting concentrations and annual nitrate recharge t_0 in year 2013

On Figure 8.30 are presented nitrate concentrations after 1 year (2013-2014).

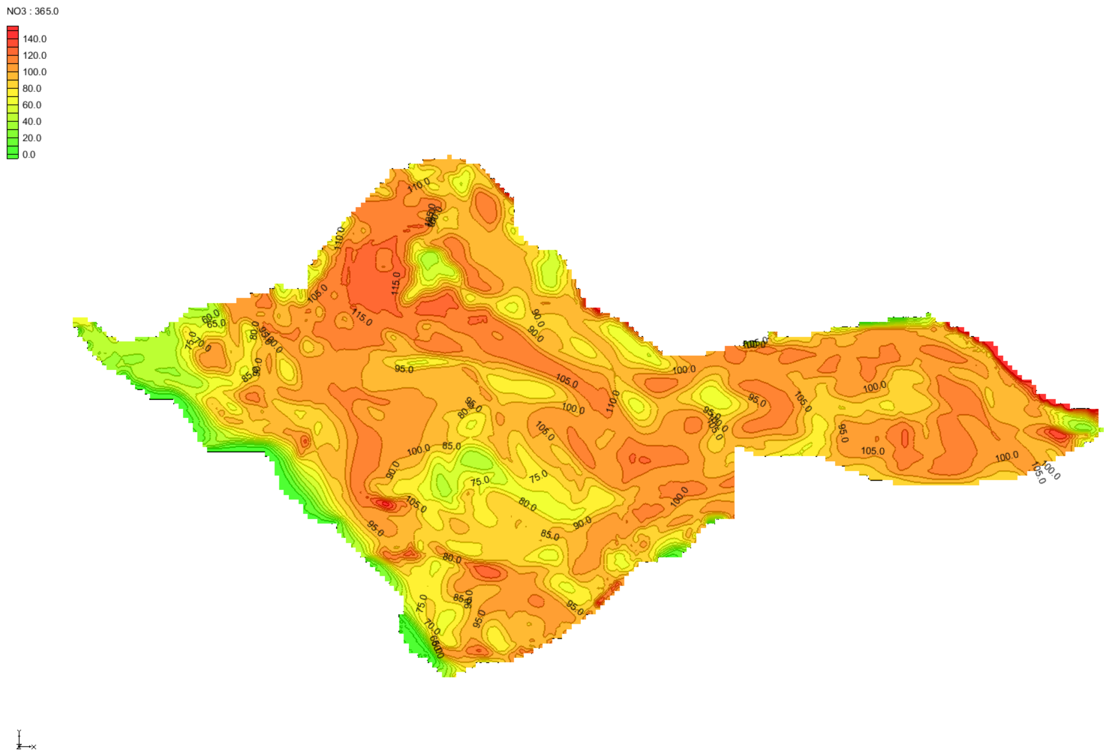

Figure 8.30. Nitrate concentrations after t_0+365 days with starting concentration from year 2013-2014

Figure 8.31 presents nitrate concentrations after 7 years (2013-2019). Values are compared with observation values shown in Table 8.18. One observation point at east most part of the modelled area showed large discrepancies between observed and modelled values. Observed concentrations are very low 2 mg/l and modelled concentration is much larger 53 mg/l. Since at this part of the model outskirt recharge does not influence the groundwater flow modelled value is not controversial. Therefor reason for low concentration is somewhere else. Other observation points give very good results.

On Ptuj field dilution of nitrate concentration is mainly influenced only by the precipitation with exception on west part where groundwater is recharged by Drava river and groundwater flow below the riverbed from Drava polje aquifer. Thus, concentration slowly decrease and are consistent on the whole area.

Based on the model results more attention should be given to nitrate intake according to low diluting processes and the trapped nature of groundwater.

Nitrate dilution is majorly affected by groundwater flow which is dependent on groundwater volume in each cell and velocity of the flow and hydraulic conductivity. Furthermore, annual nitrate concentrations roughly present the actual nitrate concentration which is of course changing from year to year based on quantity of precipitation. Therefore, with such models nitrate concentrations can be modelled but the accuracy is the assumption of predefined hydraulic model.

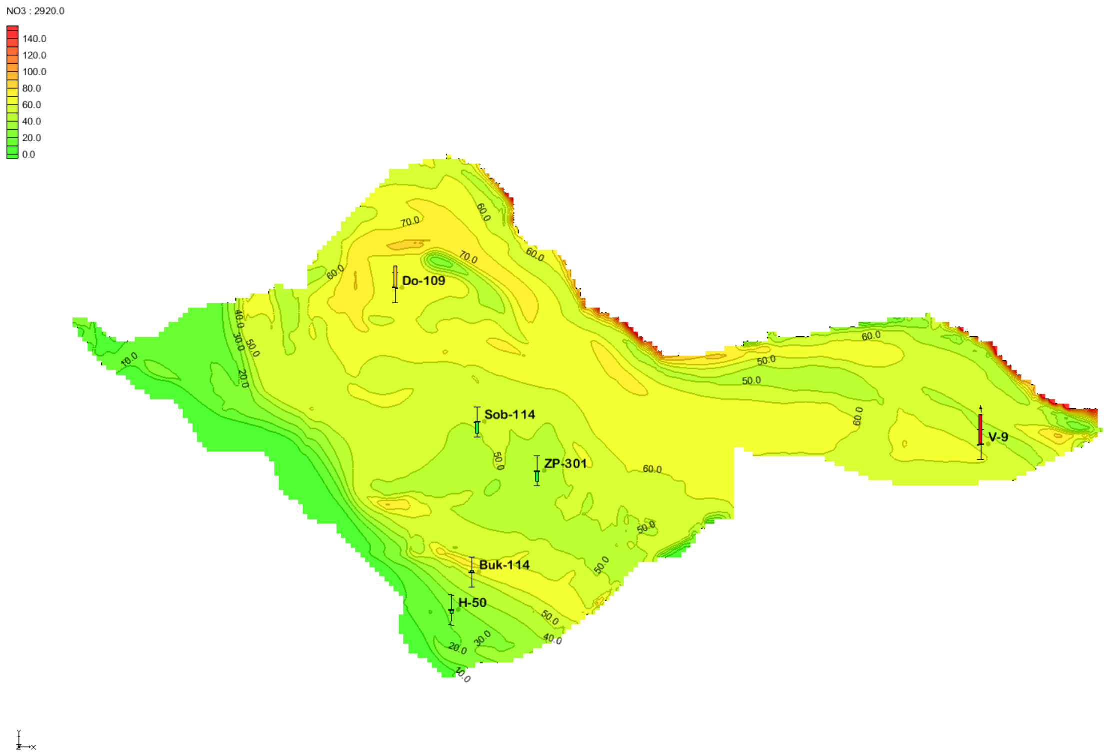

Figure 8.31. Nitrate dispersion in 7 years with starting concentrations from year 2013

Table 8.19. Ptuj polje aquifer nitrate concentration comparison between observed and modelled values

OBSERVATION POINT	GKX	GKY	OBSERVED CONCENTRATION [mg/l]	MODELLED CONCENTRATION [mg/l]	RESIDUAL
V-9	140326	585232	2.2	53.3	**51.1**
Do-1/09	143579	573030	38	66.9	28.9
ZP-3/01	139773	575990	62	48.2	13.8
Sob-1/14	140794	574744	66	50.9	15
H-50	136880	574200	31	26.6	4.41
Buk-1/14	137666	574629	62	64.3	2.3

9 MALTA

Manuel Sapiano, Henry Debattista
Energy and Water Agency, Ministry for Energy and Water Management, Malta

9.1 General Introduction – Malta

Located in the middle of the Mediterranean Sea, the Maltese islands are made up of three inhabited islands – Malta (246km^2), Gozo (67km^2) and Comino (3.5km^2) and a number of smaller uninhabited islets. The total area of the archipelago is approximately 316km^2. The populations stands at around 515,000, leading the islands to have a population density of around 1,575 inhabitants per square kilometre which stands as the highest population density amongst European Member States and the fifth highest for any country in the world. The land cover of the Maltese islands reflects this high population density and is classified as 30% urban/industrial/commercial, 52% agricultural and 18% natural vegetation.

The islands are poorly endowed with natural freshwater resources, and the availability of water resources has been, throughout the islands' history, an important limiting factor for their social and economic development. Scarcity of water resources arises due to a number of conditions, including the semi-arid Mediterranean climate with its characteristic low mean annual rainfall depths and high intra-annual variability in precipitation. The mean annual rainfall stands at around 550 mm and is mainly restricted between the months of September and April. In addition, the small size and geomorphology of the islands precludes the development of economically exploitable surface water resources whilst the high population density gives rise to a high specific demand for water per unit area of land. In fact, the availability of natural freshwater resources per capita is estimated to stand at around 70 m^3/cap/year which is far below the 500 m^3 threshold marking chronic water scarcity under the UN's water scarcity Falkenmark index.

The Malta mean sea-level aquifer (MSLA) system is by far the most important groundwater body in the Maltese islands, providing around 65% of the total mean annual groundwater yield. This groundwater body essentially takes the form of a freshwater lens floating on the denser sea-water and hence is in lateral vertical and horizontal contact with the bounding sea-water in the bedrock. It is therefore highly vulnerable to sea-water intrusion in response to abstraction activities, and therefore groundwater abstraction needs to be carefully managed to protect the quality of the abstracted water from the direct intrusion of sea-water under the abstraction point (sea-water upconing).

According to the risk-analysis undertaken during the development Malta's 2nd River Basin Management Plan (2nd RBMP), the Malta MSLA groundwater body is also at risk from contamination by nitrates originating from anthropogenic activities (such as agriculture, animal husbandry and leakages from wastewater conveyance networks) carried out in the surface catchment area of the groundwater body. In fact, nitrate contamination is identified as the main status failing condition for this body of groundwater under the qualitative status risk-assessment undertaken as part of the 2nd RBMP.

An analysis of groundwater monitoring data from the Surveillance and Operational networks in this groundwater body shows that quality data from most groundwater monitoring stations exceeds the 50mg/l Quality Standard for Nitrate as established under the EU's Groundwater Directive. As a matter of fact, and due to the high level of nitrate content, the whole surface catchment area of the groundwater body has been designated as a Nitrate Vulnerable Zone under the EU Nitrates Directive.

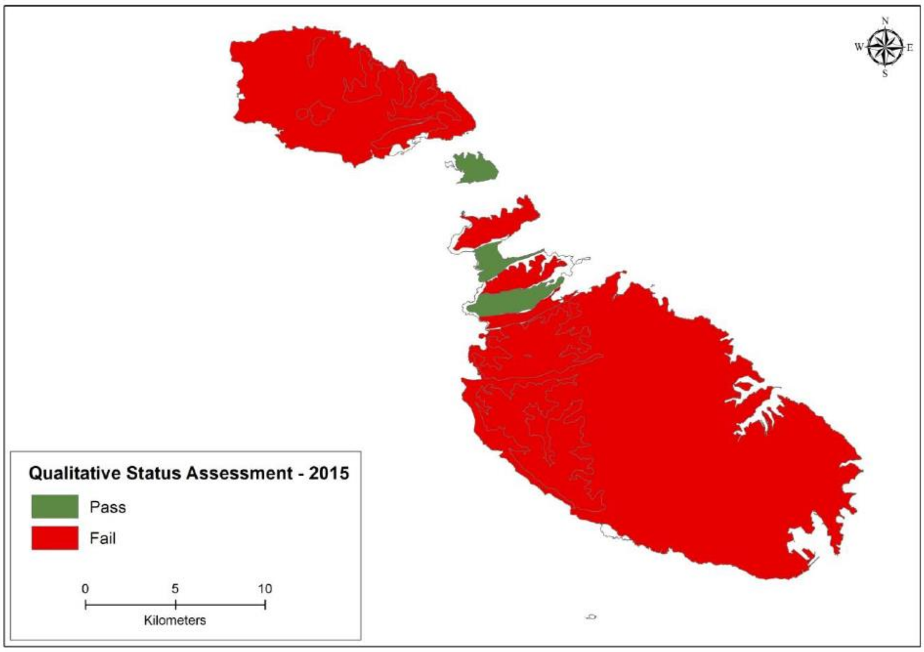

Figure 9.1. WFD Qualitative Status Assessment in the Malta River Basin District. The Malta MSLA is indicated as having poor qualitative status - with the primary status failing condition being Nitrate content. (Source – Malta 2nd Water Catchment Management Plan)

9.2 Development of Nitrate Contamination in the Malta MSLA

The oldest reference on the quality of groundwater in the Malta MSLA comes from an 1867 report on the health conditions in Malta authored by Dr John Sutherland. The report includes a set of analysis undertaken at Woolwich War Office on the quality of the main water supply resources in the Maltese islands, which include amongst other qualitative parameters an assessment of nitrate (nitrate of lime) content. Among these sources is "*the well at Marsa, within the farm of Armier, from which the water was raised by a steam pump*", which refers to the first documented source of groundwater abstraction for public supply from the mean sea level aquifer system. The nitrate content from this abstraction sources is recorded as 14mg/l Nitrate (of lime).

Although analysis of water supply continued to be undertaken in subsequent years by the local Health Authorities, analysis focused primarily on salinity and bacteriological content. This is understandable since monitoring was mainly focused on health aspects and the need to avert outbreaks of diseases such as cholera which are related to poor water supply quality.

An almost 100 year gap exists until data on nitrate assessments of groundwater abstracted from the Malta MSLA become available, with the first data sets coming from 1966. From then onwards, data is available on an annual basis with varying density of stations throughout the years, primarily depending on the number of groundwater abstraction stations in operation by the Water Works Department and subsequently the Water Services Corporation. In recent years, more spatially representative data is available from the groundwater monitoring networks established as part of the implementation of the EU Water Framework Directive. An analysis of data availability shows a good spatial representativity, in particular for the central regions of the MSLA from 1970 onwards.

The development of nitrate content in the MSLA since the 1960's is represented in Figure 9.2 below. The plots shows a historically high nitrate content in the south and north-eastern regions of the MSLA dating back to the 1970's, with the nitrate content progressively increasing in the inland regions of the aquifer systems in subsequent decades. The initially high nitrate concentrations in south and north-eastern regions can be correlated with low thicknesses of the unsaturated zone, enabling the movement of contaminants from related surface activities to reach the saturated zone quicker than in other more central and western regions of the aquifer system where the unsaturated zone is significantly thicker.

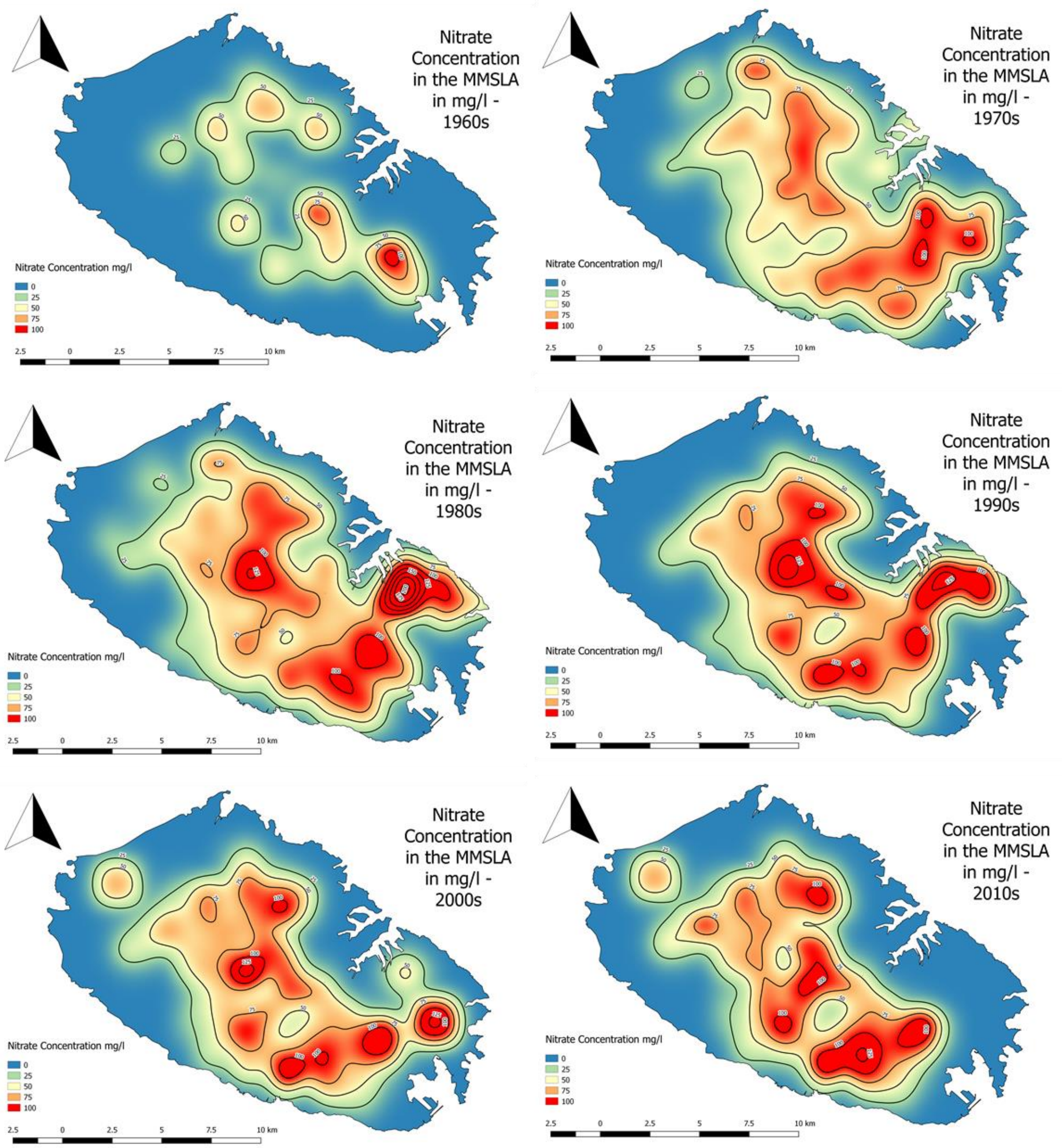

Figure 9.2. Development of Nitrate concentration in the Malta Mean Sea Level Aquifer from the 1960s to the 2010s

9.3 Identification of Nitrate contamination sources

Nitrate contamination in groundwater arises primarily as a result of human activities undertaken at the surface catchment area of the groundwater body. Within the context of the Malta MSLA, the main superficial activities which can lead to groundwater nitrate contamination are:

(i) the use of organic and artificial fertilizers in arable agriculture,
(ii) leachates from intensive animal husbandry activities,
(iii) leakages from the municipal wastewater network, and
(iv) use of nitrate containing groundwater for irrigation purposes.

The characteristics of these sources of nitrate contamination in groundwater were assessed in a study undertaken by the British Geological Survey in 2008, entitled "*A preliminary study on the identification of the sources of nitrate contamination in groundwater in Malta*". The study undertook an extensive sampling campaign and assessed the $^{15}N/^{14}N$ and $^{18}O/^{16}O$ ratios from the different potential nitrogen sources identified in the Maltese islands and of groundwater nitrate from a spatially representative array of monitoring and production boreholes, in order to enable the identification of the main contributing sources to groundwater nitrate. The main results of this study are summarized hereunder:

9.3.1 General Pattern for Groundwater Nitrate

The $^{15}N/^{14}N$ and $^{18}O/^{16}O$ analysis of groundwater nitrate are shown in Figure 9.3 below. Practically all samples have $d^{15}N$ values in the range +7.2 to +13.2‰ and $d^{18}O$ values in the range +2.8 to +6.4‰. Only two samples exhibited higher values, which is a feature generally indicative of the effects of partial denitrification.

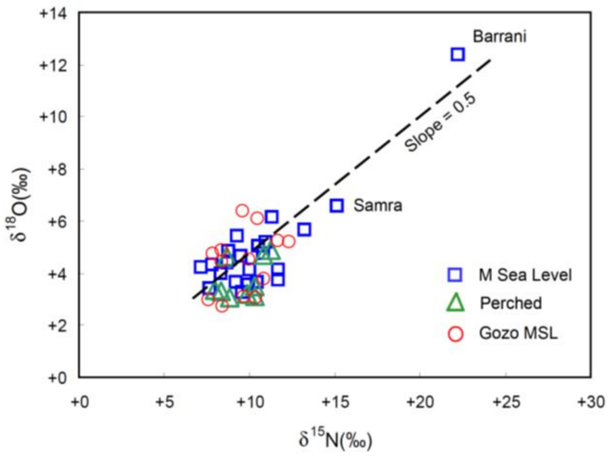

Figure 9.3. Cross-plot of nitrate $d^{18}O$ versus $d^{15}N$ for groundwater sample (Source: BGS 2008)

9.4 Analysis of identified potential nitrogen sources

9.4.1 Synthetic Fertilizers

If excessive amounts of fertilizer are applied to soil, and are immediately washed through by heavy rainfall, the fertilizer may comprise a direct supply of nitrate to groundwater – either directly as fertilizer nitrate, or by oxidation of fertilizer ammonium. This mechanism, involving little chemical interaction or nitrogen exchange with the soil, would be expected to produce nitrate with $d^{15}N$ values similar to those of fertiliser.

The $d^{15}N$ values for synthetic inorganic fertilizers utilised in Malta, -5.0 to +0.3‰ for ammonium and +1.3 to +3.5‰ for nitrate are within the typical -5 to +4‰ range reported for fertilizers in other countries (Vitòria et al., 2004, Shomar et al., 2008). These values are considerably lower than the +7.2 to +13.2‰ range for the groundwater nitrate. Direct inputs of fertilizer-derived nitrate are not therefore regarded as a major contributor to the groundwater nitrate (though fertilizer assimilated into the soil N pool could be a source).

Nitrate whose oxygen is derived solely from atmospheric sources – which includes rainfall nitrate and nitrate in synthetic fertilizer – has relatively high $d^{18}O$ values (Kendall, 1998; Heaton et al., 2004). For Maltese fertilizers the $d^{18}O$ values were +24 to +26‰, and therefore much higher than the +2.8 to +6.4‰ for groundwater nitrate. This confirms the $^{15}N/^{14}N$ data in ruling out any direct contribution of fertilizer nitrate to groundwater nitrate contamination.

9.4.2 Animal Wastes

Animal waste samples were collected direct from cesspits in animal husbandry units. The material was found to be highly anoxic and contained little nitrate but a very high concentration of ammonium. Spreading of animal waste onto land, however, could lead to rapid oxidation of ammonium to nitrate, and constitute a potentially significant source of pollution.

The $d^{15}N$ value of ammonium in animal waste is initially determined by the value for the excreted nitrogen, but thereafter is greatly dependent on the amount of ammonium lost by ammonia volatilisation. In this process kinetic and equilibrium fractionations favour the loss of ^{15}N-depleted ammonia, and result in a consequent increase in the $d^{15}N$ value of the residual ammonium (Heaton, 1986; Heaton et al., 1997). $d^{15}N$ values of ammonium and of nitrate derived from animal waste therefore tend to increase progressively with increased “age”, i.e. increased time of decomposition and oxidation (Kim et al., 2008). The $d^{15}N$ values of animal waste samples from Malta averaged +5.3‰, but had a broad range (+2.1 to +10.1‰) comparable to published values (Bateman and Kelly, 2007), and which probably reflects the different ages and degrees of decomposition of the samples.

If the oxidation of ammonium to nitrate was quantitative, there would be little isotope fractionation, and the $d^{15}N$ value of the nitrate would tend to be similar to that of the ammonium (Kendall, 1998; Kim et al., 2008). On this basis only the dry poultry and cattle waste samples, with $d^{15}N$ values of about +10‰, are comparable to the average $d^{15}N$ value for groundwater nitrate, whilst the majority of analysed animal waste samples were found to have $d^{15}N$ values lower than those in the groundwater. However, the possibility that if these wastes were subject to further decomposition as would be likely to occur with distribution onto soil, $d^{15}N$ values would rise toward levels compatible with them being sources of the nitrate in groundwater, cannot be ruled out.

9.4.3 Sewage

In common with the animal waste samples, sewer and cesspit samples were also collected from entirely anoxic environments, and so had high ammonium concentrations, but very little nitrate. If sewage were to leak into aerobic sub-surface environments, it could potentially constitute a source of nitrate contamination.

Unlike animal wastes, however, sewage constrained in sub-surface environments has much less opportunity to lose ammonia by volatilisation, and thereby increase its $d^{15}N$ value (Aravena et al., 1993). This may explain why samples from a wide variety of sewers and cesspits exhibit only a narrow range of $d^{15}N$ values, from +5.4 to +6.9‰. These are very similar to $d^{15}N$ in sewage sludges reported by Shomar et al. (2008) ranging from +4.6 to +7.4‰ and in aged, dried sludge from +5.2 to +7.4‰. As the values for Malta sewage are lower than those for the groundwater nitrate, they suggest that nitrate derived directly from leaking sewers or from cesspits is not a major source of pollution.

9.4.4 Soil Nitrogen

The $d^{15}N$ values of the soil organic nitrogen are quite high (+4 to +11‰, average +8.5‰) and at the upper end of the normal range for soils globally (Adamson et al., 2003). Insofar as the factors responsible for determining soil $d^{15}N$ are understood, it is probable that soils with high $d^{15}N$ are very 'open' with respect to nitrogen, with relatively large amounts of nitrogen loss (Handley et al, 1999; Amundson et al., 2003). This may well be a reflection of both Malta's climate (dry summers with heavy winter rain) and particularly its intensive cultivation. Cultivation has been suggested as another cause of higher soil $d^{15}N$ values (Broadbent et al., 1980), and the three soil samples marked as non-agricultural or abandoned tended to have the lowest $d^{15}N$ values.

Soil nitrification tends to produce nitrate with $d^{15}N$ values similar to those of the soil organic nitrogen (Kendall et al., 2007). On this basis, cultivation of Malta's agricultural soils ($d^{15}N$ = +6.0 to +11.2‰, average +9.1‰) could certainly produce nitrate isotopically similar to that in the groundwater ($d^{15}N$ = +7.2 to +13.2‰, average +9.7‰)

9.5 Conclusion of isotope studies

Nitrogen isotopes showed that direct inputs of fertilizer or sewage derived nitrate are probably not major contributors to groundwater nitrate. Leaching of nitrate from cultivated soils was likely to be the most important source, though derivation from animal wastes cannot be discounted. The isotope data do not rule out inorganic fertilizers and/or animal wastes as the original source of the nitrogen. The data are compatible with a process whereby nitrogen from inorganic fertilizers and/or animal wastes is assimilated into the soil organic nitrogen pool, and takes on the isotopic composition of this pool during the cycling of nitrogen attendant on cultivation, before nitrification and leaching to the underlying groundwater. Data from co-contaminants are equivocal with limited relationship between current landuse and groundwater quality.

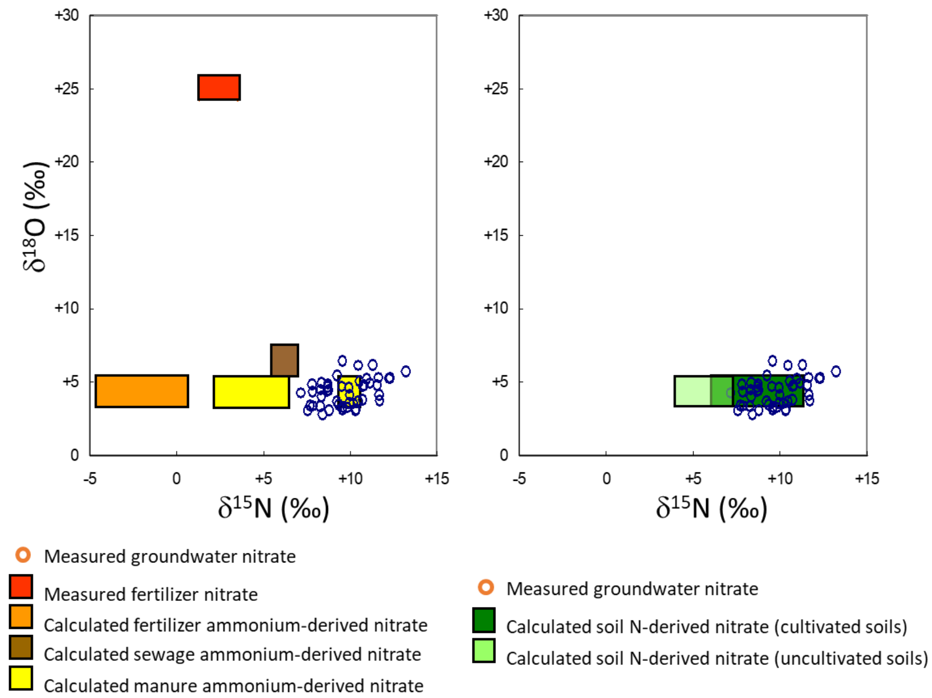

Figure 9.4. Summary of d^{15}N and d^{18}O in Nitrate in groundwater and various potential nitrate sources. (Source: BGS 2008)

9.6 Conceptual model of Malta MSLA

The Malta MSLA groundwater body stretches over an area of 216km^2, and is mostly located within the Lower Coralline Limestone formation, or the Globigerina Limestone where this formation is located at sea-level. On top of the Lower Coralline Limestone, the Globigerina Limestone outcrops to cover almost the entire island but is capped by the Blue Clay formation for an area of 36km^2 on the north-west side of the island and up to the northern bounding Pwales fault, where the LCL lies in juxtaposition at sea level to the Blue Clay formation hence giving this fault its sealing properties.

The Lower Coralline Limestone formation represents the most important aquifer formation of the Maltese islands, sustaining the major sea-level groundwater bodies which by far are the primary sources of freshwater for the islands. As the formation is predominantly composed of an algalfossiliferous limestone with sparse corals, it has a moderate, irregular and frequently layered or channel-like permeability. In fact, the high permeabilities of coral reefs are absent and are replaced instead by an irregular permeability more characteristic of algal reefs. This heterogeneity is further accentuated by the presence of scattered patch-reefs in lateral contact with lagoonal and fore reef facies.

The primary porosity of the formation is highly variable and varies from 7 to 20%. The different density indicates that a large part of the primary pore-space is not interconnected, a fact which is also stressed by the fact that the primary permeability is rather low. The effective porosity of the formation is mainly connected with fracture permeability, since otherwise the pores are very poorly interconnected. Flow and dewatering of pore-spaces rely on secondary permeability by tectonical fracturing and solution enlargement. The fractures range from microfissures to Karst solution cavities, frequently aligned in one direction. The secondary permeability is thus mainly fissure dependent and is estimated to range between 10 to 15% whilst the average hydraulic conductivity as measured from pumping tests is 400 x 10^{-6}m/s. The transmissivity of the formation is estimated to vary between 10^{-4} and 10^{-3} m^2/sec.

The groundwater bodies occurring in these mean sea-level aquifer systems are in lateral and vertical contact with sea-water. Due to the density contrast of fresh-water and salt-water a Ghyben-Herzberg system is developed. The outcome is a lens shaped body of freshwater that is dynamically floating on more saline water, having a convex piezometric surface and conversely a concave interface, both tapering towards the coast where there is virtually no distinct definition between the two surfaces. Maximum hydraulic heads of 4-5m amsl were measured for the groundwater body sustained in the Malta mean sea level aquifer in the 1940's when the system was still largely unexploited. The lens sinks to a depth below sea-level roughly 40 times its piezometric head at any point, fading into more saline water across a transition zone, the thickness of which depends on the hydrodynamic characteristics of the aquifer formation. The limits of this transition zone are commonly defined by the surface of the 1% and 95% seawater content, based on the total dissolved solids or chloride content.

The groundwater in the mean sea-level aquifers is not at rest but flows away more or less horizontally. Part of this lateral flow is recovered by public and private abstractions using galleries and boreholes, while the remaining part continues its outward journey towards the coast to be discharged into the surrounding sea. On a long term-basis, the total recharged water that is not abstracted is flowing out to the sea.

This outflow has been estimated by ATIGA (1972) to account for about 50 percent of the recharge of the sea-level aquifers. Aquifer modelling of the main mean sea-level aquifer by the BRGM has quantified outflow from this aquifer at 30 million m^3/year, or about 60 percent of the recharge.

In practice, these mean sea-level aquifer systems are very sensitive to point-form saline upconing due to their hydrogeological characteristics and the relatively small piezometric head. Wells drilled to some depth below sea-level are prone to localized upconing of saline water in response to the drawdown in the piezometric head caused by abstraction; with the direct result being an increase in the salinity of the abstracted water.

The groundwater in the mean sea level aquifer is characterized by the mixing of waters with two different infiltration processes:

(1) a very slow infiltration, through the matrix porosity, which is the dominant recharge process of the aquifers and
(2) a fast infiltration, through cracks and fractures, which is local and discrete flow occurring probably only during the main events and which most probably is responsible for the direct leaching of pollutants from the surface into the saturated zone.

According to Stuart et al.(2010) rapid infiltration of groundwater may be one of the reasons behind rapid changes in the level of the mean sea-level aquifers. Some boreholes can also act as conduits for the rapid infiltration of water by connecting fractures. Surface waters disappear quickly after intense rainfall on outcrops of Lower Coralline Limestone and some rapid infiltration routes such as sinkholes are visible from the surface. Nonetheless the geological complexity of Malta with its vertically divided sequence of aquifers may limit the amount of recharge to parts of the mean sea-level aquifers, thus increasing residence times (Stuart et al. 2010).

Therefore conceptual model developed for the Malta MSL aquifer as presented in Malta's 2nd RBMP (Figure 9.5) assumes that:

- the Lower Coralline Limestone is present across the whole island, although it is divided into horst and graben blocks north of the Pwales fault and parts are totally below sea level and are not aquifers;

- it is capped in the west part of the island by the overlying impermeable Blue Clay and the Greensand, and more extensively by less permeable strata in the Middle Globigerina Limestone;

- the water table is controlled by abstraction and is presently up to only 3 m above sea level in places.

This means that here the aquifer is protected by the overlying strata, rather than being confined in a hydraulic sense. Abstraction also leads to saline upconing and an increase in salinity;

- the relatively low porosity means that the rate of downwards movement in the aquifer matrix will be greater than in the perched aquifers, but the unsaturated travel time will be long in the thicker parts of the aquifer. The limited detections of coliforms indicate that rapid transport from the surface to the aquifer is limited;

- CFC data shows that residence times in the saturated zone are in the range 15-40 years. Combined with the low estimates of transmissivity from pumping tests, this suggests that movement in enlarged solution features is limited;

- there are a number of possible mechanisms for recharge to the part of the aquifer capped by the Blue Clay, where the groundwater appears to be of similar age to the rest of the aquifer:
– slow infiltration through the Blue Clay from the upper aquifer;

– enhanced recharge at the edge of the Blue Clay or the Middle Globigerina;

– rapid infiltration along faults or fractures.

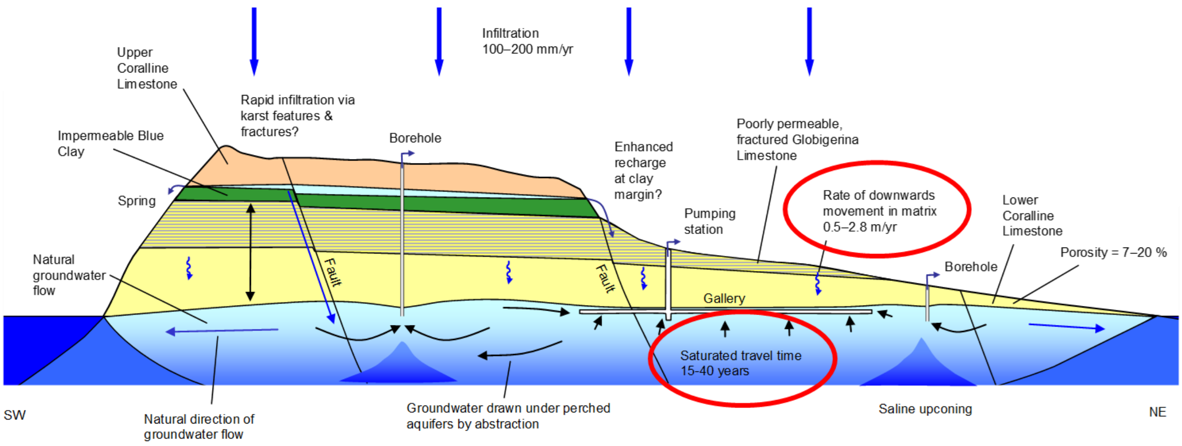

Figure 9.5. Conceptual representation of the Malta MSLA groundwater body (Source: BGS 2008)

9.7 Assessment of Nitrate development in the Malta MSLA

Nitrate stable isotope measurements suggest that the leaching from cultivated soils, spreading of animal wastes and bacterial nitrification in groundwater are the most likely sources of groundwater nitrate in the Malta MSLA. Direct inputs of fertilizer-derived nitrate ore sewage are probably not major contributors as their $d^{15}N$ is lower than that of groundwater nitrate, but transformation of these in the soil zone or the unsaturated zone may change their signatures.

The conceptual model of the Malta MSLA indicates the prevalence of slow downward movement of infiltrating water through the rock matrix in the unsaturated zone, as compared to fast flow through fissures or other secondary dissolution structures. This slow matrix flow, and the relatively long-retention time of groundwater in the saturated zone give rise to a slow responding system to changes in pollutant use or loading on the surface catchment area of the groundwater body. This slow responding system can be considered as a form of geological control related to the thickness of the unsaturated zone which is directly affected by the easterly tilt of the island. In fact, nitrate levels in groundwater from monitoring stations located in the central and western regions of the MSLA tend to be lower than those from monitoring stations in the eastern regions, where the unsaturated zone is significantly thinner and therefore the flow of surface contaminants to the saturated zone is expected to be shorter.

However, the potential historical application of fertiliser to land need also to be given due consideration. The traditional agricultural lands in the Maltese islands are located in the western regions where the occurrence of the perched (high-level) aquifer systems facilitates access to irrigation water. The western region is however underlain by a thick marly formation (the Blue Clay formation which sustains the perched aquifer systems) and hence are of limited importance with regards to infiltration to the mean sea level groundwater bodies. Whilst infiltration at the margins of the Blue Clay formation or through breaches in the formation itself is assumed to occur, still the thick unsaturated zone in these regions would delay any impact of such pollutants on the qualitative status of the underlying groundwater.

Agricultural activities in the central regions of the island were mainly rain-fed, due to the lack of access to natural freshwater sources. However, agricultural areas in the lower lying eastern regions of the islands could gain access to groundwater from the MSLA, with groundwater sources in these regions being documented as early as the early 1800's. The presence of a number of animal husbandry activities in these areas particularly around the eastern-villages of Qormi, Ghaxaq, Zejtun and Zabbar also guaranteed a supply of organic manure which would also be used as a soil conditioner to supplement their organic content. Therefore the possibility of natural fertiliser application in these regions over a long time span is an important aspect to consider.

The availability of animal manure would however have been limited by the prevailing animal husbandry practices at the time. Prior to the 1950's one finds a prevalence of sheep and goats in the animal husbandry sector of Malta, which were extensively used for both the production of milk and meat. This changed during the 1950's though the enactment of a policy measure by the British Colonial Government to address the onset of the brucellosis disease. Under this policy farmers were required to trade in 12 sheep or goats for a cow, which in economic terms provided the possibility of an increased production return. Hence the 1950's saw an important change in the animal husbandry sector in Malta with goat and sheep herds being practically eliminated and replaced by cattle herds, as is outlined in Figure 9.6. Whilst this policy was successful in eradicating brucellosis in Malta, it also resulted in the generation of significantly increased volumes of manure which had to be disposed of, and generally as per established practice such manure was applied to agricultural fields.

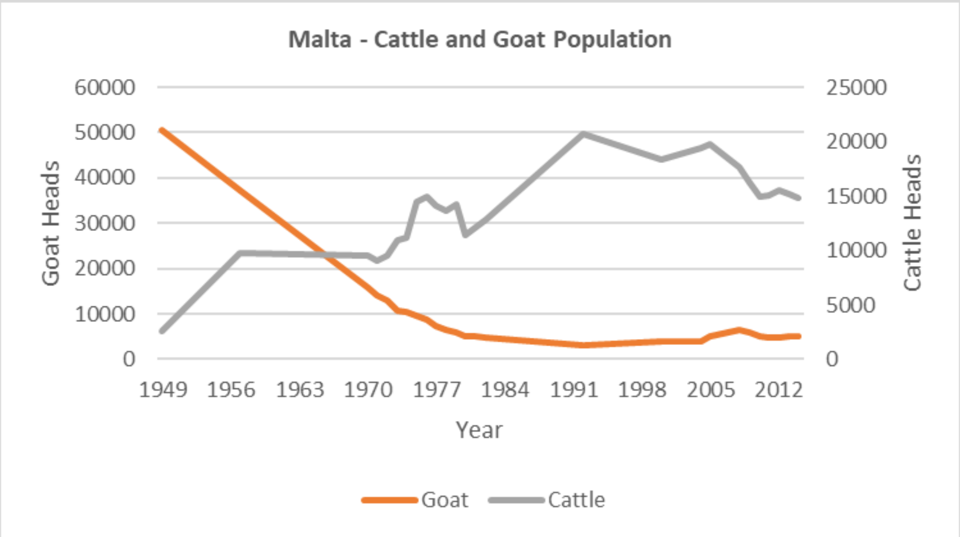

Figure 9.6. Correlation of Cattle and Goat Herd Population in the Maltese Islands

The production of manure can thus be considered to be quite limited up to the 1950's, when animal husbandry activities were predominantly based on goats and sheep. Cattle (oxen) were generally only imported for fattening and therefore kept on farm for only a limited time period. Rearing of pigs was present, however pig-farms were mainly located on the outskirts of urban areas and generally connected to the public sewer. Hence pig-manure was in most cases not applied to land.

In addition, trade records show that the importation of artificial (mineral) fertilisers started in the 1930's, although during these years limited amounts were imported. Higher importation levels were registered from the late 1950's onwards.

On the other hand Malta's increasing population, which increased from around 175,000 inhabitants in the early 1900's to over 500,000 inhabitants today, has also resulted in a decrease in the available agricultural land area to accommodate the expansion of urban areas. Today, around 30% of the island is classified as urbanised, with much of this land replacing agricultural land. In fact, registered agricultural land decreased from around 20,000 hectares in the first quarter of the 20th century to around 12,000 hectares today. Most of the sprawl of urban areas was centred in the central-eastern regions of the island. This led to a reduction in the agricultural area in which an increasing volume of manure could be applied, hence potentially resulting in the increased application of manure to unit area of land. Furthermore the increasing population would also result in an increased production of wastewater, where leakages from the sewer network would also potentially contribute to the nitrate loading in groundwater. This in particular in the increasingly urbanised central-eastern regions.

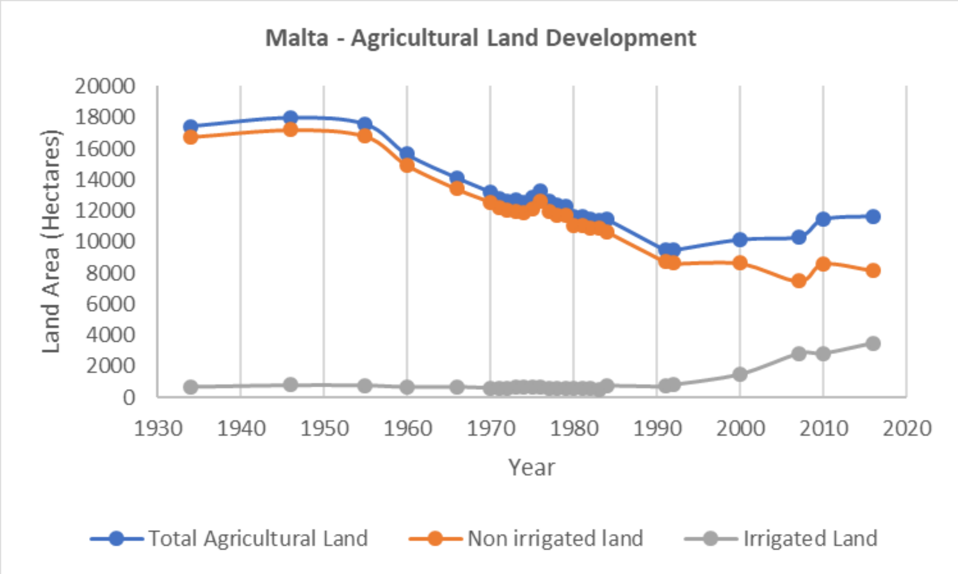

Figure 9.7. Development of Agricultural Land in the Maltese Islands

These developments in the agricultural sector when applied to the conceptual understanding of the Malta MSLA tends to sustain the observed trends in the nitrate content of groundwater.

(i) Recorded Nitrate levels in MSLA groundwater in the late 1800's are low, reflecting the lower availability of fertiliser which could be applied to land. This mainly as a result of the prevailing animal husbandry activities at the time.

(ii) Nitrate levels in the late 1960's and early 1970's already show high levels of nitrate particularly in the eastern regions of the island. This reflects the increased availability of animal manure and artificial fertiliser in the post-1950 period, in regions where the unsaturated zone is generally less thick resulting in shorter percolation times to the saturated zone.

(iii) Nitrate content in the central regions of the MSLA shows a progressive increase from the 1970's onwards, reflecting the potential increased application of fertiliser in these areas in response to the overall decreasing area of agricultural land. In addition, the thicker unsaturated zone in these area would result in a time-delay for any surface-related contamination in reaching the saturated zone.

The above considerations lead us to develop a conceptual understanding of nitrate flow from the surface catchment area to and within the saturated zone of the Malta MSLA. Water recharging the aquifer systems would take up nitrate contained in the soil on percolating down from agricultural areas. This recharging water would move slowly through the rock matrix in the unsaturated zone, the thickness of which would have a defining control on the time required to reach the saturated zone.

In the unsaturated zone, very little attenuation of the nitrate content of the percolating water is expected occur by physical processes such as sorption and hydrodynamic dispersion. Furthermore, the aerobic environment of the unsaturated zone is expected to result at best in a limited denitrification effect.

Once the percolating water reaches the saturated zone, later flow is expected to prevail depending on local and regional variations in the piezometric head. Dilution effects by mixing with resident groundwater and recharge from non-agricultural areas are expected to prevail during the movement of groundwater to the abstraction source or monitoring point.

This conceptual understanding is outlined in Figure 9.8 below.

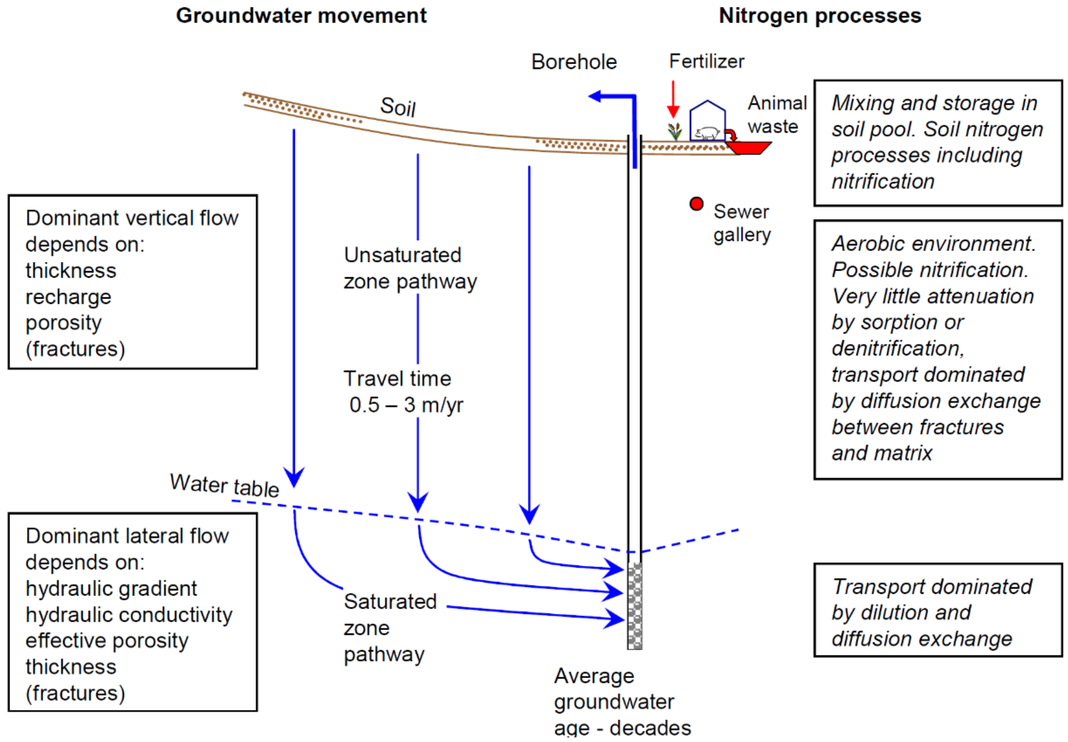

Figure 9.8. Conceptual understanding of Nitrate flow to groundwater in the Malta MSLA (Source BGS 2008)

9.8 Conclusions

The long travel times in the unsaturated zone and the residence times in the saturated zone of the Malta MSLA aquifer system have important implications for any relationship between present-day activities and nitrate concentration in groundwater. These geological and hydrogeological controls make it unrealistic to expect that a clear pattern between the application of contaminants (in this case fertilizer) and their detection in groundwater could be anticipated.

The lack of widespread rapid pathways from the surface to the water table suggest that a major part of infiltration may occur by relatively slow flow through the aquifer matrix. The travel time for nitrate from the surface to an abstraction point could be several decades at some sites. The nitrate stored in aquifer pore waters will act as a secondary source for a long period even if surface applications were to cease completely.

It is important to note that even if disposal and management of solid animal wastes were to be targeted as the most important source of nitrate contamination it is unlikely that significant improvements would be seen for several years or even decades. Hence an increased understanding of the timescale of groundwater flow in the unsaturated and saturated zone is required to enable the development of clear groundwater response timelines which can enable the modelling of the aquifer systems return to good qualitative status in response to the undertaking of pollution management actions in their surface catchment area. This is an important groundwater management issue also in relation to the application of the good status requirements under Article 4 of the EU’s Water Framework Directive.

10 IRELAND

Katie Tedd
GSI, Ireland

10.1 Introduction

This case study will focus on the Source Load Apportionment Model (SLAM) used by the Irish Environmental Protection Agency to support Water Framework Directive implementation. The model was developed by Mockler et al (2016) arising from the EPA funded PATHWAYS research project (Archbold et al, 2016). The Source Load Apportionment Model (SLAM) framework characterises sources of phosphorus (P) and nitrogen (N) emissions to water at a range of scales from sub-catchment to national. The SLAM synthesises land use and physical characteristics to predict emissions from point (wastewater, industry discharges and septic tank systems) and diffuse sources (agriculture, forestry, etc.) (Mockler et al, 2017). This case study will only discuss the nitrogen aspects of the model and is based predominantly on Mockler and Bruen (2016).

10.2 Modelling approach

10.2.1 Overarching framework

The Source Load Apportionment Model is a data driven GIS model. It is not available publicly but outputs are available to public agencies via the WFD app and to the public via the catchments.ie website.

In cases where water quality is impacted by excess nutrients, load apportionment modelling can support the proportional and pragmatic management of water resources. There are two broad approaches to load apportionment modelling, (i) load-orientated approaches which apportion origin based on measured in-stream loads (Grizzetti et al., 2005, Greene et al., 2011, Grizzetti et al., 2012), and (ii) source-orientated approaches where amounts of diffuse emissions are calculated using models typically based on export coefficients from catchments with similar characteristics (MCOS, 2002, Jordan and Smith, 2005, Smith et al., 2005, Campbell and Foy, 2008, Ní Longphuirt et al., 2016). The Source Load Apportionment Model (SLAM) framework (Mockler et al., 2016) takes the latter approach which enables estimates of the relative contribution of sources of nitrogen (N) and phosphorus (P) to surface waters in catchments without in-stream monitoring data. This allows the approach to be applied throughout Ireland, independently of the availability of measured in-stream data. It integrates information on point discharges (urban wastewater, industry and septic tank systems) and diffuse sources (pasture, arable, forestry, etc.) and catchment data, including hydrogeological characteristics where applicable (Mockler et al, 2017).The general method of source-oriented load apportionment models is an export coefficient approach as outlined in Mockler et al (2016):

1. calculate available annual average nutrient loads from each sector;
2. reduce these loads by a factor to account for treatment (e.g. urban wastewater) or attenuation in the environment (e.g. diffuse agricultural sources), where relevant this estimate the annual in-stream loads from each sector;
3. compare the estimated annual in-stream loads with annual loads calculated from measurements, where available (Bøgestrand et al., 2005).

The SLAM predicts the annual emissions of P and N to water, and does not include inter- or intra-annual variability. Changes due to hydrological variability and groundwater lag times are therefore not explicitly captured (Mockler and Bruen, 2018).

10.2.2 Source Term

Mockler and Bruen, 2018 outline the source terms for the model. The SLAM framework incorporates multiple national spatial datasets relating to nutrient emissions to surface water, including land use and physical characteristics of the sub-catchments (Table 10.1 Data sources for the SLAM framework (v2.05) (from Mockler and Bruen (2016))). Separate modules were developed for each type of nutrient source to facilitate upgrading and comparisons with new data or methods (Figure 10.1). Only the agricultural module will be discussed in this case study. The agriculture (pasture and arable) modules use spatial outputs from the Catchment Characterisation Tool (CCT) (Archbold et al., 2016).

Table 10.1 Data sources for the SLAM framework (v2.05) (from Mockler and Bruen (2016))

Sub-model	Input data and source
Waste water discharges	2014 Annual Environmental Report data (EPA, 2015)
	2014 EPA Licensing Enforcement and Monitoring Application (LEMA)
Diffuse urban sources	2012 CORINE land cover (Lydon and Smith, 2014)
Industrial discharges	Section 4 licence limits (EPA, 2015)
	2011–2013 PRTR database (EPA, 2015)
Septic tank systems	Non-sewered house dataset and surface water bodies (EPA, OSI)
	Karst feature vulnerability and subsoil permeability (GSI)
Pasture (diffuse agriculture)	2012 LPIS (DAFM dataset)
	2010 agricultural census data (Central Statistics Office, 2010)
Arable (diffuse agriculture)	2012 LPIS (DAFM dataset)
	2010 agricultural census data (Central Statistics Office, 2010)
	Good Agricultural Practices (GAP) Regulations (Government of Ireland, 2014)
	Fertiliser application rates (Lalor *et al.*, 2010)
Forestry	2012 CORINE land cover (Lydon and Smith, 2014)
Peatlands	2012 CORINE land cover (Lydon and Smith, 2014)
Atmospheric deposition	Lake segment areas (EPA dataset)
	N deposition map (Henry and Aherne, 2014)

CORINE, Coordination of Information on the Environment; PRTR, Pollutant Release and Transfer Register; OSI, Ordnance Survey, Ireland; GSI, Geological Survey Ireland; DAFM, Department of Agriculture, Food and the Marine.

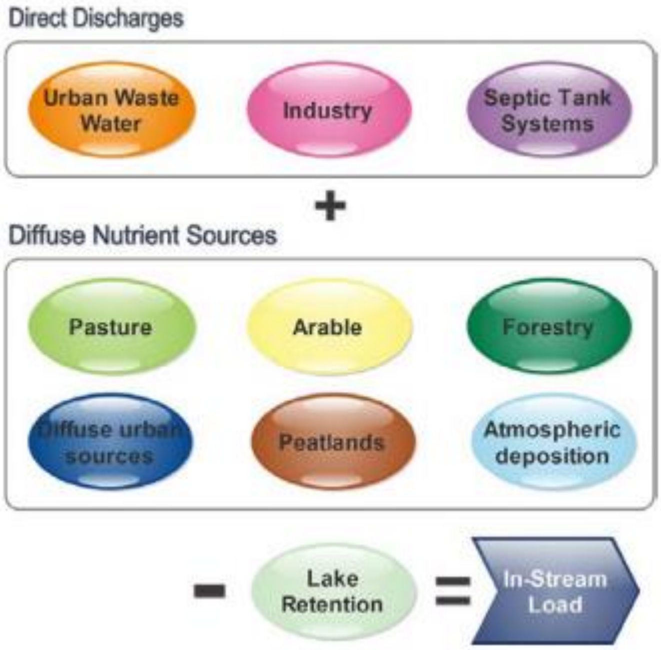

Figure 10.1 Sub-models of the SLAM framework (from Mockler and Bruen (2016))

Diffuse Agricultural losses

The agricultural module of the SLAM is the Catchment Characterisation Tool (CCT). It is an annual average export coefficient model calculating leaching rates based on methods from existing models for N (Shaffer et al., 1994; del Prado et al., 2006). The Nutrient Susceptibility maps and the Pollution impact potential maps mentioned in HOVER WP5 Deliverable 5.2 are outputs of the CCT.

The key pressure input dataset for the agriculture module (i.e. the CCT) is the Land Parcel Identification System (LPIS) from the Department of Agriculture, Food and the Marine (DAFM). The DAFM collects data from farmers who record the land use and crop description of each field they own, allowing for accurate identification of land use in a spatial context. These data were combined with DAFM data on N and P loads based on the Animal Identification System for cattle and Central Statistics Office data for sheep.

The model applied pathway-dependent attenuation coefficients related to the hydrogeological conditions, which were inferred from GIS maps of relevant properties including soil drainage, subsoil permeability and depth to bedrock. These coefficients were determined following a literature review and expert elicitation for the two pathway categories grouped into (1) “near surface” pathways, including overland and drain flow, and (2) groundwater (Archbold et al., 2016). The CCT calculated N losses from diffuse agriculture ($DiffAgri_{N,P}$) using a mass balance calculation as follows:

$$DiffAgriN,P = LeachedN,P \times [(NS \times \alpha N,P) + (GW \times \beta N,P \times \phi N,P)] \tag{10.1}$$

Where:
$Leached_{N,P}$ =loads leached from the soils for N or P ($kgyr^{-1}$);
$\alpha_{N,P}$ =near-surface pathway factors for N or P;

$\beta_{N,P}$ =groundwater pathway factors for N or P;
$\varphi_{N,P}$ =groundwater bedrock transport factor for N or P;
NS=fraction of load to surface water via near surface pathway; and
GW=fraction of load to groundwater (= 1 – NS), where:

$$NS = \frac{P_e - R}{P_e} \tag{10.2}$$

$$GW = \frac{R}{P_e} \tag{10.3}$$

where
P_e=annual effective precipitation; and
R=average annual recharge.
Note that both P_e and R data were taken from the Geological Survey of Ireland (GSI) Groundwater Recharge Map (Hunter Williams et al., 2013).

Nitrogen leaching calculation

In the CCT-N model, the $Leached_N$ from pasture was calculated using the NCYCLE_IRL (del Prado et al., 2006) modelled values for groupings of fertiliser application rate, soil drainage type and pasture type. The LPIS provided applied rates of N (kg ha^{-1} yr^{-1}) at farm level (see Zimmermann et al., 2016). Diffuse nutrient losses from arable land were calculated similarly to the Nitrogen Risk Assessment Model for Scotland (NIRAMS) (Dunn et al., 2004). The CCT-N model estimated the available (net) nutrients using the maximum allowable fertilisation rates (Government of Ireland, 2014), atmospheric deposition and average off-take values. Denitrification varies by soil texture, with rates of 5%, 15% and 75% applied to sandy, loamy or clay/peaty soils, respectively. $Leached_N$ was calculated using the Nitrate Leaching and Economic Analysis Package (NLEAP) model (Shaffer et al.,1994):

$$Leached_N = Available_N \left(1 - \exp\left[-K\left(\frac{WAL}{SATC}\right)\right]\right) \tag{10.4}$$

Where:
$Available_N$ =available (net) N (kg ha^{-1} yr^{-1});
K=leaching coefficient (0.7 for sandy soils and 1.2 for other soils);
WAL=water available for leaching (mmyr^{-1}), estimated from Pe; and
SATC=soil saturated capacity (mmyr^{-1}) estimated from Anthony et al. (1996) based on the soil drainage classification in the Irish National Soils Map (Teagasc et al., 2006).

For both pasture and arable areas, nutrient reduction factors (α_N, β_N, and ϕ_N) were then applied to the leached amount of nutrients ($Leached_N$) to predict the final losses to water ($DiffAgri_N$). The coefficients representing the delivery of N via near-surface pathways (α_N) were linked to subsoil permeability, as N tends to move through the subsoils before arriving at the surface water receptor (Table 10.2). In addition, a map of the possible location of land drains (Mockler et al., 2014) indicated a preferential delivery pathway for nitrate in low-permeability subsoils. Groundwater export coefficients (β_N) were determined following a literature and expert elicitation review (Packham et al., 2015). These coefficients vary by subsoil permeability and depth to bedrock (Table 10.3), both available as maps from GSI. The bedrock attenuation coefficient (ϕ_N) was linked to aquifer bedrock units with the potential for denitrification, mostly due to the presence of pyrite (Table 10.4).

Table 10.2 Nitrate near surface pathway factors (from Mockler and Bruen (2016))

Subsoil permeability	N near-surface factor
Low	0.2
Low and likely to have land drains	0.7
Moderate	0.55
High	1
N/A	0.95
Water/lake/rock	0.95

Table 10.3 Nitrate groundwater pathway factors (from Mockler and Bruen (2016))

Subsoil permeability (depth to bedrock)	Low	Moderate	High	N/A (DTB < 3 m)
0–1 m	1.0	1.0	1.00	1.0
1–3 m	0.60	0.95	1.00	0.95
3–5 m	0.20	0.90	1.00	–
5–10 m	0.05	0.85	1.00	–
> 10 m	0.01	0.75	1.00	–

Table 10.4 Nitrate groundwater bedrock pathway factors (from Mockler and Bruen (2016))

Bedrock unit*	Transport factor
Unit 1a, Unit 1b	0.65
All other bedrock units	1

Similar export coefficient approaches were taken for the other modules but these are not discussed here. For more information the reader is referred to Mockler et al 2016.

10.2.3 Model calibration and validation

The SLAM results were compared with monitoring data to assess the model's performance prior to its extension to cover the entire country. Sixteen major river catchments covering 50% of the area of Ireland (Figure 10.2) were selected, based on the availability of both monitoring data and loadings information. These catchments are in the national riverine inputs monitoring programme that is managed by the Irish EPA. The design of the programme followed the Comprehensive Study on Riverine Inputs and Direct Discharges (RID) principles (OSPAR, 1998). O'Boyle et al. (2016) provide details of the sampling and analysis methodologies for the TN concentration data used in this study. The locations of the flow and nutrient concentration monitoring stations are largely at the tidal limits of rivers and they are generally upstream of the large wastewater treatment plant discharges associated with the major coastal urban centres.

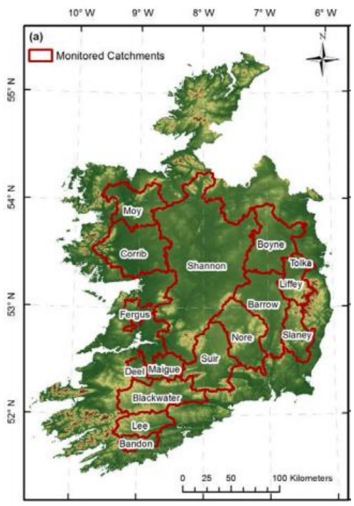

Figure 10.2 Locations of 16 catchments with monitored total nitrogen emissions to water (from Mockler and Bruen (2016))

The loadings information for diffuse and point sources used in this study relate to 3 years, 2012–2014, and hence monitoring data for only these years were used to evaluate the model performance. Annual loads were calculated as the product of the flow-weighted annual mean concentration of TP or TN and the annual flow (see O'Boyle et al., 2016).

The SLAM results provide a reasonable representation of the variance of the 3-year annual average loads (Figure 10.3 a), with satisfactory coefficient of determination (r^2) for annual TN (r^2=0.82, p=<0.01, n=16). The error bars highlight the interannual variability in the measured emissions that is not captured by the model. Figure 10.3 b indicates the individual results for each test catchment. These results compare well with other nutrient modelling studies, such as the InVEST nutrient delivery ratio model that was applied in the UK (Redhead et al., 2018), which also found a wide variation of model accuracy among 36 study catchments.

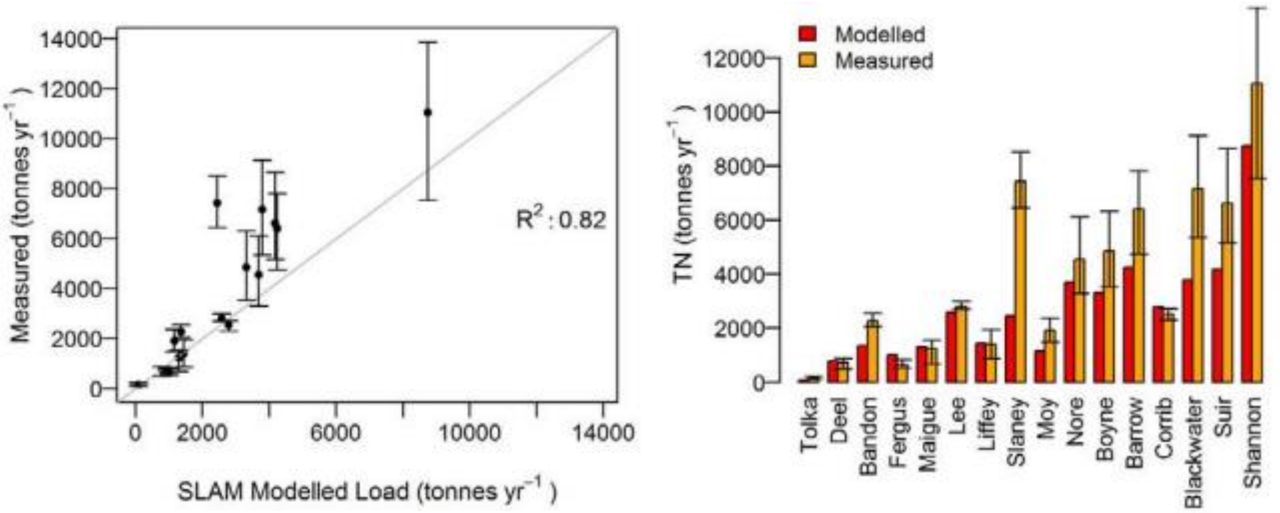

Figure 10.3 (a) Modelled SLAM nutrient emissions of total nitrogen compared with average measured annual nutrient fluxes from 2012 to 2014 (error bars show the range of measured loads). (b) Bar charts of modelled and measured total nitrogen for each catchment (ordered by increasing catchment area). (from Mockler and Bruen (2016))

10.3 Key results

Load apportionment results by sector were analysed nationally for six regional (formerly river basin) districts and at a local scale for 583 subcatchments ranging in area from 24 to 390km^2. Agriculture is the main source of N in Irish rivers, similar to other countries, including the UK (Bowes et al., 2014) and across Europe (Bøgestrand et al., 2005). In Ireland, average annual N emissions to water were estimated at over 82,000tyr^{-1} and pasture was the dominant source overall (Figure 10.4, Table 10.5). N emissions were more spatially uniform than P emissions, as nitrate from diffuse sources is typically delivered to streams via subsurface pathways, with links between increasing nitrate concentrations and groundwater contributions (Tesoriero et al., 2009). Emissions from arable land reflected the locations of the most crop-intensive areas in the more freely draining soils of the country in the East (14%) and South East (20%). The proportion of emissions of N from septic tank systems was low on average (2%), with higher contributions in the North West (5%) and West regions (4%), reflecting the relatively high density of non-sewered properties in these areas. Contributions from wastewater were low across all regions (<7%) except for the East (33%), the latter due to the high proportion of the population living in this region.

Table 10.5 Nitrogen emissions to water by region and percentage contribution from source (from Mockler and Bruen (2016))

Region	Area (km^2)	N total ($t yr^{-1}$)	Wastewater (%)	Other licensed discharges (%)	Diffuse urban (%)	Septic tank systems	Pasture (%)	Arable (%)	Forestry (%)	Peatlands (%)	Deposition on water (%)
North West	9842	4286	7	1	1	5	59	3	9	10	5
East (and Neagh-Bann)	8458	13,000	33	1	2	2	45	14	2	1	1
South East	12,850	20,594	4	1	1	2	69	20	2	1	0
South West	11,181	19,551	7	0	0	2	77	9	2	2	0
Shannon	18,014	17,171	6	1	1	2	78	3	4	2	3
West	10,458	7589	3	0	1	4	74	1	5	9	4
Total	70,803	82,190	10	1	1	2	69	10	3	2	2

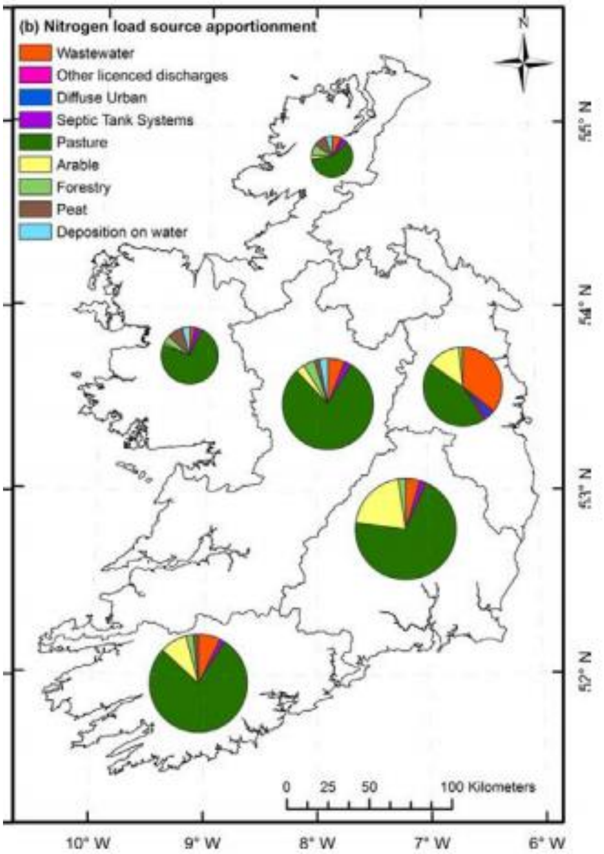

Figure 10.4 Load apportionment of nitrogen emissions to water by region. The size of the pie indicates the relative total nutrient emissions. (from Mockler and Bruen (2016))

Point vs diffuse sources at local scale

Figure 10.5 a illustrates the range of nutrient export rates of N emissions to water for each of the 583 sub-catchments in Ireland and the percentage contributions from point sources (Figure 10.5 b and c). Point sources of nutrients were classified as wastewater, other licensed discharges and septic tank systems. Farmyards as point sources are also likely contributors to emissions to water but are not included in the model (although they are somewhat implicit in the CCT). Agricultural intensity has a dominant impact on the magnitude of the total emission rates for N, with the majority of emissions coming from the East and South of the country reflecting the coincidence of higher intensity agricultural land on more freely draining soils.

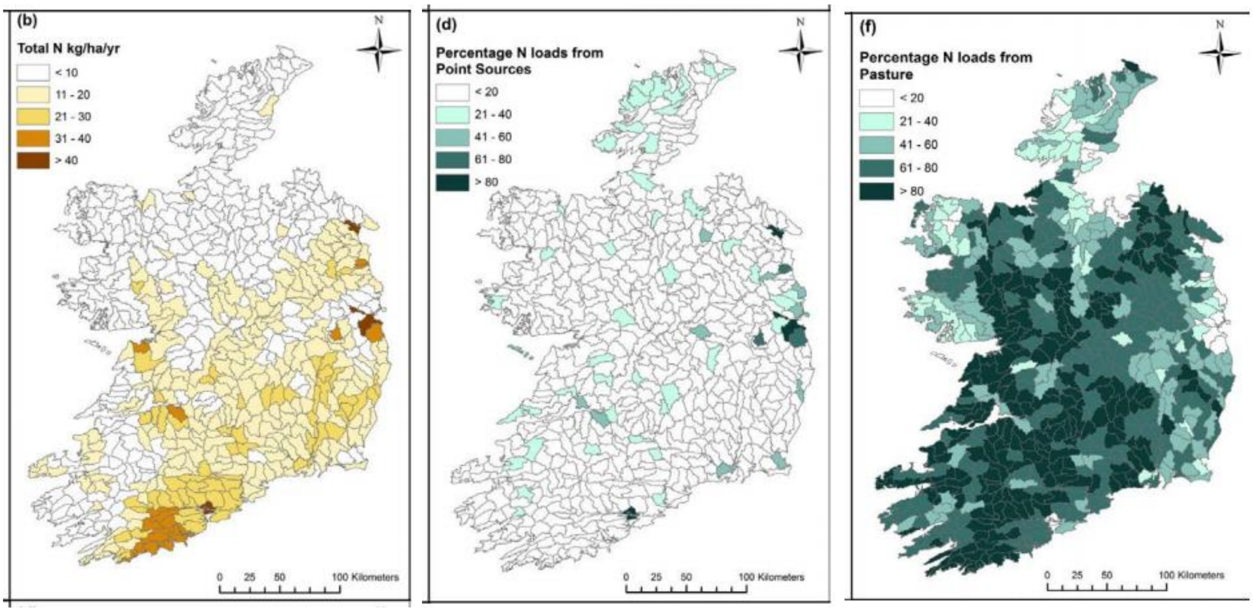

Figure 10.5 (a) Total nitrogen emissions to surface water prior to lake retention ($kgha^{-1}yr^{-1}$). Percentage contribution from (b) point sources and (c) from pasture for 583 sub-catchments. (from Mockler and Bruen (2016))

Groundwater v surface water pathways

On average, the SLAM model estimates that the groundwater pathway contributed approximately 25% of N to surface waters, increasing up to 80% of N in some hydrogeologically susceptible sub-catchments. This calculation used the SLAM modules for agriculture (pasture and arable) and septic tank systems, which calculated the emissions to surface waters through two pathway categories: (1) “near surface” pathways including overland and drain flow; and (2) groundwater. By including these pathways in the conceptual models of nutrient transport and attenuation, the threedimensional relationships of sources, pathways and receptors in catchments are accommodated. To achieve successful outcomes, water quality management strategies must be tailored to the local hydrogeological conditions and main pollutant pathways. Deakin et al. (2016) outlined two contrasting examples, showing that in a freely draining karstified catchment with predominantly subsurface pathways, measures must target managing inputs to groundwater, whereas in a catchment underlain by poorly draining soils, the transport of P by overland flow and interflow, and from small point sources, were key issues and so measures were required to intercept these pathways and mitigate discharges.

10.4 Outcomes of modelling

The SLAM framework was developed to support the proportional and pragmatic assessment of every sub-catchment within the EPA’s WFD national characterisation process. The national nutrient source apportionment results were produced at sub-catchment scale and integrated into the EPA’s WFD characterisation process (Daly et al., 2016) by the EPA’s Catchment Science and Management Unit during 2016 and 2017. The source apportionment results were included in the catchment assessments alongside other national datasets, including ecological status and trends in ecological and chemical monitoring data; information on land use, pressures, pathways and the sensitivity of receptors; licence, enforcement, audit and inspection information from regulatory agencies; and local, on-the-ground knowledge from the local authorities and fisheries agency staff (Daly et al., 2016). Inclusion of the SLAM results into this process facilitated the assessment of nutrient load information in a logical, structured, consistent and comparative way across the country and has therefore enabled robust and practical use of the available information. This systems focused approach is vital for integrated catchment management and effective WFD implementation (Voulvoulis et al., 2017). The model results, however, were only one indicator used to identify the significant pressures. During the WFD characterisation process, the results were interpreted by catchment scientists along with the other national datasets listed above. Furthermore, the SLAM results were only used in cases in which chemical and ecological monitoring data, local knowledge or other information indicated that excess nutrients were impacting on a water body. This process ensured that the several sources of uncertainty and the model under and over-estimations would not result in the incorrect identification of significant pressures. The design of measures requires integrating hydrological and social science assessments to ensure that decision makers have the best information when evaluating cost-efficiency and effectiveness (Psaltopoulos et al., 2017), and models such as the SLAM provide some of the necessary information to feed into these assessments. For example, the annual percentage contribution of loads from septic tank systems may be small overall at the sub-catchment scale, but their impact in small stream headwaters can be significant during low-flow periods (Withers et al., 2012).

Source apportionment models, such as the SLAM, can provide an indication of sources of emissions at regional or sub-catchment levels but are not suitable for detailed, site-specific assessments. Local investigative assessments are therefore required prior to implementation of specific mitigation strategies.

11 EVALUATION AND SYNTHESIS OF APPROACHES

11.1 Overview

Table 11.1 provides a summary of the different approaches used by the HOVER WP5 partners in modelling nitrate and pesticide transport. The approaches used across the partners are varied in both scale (field, regional, national, continental) and methodology (focussing on the unsaturated zone, the saturated zone or both, use of detailed process-based models or more simplified approaches).

In this chapter in section 11.2 we evaluate the different approaches used across the HOVER WP5 partners, identifying common methodologies and lessons learnt by considering approaches used at different scales. We then develop harmonised cross-partner outputs in section 11.3, and explore implications for management of nitrate and pesticide transport and an outlook for further work in sections 11.4 and 11.5 respectively.

Area	Case study	N	Pst	Source term	USZ transport	SZ transport	Attenuation processes	Model calibration, sensitivity analysis and validation	Results	Outcomes
Continental	Continental scale modelling of nitrate stored in the unsaturated zone	X		Soil N balance	Piston flow model	NA	NA	No calibration. Sensitivity analysis to leaching input and travel times conducted, with validation to previously published N storage studies and nitrate concentrations in groundwater	Nitrate stored in the unsaturated zone in continental Europe on an annual basis for 1900-2000	Increased awareness of nitrate as an issue in UK, use of global model as a regional screening tool for further investigations
UK	National scale modelling of nitrate storage and travel times	X		Empirical soil nitrogen leaching meta-model and historic N application data	Velocity based on published profiles and piston flow model, USZ thickness based on national water table depth map	Simple conceptual saturated groundwater flow model	NA	No calibration of unsaturated zone travel times and storage. Monte-Carlo calibration and sensitivity analysis for nitrate concentration trends in groundwater	National maps of nitrate travel times and storage in the unsaturated zone, modelled nitrate concentration time series in groundwater for 28 aquifer zones	Results used for updating of groundwater NVZ designation methodology in England, regional management of nitrate in the Chalk, and as evidence for UK Government enquiries on nitrate
France	National scale nitrate travel time modelling, regional studies	X		Soil N balance	Velocity based on published profiles, USZ thickness of different hydrogeological zones	NA	NA	Qualitative comparison between N pressure at the water table and nitrate concentrations in groundwater	National maps of nitrate travel times in the unsaturated zone	Results used in EU WFD reporting regarding nitrate time lags. Results can help stakeholders with decision-making regarding nitrate pollution of groundwater
Netherlands	Groundwater model evaluation in the Meuse catchment	X	X	NA	metaswap for national hydrological model, piston flow estimate of velocities for national unsaturated zone travel time map	MODFLOW + MT3D + MODPATH	NA	Modpath and MT3D ages evaluated against tracer data. Age-concentration relationships compared using ages based on tracers, MODPATH and MT3D, using nitrate, OXC, sulphate and pesticides across different parts of the study area	Reasonable agreement between tracer and model ages for c. 50% of boreholes. 10-20% of monitoring wells show large discrepancies, with too old water being predicted by the models.	Evaluation of modelled ages against tracer data helps stakeholders understand the limitations of models in linking measured nitrate and pesticides in groundwater at short screen wells to application at farmlands.
Denmark	National scale modelling of nitrate in groundwater	X		Empirical soil nitrogen leaching model	MIKE-SHE model for surface water-unsaturated zone-groundwater flow and transport		Modelled depth to redox boundary	Flow model calibration using a combination of manual trial and error and inverse modelling, validation using split-sample and proxy basin testing. National nitrogen model calibrated and validated using measurements of nitrogen transport from 340 gauging stations	National maps of depth to water table, unsaturated zone travel times, groundwater age, nitrogen leaching, nitrogen retention	Model used for national regulation of nitrogen
Denmark	Pesticide Leaching Assessment Programme Modelling	X	X	10-year nitrogen leaching time series, pesticide and degradation products	Variably saturated flow and transport models (MACRO, COMSOL, HYDRUS-1D)		Pesticide degradation included	Calibration using PEST	Detailed pesticide (fate, long term sorption and dissipation characteristics) and hydrogeological (boundary conditions, fluctuating groundwater levels, preferential flow where relevant) properties and structure need to be considered when predicting risk of pesticide contamination to shallow groundwater. Not including these processes where relevaant risks underestimating leaching of pesticides, degradation products and nitrate to groundwater and surface water.	
Croatia and Slovenia	Modelling nitrate concentration trends in the Drava aquifer	X		Empirical investigations for nitrate surplus for different land uses in Slovenia	Velocity based on lysimeter data, USZ thickness based on calibrated groundwater flow model outputs and depth to water table maps	MODFLOW + MT3D	NA	Modelled groundwater heads calibrated using PEST, no sensitivity analysis. Model evaluated and validated through comparison of flow budgets and observed and modelled groundwater nitrate concentrations	Aquifer-level maps of nitrate concentrations in groundwater in the future	Improved understanding of the future spatio-temporal evolution of nitrate concentrations in the aquifer
Malta	Summary of BGS nitrate conceptual modelling studies	X		NA					Conceptual understanding of nitrate transport in the Malta Mean Sea Level Aquifer	Improved understanding of nitrate transport can support groundwater management to achieve good status under the EU Water Framework Directive
Ireland	National Source Load Apportionment Model	X		Export coefficient model and national land use maps	Annual fluxes from groundwater and near-surface pathways to rivers derived using leaching data and export coefficients		Attenuation coefficients linked to soil drainage, subsoil permeability and depth to bedrock	Calibration through comparison of observed amd modeled riverine nutrient fluxes	National scale maps of riverine nitrogen load apportionment by region and sub-catchment	Improved understanding of N sources at national, regional and sub-catchment levels to support WFD characterisation process

Table 11.1 Summary of approaches to modelling nitrate and pesticide transport taken across different partners

11.2 Evaluation of approaches across HOVER WP5 partners

11.2.1 Hydrogeological settings influence approaches to modelling nitrate transport at the national and regional scale

The range of different approaches to modelling nitrate transport at national to regional scales reported in chapters 2 to 9 and summarised in Table 11.1 reflects the variability in hydrogeological settings and approaches to the conceptualisation of travel times across the different partners. This is illustrated conceptually in Figure 11.1 and was also evident in the approaches to monitoring of nitrate and pesticide transport as reported in previous deliverables in WP5 (D5.2).

A critical hydrogeological factor in determining the need for different approaches to modelling nitrate transport is the relative proportion (t_r) of the total travel time (t_T) in either the unsaturated zone (t_U) or saturated zone (t_S) as expressed by Sousa et al. (2013) as:

$$t_r = \frac{t_U}{t_T} \; or \; \frac{t_S}{t_T} \qquad (11.1)$$

In the UK and France some aquifers have relatively thick unsaturated zones, and thus t_U makes up a significant component of the total travel time. As a consequence, in the UK the national scale studies reported here initially focussed on unsaturated zone time lags and storage (section 3.1), before also considering the saturated zone (section 3.2). In France, the studies reported here also focus on nitrate transport in the unsaturated zone. The UK and France have adopted similar approaches to quantifying unsaturated zone time lags, using nitrate transport velocities based on observed porewater profiles and simple piston flow models. Average nitrate velocities in the Chalk unsaturated zones are 0.83 m/a and 0.93 m/a in the UK and France respectively. The nitrate velocities in the French unsaturated zones of sandstone (1.8 m/a) and limestone (1.5 m/a) are higher than that in the UK unsaturated zones of sandstone (1.06 m/a) and limestone (1.11 m/a). There are some differences in the methodologies used to estimate water table depths, with spatially distributed groundwater level depth maps (1 km x 1 km) used in the UK and average groundwater level depths for different hydrogeological zones used in France.

In contrast to the UK and France, water tables in the Netherlands are very shallow, and thus t_S dominates the total travel times. Consequently, modelling efforts at the regional and national scale reported here have focussed on the saturated zone and modelling of travel times to wells using distributed groundwater flow and transport models (MODFLOW, MT3D and MODPATH, Netherlands).

The UK/France and the Netherlands reflect end-members of a continuum of hydrogeological settings where in the former unsaturated zone travel times may be significant, and in the latter travel times in the saturated zone dominate. The other pilots show a combination of both unsaturated and saturated zone travel times depending on the hydrogeological setting. In Denmark, two conceptual models of nitrate transport are present; one with significant travel times in both the unsaturated and saturated zone, and a second with rapid shallow transport through tile drains to surface water bodies. This variability in conceptual models a necessitates the use of an integrated unsaturated zone-saturated zone-surface water model (MIKE-SHE) that can account for these different settings. Similarly, the Drava aquifer pilot shows significant travel times in both the unsaturated zone and saturated zone in some areas, and as a consequence the modelling approach adopted in Croatia and Slovenia considers both the unsaturated zone and saturated zone in detail using observed lysimeter data and distributed flow and transport models (MODFLOW and MT3D). In Malta, whilst no numerical model has been reported in this deliverable, the conceptual model reported considers travel times in both the unsaturated and saturated zone. Ireland's hydrogeology is dominated by a wet climate, shallow water tables and fractured or karstic bedrock aquifers (generally with no primary porosity) meaning that unsaturated and saturated travel times can be relatively short. This is particularly the case in areas with high groundwater nitrate (such as the well-drained soils with higher agricultural inputs in the south east). The Irish source load apportionment model uses annual fluxes to support WFD objectives without explicitly capturing groundwater lag times.

The variability in hydrogeological settings across the different national and regional pilots is also reflected in the model inputs and outputs for the continental scale modelling of nitrate stored in the unsaturated zone reported in section 2. Figure 11.2 shows modelled water table depth (Fan et al., 2013) used as a model input in this global scale research across the HOVER WP5 partners contributing national-scale pilots to this report. It can be observed that the modelled depth to water table is significantly greater in the UK and France than in the Netherlands and Denmark. Moreover, despite the high modelled nitrate leaching rates in the Netherlands and Denmark (Figure 2.5), modelled unsaturated zone nitrate storage is low due to the shallow water table in these areas. This broad agreement between the continental scale and national scale modelling approaches in which areas the unsaturated zone may be significant provides some confidence in the continental scale modelling, and corroborates previous work which has suggested global scale models are a potentially useful screening tool, but require refinement for local scale applications (Turkeltaub et al., 2020).

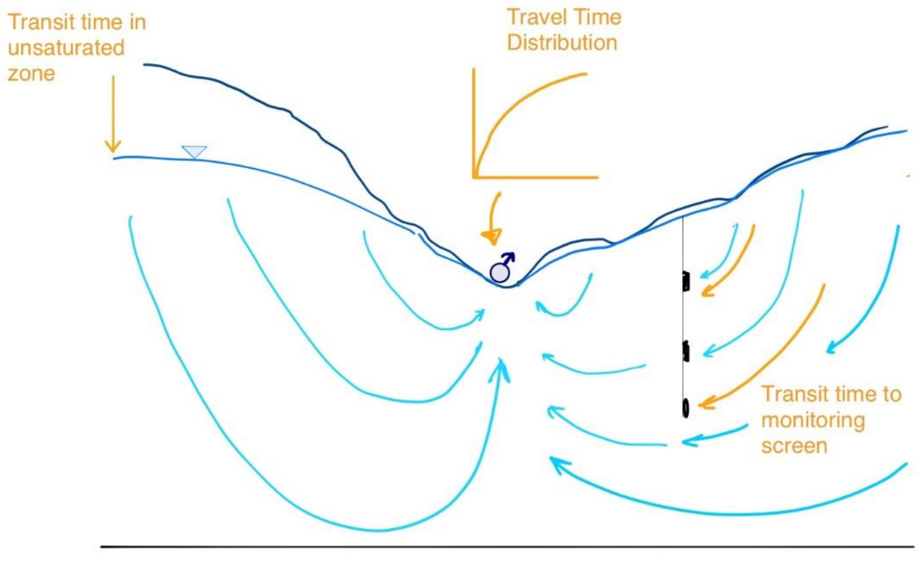

Figure 11.1 Different conceptual models of travel times used by HOVER WP5 partners. The UK and France have focussed on transit times in the unsaturated zone (left), whilst the Netherlands have focussed on transit times in the saturated zone to wells (right). Pilots in Denmark, Croatia, Slovenia and Malta reflect a combination of both conceptualisations, where both unsaturated and saturated zone travel times are significant depending on the hydrogeological setting. Reproduced from HOVER D5.2.

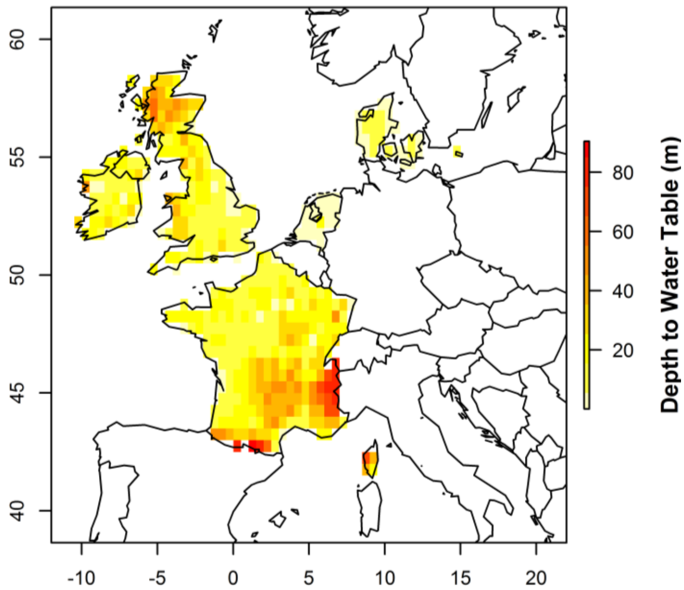

Figure 11.2. Modelled water table depth across HOVER WP5 partners contributing national-scale pilots. Reproduced after Fan et al. (2013).

11.2.2 Insights from model-tracer age comparison and local scale analyses

With the exception of the PLAP modelling in Denmark reported in section 6.1, all the pilot studies reported in this deliverable consist of modelling approaches at large scales (regional, national or continental scale). The development of models of nitrate and pesticide transport at these scales requires invoking assumptions regarding groundwater flow and transport (e.g. ignoring preferential flow). Given these assumptions, what are the limitations to the use of such large scale modelling approaches? Two of the pilots, the model-tracer age comparison in the Netherlands and the PLAP modelling in Denmark, provide insights.

In the Netherlands pilot, comparison of observed (tracer) and modelled groundwater ages showed a reasonable agreement for c. 50% of boreholes. 10-20% of monitoring wells showed large discrepancies, with the model predicting too old water. This evaluation of modelled ages against tracer data helps stakeholders understand the limitations of models in linking measured nitrate and pesticides in groundwater at short screen wells to application at farmlands. A similar modelling approach (MODFLOW + MT3D) was used in the Drava pilot, and thus the results of the Netherlands pilot should be borne in mind when evaluating model results in the Drava pilot.

In the Netherlands pilot discrepancies between observed (tracer) and modelled groundwater age are associated with numerical model discretisation, with model grid cells being significantly larger than the spatial dimensions of the drainage networks which cause small scale variations of flow paths and resulting groundwater age patterns (e.g. Broers 2004). Although using a national scale model has merits in demonstrating the large scale patterns of groundwater age, these models are less useful to link contaminants in specific short-screened wells to their infiltration history as the probability of missing the small scale flow path variations is significant. Groundwater age tracer sets remain a prerequisite of validating these kind of models and for using groundwater age as a forensic tool to link contaminant temporal and spatial patterns to the infiltration history. However, detailed, small-scale modelling of nitrate and pesticide transport below agricultural fields from the PLAP modelling pilot in Denmark is able to provide insight into controlling processes at the field scale. Pesticide (fate, long term sorption and dissipation characteristics) and hydrogeological (boundary conditions, fluctuating groundwater levels, preferential flow where relevant) properties and structure need to be considered when predicting risk of pesticide contamination to shallow groundwater. Not including these processes where relevant risks underestimating leaching of pesticides, degradation products and nitrate to groundwater and surface water.

A significant challenge that follows from these insights this is how to utilise such detailed local-scale knowledge at the large scale, where there is limited information on both the significance of many of the processes highlighted by the PLAP modelling, and limited tracer age datasets. A conservative approach would be to consider such large scale modelling approaches, in particular simplified continental-scale modelling in section 2, as screening tools prior to further investigation. This has been previously highlighted by Turkeltaub et al. (2020), who compared the results of a gridded 1D Richards equation model of nitrate transport in the unsaturated zone with the results of the global model used in section 2. This comparison showed similar spatial patterns of nitrate storage in the unsaturated zone between the models, but some significant discrepancies in the magnitude of nitrate and recharge fluxes. It was concluded that any application of global scale models at regional to local scales requires detailed refinement to represent the relevant processes occurring. Further refinement and evaluation of the travel time models reported in this deliverable would benefit from the international databases of tracer age data as are currently being collated in HOVER WP6.

11.3 Development of harmonised cross-partner outputs

11.3.1 Unsaturated zone travel times

Figure 11.3 shows unsaturated zone travel times derived from national scale modelling undertaken in Great Britain (UK), France, Netherlands and Denmark. Travel times for the Drava aquifer (Croatia and Slovenia) are also shown. The map highlights differences between and within the partner countries as to the significance of travel times in the unsaturated zone. The longest travel times are present in the Great Britain (UK) and France, where they may be > 50 years in the Chalk of SE East England and northern France. In the Drava aquifer, Denmark and in the Netherlands there are also areas of relatively long travel times (up to 20 years). However, in the largest part of Netherlands travel times in the unsaturated zone are <2 years across much of the country.

Figure 11.4 shows areas across the pilots where travel times for nitrate in the unsaturated zone are > or < 10 years. This is further summarised in Table 11.2, which shows the % of land area across each pilot where travel times are > 10 years. This highlights the differences between the UK/France and the other pilots. Approximately 50% of the land area in Great Britain (UK) and France has travel times > 10 years, whereas this < 10% in the Netherlands, Denmark, and the Drava pilots.

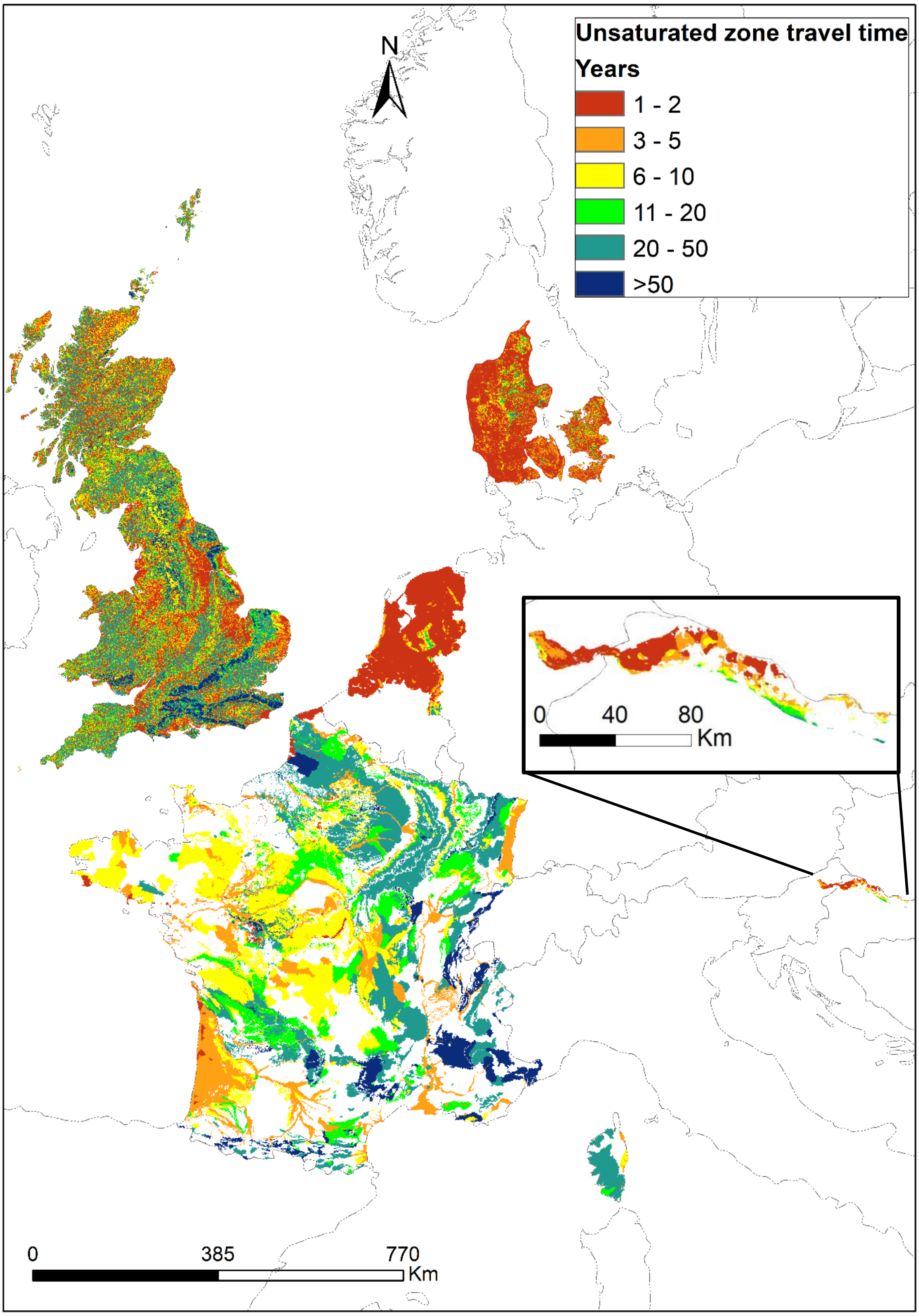

Figure 11.3. Travel times for nitrate in the unsaturated zone across selected pilots in this deliverable

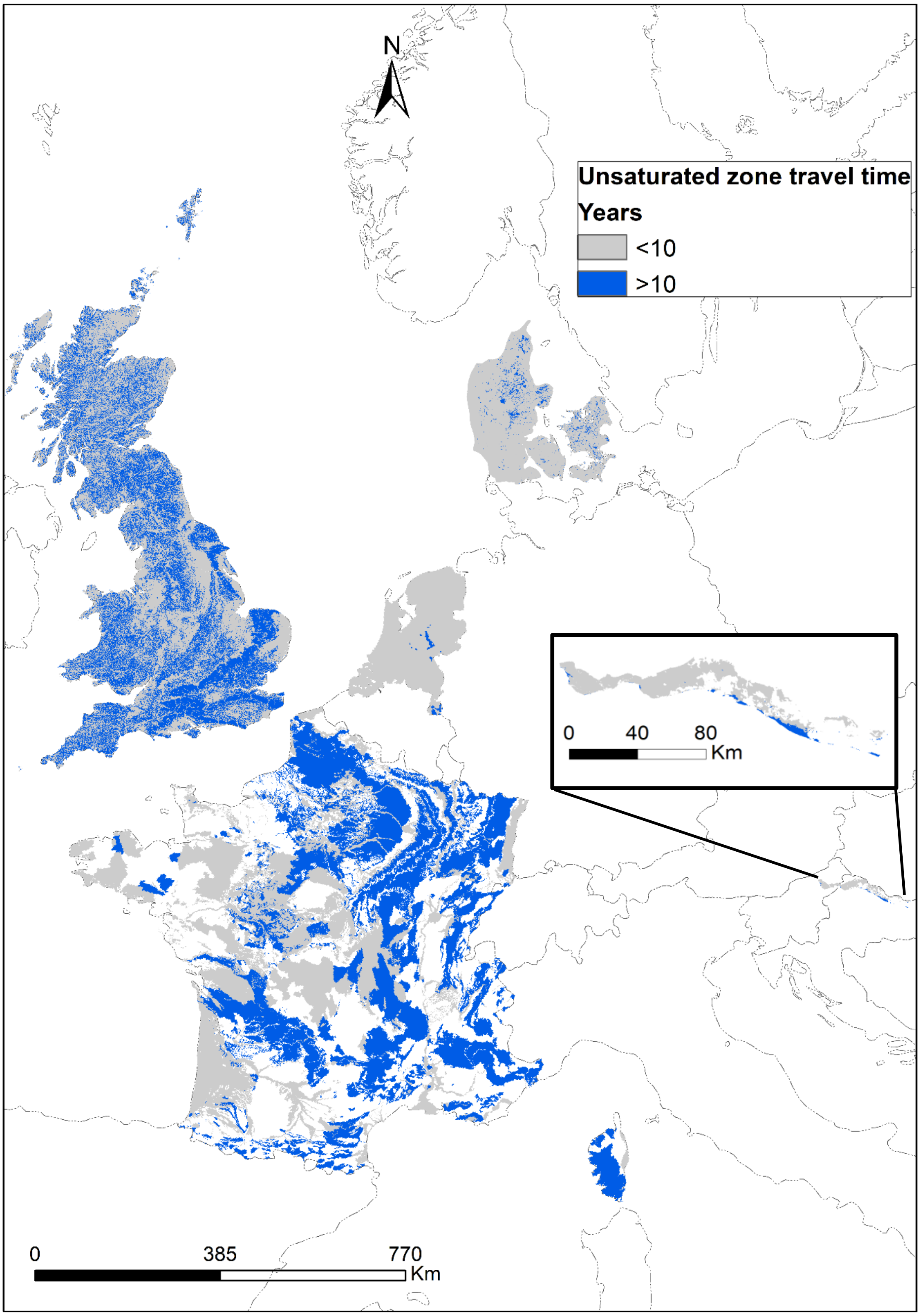

Figure 11.4 Areas where travel times for nitrate in the unsaturated zone are > or < 10 years across selected pilots in this deliverable

Table 11.2 % of area where unsaturated zone travel time > 10 years across selected pilots in this deliverable

Pilot	**% of area where unsaturated zone travel time > 10 years**
Great Britain (UK)	47.6
France	56
Denmark	5.5
Netherlands	2.3
Drava (Slovenia)	1.5
Drava (Croatia)	9.2
Overall	45.6

11.4 Implications for management of nitrate and pesticide transport

The pilots reported in this deliverable have shown significant travel times for nitrate from the base of the soil zone to receptors (abstraction wells, groundwater dependent streams and terrestrial ecosystems), either in the unsaturated zone, the saturated zone or both. These travel times have significant implications for management of nitrate pollution. In Europe, the Water Framework Directive (European Union, 2000) has been implemented as a supra-national policy directive obliging member states to achieve “good” qualitative status for all groundwaters and surface waters. Status is measured relative to fixed thresholds (e.g. 11.3 mg NO3/L in drinking water), with reporting of status every six years and an initial deadline of achieving good status as 2015. It has been previously stated by the European Environmental Bureau that travel times for nitrate are a “generic excuse” to escape more stringent policy measures to reduce nitrate loadings (Vero et al., 2018). However, the pilots in this deliverable show that this is not the case and that there are significant time lags between nitrate losses at the base of the soil zone and receptors. These time lags have been shown to be up to the order of decades, substantially longer than timescales for WFD status reporting. Consequently, the evidence presented here supports previous assertions (Vero et al., 2018) that trend (rather than threshold)-based, multidecadal scale monitoring and evaluation of the impacts of measures to reduce nitrate concentrations at receptors are required.

Whilst the pilots all show significant time lags, the variability of where in the hydrogeological system (unsaturated zone, saturated zone or both) these time lags occur and resulting differences in modelling approaches has significant implications for the management of nitrate pollution. Evaluations of measures put in place to reduce nitrate and pesticide concentrations in groundwater and surface water receptors under directives such as the WFD should take into consideration this diversity of hydrogeological settings. For example, if considering groundwater at the water table as a receptor, measures put in place to reduce nitrate losses from soils in parts of the UK and France where the water table is deep are likely to take longer to impact groundwater than in areas with shallow water tables in the Netherlands and Denmark. In contrast, travel times in the saturated zone may be relatively more significant when considering receptors such as streams or long-screened abstraction boreholes receiving groundwater from an aquifer with a shallow water table (e.g Netherlands). As a consequence of this diversity of hydrogeological settings, application of any “one-size-fits-all” approach to evaluation of impacts of measures is unlikely to be successful.

The models reported in this deliverable cover a wide range of scales including field, regional, national, and continental scale approaches. Evaluation across the pilots provides some insight into the utility of the different scales of modelling for managing nitrate pollution. Continental scale modelling of nitrate stored in the unsaturated zone is beneficial to highlight the potential significance of the legacy nitrate, and as a high level screening tool to identify large areas (country scale or greater) which may be affected. However, such tools cannot be used for management of nitrate pollution at the national or regional scale without significant refinement (Turkeltaub et al., 2020). Modelling approaches used in the national scale pilots (UK, France, Netherlands, Denmark) have been used for decision support, setting stakeholder expectations and regulatory reporting under the WFD. These models have been shown to be effective in delineating overarching patterns of nitrate travel times, but regional analysis in the Netherlands has shown models to fail to capture detailed local travel time distributions to short screened wells. Whilst challenging to apply directly at large scales, modelling at the field scale (PLAP, Denmark) provides insight into local processes (e.g. preferential flow, fluctuating water table dynamics) that should be taken into consideration when evaluating national and regional scale modelling approaches.

11.5 Outlook for further work

This deliverable has reported approaches to modelling nitrate and pesticide transport across different partners in HOVER WP5. A number of the datasets synthesised here will be uploaded to the EGDI:

1. Conceptual models of nitrate transport (from deliverable D5.1)
2. Maps of nitrate travel times in the unsaturated zone (as reported in section 11.3 of this report)
3. Maps of nitrate stored in the unsaturated zone at the continental scale (as reported in section 2 of this report)

Future HOVER WP5 deliverables will consider approaches mapping denitrification potential across different partners (D5.4), before summarising all the maps and data products of nitrate time lags and attenuation processes in D5.5.

REFERENCES

Addiscott, TM 2005. Nitrate, Agriculture and the Environment. CAB International: Wallingford; 279.

Addiscott, TM, Whitmore, AP, Powlson, DS 1991. Farming, Fertilizers and the Nitrate Problem. CAB International: Wallingford; 170.

Albers, C.N., Ernstsen, V., Johnsen, A.R. 2019. Soil Domain and Liquid Manure Affect Pesticide Sorption in Macroporous Clay Till. J Environ Qual. 48(1): 147-155. Doi: 10.2134/jeq2018.06.0222. PMID: 30640346.

Allen, D.J., Brewerton, L.J., Coleby, L.M., Gibbs, B.R., Lewis, M.A., MacDonald, A.M., Wagstaff, S.J., Williams, A.T., 1997. The physical properties of major aquifers in England and Wales, British Geological Survey Technical Report WD/97/34, Environment Agency R&D Publication 8.

Amundson, R., Austin, A. T., Schuur, E. A. G., Yoo, K., Matzek, V., Kendall, C., Uebersax, A., Brenner, D. and Baisden,W. T. 2003. Global patterns of the isotopic composition of soil and plant nitrogen. . Global Biogeochemical Cycles, Vol. 17, Article no. 1031

Anglade, J., Billen, G., Garnier, J., 2015. Relationships for estimating N2 fixation in legumes: incidence for N balance of legume-based cropping systems in Europe. Ecosphere 6(3), 1-24

Anthony, S., Quinn, P. and Lord, E., 1996. Catchment scale modelling of nitrate leaching. Aspects of Applied Biology 46: 23–32.

Aravena, R., Evans,M. L. and Cherry, J. A. 1993. Stable isotopes of oxygen and nitrogen in source identification of nitrate from septic systems. Ground Water, Vol. 31, 2, 180-186.

Arnaud L., Baran N., Branellec M. et al. 2009. Détermination des vitesses de transfert de l’eau et des nitrates dans la zone non saturée de l’aquifère crayeux en Haute-Normandie. BRGM

Arso, 2008. Kakovost podzemne vode v Sloveniji v letih 2007 in 2008. Ministry of environment and spatial planning of Republic of Slovenia, Ljubljana.

Arso, 2018. Ministry of environment and spatial planning of Republic of Slovenia. Found online (30.03.2020): https://meteo.arso.gov.si/uploads/probase/www/hidro/watercycle/text/sl/projects/mGROWA-SI/Prezentacija_mGROWA_201801a.pdf

Arso, 2019. Ministry of environment and spatial planning of Republic of Slovenia. Found online (30.09.2020): https://www.arso.gov.si/vode/podatki/arhiv/kakovost_arhiv2019.html

Ascott, M.J., 2018. Gridded model estimates of nitrate-N stored in the vadose (unsaturated) zone at the global scale from 1900 to 2000, British Geological Survey.

Ascott, M.J., Gooddy, D.C., Wang, L., Stuart, M.E., Lewis, M.A., Ward, R.S., Binley, A.M., 2017. Global patterns of nitrate storage in the vadose zone. Nat. Commun., 8(1): 1416. DOI:10.1038/s41467-017-01321-w

Ascott, M.J., Wang, L., Stuart, M.E., Ward, R.S., Hart, A., 2016. Quantification of nitrate storage in the vadose (unsaturated) zone: a missing component of terrestrial N budgets. Hydrol. Processes, 30(12): 1903-1915. DOI:10.1002/hyp.10748

Ascott, M.J., Ward, R.S., 2018. Written evidence submitted by the British Geological Survey. http://data.parliament.uk/writtenevidence/committeeevidence.svc/evidencedocument/environmental-audit-committee/nitrate/written/77020.html

ATIGA. 1972. Wastes disposal and water supply project in Malta. UNDP.

Auterive, C., Baran, N., 2017. Méthode appliquée à l'échelle nationale pour l'étude pression-impact des substances phytosanitaires sur les eaux souterraines. Rapport final., p. 97, BRGM.

Aziz, C.E., Newell, C.J., Gonzales, J.R., Haas, P., Prabhakar Clement, T. & Yunwei Sun, 2000. BIOCHLOR: Natural Attenuation Decision Support System; User's manual, version 1.0. EPA/600/R-00/008, U.S. Environmental Protection Agency, Office of Research and Development, 46 p., Washington, D.C.

Babić, Ž., Čakarun, I., Sokač, A. & Mraz, V. 1978. On geological features of quaternary sediments of Drava basin on Croatian territory. Geol. vjesnik, 30/1, 43-61

Badawi, N., Johnsen, A.R., Sørensen, J., Aamand, J. 2013. Centimeter-Scale Spatial Variability in 2-Methyl-4-Chlorophenoxyacetic Acid Mineralization Increases with Depth in Agricultural Soil. J Environ Qual. 42(3): 683-689. https://doi.org/10.2134/jeq2012.0397

Badawi, N., Rosenbom, A.E., Jensen, A.M.D., Sørensen, S.R. 2016. Degradation and sorption of the fungicide tebuconazole in soils from golf greens. Environ Pollut. 219: 368-378. Doi: 10.1016/j.envpol.2016.10.045.

Baillon, K., Lacherez, S., Six, P., Caulier, P., Risbourg, D., Maillot, H., 2001. Gestion de la nappe de la craie dans le nord de la France. Premiers résultats sur le transfert des nitrates d'origine agricole dans le non saturé de l'arrondissement de Cambrai. Techniques Sciences Méthodes 4, 33-46.

Ballif, J. L., Muller, J. C., 1993. Historique cultural et profils d'azote minéral dans la zone non saturée de la craie : conséquences sur le transfert et le bilan de l'azote. Résultats de dix années d'observation. Cahiers Agricultures 2, 330-337.

Baran, N., Bourgeois, M., Fléhoc, C., Normand. B., 2005. Détermination de la vitesse de transfert de l'eau, des nitrates et autres solutés en zone non saturée dans un loess profond. BRGM.

Baran, N., Chabart, M., 2006. Détermination de la vitesse de transfert des nitrates en zone crayeuse sur deux bassins versants à enjeux : La Retourne (08) et la Superbe (51). – Rapport final. BRGM

Barlebo, H.C., Rosenbom, A.E., Kjær, J. 2007. Evaluation of Pesticide Scenarios for the Registration Procedure. Environmental Project No. 1178. https://www2.mst.dk/Udgiv/publications/2007/978-87-7052-540-4/html/default_eng.htm

Barraclough, D. Gardner, CMK, Wellings, SR, Cooper, JD 1994. A tracer investigation into the importance of fissure flow in the unsaturated zone of the British Upper Chalk. Journal of Hydrology 156: 459469

Batu, V. 2006. Applied Flow and Solute Transport Modeling in Aquifers. Taylor & Francis, 667 p., New York.

Bear, J. 1972. Dynamics of Fluids in Porous Media. American Elsevier, 784 p., New York.

Bedekar, V., Morway, E.D., Langevin, C.D., and Tonkin, M. 2016. MT3D-USGS version 1: A U.S. Geological Survey release of MT3DMS updated with new and expanded transport capabilities for use with MODFLOW: U.S. Geological Survey Techniques and Methods 6-A53, 69 p., http://dx.doi.org/10.3133/tm6A53

Bedekar, V., Morway, E.D., Langevin, C.D., and Tonkin, M. 2016. MT3D-USGS version 1.0.0: Groundwater Solute Transport Simulator for MODFLOW: U.S. Geological Survey Software Release, 30 September 2016, http://dx.doi.org/10.5066/F75T3HKD

Beusen, A.H.W., Van Beek, L.P.H., Bouwman, A.F., Mogollón, J.M., Middelburg, J.J., 2015. Coupling global models for hydrology and nutrient loading to simulate nitrogen and phosphorus retention in surface water – description of IMAGE-GNM and analysis of performance. Geosci. Model Dev. Discuss., 8(9): 7477-7539. DOI:10.5194/gmdd-8-7477-2015

Blicher-Mathiesen, G., J. Windolf, S. E. Larsen, J. Rolighed, M. V. Carstensen, A. L. Højberg, H. Tornbjerg, and B. Kronvang. 2020. "The Effect of Nitrogen Mitigation Measures Evaluated by Monitoring of Nitrogen Concentrations and Loadings in Danish Mini-Catchments - 1990-2015." Water Science and Technology: Water Supply 20 (2): 586–93. https://doi.org/10.2166/ws.2020.002.

Bloomfield, JP, Brewerton, LJ, Allen, DJ 1995. Regional trends in matrix porosity and dry density of the Chalk of England, Quarterly Journal of Engineering Geology 28: S131-S142.

Bøgestrand, J., Kristensen, P. and Kronvang, B., 2005. Source Apportionment of Nitrogen and Phosphorus Inputs into the Aquatic Environment. European Environment Agency, Copenhagen.

Böhlke J-K (2002) Groundwater recharge and agricultural contamination. Hydrogeol J 10:153–179.

Boorman, D.B., Hollist, J.M., Lilly, A., 1995. Hydrology of soil types: a hydrologically based classification of the soils of the United Kingdom. Institute of Hydrology, Report No. 126, Oxford, UK.

Bouwman, L., Goldewijk, K.K., Van Der Hoek, K.W., Beusen, A.H.W., Van Vuuren, D.P., Willems, J., Rufino, M.C., Stehfest, E., 2013. Exploring global changes in nitrogen and phosphorus cycles in agriculture induced by livestock production over the 1900–2050 period. Proceedings of the National Academy of Sciences, 110(52): 20882-20887. DOI:10.1073/pnas.1012878108

Brenčič, M. 2002. Presoja sprememb gladine podzemne vode na območju Ptujskega polja. Geological Survey of Slovenia, Ljubljana.

Brilly, M. 1994. Model podtalnice Vrbanskega platoja In: Sanacija kvalitete podtalne vode na Vrbanskem platoju – novelacija varstvenih pasov. Inštitut za geologijo, geotehniko in geofiziko, Ljubljana.

Brkić, Ž. 1999. Alluvial aquifer recharge through semipermeable covering deposits in northern Croatia. PhD thesis (in Croatian), University of Zagreb, 157 p.

Brkić, Ž., Kuhta, M., Larva, O. & Marković, T. 2019. Groundwater age dating as a tool for nitrogen pollution risk assessment in Croatia. 6th Croatian Geological Congress. Abstracts Book / Horvat, Marija ; Matoš, Bojan ; Wacha, Lara (eds). Zagreb.

Broers, H. P., & Vliet, M. V. 2018b. Tritium-based Travel Time Distributions and Nitrate Forecasts in Dutch Chalk Springs. AGUFM, 2018, H11G-08.

Broers, H.P. & B. van der Grift 2004. Regional monitoring of temporal changes in groundwater quality. Journal of Hydrology 296:192-220

Broers, H.P. 2004. The spatial distribution of groundwater age for different geohydrological situations in The Netherlands: implications for groundwater quality monitoring at the regional scale. Journal of Hydrology 299: 84-106

Broers, H.P., van Vliet, M.E. 2018a. Dateringsonderzoek bronnen en bronbeken Zuid-Limburg. Prognose van de nitraatconcentraties in Limburgse bronnen voor het KRW-jaar 2027. TNO-rapport R10421

Bureau de Recherche Géologique et Minière (BRGM). 1991. Study of the fresh-water resources of Malta. Government of Malta.

Campbell, E. and Foy, B., 2008. Lough Melvin Catchment Management Plan. INTERREG Programme. Fisheries Ireland. Available online: https://www.fisheriesireland. ie/documents/49-lough-melvin-cachmentmanagement-plan-executive-summary-1/file.html (accessed 20 April 2018).

Caous, .J.Y.; Comon, D., Seguin, J-J., 1984. Agence de l'eau Artois Picardie. Evolution des teneurs en nitrates de la nappe de la craie : essai de prévision. BRGM.

Cerar, S., Mezga, K., Žibret, G., Urbanc, J. 2016: Vsebnost nitrata v podzemni vodi v Sloveniji = Nitrate concentrations in Slovenian groundwater. Geological Survey of Slovenia.

Chilton, PJ, Foster, SS. 1991. Control of groundwater nitrate contamination pollution by land-use change. In Nitrate Contamination: Exposure, Consequence and Control. NATC ASI Series Vol G30, Bogardi, I, Kuzelka, RD, Ennenga, WG (eds). New York, Springer-Verlag; 333�347.

Costa, J.L., Massone, H., Martínez, D., Suero, E.E., Vidal, C.M., Bedmar, F., 2002. Nitrate contamination of a rural aquifer and accumulation in the unsaturated zone. Agricultural Water Management, 57(1): 33-47. DOI:https://doi.org/10.1016/S0378-3774(02)00036-7

Crampon, N., Roux, J.C, Bracq, P. 1993. Hydrogéologie de la craie en France. Hydrogéologie 2, 81-123

Daly, D., Deakin, J., Craig, M., Mannix, A., Archbold, M. and Mockler, E., 2016. Progress in implementation of the Water Framework Directive in Ireland. Proceedings of International Association of Hydrogeologists (Irish Group) Conference “Sustaining Ireland’s Water Future: The Role of Groundwater”, Tullamore. Available online: http://hdl.handle.net/10197/7910

De Lange, W. J., Prinsen, G. F., Hoogewoud, J. C., Veldhuizen, A. A., Verkaik, J., Essink, G. H. O., ... & Kroon, T. 2014. An operational, multi-scale, multi-model system for consensus-based, integrated water management and policy analysis: The Netherlands Hydrological Instrument. Environmental Modelling & Software, 59, 98-108.

del Prado, A., Brown, L., Schulte, R., Ryan, M. and Scholefield, D., 2006. Principles of development of a mass balance N cycle model for temperate grasslands: an Irish case study. Nutrient Cycling in Agroecosystems 74: 115–131. Available online: http:// dx.doi.org/10.1007/s10705–005–5769-z

Delsman et al. 2020a. Presentation NHI. https://edepot.wur.nl/515003

Delsman, J. et al. 2020b. Actualisatie zout in het NHI. Toolbox NHI zoet-zout modellering en landelijk model. Deltares rapport 11205261-003-BGS-0001.

Doherty, J. 2015. Calibration and Uncertainty Analysis for Complex Environmental Models. Watermark Numerical Computing, Brisbane, Australia. ISBN: 978-0-9943786-0-6. http://docs.pesthomepage.org.s3.amazonaws.com/documents/pest_book_toc.pdf

Dunn, S.M., Vinten, A.J.A., Lilly, A., DeGroote, J., Sutton, M.A. and McGechan, M., 2004. Nitrogen risk assessment model for Scotland: I. Nitrogen leaching. Hydrology and Earth System Sciences 8: 191–204. Available online: http://dx.doi.org/10.5194/ hess-8-191-2004

E.M. Mockler, J. Deakin, M. Archbold, D. Daly, M. Bruen. Nutrient load apportionment to support the identification of appropriate water framework directive measures. Biology and Environment, 116B (3) (2016), pp. 245-263, 10.3318/bioe.2016.22

Engesgaard, P. 1996. "Simulation of Subsurface Transport of Environmental Tritium". Water Resources Research, 32 (11): 3253–66.

Engesgaard, P. and Molson, J. 1998. Direct simulation of groundwater age in the Rabis Creek, Denmark. Groundwater, 36, 577-582.

Engesgaard, P., A.L. Højberg, K. Hinsby, K.H. Jensen, T. Laier, F. Larsen, E. Busenberg, and L. Niel Plummer. 2004. "Transport and Time Lag of Chlorofluorocarbon Gases in the Unsaturated Zone, Rabis Creek, Denmark." Vadose Zone Journal 3 (4).

Environment Agency, 2007. Making Information Available for Integrated Catchment Management, Science Report – SC060035/SR2007, Bristol, UK, pp. 114p.

Ernstsen, V., Olsen, P., Rosenbom, A.E. 2015. Long-term monitoring of nitrate transport to drainage from three agricultural clayey till fields. Hydrol. Earth Syst. Sci. 19: 3475–3488. www.hydrol-earth-syst-sci.net/19/3475/2015/ https://doi:10.5194/hess-19-3475-2015.

European Environment Agency, 2015. Waterbase - Groundwater. https://www.eea.europa.eu/data-and-maps/data/waterbase-groundwater-6

European Union, 2000. Directive 2000/60/EC of the European Parliament and of the Council establishing a framework for the Community action in the field of water policy. European Union, Brussels.

Eva M. Mockler, Jenny Deakin, Marie Archbold, Laurence Gill, Donal Daly, Michael Bruen. Sources of nitrogen and phosphorus emissions to Irish rivers and coastal waters: Estimates from a nutrient load apportionment framework. Science of The Total Environment. Volumes 601–602, 1 December 2017, Pages 326-339. https://doi.org/10.1016/j.scitotenv.2017.05.186

Fan, Y., Li, H., Miguez-Macho, G., 2013. Global Patterns of Groundwater Table Depth. Science, 339(6122): 940-943. DOI:10.1126/science.1229881

FAO 2006, Malta Water Resources Review. Rome.

Fenton, O., Schulte, R.P.O., Jordan, P., Lalor, S.T.J., Richards, K.G., 2011. Time lag: a methodology for the estimation of vertical and horizontal travel and flushing timescales to nitrate threshold concentrations in Irish aquifers. Environ. Sci. Policy, 14(4): 419-431. DOI:http://dx.doi.org/10.1016/j.envsci.2011.03.006

FOCUS 2000. FOCUS Groundwater Scenarios in the EU Review of Active Substances, Report of the FOCUS Groundwater Scenarios Workgroup. EC Document Reference Sanco/321/2000 rev.2, p. 202.

Foster, S.S.D., Cripps, A.C., Smith-Carington, A., 1982. Nitrate Leaching to Groundwater. Philos. Trans. R. Soc., B, 296(1082): 477-489. DOI:10.1098/rstb.1982.0021

Geake, AK, Foster, SSD. 1989. Sequential isotope and solute profiling in the unsaturated zone of British Chalk. Hydrological Sciences Journal 34: 7995.AS 2003

Gehrels, J.C. 1999. Groundwater level fluctuations; separation of natural from anthropogenic influences and determination of groundwater recharge in the Veluwe area, the Netherlands. Doctoral Thesis Vrije Universiteit Amsterdam.

GEUS, 2020. Map viewer of nitrate distribution in Danish groundwater monitoring wells. nitrate map viewer - accessed 01-12-2020.

Gill, L.W. & Mockler, E.M. (2016) Modeling the pathways and attenuation of nutrients from domestic wastewater treatment systems at a catchment scale. Environmental Modelling & Software 84 363-377. http://dx.doi.org/10.1016/j.envsoft.2016.07.006

Gjetvaj, G. 1990. Identification of dispersivity parameters in radial flow. Proceedings of the 10th Conference of the Yugoslav Society for Hydraulic Research, 436-440, Sarajevo.

Gleeson, T., Moosdorf, N., Hartmann, J., van Beek, L.P.H., 2014. A glimpse beneath earth's surface: GLobal HYdrogeology MaPS (GLHYMPS) of permeability and porosity. Geophys. Res. Lett., 41(11): 2014GL059856. DOI:10.1002/2014GL059856

Gleeson, T., Smith, L., Moosdorf, N., Hartmann, J., Dürr, H.H., Manning, A.H., van Beek, L.P.H., Jellinek, A.M., 2011. Mapping permeability over the surface of the Earth. Geophys. Res. Lett., 38(2). DOI:10.1029/2010GL045565

Gonod, L.V., Chadoeuf, J., Chenu, C. (2006). Spatial distribution of microbial 2,4-dichlorophenoxy acetic acid mineralization from field to microhabitat scales. Soil Sci. Soc. Am. J. 70: 64–71. doi: https://doi-org.ep.fjernadgang.kb.dk/10.2136/sssaj2004.0034

Goode, D. J. (1996). Direct simulation of groundwater age. Water Resources Research, 32(2), 289-296.

Gourcy, L., Pinson, S. and Surdyk, N., 2017. Description de la méthode appliquée à l'échellenationale pour l'analyse pression–impact du nitrate sur les eaux souterraines, p. 106, BRGM.

Government of Ireland, 2014. Statutory Instruments – Eurpoean Union (Good Agricultural Practice for the Protection of Waters) Regulations 2014. S.I. 31 of 2014. Government of Ireland, Dublin.

Government of Malta 2005, Initial Characterisation of Groundwater Bodies in the Maltese River Basin District.

Government of Malta 2015 The 2nd Water Catchment Management Plan for the Malta Water Catchment District 2015-2021.

Greene, S., Taylor, D., McElarney, Y.R., Foy, R.H. and Jordan, P., 2011. An evaluation of catchment-scale phosphorus mitigation using load apportionment modelling. Science of the Total Environment 409: 2211–2221. Available online: http://dx.doi. org/10.1016/j.scitotenv.2011.02.016

Griffiths KJ, MacDonald AM, Robins NS, Merritt J, Booth SJ, Johnson D and McConvey PJ, 2010. Improving the characterisation of Quaternary deposits for groundwater vulnerability assessments using maps of recharge and attenuation potential. Quarterly Journal of Engineering Geology and Hydrogeology, 43: 1-14

Grizzetti, B., Bouraoui, F. and Aloe, A., 2012. Changes of nitrogen and phosphorus loads to European seas. Global Change Biology 18: 769–782. Available online: http://dx.doi.org/10.1111/j.1365–2486.2011.02576.x

Grizzetti, B., Bouraoui, F., de Marsily, G. and Bidoglio, G., 2005. A statistical method for source apportionment of riverine nitrogen loads. Journal of Hydrology 304: 302–315. Available online: http://dx.doi.org/10.1016/j. jhydrol.2004.07.036

Gvirtzman, H., Magaritz, M., 1986. Investigation of Water Movement in the Unsaturated Zone Under an Irrigated Area Using Environmental Tritium. Water Resour. Res., 22(5): 635-642. DOI:10.1029/WR022i005p00635

Handley, L. L., Austin, A. T., Robinson, D., Scrimgeour, C.M., Raven, J. A., Heaton, T. H. E.,Schmidt, S. and Stewart, G. R. 1999. The 15N natural abundance (δ15N) of ecosystem samples reflects measures of water availability. Australian Journal of Plant Physiology, Vol. 26, 185-199.

Hansen, B., Thorling, L., Dalgaard, T., & Erlandsen, M. (2010). Trend reversal of nitrate in Danish groundwater-A reflection of agricultural practices and nitrogen surpluses since 1950. Environmental science & technology, 45(1), 228-234.

Hansen, Birgitte, Lærke Thorling, Hyojin Kim, and Gitte Blicher-Mathiesen. 2019. “Long-Term Nitrate Response in Shallow Groundwater to Agricultural N Regulations in Denmark.” Journal of Environmental Management 240 (February): 66–74. https://doi.org/10.1016/j.jenvman.2019.03.075.

Hansen, Birgitte, Lærke Thorling, Jörg Schullehner, Mette Termansen, and Tommy Dalgaard. 2017. “Groundwater Nitrate Response to Sustainable Nitrogen Management.” Scientific Reports 7 (1): 1–12. https://doi.org/10.1038/s41598-017-07147-2.

Hansen, S., Abrahamsen, P., and Petersen, C. 2010a. Daisy 2d simulation of silstrup and estrup, Report, University of Copenhagen.

Hansen, S., Abrahamsen, P., Petersen, C. T., and Styczen, M. 2012. Daisy: Model use, calibration, and validation, Transactions of the Asabe, 55, 1315–1333, URL ://WOS: 000309089900017.

Hansen, S., Petersen, C., Abrahamsen, P., Nielsen, M., and Mollerup, M. 2010b. Daisy 2d simulation of rørrendegård, Technical report, University of Copenhagen.

Harbaugh, A.W. 2005. MODFLOW-2005, the U.S. Geological Survey modular ground-water model -- the Ground-Water Flow Process: U.S. Geological Survey Techniques and Methods 6-A16.

Harbaugh, A.W., Langevin, C.D., Hughes, J.D., Niswonger, R.N., and Konikow, L. F. 2017. MODFLOW-2005 version 1.12.00, the U.S. Geological Survey modular groundwater model: U.S. Geological Survey Software Release, 03 February 2017, http://dx.doi.org/10.5066/F7RF5S7G

Heaton, T. H. E. 1986. Nitrate pollution of groundwater. South African Journal of Science, Vol. 82,6, 279.

Heaton, T. H. E., Spiro, B. and Robertson, S.M. C. 1997. Potential canopy influences on the isotopic composition of nitrogen and sulphur in atmospheric deposition. Oecologia, Vol. 109, 600-607.

Heaton, T. H. E., Wynn, P. and Tye, A. 2004. Low 15N/14N ratios for nitrate in snow in the High Arctic (79°N). . Atmospheric Environment, Vol. 38, 5611-5621.

Henriksen HJ, Troldborg L, Højberg AL, Refsgaard JC, 2008. Assessment of exploitable groundwater resources of Denmark by use of ensemble resource indicators and a numerical groundwater–surface water model. Journal of Hydrology, 348, 224-240

Henriksen HJ, Troldborg L, Nyegaard P, Sonnenborg TO, Refsgaard JC, Madsen B., 2003. Methodology for construction, calibration and validation of a national hydrological model for Denmark. Journal of Hydrology, 280(1-4), 52-71

Henriksen, HJ, Voutchkova, D., Troldborg, L., Ondracek, M., Schullehner, J., and Hansen, B. National Water Resources Model - estimation of degree of exploitation, decline of water tables and impacts on runnoff with DK-Model 2019. GEUS report 2019/31, In Danish.

Hill, M.C. 2006. The practical use of simplicity in developing ground water models. Ground Water, 44, 775-781.https://doi.org/10.1016/j.envpol.2015.03.002.

Hinsby, K., Markager, S., Kronvang, B., Windolf, J., Sonnenborg, T. O., & Thorling, L. (2012). Threshold values and management options for nutrients in a catchment of a temperate estuary with poor ecological status. Hydrology and Earth System Sciences, 16(8), 2663–2683. https://doi.org/10.5194/hess-16-2663-2012

Hinsby, K., Markager, S., Kronvang, B., Windolf, J., Sonnenborg, T. O., & Thorling, L., 2012. Threshold values and management options for nutrients in a catchment of a temperate estuary with poor ecological status. Hydrology and Earth System Sciences, 16(8), 2663–2683.

Hinsby, Klaus, M. Teresa Condesso de Melo, and Mette Dahl. 2008. "European Case Studies Supporting the Derivation of Natural Background Levels and Groundwater Threshold Values for the Protection of Dependent Ecosystems and Human Health." Science of the Total Environment 401 (1–3): 1–20.https://doi.org/10.5194/hess-16-2663-2012

Højberg AL, Troldborg L, Stisen S, Christensen BSB, Henriksen HJ, 2013. Stakeholder driven update and improvement of a national water resources model. Environmental Modelling & Software 40, 202-213.

Højberg, A.L., Windolf, J., Børgesen, C.D., Troldborg, L., Tornbjerg, H., Blicher-Mathiasen, G., Kronvang, B., Thodsen, H., Ernstsen, V., 2015. National kvælstofmodel - Oplandsmodel til belastning og virkemidler. Metode rapport, revideret udgave september 2015 (National nitrogenmodel - Catchment model for load and measures. Method report, revised version September 2015). In: Report from Geological Survey of Denmark and Greenland and Aarhus University, ISBN 978-87-7871-418-3.

Højberg, A.L., Windolf, J., Børgesen, C.D., Troldborg, L., Tornbjerg, H., Blicher-Mathiasen, G., Kronvang, B., Thodsen, H., Ernstsen, V., 2015. National nitrogenmodel - Catchment model for load and measures. Method report, revised version September 2015. Report from Geological Survey of Denmark and Greenland and Aarhus University, ISBN 978-87-7871-418-3, 111 pp., In Danish.

Højberg, Anker Lajer, Anne Lausten Hansen, Przemysław Wachniew, Anna J. Żurek, Seija Virtanen, Jurga Arustiene, Johan Strömqvist, Katri Rankinen, and Jens Christian Refsgaard. 2017. “Review and Assessment of Nitrate Reduction in Groundwater in the Baltic Sea Basin.” Journal of Hydrology: Regional Studies 12 (December 2016): 50–68. https://doi.org/10.1016/j.ejrh.2017.04.001.

Hunter Williams, N.H., Misstear, B.D.R., Daly, D. and Lee, M., 2013. Development of a national groundwater recharge map for the Republic of Ireland. Quarterly Journal of Engineering Geology and Hydrogeology 46: 493–506. Available online: http://dx.doi.org/10.1144/ qjegh2012–016

Jakobsen, Rasmus, Anne Lausten Hansen, Klaus Hinsby, Dieke Postma, and Jens Christian Refsgaard. 2019. “Reactive Nitrogen in a Clay till Hill Slope Field System.” Ambio 48 (11): 1240–51. https://doi.org/10.1007/s13280-019-01228-4.

Jauffret, D., Seguin, J.J., Panel, R., Hole, J.P. 1984. Prévision de l’évolution des teneurs en nitrates de la nappe de la craie dans les régions de grandes cultures du département de l’Eure. BRGM

Johnsen, A.R, Albers, C., Rosenbom, A.E., Ernstsen, V., Haarder, E.B. 2020. TRANSPORER Sorberende pesticiders mobilisering, tilbageholdelse og transport i makroporer. Miljø- og Fødevareministeriet, Miljøstyrelsen, Bekæmpelsesmiddelforskning nr. 187 pp. 120. ISBN: 978-87-7038-187-1 (In Danish).

Johnston, C.T., Cook, P.G., Frape, S.K., Plummer, L.N., Busenberg, E., Blackport, R.J., 1998. Ground Water Age and Nitrate Distribution Within a Glacial Aquifer Beneath a Thick Unsaturated Zone. Groundwater, 36(1): 171-180. DOI:10.1111/j.1745-6584.1998.tb01078.x

Johnston, C.T., Cook, P.G., Frape, S.K., Plummer, L.N., Busenberg, E., Blackport, R.J., 1998. Ground Water Age and Nitrate Distribution Within a Glacial Aquifer Beneath a Thick Unsaturated Zone. Groundwater, 36(1): 171-180. DOI:10.1111/j.1745-6584.1998.tb01078.x

Karan, S., Badawi, B., Jensen, A.M.D., Rosenbom, A.E. (2020). Impact of fate properties, groundwater fluctuations and the presence of worm burrows on pesticide leaching assessments. (Under review)

Karlović, I., Marković, T. & Larva, O. 2019. Developing a Conceptual Model for Groundwater Flow and Transport Model of Nitrate in the Varaždin Alluvial Aquifer. 6th Croatian Geological Congress. Abstracts Book / Horvat, Marija ; Matoš, Bojan ; Wacha, Lara (eds). Zagreb.

Kendall, C. 1998. Tracing nitrogen sources and cycling in catchments. 519-576 in Isotope Tracers in Catchment Hydrology. Kendall, C. and McDonnell, J. J. (editor). (Amsterdam: Elsevier Science B.V.)

Kerbaul, A., Morfaux, P., Landreau, A. L'épandage d'effluents sur terrain agricole. - Effets sur la zone non saturée de la craie en Champagne. BRGM

Kim, Hyojin, Anne Sophie Høyer, Rasmus Jakobsen, Lærke Thorling, Jens Aamand, Pradip Kumar Maurya, Anders Vest Christiansen, and Birgitte Hansen. 2019. "3D Characterization of the Subsurface Redox Architecture in Complex Geological Settings." Science of the Total Environment 693. https://doi.org/10.1016/j.scitotenv.2019.133583.

Kim, Y. J., Choi W. J., Lim, S. S., Kwak J.H., Chang S.X., Kim H.Y., K.S., Y. and Ro, H.M. 2008. Changes in nitrogen isotopic compositions during composting of cattle feedlot animal waste: effects of bedding material type. Bioresource Technology, Vol. 99, 13, 5452-5458.

Kinniburgh, D.G., Gale, I.N., Gooddy, D.C., Darling W.G., Marks R.J., Gibbs B.R., Coleby L.M, Bird M.J., West J.M, 1994. Denitrification in the unsaturated zones of the British Chalk and Sherwood Sandstone aquifers, British Geological Survey, Keyworth, UK.

Kivits, T. H.P. Broers, Mariëlle van Vliet 2019. Dateren grondwater van het Provinciaal Meetnet Grondwaterkwaliteit Noord-Brabant. Inzicht in de toestand en trends van 12 indicatoren van de grondwaterkwaliteit. Rapport TNO 2019 R11094, TNO, Utrecht.

Kivits, T., Broers, H.P., Beeltje, H., van Vliet, M., Griffioen, J. 2018. Presence and fate of veterinary antibiotics in age-dated groundwater in areas with intensive livestock farming. Environmental Pollution, 241: 988-998.

Koch, Julian, Simon Stisen, Jens C. Refsgaard, Vibeke Ernstsen, Peter R. Jakobsen, and Anker L. Højberg. 2019. "Modeling Depth of the Redox Interface at High Resolution at National Scale Using Random Forest and Residual Gaussian Simulation." Water Resources Research 55 (2): 1451–69. https://doi.org/10.1029/2018WR023939.

Koroša, A. 2019. Origin and transport of organic pollutants in intergranular aquifers. Ph. D. Thesis. University of Ljubljana, Faculty of Civil and Geodetic Engineering: f. 207.

Koroša, A., Brenčič, M. & Mali, N. 2020. Estimating the transport parameters of propyphenazone, caffeine and carbamazepine by means of a tracer experiment in a coarse-gravel unsaturated zone. Water Research, 175: 1-12. doi: 10.1016/j.watres.2020.115680.

Koroša, A., Mali, N. 2015. Water and nitrate transport in an unsaturated zone. Case study: lysimeter Selniška dobrava, Slovenia. In: Bericht. Irdning: Höhere Bundeslehr- und Forschunganstalt für Landwirtschaft Raumberg-Gumpenstein, cop. 2015. Str. 33-38. Bericht (Höhere Bundeslehr- und Forschungsanstalt für Landwirtschaft Raumberg Gumpenstein).

Kurtzman, D., Shapira, R.H., Bar-Tal, A., Fine, P., Russo, D., 2013. Nitrate fluxes to groundwater under citrus orchards in a Mediterranean climate: Observations, calibrated models, simulations and agro-hydrological conclusions. J. Contam. Hydrol., 151: 93-104. DOI:https://doi.org/10.1016/j.jconhyd.2013.05.004

Lacherez-Bastin, S. 2005. Contribution à l'étude de la migration des nitrates dans le sol et la zone non saturée de la nappe de la craie dans le Nord de la France – Modélisation intégrée des nitrates dans le bassin versant de l'Escrebieux. Thèse à l'université des sciences et technologies de Lille. 191p.

Landreau, A., Morisot, A., 1983. Evaluation de la vulnérabilité des aquifères libres aux nitrates d'origine agricole. BRGM

Lapajne, V. Nekateri vidiki hidrološkega in kmetijskega stanja podzemne vode dravsko-ptujskega polja. Zavod za zdravstveno varstvo Maribor, Maribor.

Larsbo, M., Roulier, S., Stenemo, F., Kasteel, R., Jarvis, N 2005. An improved dual-permeability model of water flow and solute transport in the vadose zone Vadose Zone J. 4 (2) 398– 406.

Larva, O. 2008. Aquifer vulnerability at catchment area of Varaždin pumping sites. PhD thesis (in Croatian), University of Zagreb, 198 p.

Legout, C., Moléna,t J., Aquilina, L. et al. 2007. Solute transfer in the unsaturated zone-groundwater continuum of a headwater catchment. Journal of Hydrology 332, 421-441

Leonard, R.A., Knisel, W.G., 1988. Evaluating groundwater contamination potential from herbicide use. Weed Technology 2(2), 207–216.

Limousin, G. 2007. Transfert de solutés réactifs dans la zone non saturée des sols à différentes échelles d'observation. Thèse de doctorat de l'Université Joseph Fourier, Grenoble I., 194p.

Lin, B.-L., Sakoda, A., Shibasaki, R., Goto, N., Suzuki, M., 2000. Modelling a global biogeochemical nitrogen cycle in terrestrial ecosystems. Ecological Modelling, 135(1): 89-110.

Lord, E., Anthony, S., 2000. MAGPIE: A modelling framework for evaluating nitrate losses at national and catchment scales. Soil Use and Management 16, 167–174.

Lord, E.I., 1992. Modelling of nitrate leaching: Nitrate Sensitive Areas. Aspects of Applied Biology 30, 19-28.

Lord, EI, Johnson, PA, Archer, JR. 1999. Nitrate Sensitive Areas: a study of large scale control of nitrate loss in England. Soil Use and Management 15: 201�207.

Macdonald, D M J, et al. Review of the Hydrological and Hydrogeological Characteristics of the Maltese Islands - CT3069/2019 - Activity 1.2 Report. British Geological Survey, 2020.

MACRO. Hydrol. Earth Syst. Sci. 16, 2069e2083.

Mali, N. & Koroša, A. 2015. Assessment of nitrate transport in the unsaturated (coarse gravel) zone by means of tracing experiment (Selniška dobrava, Slovenia). Geologija, 58/2: 183-194.

Mali, N. 2006. Characterization of transport processes in the unsaturated zone of a gravel aquifer by natural and artificial tracers. – Univerza v Novi Gorici, Fakulteta za podiplomski študij, Doktorska naloga podiplomskega programa Znanosti o okolju, 96 pp, 24 app., Nova Gorica.

Mangion, J. and Sapiano. M. 2008, The Mean Sea Level Aquifer, Malta and Gozo. in Natural Groundwater Quality, Blackwell Publishing 400-420.

Marie Archbold, Jenny Deakin, Michael Bruen, Mesfin Desta, Ray Flynn, Mary Kelly- Quinn, Laurence Gill, Pamela Maher, Bruce Misstear, Eva Mockler, Ronan O'Brien, Alison Orr, Ian Packham and Joshua Thompson 2016. Research 165 - Contaminant Movement and Attenuation along Pathways from the Land Surface to Aquatic Receptors: the PATHWAYS Project. Environmental Protection Agency Research report, Wexford, Ireland. https://www.epa.ie/researchandeducation/research/researchpublications/researchreports/research report165.html

Marković, T. 2007. Vulnerability assessment of unsaturated zone by geochemical modelling. PhD thesis (in Croatian), University of Zagreb, 155 p.

Marković, T., Brkić, Ž., Ćućuzović, H., Larva, O., & Briški, M. 2015. Behaviour of heavy metals and nitrates in the alluvial aquifer of Koprivnica region. // Abstracts Book. Sapienza University of Rome.

Marković, T., Karlović, I., Perčec Tadić, M. & Larva, O. 2020. Application of stable water isotopes to improve conceptual model of alluvial aquifer in the Varaždin area. Water, 12, 1-13.

Marković, T., Šparica Miko, M., Đumbir, A., Gligora Uvodič, M., Kulaš, A., Larva, O. & Brkić, Ž. 2018. Variations of nitrate concentrations in ground and surface waters of Varaždin alluvial system. Abstracts Book / Novak, M., Rman, N. (eds). Ljubljana.

Mayer, D. 1993. Groundwater quality and protection. Croatian Water and Sea Pollution Control Society, (in Croatian) 146 p., Zagreb.

McMahon, P.B., Dennehy, K.F., Bruce, B.W., Böhlke, J.K., Michel, R.L., Gurdak, J.J., Hurlbut, D.B., 2006. Storage and transit time of chemicals in thick unsaturated zones under rangeland and irrigated cropland, High Plains, United States. Water Resour. Res., 42(3). DOI:10.1029/2005WR004417

MCOS (M.C. O'Sullivan), 2002. Three Rivers Project Final Technical Report. Environmental Protection Agency, Johnstown Castle, Ireland.

Mercado, A., 1976. Nitrate and chloride pollution of aquifers: A regional study with the aid of a single-cell model. Water Resour. Res., 12(4): 731-747. DOI:10.1029/WR012i004p00731

MKGP, 2020. Ministry of Agriculture, Forestry and Food. Found online 1.6.2020: https://rkg.gov.si/vstop/

Mockler and Bruen, 2018. Catchment Management Support Tools for Characterisation and Evaluation of Programme of Measures (CatchmentTools Project). Environmental Protection Agency Research report, Wexford, Ireland. http://www.epa.ie/pubs/reports/research/water/Research_Report_249.pdf

Mockler, E. M., Deakin, J., Archbold, M., Gill, L., Daly, D. and Bruen, M., 2017b. Sources of nitrogen and phosphorus emissions to Irish rivers and coastal waters: estimates from a nutrient load apportionment framework. Science of the Total Environment 601–602: 326–339. Available online: https://doi.org/10.1016/j. scitotenv.2017.05.186

Mockler, E., Bruen, M., Desta, M. and Misstear, B., 2014. Pathways Project Final Report Volume 4: Catchment Modelling Too. Environmental Protection Agency, Johnstown Castle, Ireland. Available online: http:// epa.smartsimple.ie/files/347278/102779/Pathways_ Project_Vol_4.pdf

Mockler, E.M., Deakin, J., Archbold, M., Daly, D. and Bruen, M., 2016. Nutrient load apportionment to support the identification of appropriate Water Framework Directive measures. Biology and Environment: Proceedings of the Royal Irish Academy 116B: 245–263. Available online: http://dx.doi. org/10.3318/bioe.2016.22

Moeys, J., Larsbo, M., Bergstrom, L., Brown, C.D., Coquet, Y., Jarvis, N.J. 2012. Functional test of pedotransfer functions to predict water flow and solute transport with the dual-permeability model

Molenat, J., Gascuel-Odoux, C., Aquilina, L. et al. 2013. Use of gaseous tracers (CFCs and SF6) and transit-time distribution spectrum to validate a shallow groundwater transport model. Journal of Hydrology 480, 1-9

Mollerup, M. 2010. Daisy 2d numerics, URL http://daisy.ku.dk/publications/Num2D-v2.pdf.

MOP. 2020. Ministry of the environment and spatial planning. Found online 1.6.2020: https://egp.gu.gov.si/egp/

Morris, T. O. 1952. The water supply resources of Malta. Valletta: Government Printing Office

Nagy, D. (2020). Quantifying the transport and fate of dissolved nitrogen at different scales in drained agricultural landscapes. Ph.D.-thesis, pp 219. https://pure.au.dk/portal/en/publications/quantifying-the-transport-and-fate-of-dissolved-nitrogen-at-different-scales-in-drained-agricultural-landscapes(cbb43ba8-4922-42ef-814e-b4fb88e532e2).html or https://hess.copernicus.org/preprints/hess-2019-666/

National Statistics Office, 2010 Census of Agriculture, Government of Malta

Ní Longphuirt, S., Mockler, E., O'Boyle, S., Wynne, C. and Stengel, D.B., 2016. Linking changes in nutrient load source apportionment to estuarine responses: an Irish perspective. Biology and Environment: Proceedings of the Royal Irish Academy 116B: 295–311. Available online: http://dx.doi.org/10.3318/bioe.2016.21

Nimmo , John R 2020. The processes of preferential flow in the unsaturated zone. Invited review. Soil Science Society of America Journal. https://doi.org/10.1002/saj2.20143

Niswonger, R.G., Panday, Sorab, and Ibaraki, Motomu (2011): MODFLOW-NWT, A Newton formulation for MODFLOW-2005: U.S. Geological Survey Techniques and Methods 6–A37, 44 p.

Normand, B., Czernichowski, I., Mouvet, C. 1999. Suivi de la nappe et de la zone non saturée dans le bassin de l'Hallue (Somme). BRGM

O'Boyle, S., Quinn, R., Dunne, N., Mockler, E.M. and Ní Longphuirt, S., 2016. What have we learned from over two decades of monitoring riverine nutrient inputs to Ireland's marine environment? Biology and Environment: Proceedings of the Royal Irish Academy 116B: 313–327. Available online: https://doi. org/10.3318/bioe.2016.23

Oenema, O., Kros, H., de Vries, W., 2003. Approaches and uncertainties in nutrient budgets: implications for nutrient management and environmental policies. European Journal of Agronomy 20, 3-16

OSPAR, 1998. Principles of the Comprehensive Study on Riverine Inputs and Direct Discharges (RID). OSPAR Commission, London.

Packham, I., Archbold, M., Desta, M., Flynn, R., Deakin, J., Gill, L., Mockler, E., Bruen, M. and Misstear, B., 2015. Pathways Project Final Report Volume 3: Catchment Characterisation Tools. Environmental Protection Agency, Johnstown Castle, Ireland.

Paquer, A., Massart, S., Krzyk M., Četina M. 1999. 2-D models for suspended sediment transport – comparitive use for case of Ptuj Lake. V: Hydraulic engineering for Substainable Water Resources Management at the Turn of the Millenium. Graz, Technical University Gray, Institute for Hydraulics and Hydrology. (online). URL: https://www.sv-jme.eu/?ns_articles_pdf=/ns_articles/files/ojs3/1010/submission/1010-1-1081-1-2-20170705.pdf&id=4405

Patrčević, V. 1995. Hydrological analysis of vertical water balance of groundwater at the area of river alluvium. PhD thesis (in Croatian), University of Zagreb, 161 p.

Pestotnik, S., Prestor, J., Meglič, P., Janža, M., Šram, D., 2019. D. T2.2.4 - Report on actualized contaminants mass balance and pressures-impacts model, Version 2. Project AMIIGA (Interreg, Central Europe). Geological Survey of Slovenia.

Philippe, E. 2011. Contribition à la modélisation du transfert de nitrates au travers de la zone non saturée à l'échelle régionale : application au bassin de la Seine. Thèse de doctorat de l'école nationale supérieure des mines de Paris. 207p

Poisvert, C., Curie, F., Moatar, F., 2017. Annual agricultural N surplus in France over a 70-year period. 2017. Nutr Cycl Agroecosyst 107, 63–78

Pratt, P.F., Jones, W.W., Hunsaker, V.E., 1972. Nitrate in Deep Soil Profiles in Relation to Fertilizer Rates and Leaching Volume. J. Environ. Qual., 1(1): 97-101. DOI:10.2134/jeq1972.00472425000100010024x

Prentice, I., 2008. Terrestrial nitrogen cycle simulation with a dynamic global vegetation model. Global Change Biology, 14(8): 1745-1764.

Prestor, J., Pestotnik, S., Janža, M., Meglič, P., 2014. Načrtovanje zaščitnih ukrepov na podlagi modela obremenitev in vplivov na podzemno vodo. V: Kladnik, D., Topole, M. ur. Skrb za vodo. Ljubljana: Založba ZRC. 79-92 str.

Psaltopoulos, D., Wade, A.J., Skuras, D., Kernan, M., Tyllianakis, E. and Erlandsson, M., 2017. False positive and false negative errors in the design and implementation of agri-environmental policies: a case study on water quality and agricultural nutrients. Science of the Total Environment 575: 1087–1099. Available online: http://dx.doi.org/10.1016/j. scitotenv.2016.09.181

Raats, P. A. C. 1981. Residence times of water and solutes within and below the root zone. In Developments in Agricultural Engineering (Vol. 2, pp. 63-82). Elsevier.

Rao, R.S.C., Davidson, J.M., 1985. Indices for ranking the potential for pesticide contamination of groundwater. Soil and Crop Science Society of Florida proceedings 44, 1–8.

Rao. P.S.C., Jessup, R.E., 1983. Sorption and movement of pesticides and other toxic organic substances in soils. P.183–201. In: D.W., Nelson, K.K., Tanji, D.E., Elrick (ed) Chemical Mobility and Reactivity in Soil Systems. American Society of Agronomy, Madison. WI.

Redhead, J.W., May, L., Oliver, T.H., Hamel, P., Sharp, R. and Bullock, J.M., 2018. National scale evaluation of the InVEST nutrient retention model in the United Kingdom. Science of the Total Environment 610–611: 666–677. Available online: https://doi.org/10.1016/j. scitotenv.2017.08.092

Rivett, M.O., Buss, S.R., Morgan, P., Smith, J.W., Bemment, C.D., 2008. Nitrate attenuation in groundwater: a review of biogeochemical controlling processes. Water Res., 42(16): 4215-4232.

Rivett, M.O., Smith, J.W.N., Buss, S.R., Morgan, P., 2007. Nitrate occurrence and attenuation in the major aquifers of England and Wales. Quarterly Journal of Engineering Geology and Hydrogeology, 40(4): 335-352. DOI:10.1144/1470-9236/07-032

Romić, D., Husnjak, S., Mesić, M., Salajpal, K., Barić, K., Poljak, M., Romić, M., Konjačić, M., Vnučec, I., Bakić, H., Bubalo, M., Zovko, M., Matijević, L., Lončarić, Z., Kušan, V., Brkić, Ž. & Larva, O. 2015. The impact of agriculture on surface and groundwater pollution in the Republic of Croatia. Faculty of Agriculture, Univrsity of Zagreb, 302 p.

Rosenbom, A.E., Badawi, N., Karan, S., Jensen, A.M.D. 2020. PESTGOLF - Pesticidudvaskning fra golfbanearealer. Miljø- og Fødevareministeriet, Miljøstyrelsen, Bekæmpelsesmiddelforskning nr. 188 pp. 70. ISBN: 978-87-7038-210-6 (In Danish).

Rosenbom, A.E., Binning, P.J., Aamand, J., Dechesne, A., Smets, B.F., Johnsen, A.R. 2014. Does microbial centimeter-scale heterogeneity impact MCPA degradation in and leaching from a loamy agricultural soil? Science of The Total Environment 472: 90-98. ISSN 0048-9697. https://doi.org/10.1016/j.scitotenv.2013.11.009.

Rosenbom, A.E., Kjær, J., Henriksen, T., Ullum, M., Olsen, P. 2009. Ability of the MACRO Model to Predict Long-Term Leaching of Metribuzin and Diketometribuzin. Environ. Sci. Technol. 43(9): 3221–3226. https://doi-org.ep.fjernadgang.kb.dk/10.1021/es802752

Rosenbom, A.E., Olsen, P., Plauborg, F., Grant, R., Juhler, R.K., Brüsch, W., Kjær, J. 2015. Pesticide leaching through sandy and loamy fields – Long-term lessons learnt from the Danish Pesticide Leaching Assessment Programme. Environmental Pollution 201:75-90. ISSN 0269-7491.

Rousseau, M., Seguin, J.J., Croiset, N., Surdyk, N., 2016. Modélisation du transfert des nitrates en zone non saturée dans les alluvions fluvio-glaciaires du couloir de Meyzieu (Rhône). BRGM

Rudolph, D.L., Devlin, J.F., Bekeris, L., 2015. Challenges and a Strategy for Agricultural BMP Monitoring and Remediation of Nitrate Contamination in Unconsolidated Aquifers. Groundwater Monitoring & Remediation, 35(1): 97-109. DOI:10.1111/gwmr.12103

Scholefield, D., Lockyer, D.R., Tyson, K.C., Whitehead, D.C., 1991. A model to predict transformations and losses of nitrogen in UK pastures grazed by beef cattle. Plant Soil 132, 165–177.

Schullehner, Jörg, Birgitte Hansen, Malene Thygesen, Carsten B. Pedersen, and Torben Sigsgaard. 2018. "Nitrate in Drinking Water and Colorectal Cancer Risk: A Nationwide Population-Based Cohort Study." International Journal of Cancer 143 (1): 73–79. https://doi.org/10.1002/ijc.31306.

Seguin, J.-J., Moreau, F., 1986. Migration des nitrates dans la zone non-saturée de la craie de champagne. Interprétation des résultats d'une campagne de carottages sous un champ d'épandages d'effluents agricoles, Connantre-Marne. BRGM.

Serhal, H. 2006. Influence des pressions anthropiques sur l'évolution des concentrations en nitrates dans la nappe de la craie du Nord de la France (application au Cambrésis et au nord Audomarois) - Thèse de doctorat de l'Université de Lille.

Serhal, H., Bastin-Lacherez, S., Bernard D., El Khattabi J. 2006. Etude de la migration des nitrates dans la nappe à travers la zone non saturée: enjeux et impact sur la qualité de l'eau exploitée. Gestion des grands aquifères, 30 mai-1er juin 2006, Dijon. France.

Shaffer, M.J., Wylie, B.K., Follett, R.F. and Bartling, P.N.S., 1994. Using climate/weather data with the NLEAP model to manage soil nitrogen. Agricultural and Forest Meteorology 69: 111–123. Available online: http://dx.doi.org/10.1016/0168–1923(94)90084-1

Shomar, B., Osenbrück, K. and Yahya, A. 2008. Elevated nitrate levels in the groundwater of the Gaza Strip: Distribution and sources. Science of The Total Environment, Vol. 398, 164-174.

Šimůnek, J., M. Šejna, H. Saito, M. Sakai, van Genuchten, M. Th. 2018. The HYDRUS-1D Software Package for Simulating the Movement of Water, Heat, and Multiple Solutes in Variably Saturated Media. Version 4.17, HYDRUS Software Series 3, Department of Environmental Sciences, University of California Riverside, Riverside, California, USA, pp. 348.

Smith, R.V., Jordan, C. and Annett, J.A., 2005. A phosphorus budget for Northern Ireland: inputs to inland and coastal waters. Journal of Hydrology 304: 193–202. Available online: http://dx.doi.org/10.1016/j. jhydrol.2004.10.004

SNIFFER. 2006. An approach to hydrogeological assessment of Quaternary deposits in the UK. Project WFD34, Scotland and Northern Ireland Forum for Environmental Research: Edinburgh.

Sonnenborg, T.O., K. Hinsby, L. van Roosmalen, and S. Stisen. 2012. "Assessment of Climate Change Impacts on the Quantity and Quality of a Coastal Catchment Using a Coupled Groundwater-Surface Water Model." Climatic Change 113 (3–4): 1025–48.

Sousa, M.R., Jones, J.P., Frind, E.O., Rudolph, D.L., 2013. A simple method to assess unsaturated zone time lag in the travel time from ground surface to receptor. J. Contam. Hydrol., 144(1): 138-151. DOI:https://doi.org/10.1016/j.jconhyd.2012.10.007

Spalding, R.F., Kitchen, L.A., 1988. Nitrate in the Intermediate Vadose Zone Beneath Irrigated Cropland. Ground Water Monitoring & Remediation, 8(2): 89-95. DOI:10.1111/j.1745-6592.1988.tb00994.x

Stisen, S., Ondracek, M., Troldborg, L., Schneider, RJM, van til MJ. & Michael John van Til. The National Water Resources Model - model setup and calibration of DK-model 2019. GEUS report 2019/31, 2019, in Danish.

Stuart, M E, et al. 2008. A Preliminary Study on the Identification of the Sources of Nitrate Contamination in Groundwater in Malta Results and Interpretation. British Geological Survey.

Stuart, M.E., et al 2010. Groundwater residence time and movement in the Maltese islands – A geochemical approach. - Applied Geochemistry, 25, 609-620.

Stuart, ME. 2005. Development of nitrate profiles database. British Geological Survey Internal Report IR/05/058.

Surdyk N., Gourcy L., Baran N., Picot G., 2014. Etude du transfert des nitrates dans la zone non saturée et dans les eaux souterraines des aires d'alimentation de captage en Picardie, bassin Seine Normandie. Rapport provisoire. BRGM

Surdyk, N., Gourcy, L., Bault, V., 2016. Etude du transfert des nitrates dans la zone non saturée et dans les eaux souterraines des aires d'alimentation de captage dans l'Oise. BRGM

Teagasc, EPA and GSI, 2006. National Soils Map. Available online: gis.epa.ie/GetData/Download

Tesoriero, A.J., Duff, J.H., Wolock, D.M., Spahr, N.E. and Almendinger, J.E., 2009. Identifying pathways and processes affecting nitrate and orthophosphate inputs to streams in agricultural watersheds. Journal of Environmental Quality 38: 1892–1900. Available online: http://dx.doi.org/10.2134/jeq2008.0484

Thorling L. et al., GEUS report 2020/4, 2020, In Danish.

Troldborg, L. et al. GEUS report 2020/1, 2020, in Danish.

Turkeltaub, T., Ascott, M.J., Gooddy, D.C., Jia, X., Shao, M.-A., Binley, A., 2020. Prediction of regional-scale groundwater recharge and nitrate storage in the vadose zone: A comparison between a global model and a regional model. Hydrol. Processes, 34(15): 3347-3357. DOI:https://doi.org/10.1002/hyp.13834

Turkeltaub, T., Kurtzman, D., Russak, E.E., Dahan, O., 2015. Impact of switching crop type on water and solute fluxes in deep vadose zone. Water Resour. Res., 51(12): 9828-9842. DOI:doi:10.1002/2015WR017612

Turnšek, A. 2016. Groundwater storage quaternary aquifer of Dravsko polje. Master's thesis. University of Ljubljana, Faculty of Natural Sciences and Engineering. Available online (30.03.2020): https://repozitorij.uni-lj.si/Dokument.php?id=86650&lang=slv

Urbanc, J., Krivic, J., Mali, N., Ferjan, S., T., Koroša, A., Šram, D., Mezga, K., Bizjak, M., Medić, M., Bole, Z., Lojen, S., Pintar, M., Udovč, A., Glavan, M., Kacjan-Maršić, N., Jamšek, A., Valentar, V., Zadravec, D., Pušenjak, M., Klemenčič Kosi, S. 2014. Možnosti kmetovanja na vodovarstvenih območjih : zaključno poročilo projekta. Ljubljana : Geološki zavod Slovenije : Univerza v Ljubljani, Biotehniška fakulteta : Institut Jožef Stefan ; Maribor : Kmetijsko gozdarski zavod, 2 zv. (183; 154 str.). Arh. št.: K-II-30d/c-1/1826.

Urumović, K. 1971. On quaternary aquifer complex in Varazdin area. Geol. vjesnik 24,183-191

Urumović, K., Hlevnjak, B., Prelogović, E. & Mayer, D. (1990): Hydrogeological conditions of Varaždin aquifer. Geol. vjesnik 43,149-158

Urumović, K., Šarin, A. & Donadini, K. 1981. Groundwater balance in the river basin district Drava-Dunav for 1979-1980. IGI, Zagreb.

USGS, 2015. Water Quality Portal. http://waterqualitydata.us/

Van der Aa & Swartjes 2017. Bestrijdingsmiddelen bij drinkwaterwinningen en maatregelen om uitspoeling naar grondwater te verminderen, H2O-online.

Van Drecht, G., Bouwman, A.F., Knoop, J.M., Beusen, A.H.W., Meinardi, C.R., 2003. Global modeling of the fate of nitrogen from point and nonpoint sources in soils, groundwater, and surface water. Global Biogeochem. Cycles, 17(4). DOI:10.1029/2003GB002060

Van Engelen, J., Verkaik, J., King, J., Nofal, E. R., Bierkens, M. F., & Oude Essink, G. H. 2019. A three-dimensional palaeohydrogeological reconstruction of the groundwater salinity distribution in the Nile Delta Aquifer. Hydrology and Earth System Sciences, 23(12), 5175-5198.

Van Meter, K.J., Basu, N.B., Veenstra, J.J., Burras, C.L., 2016. The nitrogen legacy: emerging evidence of nitrogen accumulation in anthropogenic landscapes. Environ. Res. Lett., 11(3): 035014.

Vero, S.E., Basu, N.B., Van Meter, K., Richards, K.G., Mellander, P.-E., Healy, M.G., Fenton, O., 2018. Review: the environmental status and implications of the nitrate time lag in Europe and North America. Hydrogeology Journal, 26(1): 7-22. DOI:10.1007/s10040-017-1650-9

Vero, S.E., Ibrahim, T.G., Creamer, R.E., Grant, J., Healy, M.G., Henry, T., Kramers, G., Richards, K.G., Fenton, O., 2014. Consequences of varied soil hydraulic and meteorological complexity on unsaturated zone time lag estimates. J. Contam. Hydrol., 170: 53-67. DOI:https://doi.org/10.1016/j.jconhyd.2014.10.002

Veršič, B. 2007. Geografske značilnosti Ptujskega jezera. Diplomska naloga. Univerza v Ljubljani, Filozofska fakulteta, oddelek za geografijo. URL: https://repozitorij.uni-lj.si/Dokument.php?id=111442&lang=slv

Veselič, M. 1984. Hidrogeologija. FNT, VTOZD Montanistika, Odsek za geologijo.

Visser, A. H.P. Broers, R. Heerdink and M.F.P. Bierkens 2009. Trends in pollutant concentrations in relation to time of recharge and reactive transport at the groundwater body scale. Journal of Hydrology, 369:427-439.

Visser, A., H.P. Broers, & M.F.P. Bierkens 2007. Demonstrating trend reversal in groundwater quality in relation to time of recharge determined by 3H/3He dating. Environmental Pollution 148(3)

Vogel, J. C. (1967). Investigation of groundwater flow with radiocarbon. In Isotopes in hydrology. Proceedings of a symposium.

Voulvoulis, N., Arpon, K.D. and Giakoumis, T., 2017. The EU Water Framework Directive: from great expectations to problems with implementation. Science of the Total Environment 575: 358–366. Available online: http://dx.doi.org/10.1016/j. scitotenv.2016.09.228

Wada, Y., van Beek, L.P., van Kempen, C.M., Reckman, J.W., Vasak, S., Bierkens, M.F., 2010. Global depletion of groundwater resources. Geophys. Res. Lett., 37(20).

Wang, L., Butcher, A., Stuart, M., Gooddy, D., Bloomfield, J., 2013. The nitrate time bomb: a numerical way to investigate nitrate storage and lag time in the unsaturated zone. Environ. Geochem. Health, 35(5): 667-681.

Wang, L., Stuart, M., Lewis, M., Ward, R., Skirvin, D., Naden, P., Collins, A., Ascott, M., 2016. The changing trend in nitrate concentrations in major aquifers due to historical nitrate loading from agricultural land across England and Wales from 1925 to 2150. Science of the Total Environment, 542: 694-705.

Wang, L., Stuart, M.E., Bloomfield, J.P., Butcher, A.S., Gooddy, D.C., McKenzie, A.A., Lewis, M.A., Williams, A.T., 2012. Prediction of the arrival of peak nitrate concentrations at the water table at the regional scale in Great Britain. Hydrol. Processes, 26(2): 226-239. DOI:10.1002/hyp.8164

Weissmann, G. S., Zhang, Y., LaBolle, E. M., & Fogg, G. E. 2002. Dispersion of groundwater age in an alluvial aquifer system. Water Resources Research, 38(10), 16-1.

Wellings, S.R., Bell, J.P., 1980. Movement of water and nitrate in the unsaturated zone of Upper Chalk near Winchester, Hants., England. J. Hydrol., 48(1): 119-136. DOI:http://dx.doi.org/10.1016/0022-1694(80)90070-0

Wiedemeier, T.H., Swanson, M.A., Moutoux, D.E. Gordon, E.K., Wilson, J.T., Wilson, B.H., Kampbell, D.H., Haas, P.E., Miller, R.N., Hansen, J.E. & Chapelle, F.H. 1998. Technical protocol for evaluating natural attenuation of chlorinated solvents in ground water. EPA/600/R-98/128, U.S. Environmental Protection Agency, Office of Research and Development, Washington, D.C.

Wilson, S., Shokri, A., 2015. Estimation of lag time of water and nitrate flow through the Vadose Zone: Waikato and Waipa River Catchments.

Withers, P.J.A., May, L., Jarvie, H.P., Jordan, P., Doody, D., Foy, R.H., Bechmann, M., Cooksley, S., Dils, R. and Deal, N., 2012. Nutrient emissions to water from septic tank systems in rural catchments: uncertainties and implications for policy. Environmental Science & Policy 24: 71–82. Available online: http://dx.doi. org/10.1016/j.envsci.2012.07.023

Worrall, F., Burt, T., Howden, N., Whelan, M., 2009. Fluvial flux of nitrogen from Great Britain 1974–2005 in the context of the terrestrial nitrogen budget of Great Britain. Global Biogeochem. Cycles, 23(3).

Worrall, F., Howden, N.J.K., Burt, T.P., 2015. Evidence for nitrogen accumulation: the total nitrogen budget of the terrestrial biosphere of a lowland agricultural catchment. Biogeochemistry, 123(3): 411-428. DOI:10.1007/s10533-015-0074-7

Zhang, Y., Collins, A.L., Murdoch, N., Lee, D. and Naden, P.S., 2014. Cross sector contributions to river pollution in England and Wales: updating waterbody scale information to support policy delivery for the Water Framework Directive. Environmental Science and Policy 42, 16–32.

Zheng, C. & Wang, P.P. 1999. MT3DMS – A modular three - dimensional multispecies transport model for simulation of advection, dispersion, and chemical reactions of contaminants in groundwater systems. Contract Report for U.S. Army Corps of Engineers. SERDP 99, 239, Tuscalossa, Alabama.

Zimmermann, J., Fealy, R.M., Lydon, K., Mockler, E.M., O'Brien, P., Packham, I., Smith, G. and Green, S., 2016. The Irish Land-Parcels Identification System (LPIS): experiences in ongoing and recent environmental research and land cover mapping. Biology and Environment: Proceedings of the Royal Irish Academy 116B: 53–62. Available online: http:// dx.doi.org/10.3318/bioe.2016.04

Žlebnik, J. 1982. Hydrogeology of the Drava field. Geologija, 25/1: 151-164, Ljubljana.

Žlebnik, L. 1991. Hydrogeology of the Ptuj field. Geologija, 34: 337-352.